

Advanced energy planning of Smart Islands

Mimica, Marko

Doctoral thesis / Disertacija

2022

Degree Grantor / Ustanova koja je dodijelila akademski / stručni stupanj: **University of Zagreb, Faculty of Mechanical Engineering and Naval Architecture / Sveučilište u Zagrebu, Fakultet strojarstva i brodogradnje**

Permanent link / Trajna poveznica: <https://um.nsk.hr/um:nbn:hr:235:077703>

Rights / Prava: [In copyright](#) / [Zaštićeno autorskim pravom.](#)

Download date / Datum preuzimanja: **2024-04-26**

Repository / Repozitorij:

[Repository of Faculty of Mechanical Engineering
and Naval Architecture University of Zagreb](#)





University of Zagreb

FACULTY OF MECHANICAL ENGINEERING AND NAVAL
ARCHITECTURE

Marko Mimica

ADVANCED ENERGY PLANNING OF SMART ISLANDS

DOCTORAL THESIS

Zagreb, 2022.



University of Zagreb

FACULTY OF MECHANICAL ENGINEERING AND NAVAL
ARCHITECTURE

Marko Mimica

ADVANCED ENERGY PLANNING OF SMART ISLANDS

DOCTORAL THESIS

Supervisor: Associate Professor Goran Krajačić, PhD

Zagreb, 2022.



Sveučilište u Zagrebu

FAKULTET STROJARSTVA I BRODOGRADNJE

Marko Mimica

NAPREDNO ENERGETSKO PLANIRANJE PAMETNIH OTOKA

DOKTORSKI RAD

Mentor: izv. prof. dr. sc. Goran Krajačić

Zagreb, 2022

TABLE OF CONTENTS

PREFACE	iii
ACKNOWLEDGEMENT	iv
SPECIAL ACKNOWLEDGEMENT	v
SUMMARY	vii
PROŠIRENI SAŽETAK	ix
LIST OF FIGURES	xiv
LIST OF TABLES	xv
1 INTRODUCTION.....	1
1.1. Background.....	1
1.1.1. Global perspective.....	1
1.1.2. EU energy transition policy.....	2
1.1.3. EU policy on islands	3
1.2. Motivation	4
1.3. Objectives and hypothesis of the research.....	8
1.4. Scientific contributions.....	8
2 METHODS.....	10
2.1. Formulation of the optimization problem.....	12
2.2. Unit commitment.....	13
2.2.1. Transmission system approximation model.....	15
2.2.2. Distribution system representation.....	16
2.3. The Smart Islands method	17
2.4. Risk assessment method of the energy planning scenarios on islands	18
2.5. Advanced capacity expansion energy planning model soft-linked with the power flow	19
2.6. Demand response model.....	21
2.7. Demand response and energy storage in joint energy and reserve markets	23
2.8. Maritime transport electrification model	24
3 SELECTED RESULTS AND	27
DISCUSSION	27
3.1. Meeting islands' needs with local resources	27
3.1.1. Krk island	27
3.1.2. Vis island.....	29
3.2. Risk assessment for island energy planning scenarios	31
3.2.1. Unije	31
3.2.2. Tilos island	34
3.3. Advanced energy planning approach for smart islands.....	36

3.4.	A novel demand response model for the development of a smart archipelago	42
3.4.1.	The impact of the demand response and battery storage system on the financial and technical aspects	43
3.4.2.	The incentive value for providing the demand response.....	46
3.5.	Demand response and energy storage system models in a joint network constrained energy and reserve market.....	49
3.5.1.	DR and ESS impact on the financial aspects	50
3.5.2.	DR and ESS impact on the technical aspects of the system.....	52
3.6.	Maritime transport electrification and integration with the energy system.....	54
4	CONCLUSIONS AND	59
	FUTURE WORK	59
5	LITERATURE	62
6	CURRICULUM VITAE	71
7	SUMMARY OF PAPERS	72

PREFACE

The research presented in this thesis is a result of four-year research work carried out at the Department of Energy, Power and Environmental Engineering of the Faculty of Mechanical Engineering and Naval Architecture, University of Zagreb. Over these four years, I had the opportunity to participate in six conferences in order to promote, discuss and disseminate my work. At these conferences, I co-authored numerous papers, however, they are not an integral part of this thesis.

The ultimate motivation for this work lies in the fact that human activity is causing global climate changes. This presents perhaps the most important issue of the 21st century and the extent to which we will address these issues will have a significant impact on our future. Decarbonisation of island energy systems will not directly impact the emissions reduction, however, the knowledge obtained from testing and implementing new approaches and solutions on islands can have a wide-scale impact on the energy transition. This thesis brings several novel concepts tested on islands as well as new approaches for the planning of island energy transition. The results clearly showed that different approaches generate different results, thus many new questions can be set out. How can we optimally utilize the increasing data streams for optimal energy planning? What is the proper trade-off between the energy system model complexity and the desired outcomes? How to transfer and scale-up positive solutions from the islands to the mainland? How do we accelerate the energy transition on islands and on the mainland by exploiting the benefits of increased digitalization? How to create market and policy frameworks in order to create viable business models for flexibility units?

These and many more questions can be asked based on the results of this thesis. However, this should not discourage us as the past ten to fifteen years showed us that change is possible and that we can turn the challenges we face into opportunities. As famous physicist Richard Feynman once said *“I would rather have questions that can’t be answered than answers that can’t be questioned”*. With that in mind, let us continue answering these questions.

In Mimice, 25th of August 2022

Marko Mimica

ACKNOWLEDGEMENT

Most importantly I would like to thank my parents Meri and Dobromir, sister Karla and brother Roko for constant support without which it wouldn't be possible to obtain degrees from two most prominent technical faculties in Croatia – FSB and FER.

I would also like to thank my mentor and supervisor prof. Goran Krajačić for his advice and availability not only regarding the PhD study but any other issue even in the late night (or early morning) hours.

My thanks also goes to prof. Neven Duić and prof. Tomislav Pukšec for their valuable advices during the PhD study. I would also like to express my gratitude to Mr. Mirko Tunjić whose support was always recognised and appreciated.

Special thanks goes to the colleagues and fellow PhD students from Powerlab, who were a big support during these 4 years of the PhD study: Goran Stunjek, Nikola Matak, Antun Pfeifer, Hrvoje Dorotić, Borna Doračić, Ana Lovrak, Filip Jurić, Tibor Bešenić, Marijan Marković, Hrvoje Stančin, Josip Miškić, Ivan Pađen, Hrvoje Mikulčić, Marko Ban, Doris Beljan, Luka Herc, Boris Ćosić and all other colleagues from the Powerlab and Department. I would also like to thank Dominik Franjo Dominković for his valuable advice and support. My thanks goes to all of my friends, especially Žara, Andrija, Ivan, Josip Lucijan, Toni, Zdenko, Joško, Ante, Domagoj, Luka, Nikolina and Ana for always being there for a good laugh in the moments of relaxation.

At the end of my study, I would also like to thank my colleagues and professors from Faculty of electrical engineering and computing, especially members of the EESTEC LC Zagreb where I learned to think openly and always challenge myself to achieve better and more.

Finally, I would like to thank my Irma for being my biggest support in the moments of difficulty and for always being a sweet comfort in a bitter world of a PhD student.

SPECIAL ACKNOWLEDGEMENT

The research presented in this thesis was carried out at the Department of Energy, Power and Environmental Engineering of the Faculty of Mechanical Engineering and Naval Architecture in scope of the Young researchers' Career Development Programme (DOK-01-2018) financed by Croatian Science Foundation from European Social Fund. The thesis was also completed in the scope of Horizon 2020 project INSULAE - Maximizing the impact of innovative energy approaches in the EU islands (Grant number ID: 824433) financed by the European Union. This support is gratefully acknowledged and recognized.

*“Some men see things as they are and say why, I dream
things that never were and say, why not!”*

George Bernard Shaw

SUMMARY

Climate change represents one of the greatest challenges of our time. Human activity is causing global temperature to rise and failure to act swiftly and efficiently on this issue will result in irreversible consequences. European union has recognised this and set ambitious goals for tackling this issue. The role of geographical islands is also recognised in the European union legislation. Thus, many studies deal with the analysis of energy systems on islands and offer solutions for their energy transition.

The main objective of this thesis is to show that the transition of energy systems on islands to fully renewable is possible and that it is possible to quantify the risks of energy planning scenarios on islands. Additionally, the objectives of this thesis are to provide new models and methods for design of the smart energy systems on the islands. For this purpose, the Smart Islands method that automatically generates energy planning scenarios for islands and that considers seven different sectors was developed. The method bases its results on the indexation method with quantified indicators developed in the scope of this thesis and on the linear optimization model that minimizes the investment cost of the energy planning scenarios on islands. In order to quantify the risk of the energy planning scenarios for islands, a method based on the probability of outages and the damage caused by particular outage was developed. The multiplication of the outage probability and damage results in risk vectors that quantifies the risk of each energy planning scenario. Novel models and methods for the demand response, maritime transport electrification, detailed spatio-temporal modelling soft-linked to the power flow, participation of flexibility providers in the joint energy and reserve network-constrained markets were developed and tested on islands. Models and methods are based on different formulations of the optimization problem and also include different sensitivity and well as uncertainty management methods such as robust optimization and Monte Carlo method.

The results of the study showed that it is possible to design fully renewable systems on islands with defined type and capacities of technologies that meet local needs with local resources. It was also shown that the integration of different flows results in increased flexibility in the energy system. The results also showed that it is possible to quantify the risk level of energy planning scenarios for islands and that increased penetration of renewable energy sources and flexibility sources lead towards lower levels of risk. Additionally, the results showed that spatial distribution can have a significant impact on the energy system modelling. Finally, the results

showed that different solutions that increase the flexibility of the island energy systems such as energy storage systems, cross-sector integration and different market frameworks can increase the possibility for the integration of the renewable energy sources and reduce the overall cost of the island energy systems.

PROŠIRENI SAŽETAK

Ključne riječi:

Pametni otoci, analiza energetske sustava, Smart Islands, procjena rizika, detaljno prostorno i vremensko energetske planiranje.

Klimatske promjene su danas prepoznate kao jedna od najozbiljnijih prijetnja čovječanstvu. Kontinuirana emisija stakleničkih plinova dovodi do povećanja prosječne temperature koja posljedično može dovesti do nepovratnih negativnih promjena. Iako su klimatske promjene već odavno prepoznate kao prijetnja, konkretnije djelovanje u svrhu sprječavanja klimatskih promjena je nastupilo tek u devedesetim godinama prošlog stoljeća. Tek su se Pariškim sporazumom 2015. godine zemlje svijeta obvezale poduzeti akcije u svrhu sprječavanja porasta temperature. Znanstvenici se slažu da bi porast prosječne temperature od 2 °C predstavljao točku u kojoj bi nastupile nepovratne negativne posljedice te postoji jasan konsenzus da je sprječavanje takvog porasta moguće jedino provođenjem ubrzane dekarbonizacije svih sektora.

Europska Unija je prepoznala važnost djelovanja po pitanju klimatskih promjena te je definirala tzv. 20-20-20 ciljeve za 2020. godinu. Ti ciljevi uključuju smanjenje emisija ugljikovog dioksida za 20% u odnosu na 1990. godinu, 20% povećanja obnovljivih izvora energije u ukupnoj potrošnji energije te povećanje energetske efikasnosti za 20% te su ti ciljevi u velikom broju država članica ispunjeni. Nedavno je donesen novi, ambiciozniji plan koji za svoj cilj ima klimatsku neutralnost Europske unije do 2050. s novim ciljevima za 2030. godinu. Nadalje, od država članica se očekuje donošenje nacionalnih planova kojima će se definirati akcije za postizanje propisanih ciljeva.

U svom cilju energetske tranzicije kontinenta, Europska unija je također prepoznala ulogu geografskih otoka pa je tako donijela nekoliko važnih dokumenata koji promoviraju energetske tranzicije na otocima. Jedan od njih je Čista energija za otoke Europske unije kojima je formalizirana namjera za dekarbonizaciju otoka. Također je formirano i tajništvo za energetske tranzicije otoka koji imaju ulogu pružanja potpore otocima u njihovim nastojanjima provođenja akcija energetske tranzicije. Drugi važan dokument je Deklaracija o pametnim otocima koja je postavila deset akcijskih točaka koji promoviraju razvoj pametnih otoka kroz digitalizaciju i zelene tehnologije. Nadalje, Deklaracija prepoznaje otoke kao žive laboratorije koji mogu predstavljati pilote za demonstraciju naprednih tehnologija i rješenja koji se mogu skalirati i transferirati na kopno.

Prilikom analize otočnih sustava, potrebno je nastojati lokalne potrebe zadovoljiti lokalnim resursima. Naime, rješenja metoda planiranja energetske sustava prilagođenih za prilike na kopnu ne moraju nužno biti optimalna rješenja za otočne sustave iz razloga što su cijene dobara, ali i dostupnost resursa bitno drugačija. Stoga je prilikom planiranja otočnih sustava potrebno identificirati dostupne resurse i potrebe. Za te potrebe je razvijena RenewIslands metoda koja se sastoji od niza kvalitativnih indikatora koji služe za mapiranje resursa i potreba otoka za sedam različitih sektora. Iako sveobuhvatna metoda, RenewIslands je podložna subjektivnoj interpretaciji pojedinih eksperata pa je to dovelo do toga da pojedini eksperti dodjeljuju različite kvalitativne indikatore za iste otoke.

U posljednjih dvadesetak godina izrađen je značajan broj znanstvenih studija koji analiziraju energetske sustave na otocima. U samim počecima znanstvene analize energetske sustava na otocima, stručnjaci su uglavnom predlagali integraciju varijabilnih obnovljivih izvora energije uz reverzibilne hidroelektrane ili podmorskog kabela za održavanje stabilnosti sustava. Otočni sustavi su također služili ispitivanju mogućnosti integracije vodika, kao i desalinizacijskih postrojenja u energetske sustave na otocima. Sa sve većim korištenjem informacijsko-telekomunikacijske tehnologije i naprednih tehnologija poput baterijskih spremnika energije dolazi do značajnijeg broja analiza i prijedloga rješenja za dekarbonizaciju otoka i stvaranja pametnih otoka. Tako sve više postaju zastupljene ideje koje zagovaraju međusektorsku integraciju, elektrifikaciju transporta, korištenje spremnika energije te uključivanje otocana u energetske tranzicije otoka uz pomoć informacijsko-komunikacijske tehnologije. Iako su predložene metode rezultirale s relevantnim scenarijima za otočne zajednice, potrebno je analizirati različite pristupe energetskom planiranju koje prije svega podrazumijevaju razinu prostorno vremenske rezolucije te istražiti i razviti dodatne mogućnosti za samoodrživost otočnih zajednica temeljem njihovih resursa i potreba.

CILJEVI I HIPOTEZA

Ciljevi ovog rada su sljedeći:

Razviti indeksacijski model za procjenu stupnja razvijenosti otoka koji može služiti kao temelj za planiranje strateškog razvoja otoka s posebnim osvrtom na energetske sustav

Razviti sveobuhvatnu Smart Islands metodu za proračun scenarija energetskeg planiranja s posebnim naglaskom na integraciju različitih tokova u svrhu postizanja sinergije energetskeg sektora s ostalim sektorima

Izraditi metodu za procjenu rizika pojedinih energetskeg scenarija uzimajući u obzir vjerojatnost pojave kvara na pojedinim elementima elektroenergetskeg sustava i potencijalnu štetu nastalu kao posljedica kvara.

Hipoteza ovog istraživanja jest da se primjenom Smart Islands metode i metode za procjenu rizika energetskeg sustava može pokazati da je moguća transformacija energetskeg sustava na otocima prema potpuno obnovljivim sustavima uz precizno definiranu količinu i vrstu potrebne tehnologije te uz kvantificiranu razinu rizika pojedinog scenarija energetskeg planiranja.

ZNANSTVENI DOPRINOSI

Znanstveni doprinosi ovog rada su sljedeći:

Smart Islands metoda za razvoj scenarija energetskeg planiranja koja pruža potporu za strateško odlučivanje i daje podlogu za izradu planova energetske tranzicije otoka.

Metoda za procjenu rizika pojedinih scenarija energetskeg planiranja koja će evaluirati utjecaj spremnika energije, odziva potrošnje i ostale napredne tehnologije na smanjenje rizika prilikom promjena pogonskih i topoloških stanja u elektroenergetskim sustavima na otocima.

METODE I POSTUPCI

Za potrebe doktorskog rada razvijeno je nekoliko metoda i postupaka koji doprinose naprednom energetskeg planiranju na pametnim otocima. Predložene metode i postupci razmatraju problematiku planiranja energetskeg sustava na otocima s nekoliko stajališta, a predstavljeni su kroz šest znanstvenih članaka u prilogu ovog doktorskog rada. Za potrebe planiranja energetskeg sustava na otocima razvijena je Smart Islands metoda. Smart Islands metoda automatski generira potreban tip i količinu tehnologija potrebnih za zadovoljavanje lokalnih potreba s lokalnim resursima te prelazak na potpuno obnovljive sustave. U svom prvom koraku, Smart Islands metoda generira liste tehnologija kojima je moguće zadovoljiti lokalne potrebe s lokalnim resursima za sedam različitih sektora. Za te potrebe, razvijen je indeksacijski model koji sadrži kvantitativne indikatore koji služe za mapiranje resursa i potreba otoka za sedam

različitih sektora. U svom drugom koraku, Smart Islands metoda proračunava moguće energetske scenarije te za svaki scenarij proračunava potreban kapacitet pojedine tehnologije. Za te potrebe razvijen je linearni optimizacijski model koji minimizira ukupan investicijski trošak za svaki scenarij energetskog sustava na otocima. Kako bi se ispitala robusnost Smart Islands metode, primijenjena je Monte Carlo metoda.

Kako bi se kvantificirao rizik energetskih scenarija na otocima, razvijena je metoda za procjenu rizika. Metoda razmatra topologiju sustava te pomoću Poissonove distribucije proračunava vjerojatnost ispada pojedinog elementa sustava. Za potrebe proračuna nastale štete kao posljedica ispada pojedinih elemenata razvijen je mješoviti cjelobrojni linearni optimizacijski model. Umnoškom vjerojatnosti ispada pojedinih elemenata i posljedično nastale štete moguće je proračunati vektor rizika gdje svaki član vektora predstavlja rizik pojedinog energetskog scenarija. Optimizacijski model je razvijen kao robusni model kako bi se istražio utjecaj nesigurnosti potražnje za električnom energijom.

Kako bi se evaluiralo detaljno prostorno i vremensko energetske planiranje razvijena je metoda koja omogućuje usporedbu različitih pristupa planiranju otočnih energetski sustava. S jedne strane, razmatrane su metode koje sve tehnologije razmatraju na jednoj lokaciji te modeliraju sustav na satnoj razini, dok su s druge strane razmatrane metode koje modeliraju više lokacija na polusatnoj razini. Metoda je također povezana s proračunom tokova snaga kako bi se evaluirale mogućnosti za implementaciju pojedinih energetskih scenarija na otocima.

Razvijen je također model odziva potrošnje koji se temelji na razlikama u cijeni na dan unaprijed tržištu električne energije. Model je integriran u detaljan optimizacijski model distribucijske mreže koji uvažava sva relevantna ograničenja koja razmatra i operator distribucijskog sustava. Nadalje, razvijena je metoda koja evaluira financijski i tehnički utjecaj modela odziva potrošnje. Funkcija cilja optimizacijskog modela također uključuje i poticajnu naknadu za pružatelja usluga odziva potrošnje što omogućuje analizu utjecaja različitih poticaja na rad sustava i ukupan trošak pogona.

Za potrebe evaluacije utjecaja naprednih tehnologija odziva potrošnje i spremnika električne energije na otocima kada oni mogu sudjelovati na tržištu energije i tržištu rezerve, predstavljen je pristup koji uspoređuje ta dva slučaja. Također je razvijen optimizacijski model zajedničkog tržišta energije i rezerve koji uvažava ograničenja relevantna za prijenosnu elektroenergetsku mrežu. Potražnja za električnom energijom je uzeta kao nesiguran parametar, a da bi se to uvažilo razvijen je robusni optimizacijski model.

Konačno, metoda za evaluaciju utjecaja elektrifikacije pomorskog transporta je također razvijena u sklopu ovog doktorskog rada. Metoda uključuje i novi model električnog broda integriran u optimizacijski model koji predstavlja distribucijsku mrežu. Metoda omogućuje evaluaciju utjecaja elektrifikacije pomorskog transporta na pogonske uvjete u distribucijskoj mreži te utjecaj na mogućnost integracije obnovljivih izvora energije u energetske sustav.

Scientific area: Technical sciences

Scientific field: Mechanical engineering

Institution: Faculty of Mechanical Engineering and Naval Architecture

Doctoral dissertation mentors: Associate Professor Goran Krajačić, PhD

Number of pages: Without enclosed articles 77, with articles 316

Number of figures: 38

Number of tables: 3

Number of references: 104

Date of examination: November 12, 2022

Doctoral dissertation defence commission:

Professor Neven Duić, PhD – Chairman of defence commission

Associate Professor Tomislav Capuder, PhD – external member

Professor Henrik Madsen, PhD – external member

LIST OF FIGURES

<i>Figure 1 Credibility gap between targets in 2030 and net zero targets for 2050 or later [11].</i>	<i>2</i>
<i>Figure 2 Overview of the used approaches and scientific novelties of the thesis.....</i>	<i>11</i>
<i>Figure 3 Overview of the scientific contributions of the thesis.....</i>	<i>12</i>
<i>Figure 4 Overview of the Smart Islands method.....</i>	<i>17</i>
<i>Figure 5 Risk assessment method for the energy planning scenarios on islands</i>	<i>19</i>
<i>Figure 6 Proposed soft-linking method of the energy planning and power flow models</i>	<i>21</i>
<i>Figure 7 Overview of the method for the impact evaluation of maritime transport electrification and integration with the energy system</i>	<i>26</i>
<i>Figure 8 The results of the Krk island case study with the consideration of the uncertainty of technical input parameters.....</i>	<i>28</i>
<i>Figure 9 Energy planning scenarios for the electricity generation technologies for Krk island when the uncertainty of the specific investment cost of technologies was considered.....</i>	<i>29</i>
<i>Figure 10 Considered uncertainty range for the Unije island risk assessment calculation</i>	<i>32</i>
<i>Figure 11 The risk values for different Unije island energy system scenarios considering the uncertainty budget.....</i>	<i>33</i>
<i>Figure 12 The results of the risk assessment analysis for finding a “zero-import” scenario .</i>	<i>34</i>
<i>Figure 13 The topology of the Tilos power system and its graph representation.....</i>	<i>34</i>
<i>Figure 14 The results of the deterministic risk assessment analysis for the Tilos island</i>	<i>35</i>
<i>Figure 15 Considered case study with eight locations and interconnections.....</i>	<i>37</i>
<i>Figure 16 Installed production capacities for different locations and scenarios</i>	<i>37</i>
<i>Figure 17 Installed storage technologies for different scenarios and locations.....</i>	<i>38</i>
<i>Figure 18 Total costs for different analysed scenarios.....</i>	<i>39</i>
<i>Figure 19 Transport sector operation for S3 and S5 scenarios.....</i>	<i>39</i>
<i>Figure 20 Battery system operation for S3 and S5 scenarios</i>	<i>40</i>
<i>Figure 21 Battery storage operation for X1 and X2 locations and S3 and S4 scenarios</i>	<i>41</i>
<i>Figure 22 Voltage values for nodes in the power system for minimum demand case</i>	<i>42</i>
<i>Figure 23 The topology of the observed distribution system – red line represents a transmission 110 kV line to Krk island, black lines are the distribution lines and black nodes are the distribution transformers 10(20)/0.4 kV</i>	<i>43</i>
<i>Figure 24 Operation cost reduction for different scenarios in comparison to the base case scenario</i>	<i>44</i>
<i>Figure 25 The voltage magnitude at node 10 for different electricity price values for Scenario C (a) and Scenario D (b).....</i>	<i>45</i>
<i>Figure 26 Available and activated demand response for the different price scenarios.....</i>	<i>46</i>
<i>Figure 27 The operation cost for different incentives and available flexible load values.....</i>	<i>47</i>
<i>Figure 28 Provided demand response (a) and the percentage of used demand response (b) for different incentive and flexibility values.....</i>	<i>48</i>
<i>Figure 29 Dual variable of the power balance constraint for energy only and joint energy and reserve market</i>	<i>51</i>
<i>Figure 30 Revenues for the demand response providers and energy storage systems for different RES shares and conservativeness factors.....</i>	<i>52</i>

<i>Figure 31 Energy storage operation for two nodes in energy only and joint energy and reserve markets</i>	<i>53</i>
<i>Figure 32 Battery storage operation in node 1 for minimum (a) and maximum (b) VRES share where SOC is measured in MWh and other parameters in MW</i>	<i>53</i>
<i>Figure 33 Modelled power system for the maritime transport electrification analysis.....</i>	<i>55</i>
<i>Figure 34 Maximum demand: Charging schedule for Krk and Kornati electric ships for different RES shares</i>	<i>56</i>
<i>Figure 35 Maximum demand: State of the charge of the Krk and Kornati for different RES shares</i>	<i>56</i>
<i>Figure 36 Minimum demand: Charging schedule for Krk and Kornati electric ships for different RES shares</i>	<i>57</i>
<i>Figure 37 Minimum demand: State of the charge of the Krk and Kornati for different RES shares</i>	<i>57</i>
<i>Figure 38 Voltage magnitude at node 4 for different scenarios and RES shares</i>	<i>58</i>

LIST OF TABLES

<i>Table 1 Results of the case study for the Vis island with and without the interconnection</i>	<i>30</i>
<i>Table 2 Analysed scenarios for the Tilos island</i>	<i>35</i>
<i>Table 3 Curtailed energy in the energy system for different scenarios and RES shares</i>	<i>58</i>

1 INTRODUCTION

This chapter presents the background and motivation for the work. The background provides a brief summary of relevant policy and historical events that lead to the current energy transition and the role of islands in the energy transition position. The motivation presents relevant references and summarizes the current state-of-the-art in energy system research on islands as well as briefly states the advantages and contributions of this thesis. Finally, Introduction ends with the research objectives and scientific contributions.

1.1. Background

1.1.1. Global perspective

Modern science is clear and compelling: Human activity is causing global climate changes [1]. Environmental issues have moved to the top of the global agenda and, depending on how well the nations address these issues, they will have a significant impact, for good or ill, on the people around the world. Although the first conference that underlined the environment as a major global issue was held back in 1972 in Stockholm [2], a more decisive action took place in Rio de Janeiro twenty years later [3]. In that conference held in 1992, the concept of sustainable development was recognized as an adequate global concept suitable for all nations and all levels, from local to international. A simple proposition of that conference was that today's progress should not be realized at tomorrow's expense. This means that the economic growth and the energy that drives it must be based on advanced and renewable technologies. By combining new technology with increased energy efficiency and productivity it is possible to turn the facing issues into new opportunities.

The resolutions from these and other conferences up to the last one in Stockholm in 2022 identify greenhouse gas (GHG) emissions as the main cause of global warming and suggest different actions for their reduction [4]. The GHG emissions and their effect have extensively been a topic of scientific research over the years [5] and the consensus reached was that a global temperature rise beyond 2 °C would cause irreversible climate changes [6]. This fact makes global warming and climate change one of the most important issues in history that requires immediate and efficient global action.

The nation's efforts to tackle this challenge cumulated in 2015 in Paris at the 21st Conference of the Parties (COP 21) where nations legally obliged to the framework that aims to avoid a 2°C global temperature limit by signing the Paris Agreement [7]. The researchers widely agree that the objectives set by the Paris Agreement can be achieved only by decarbonising the energy system by large-scale penetration of renewable energy sources (RES) and deployment of cross-sector technologies that result in a highly interconnected smart energy system [8], [9], [10]. Nevertheless, the actions to meet the ambitious objectives are not sufficient as shown in **Figure 1** [11], which means that more effort has to be taken in order to increase RES integration and advanced technology implementation in order to decarbonise the energy system.

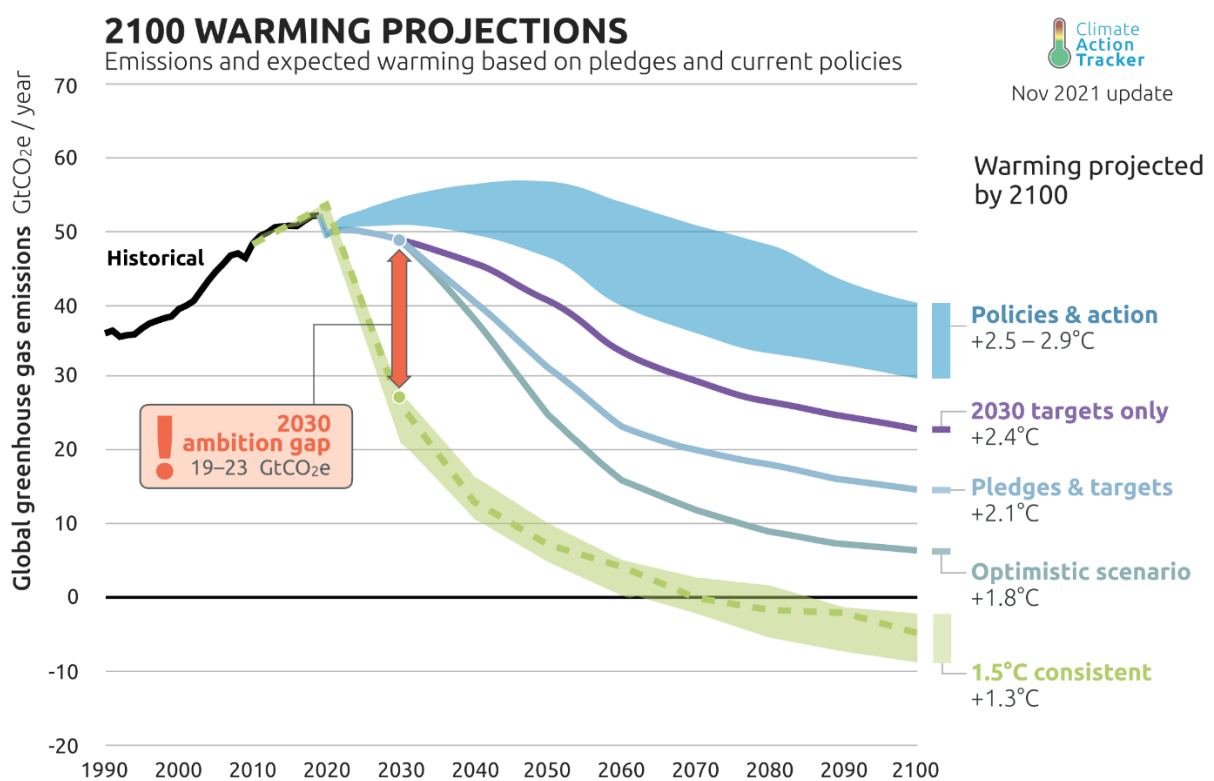


Figure 1 Credibility gap between targets in 2030 and net zero targets for 2050 or later [11]

1.1.2. EU energy transition policy

By setting so-called 20-20-20 climate targets in The 2020 Climate & Energy Package [12], European Union (EU) has set obligatory objectives for its member states for tackling climate change and global warming. The package provided the set of laws to tackle climate change in three directions: 20% GHG emissions reduction in comparison to 1990 levels, 20% of EU

energy produced from RES, and a 20% increase in energy efficiency. According to the European Environment Agency (EEA), these objectives were fully achieved [13]. The EEA estimated that the GHG emissions were reduced by 31% (in comparison to 1990 levels) and that 21.3% of energy consumption was from RES. The objectives were met by 21 member states, while other member states have to use other mechanisms (e.g. buying emission quotas) to meet their obligations.

Recently, a more ambitious plan called The European Green Deal [14] was set out by the European Commission aiming at 55% GHG emission reduction, which will lead to EU climate neutrality in 2050. The plan was further supported by the Sustainable Europe Investment Plan [15] aiming to provide the framework for the financing of The European Green Deal. All EU member states have to comply with these goals and have to develop their National Energy Climate Plans (NECPs) to set out a strategy for meeting these objectives. Furthermore, EU efforts to decarbonise the energy system and reduce its dependence on fossil fuel imports in the EU have increased with the recent REpowerEU plan [16] launched as a response to the recent energy market disturbance caused by the war between Russia and Ukraine.

1.1.3. EU policy on islands

In addition to the general policy and targets regarding the energy transition, the EU has recognised the importance of more specific areas that can contribute to the energy transition. One such area is the EU islands. The EU formalized its intentions to decarbonise the EU islands with the Clean energy for EU islands initiative [17] and established the Clean energy for EU islands secretariat in 2018. The objective of the established secretariat is to implement the targets of the Clean energy for EU islands initiative. They also support the implementation of the long-term support to EU islands in their decarbonisation by ensuring that the Memorandum of Split [18] from 2020 is implemented.

Another important initiative was the Smart Islands Initiative [19] which summarized its ambitions in the document Smart Islands Declaration. The Initiative is a bottom-up approach to make islands smart, green and inclusive through ten action points that promote the digitalization and RES penetration on islands. The Declaration recognised the benefits of islands as Living Labs, a concept that aims to identify the needs of the citizens and engage them early in the transition process (the concept is explained in more detail in [20]). Furthermore, this concept enables the testing of the new technologies that engage citizens, thus creating effective pilots

on the islands (e.g. in the Kvarner archipelago [21] or Samsø [22]). This means that the new, smart and green technologies (e.g. [23]) are implemented on the islands and, after a successful demonstration, replicated and scaled to the mainland. Such a concept adds significantly to the importance of the islands as stakeholders in the energy transition and promotes the islands as the leaders of the EU energy transition process. In this context, this thesis focuses on the small islands and their possibilities for policies and market contributions and not on the larger islands and their contributions as in [24].

1.2. Motivation

The motivation for the research work presented in this thesis was based on two key points. Firstly, the energy system is currently going through significant changes. Besides the increased RES penetration and the decentralisation of the power system [25], the power system is increasingly merging with other sectors such as transport, water or thermal system and forming smart energy systems [26], [27]. Such transformation requires the application of new approaches and techniques by energy planners in order to evaluate and adjust the models to have appropriate tools for decision-making. Accurate models will lead toward low-cost energy systems which will be the basis of global economic growth and sustainability [28].

Secondly, the need for the energy transition of islands and their role in the EU energy transition has to be evaluated [29], [30], [31]. Since the islands are one of the most vulnerable groups that are affected by climate change [32], their role and motivation in the energy transition process are even more enhanced. More challenging conditions on the islands such as a weaker grid, more expensive goods and fuels [33], and overall more difficult achievement of energy access [34] make the energy transition of the islands relevant for both, the islanders which will have a direct benefit of the energy transition and the mainland stakeholders which will be able to learn from the good islands practices. The case for the energy transition of islands is even stronger considering many co-benefits (increased income, job creation and others) that are generated by the transition [35].

Duić et al [36] suggested that islands should meet their local needs with local resources and developed a RenewIslands method that supports islands in their energy transition. RenewIslands method included electricity, thermal, transport, water, waste and wastewater sectors making it suitable for recognising the potential flow integration of different sectors.

Krajačić et al [37] later used the RenewIslands method for evaluating the hydrogen as an energy vector on the islands. The method was further used in [38] as a part of a superstructure-based optimization. The method was also used in some of the research conducted in the scope of this thesis as a basis for island energy planning. However, although detailed and comprehensive, the RenewIslands is based on the qualitative indicators and is subjugated to the subjective opinions of the experts. This lead toward different interpretation of authors for the same island (e.g. Mljet grid connection is mapped as strong in [36], while in it is mapped as medium in [39]).

Renewable energy systems have been examined in numerous research as evident from the latest review [40]. According to the review, the first research on renewable energy systems was conducted by Duić in [41] where the authors presented the case for a 100% renewable island of Porto Santo. Following this study, a total of 97 research articles on 100% renewable energy systems on islands were published (until March 2022). This indicates the importance of the islands as a research field for renewable energy systems, however, due to the technology, market and policy developments in the past 20 years, it is necessary to develop new advanced energy planning approaches for the islands.

Over the course of years, authors developed and applied different strategies and tools for the analysis of energy systems on islands. H2RES [42] was used in the first study that focused on the renewable energy system planning on islands [41] and was also used for the analysis of hydrogen integration in the renewable energy systems on islands [43], [44], [45]. H2RES was also compared to another tool - EnergyPLAN [46] in [47]. The latest, EnergyPLAN tool, was also extensively used for the energy system analysis on the islands (e.g. in [48] for energy system planning of Wang-An island, in [49] for the Sardinia island or for Galapagos islands in [50]). The full review of the application of the EnergyPLAN is conducted in [51]. Other tools used for energy planning of islands include HOMER software [52] that was used for the feasibility assessment of RES integration of Popova Island [53], for the planning of the Favignana island [54] where authors aimed to exploit the synergies between HOMER and EnergyPLAN tool as well as for energy planning of hybrid energy system on St. Martin island [55]. TIMES model [56] was also used in several studies regarding island energy systems planning as in [57] where it was coupled with the EnergyPLAN tool for the case study of the Norwegian island Hinnøya. However, the research regarding more detailed modelling with emphasis on the spatio-temporal resolution should be further investigated.

Presented tools use indicators as a simplified method for the representation of certain constraints (e.g. power grid representation and limitations), while other authors apply different unit commitment (UC) models that deploy a direct approach to modelling such constraints. Dominković et al. [58] used PLEXOS for the planning of Caribbean islands and Barone et al. [59] used TRANSYS for the development of a new dynamic simulation model applied on El Hierro island for the creation of self-sufficient island communities. A mathematical UC model was developed in [60] for designing a hybrid system on Astypalaia Island based on the concentrating solar power connected to the desalination plant. Another energy system model that included the vehicle-to-grid (V2G) technology was presented in [61] where the authors analysed the possibility of electric vehicles (EVs) providing ancillary services to the power system. Although they provide a possibility to directly represent previously mentioned energy system constraints, the UC models are also more computationally complex. Thus, the challenge in energy system planning on the islands is in finding the optimal trade-off between the model complexity and desired outcome precision [62]. Although many tools and methods were applied to the island energy systems, there is no objective method that designs scenarios that meet local needs with resources.

In the research of the energy systems on the island pumped hydropower plants (PHP) were an important factor for maintaining the stability of the power system. PHPs were considered in numerous studies such as in [63] for El Hierro island, in [64] for the Canary islands or [65] for Sifnos island. However, with the development of the information and communication technologies (ICT) and the energy storage systems authors are proposing additional flexibility sources as well as production units. Groppi et al. [66] conducted a review on the more advanced technology such as energy storage and the demand response in island energy systems. The inclusion of such technologies helps create smart energy systems on islands, which is important not only from the technical aspect (e.g. for synthetic inertia and grid stability improvements on small islands as in [67]), but for citizen engagement as well. Historically, citizen engagement has always been high on islands, making them a suitable candidate for testing new technologies and frameworks that include the citizens in the energy transition [68].

The authors in [69] considered the biogas production on the island of Procida and analysed its energy, environmental and cost impacts when biogas is utilized in the residential and transport sector. Advanced RES technologies were considered in [70] where the authors presented a case for the integration of tidal energy into the island energy system. They concluded that the

inclusion of tidal energy can increase system efficiency by 42.5%, however, they also indicated the need for a detailed economic evaluation as the technology is highly dependent on the site and device specifications. Blue Energy was also considered with its potential in the Mediterranean being explored in [71] and with the offshore wind being integrated into the energy system of Crete in [72]. The analysis of the DR potential from the hotels for Canary islands was investigated in [73]. The options for islands power supply supported by the electric and hydrogen storage systems was investigated in [74]. Many different technologies were modelled and integrated into the island energy systems, however the impact of advanced technologies for different energy planning approaches should further be investigated. For example, how would the energy system cost and operation change if more detailed spatial models are used or if ancillary services were considered as well in the models?

The research regarding the maritime electrification and its integration with the island energy systems has also been conducted in the recent years [75]. Norway is perhaps the most advanced country in the maritime electrification and lessons from its maritime electrification process [76] suggests that social acceptance may be an issue because of the high costs of the system. However, benefits of the maritime transportation with regard to the RES integration has been shown on the example of Korčula island [77] and on additional three lines [78]. Current research suggests that the maritime transport electrification is feasible for shorter lines and that the development of the battery technology will lead towards large-scale electrification of maritime transport [79]. However, the impact of the maritime transport electrification on the distribution grids and its connection to the RES penetration should be further investigated.

It is evident that the research of the island energy systems is interesting from various points of view. Although a significant number of research has already been conducted on islands, there is a significant number of findings that still need to be investigated. This thesis offers several contributions to the existing literature. It offers methods that generate renewable scenarios for the energy system on islands; method for risk assessment of the energy planning scenarios; it analyses the impacts of different energy planning approaches on islands; it provides novel models for demand response and energy storage technologies and it evaluates their impact on the island energy system; and it provides a model for the electrification of the maritime transport.

1.3. Objectives and hypothesis of the research

The objectives of this research were to provide models and methods that will enable the representation of the advanced energy planning aspects on the islands. This means that the developed methods have to support and account for the effects of the new emerging technologies such as energy storage, demand response and cross-sector integration as well as market frameworks that will support the successful integration of advanced technology into high RES energy systems on islands. For this purpose, this research developed: an indexing model for assessing the degree of development of an island that can serve as a basis for strategic planning of island development with particular reference to the energy system; a comprehensive Smart Islands method for calculating energy planning scenarios with particular emphasis on integrating different flows to achieve synergy with the other sectors; a method for risk assessment of individual energy scenarios by taking into account the probability of failure of elements of the power system and the potential damage resulting from the failure. The hypothesis of this research is that using the Smart Islands method and the energy systems risk assessment method, it can be shown that the transformation of energy systems on islands to fully renewable systems is possible with a precisely defined amount and type of technology required and with a quantified level of risk for each energy planning scenario.

1.4. Scientific contributions

This doctoral thesis has several scientific contributions:

- Smart Islands method for developing energy planning scenarios that support strategic decision making and provides the basis for developing energy transition plans for islands
- A risk assessment method for individual energy planning scenarios that will evaluate the impact of energy storage, demand response and other advanced technologies on reducing the risk of changes in operating and topological conditions in the power systems on islands
- A mathematical model of DR that includes final users in the day-ahead electricity market and that reduces the energy system operation cost and contributes to the creation of the smart islands
- A detailed spatio-temporal capacity expansion model soft-linked to the power flow calculation for energy planning of islands

- A joint network constrained energy and reserve market model suitable for assessing the role of DR and energy storage on islands

2 METHODS

This section presents the overview of used methods and tools in this thesis. Research on advanced energy planning approaches presents a challenging topic in the era of digitalization, dramatic transformation and fundamental change of the energy systems. It is not enough to observe the power system alone, the impact of other systems (e.g. thermal, transport, water etc.) has to be accounted for as well. The cross-sector integration aspect is important for two main reasons – it increases social welfare and reduces the overall cost of energy system operation, and it unlocks additional flexibility potentials necessary for increasing the penetration of the variable renewable energy sources.

When considering the advanced energy planning approaches on the islands, one has to include specific islands' features. Since the islands are significantly dependent on the mainland as described in the papers (especially PAPER1 and 2), the energy planning approaches on islands have to differ from the ones on the island. On the islands, it is necessary to consider local resources to meet local needs. Although such an approach may not be the optimal one in the mainland cases, for islands, such an approach can assure self-sustainability and increase their independence from the mainland.

The methods developed and used in this thesis include a wide spectrum of capacity expansion and operation. Depending on the objectives of the research, the developed methods are suitable for the representation of the islands' energy system, its inclusion and its interaction with the surrounding distribution system and transmission system. The input data is based on islands' needs, resources, infrastructure and other islands-specific data which include maritime transportation data, desalination plants etc. The proposed approach is suitable for addressing both technical and financial aspects of specific energy system interventions on islands in various market conditions. The presented approach resulted in six journal papers and six scientific contributions as presented in Figure 2.

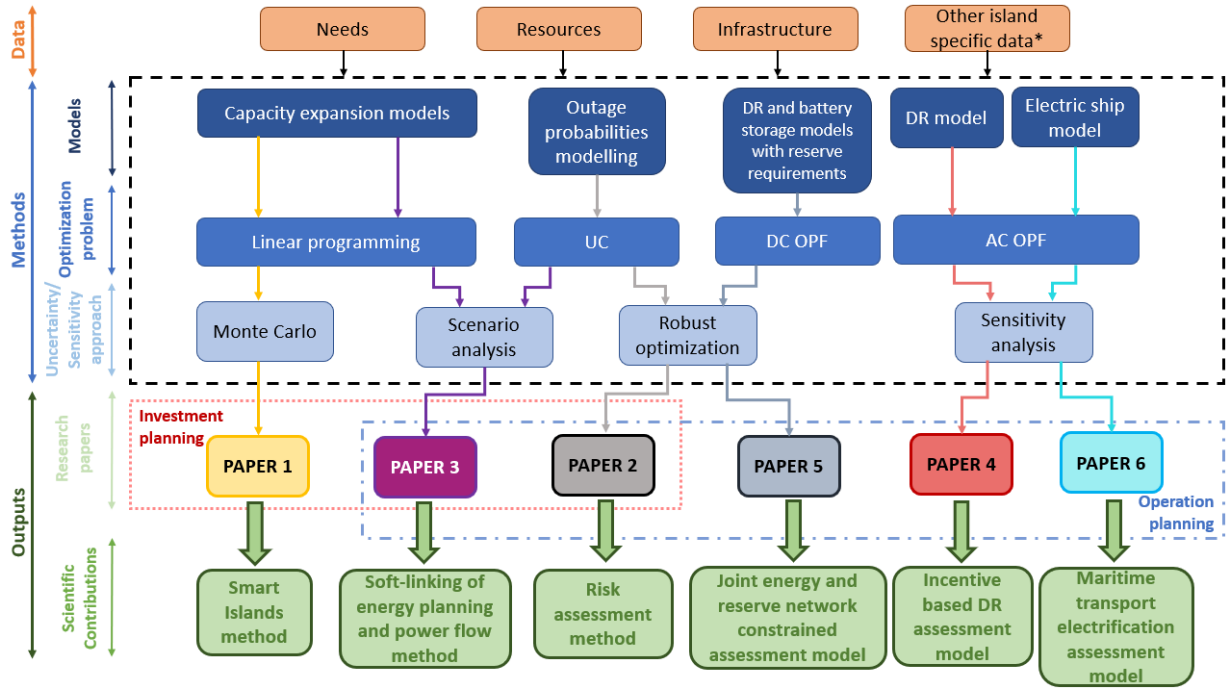


Figure 2 Overview of the used approaches and scientific novelties of the thesis

The overview of the scientific contributions is shown in Figure 3. The table shows which modelling approach was taken in the operational models in terms of the spatio-temporal distribution, what grid aspects were considered, what were considered advanced technologies and what were the implementation tools of the models. It can be seen that all operational models use spatially distributed modelling and almost all use time resolution of less than one hour which is beyond the current state-of-the-art in energy planning where authors based their results on the courser and/or one-hour time resolution modelling. Grid aspects were also largely considered either by considering non-linear or linearized power flow and by considering the reserve requirements as well. Although power flow was not calculated in the risk assessment method, the grid topology was also considered. The advanced technology column represents assets that should be significantly represented in future energy systems. In this sense, the battery storage systems and demand response were largely considered, while hydrogen and biofuel technologies were also included in several models. Finally, Figure 3 shows the tools with which the models were implemented. These include modelling in Python and optimization problem solving using Gurobi [80], GAMS [81] as a mathematical programming tool for solving the optimization problems, Calliope [82] as a tool suitable for detailed spatio-temporal modelling of the energy systems and NEPLAN [83] as tool specialized for performing the power flow calculations.

	Modelling approach		Grid aspects		Considered advanced technology				Implementation tools			
	Spatially distributed	Time resolution <1 hour	Linear or non-linear power flow	Reserve	Battery storage	Demand response	Hydrogen	Biofuels	Python/Gurobi	GAMS	Calliope	NEPLAN
Smart Islands		-										
Risk assessment		0.5h										
Soft-linking of energy planning and power flow		0.5h										
Incentive based DR model assessment												
Joint energy and reserve assessment model		0.25h										
Maritime transport electrification assessment model		0.5h										

Figure 3 Overview of the scientific contributions of the thesis

2.1. Formulation of the optimization problem

At the core of all research conducted in this thesis is the formulation of the optimization problem. All research papers include some type of optimization problem. The optimization problem consists of two main parts – the objective function and constraints. The form of the optimization problem can be written as in [84] (1):

$$\begin{aligned}
 &\text{Minimize } f(x) \\
 &\text{Subject to } g_i(x) \leq b_i, \quad i = 1, \dots, m
 \end{aligned} \tag{1}$$

Where $x = \{x_1, \dots, x_n\}$ are the optimization or the decision variables of the problem, function f is the objective function of the problem and $g_i, i = 1, \dots, m$ are the constraints of the problem. Limits or bounds of the constraints are represented with b_1, \dots, b_m . A vector of decision variables x^* is an optimal solution to the optimization problem if it has the smallest value of the objective function. This means that for any z with $g_1(z) \leq b_1, \dots, g_m(z) \leq b_m$ it is $f(z) \geq f(x^*)$. If the objective function and constraints are linear, the optimization problem can be called a *linear program* (LP). If some of the variables of LP are not continuous (integer or binary values), LP becomes a *mixed-integer linear program* (MILP). LP and MILP are formulated in most of the papers in this thesis. However, a *non-linear program* (NLP) is also

presented in two research papers in this thesis. An NLP has non-linear expressions in the objective function and/or constraints of the problem (e.g. NLP formulated in [85] for deciding on measures to reduce CO₂ emissions). Although the NLP does not guarantee the global optimum of the problem, it can be solved efficiently on relatively small problems as was the case in the two research papers that are presented in this thesis. All of the problems are solved with solvers available in GAMS or Gurobi solver.

2.2. Unit commitment

One of the most widely used formulations for the representation of the power system is the so-called – unit commitment (UC) formulation [86]. UC is usually formulated as a MILP with the objective of minimizing the total operation cost of the system. It aims to represent factors that affect the operation of the system such as generator ramping constraints, fuel cost, emissions, energy import and export, specific operation costs etc. The objective of the UC problem with photovoltaic and wind generation can be formulated as follows (2):

$$\begin{aligned} \min \sum_{t \in \Omega^T} \left(\sum_{g \in \Omega^G} (SU_g \cdot x_{g,t} + SD_g \cdot z_{g,t}) + \sum_{g \in \Omega^G} F_g(p_{g,t}) + VWC \cdot \sum_{w \in \Omega^W} p_{w,t}^{curt} \right. \\ \left. + VPVC \cdot \sum_{pv \in \Omega^{PV}} p_{pv,t}^{curt} + VoLL \cdot LS_t \right) \end{aligned} \quad (2)$$

Where SU_g and SD_g are the start-up and shut-down costs of the thermal units and $x_{g,t}$ and $z_{g,t}$ are the binary variables describing whether a unit is being shut-down or started up. Thermal unit generation is given with $p_{g,t}$, while $p_{w,t}^{curt}$ and $p_{pv,t}^{curt}$ represent the curtailment from the wind and photovoltaic plants respectively. The fuel cost function of the thermal unit is given with $F_g(p_{g,t})$, which is usually a quadratic function. This results in a quadratic mixed integer problem which represents a complex problem to solve. Thus, a linearization of the fuel cost function is applied for lowering the complexity of the problem as described in [87]. Parameters VWC and $VPVC$ are penalties for curtailed values of wind and photovoltaic plants respectively, that represent a compensation for the lost production of the producer. Variable LS_t denotes the load shed at customer nodes, that is the failure to deliver the electricity to the final customer.

The failure to deliver the electricity to the customer is penalized with $VoLL$, or the value of the lost load.

In addition to the objective function, a power balance constraint where all generation has to equal all consumption has to be formulated. Other constraints specific to the operation of different assets can also be included. The constraints for thermal generator output $p_{g,t}$ are presented with (3) and (4) where P_g^{min} and P_g^{max} represent the minimum and maximum possible output from a certain generator and where $u_{g,t}$ represents the binary variable for thermal generator activation. Equation (5) defines the ramping capabilities of the thermal generator according to up RU_g and down RD_g ramping limits.

$$P_g^{min} \cdot u_{g,t} \leq p_{g,t} \leq P_g^{max} \cdot u_{g,t}, \forall g \in \Omega^G, \forall t \in \Omega^T \quad (3)$$

$$p_{g,t} \geq 0, \forall g \in \Omega^G, \forall t \in \Omega^T \quad (4)$$

$$-RD_g \leq p_{g,t} - p_{g,t-1} \leq RU_g, \forall g \in \Omega^G, \forall t \in \Omega^T \quad (5)$$

Usually, an additional set of constraints (6) – (11) is also modelled. Equations (6) and (7) limit that generator is running for the minimum running or up-time UT_g and that is being shut down for the minimum down-time DT_g . Action for the start-up and shut-down of the thermal generators are defined with (8) and (9). Finally, simultaneous start-up and shut-down of the thermal generators are prevented with (10).

$$u_{g,t} - u_{g,t-1} \leq u_{g,k}, \forall g \in \Omega^G, \forall t \in \Omega^T, k = t, \dots, \min\{t + UT_g - 1, |\Omega^T|\} \quad (6)$$

$$u_{g,t-1} - u_{g,t} \leq 1 - u_{g,k}, \forall g \in \Omega^G, \forall t \in \Omega^T, k = t, \dots, \min\{t + DT_g - 1, |\Omega^T|\} \quad (7)$$

$$x_{g,t} \geq u_{g,t} - u_{g,t-1}, \forall g \in \Omega^G, \forall t \in \Omega^T \quad (8)$$

$$z_{g,t} \geq u_{g,t-1} - u_{g,t}, \forall g \in \Omega^G, \forall t \in \Omega^T \quad (9)$$

$$x_{g,t} + z_{g,t} \leq 1, \forall g \in \Omega^G, \forall t \in \Omega^T \quad (10)$$

$$x_{g,t}, z_{g,t}, u_{g,t} \in \{0,1\}, \forall g \in \Omega^G, \forall t \in \Omega^T \quad (11)$$

The deterministic representation of the RES production is given with (12) where Λ_t^{RES} presents the total potential production from RES (e.g. calculated based on wind or solar potential), p_t^{RES}

presents the actual RES production and $p_t^{RES,crut}$ presents the curtailed RES values. Curtailed RES values are usually penalized in the objective function of the UC problem to compensate for the producers' loss.

$$p_t^{RES} + p_t^{RES,crut} = \Lambda_t^{RES}, \quad \forall t \in \Omega^T \quad (12)$$

A standard model of the ESS is provided with equations (13) – (16). It includes state of charge SOC_t of the ESS, charging $p_{c,t}$ and discharging $p_{d,t}$ of the ESS and parameters of ESS charging and discharging efficiency (η_c, η_d), minimum and maximum SOC (SOC^{min}, SOC^{max}) and minimum and maximum charging and discharging values ($P^{c,max}, P^{d,max}$). Binary variable μ_t is used to prevent the simultaneous charging and discharging of the ESS. Recently, more advanced models that linearize the battery charging depending on the current SOC of the ESS have been proposed [88]. However, in this thesis, a limitation is placed on the minimum and maximum SOC so that different charging speeds at very high and very low SOC would not be part of the model (this is justified as it also slows down the battery degradation).

$$SOC_t = SOC_{t-1} + (p_{c,t} \cdot \eta_c - \frac{p_{d,t}}{\eta_d}) \cdot \Delta t, \quad \forall t \in \Omega^T \quad (13)$$

$$SOC^{min} \leq SOC_t \leq SOC^{max}, \quad \forall t \in \Omega^T \quad (14)$$

$$p_{c,t} \cdot \Delta t \leq P^{c,max} \cdot \mu_t, \quad \forall t \in \Omega^T \quad (15)$$

$$p_{d,t} \cdot \Delta t \leq P^{d,max} \cdot (1 - \mu_t), \quad \forall t \in \Omega^T \quad (16)$$

The DR models have also been introduced several times in the research in this thesis, however, they differentiate depending on the type of flexible load considered and on the final objective of models in the research papers of this thesis. Some of the models are presented in this chapter and detailed descriptions of DR models can be found in the research papers in the annexe of this thesis.

2.2.1. Transmission system approximation model

In order to represent the transmission system, the UC is upgraded so that it represents nodes and connections between them. In the literature, this is often referred to as a DC power flow

[89]. In such a model, active power flows are modelled and the power flow p_{ij} between the two nodes i and j is represented with (17).

$$p_{ij} = -p_{ji} = \frac{\delta_i - \delta_j}{x_{ij}} \quad (17)$$

Voltage angle at node i is denoted with δ_i and the reactance (imaginary part of the impedance) between the two nodes i and j is represented with x_{ij} . As can be seen from the equation (17), this model assumes that there are no power losses or $p_{ij} = -p_{ji}$. For the presented model of the power system, the power balance has to be defined for every node i . However, this model presents a linearisation of a more complex problem – AC power flow. Thus, the model has several assumptions:

- The reactance x_{ij} between the two nodes is significantly higher than the resistance r_{ij} , thus it is assumed $r_{ij} \approx 0$.
- The voltage magnitude at each node i is equal to the nominal voltage magnitude
- The voltage angle difference $\delta_i - \delta_j$ is sufficiently small so that it is possible to write $\cos(\delta_i - \delta_j) \approx 1$ and $\sin(\delta_i - \delta_j) \approx [\delta_i - \delta_j]$

2.2.2. Distribution system representation

The previously defined model is suitable for high voltage grids where it can be assumed that the reactive power flows are balanced and the voltage magnitude at each node is nominal. However, the nodes in the distribution system mostly have only loads, thus they do not have the regulation possibilities. Additionally, the physical characteristics of the distribution system are different in comparison to the transmission system. Thus, the power flow equations for the distribution system are written in their non-linear form – AC power flow (a more detailed comparison between the two models is provided in [90]).

Because such formulation is non-linear, the solution to this problem does not guarantee the global optimum. Although there are other linearization techniques, the research in this thesis solved AC power flow in its original form by using non-linear solvers in the GAMS tool. Another example of the non-linear formulation can be found in [91], where the authors verified their findings in Matpower [92].

2.3. The Smart Islands method

The Smart Islands method builds on the existing RenewIslands method. Firstly, it introduces the indexing model which enables the mapping of the island. As in the RenewIslands method, the mapping model includes islands' needs, resources, infrastructure and water, however, in Smart Islands, the indicators are quantified and expanded. A full list of the indicators can be found in PAPER 1. Secondly, the algorithm was developed in Python language that loads the indicators from the indexing model as input data. Based on the indicators, the algorithm matches islands' resources with needs. After the matching, the algorithm generates a list of the possible technologies for meeting the needs with local resources for electricity, heating, cooling, transport, waste, wastewater and water sectors. Finally, the selected technologies enter the optimization algorithm that selects optimal capacities of the technologies and generates possible energy planning scenarios for the analysed islands. The graphical representation of the Smart Islands method is provided in Figure 4, while more detailed explanations can be found in PAPER 1.

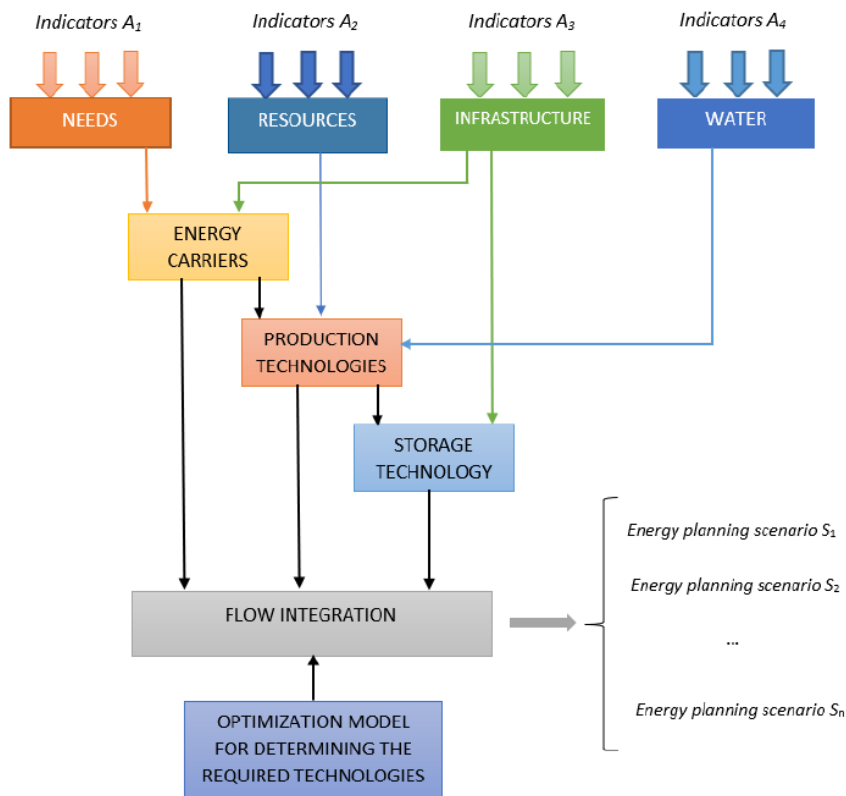


Figure 4 Overview of the Smart Islands method

2.4. Risk assessment method of the energy planning scenarios on islands

In order to quantify the risk of a particular island energy planning scenario, a risk assessment method was developed and presented in PAPER 2. In this context, the risk is referred to as the risk of supply loss, as the stable electric energy supply is one of the key drivers of the development of islands. In order to calculate the risk, it is first necessary to form an undirected graph $G = (N, \mathcal{E}, A)$ where $N = \{n_1, \dots, n_n\}$ is a set of nodes of the island power system, $\mathcal{E} \subseteq N \times N$ is a set of links or edges and where A is a matrix of ratios of an event occurring obtained by the historical data. The set of undirected edges has a cardinality $|\mathcal{E}|$. By using Poisson distribution and matrix A , it is possible to generate a vector of probabilities $\theta = [\vartheta_1, \dots, \vartheta_{|\mathcal{E}|}]$, where $\vartheta_m \in \langle 0, 1 \rangle$ and $m = 1, 2, \dots, |\mathcal{E}|$ that describes the outage probability of island power system elements.

After calculating the outage probability vector it is necessary to calculate the damage caused by each outage. For this purpose, a previously defined UC problem is formulated and each outage from the set of outages $V = \{v_1, \dots, v_{|\mathcal{E}|}\}$ is applied to power system elements. The optimization problem is solved for every outage and the damage matrix can be formed based on the solutions of the optimization problem. If $S = \{S_1, \dots, S_Y\}$ is a set of energy planning scenarios, the damage matrix can be written as $\mathcal{D} \in \mathbb{R}^{|\mathcal{E}| \times Y}$. Multiplication of the damage matrix and the outage probability vector generate the risk vector as presented in Figure 5.

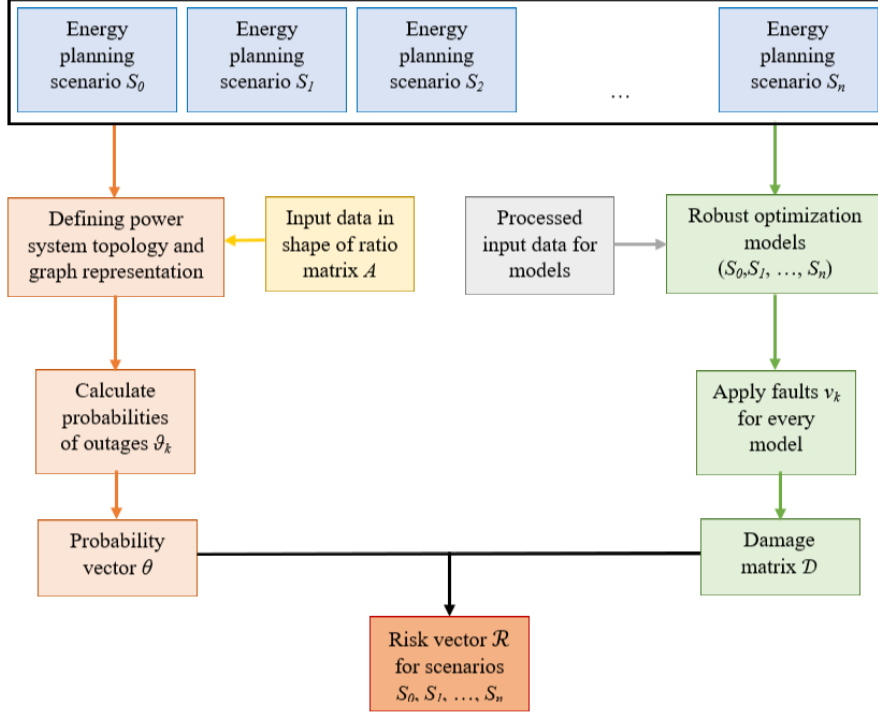


Figure 5 Risk assessment method for the energy planning scenarios on islands

Finally, risk vector $\mathcal{R} \in \mathbb{R}^{1 \times Y}$ presents the risk of each energy planning scenario for the island and can be defined as follows (18):

$$\begin{bmatrix} \vartheta_1 \\ \vartheta_2 \\ \vdots \\ \vartheta_m \end{bmatrix}^T \cdot \begin{bmatrix} \mathcal{D}_{11} & \dots & \mathcal{D}_{1Y} \\ \vdots & \ddots & \vdots \\ \mathcal{D}_{|\mathcal{E}|1} & \dots & \mathcal{D}_{|\mathcal{E}|Y} \end{bmatrix} = \begin{bmatrix} \mathcal{R}_1 \\ \mathcal{R}_2 \\ \vdots \\ \mathcal{R}_Y \end{bmatrix}^T \quad (18)$$

2.5. Advanced capacity expansion energy planning model soft-linked with the power flow

The novel approach presented in PAPER 3 provided a framework for energy system analysis on the islands. The open-source Calliope modelling framework [93] is used for energy system modelling and it enables the modelling on a detailed spatio-temporal resolution. The objective of the defined linear continuous optimization problem was the minimization of the socio-economic cost of the observed system. In addition to the installation, fixed and variable O&M costs, the objective function also considered the EU Emissions Trading System (ETS) which was used to account for CO₂ emissions cost. Although the ETS price was already included in the clearing price of the day-ahead electricity market, the future higher prices on ETS were also

considered and included as a fixed carbon tax by deducting the ETS price for the referent year from the projected ETS price in 2030. The model is suitable for half-hourly input data and it included electricity, transport, heating and cooling sector. The solution of the solved problem included capacity expansion results as well as the operational aspects of the observed system. A detailed description of the Calliope modelling framework can be found in [94].

The described framework was soft-linked with the power flow. The power flow is a well-known calculation that is used for grid analyses and that provides application possibilities insights for particular energy planning scenarios. In this research, it was solved using the Newton-Raphson algorithm [95] included in NEPLAN software [83]. The term soft-linking refers to running the models one after another, and not in parallel which would be the case in hard linking that would result in one complex model. The soft-linking approach significantly reduced the complexity of the problem, which would otherwise be extremely complex due to the very high number of variables and because of the non-linear expressions in the power flow. The proposed soft-linking approach developed in this thesis is presented in Figure 6.

Finally, a more detailed socio-economic analysis was performed by including the job creation analysis. The objective of this analysis is to provide insight into the energy transition impact on the local island economy. For this purpose, the impact of different technologies on job creation was considered as in [96]. However, when considering the island communities the important difference is that only O&M jobs contribute to the local economic development, while other jobs regarding R&D are usually connected to the mainland.

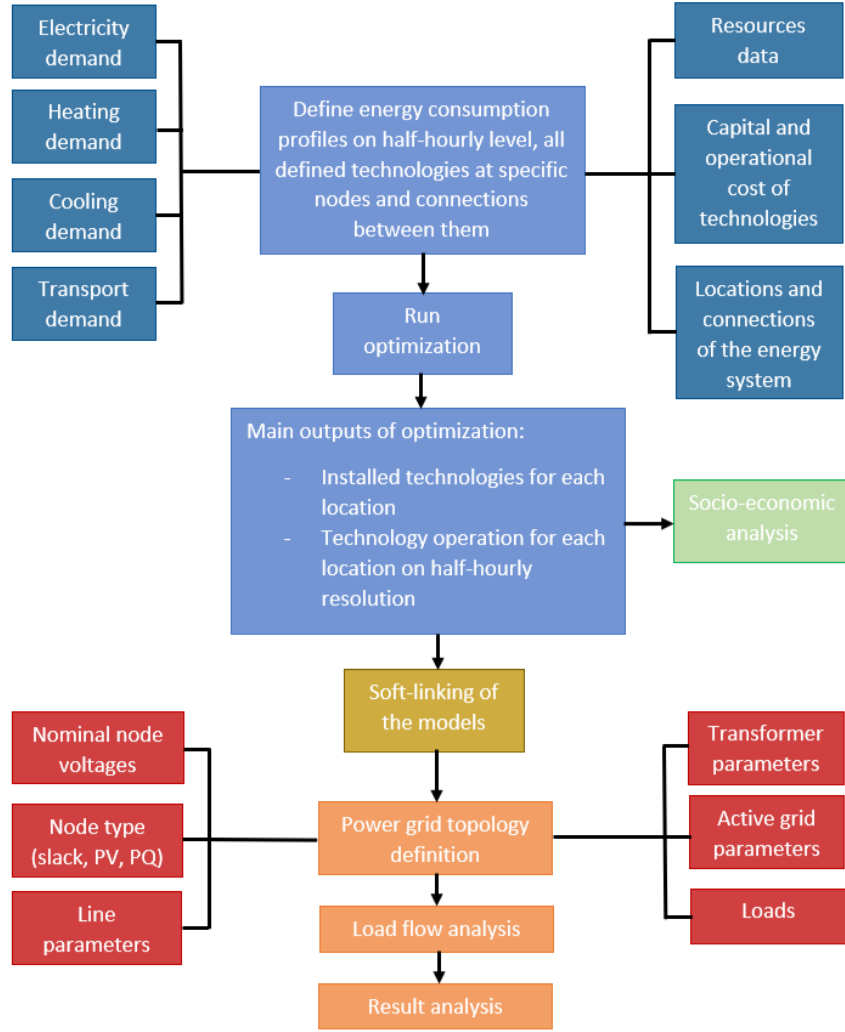


Figure 6 Proposed soft-linking method of the energy planning and power flow models

2.6. Demand response model

The DR represent one of the important aspects of smart energy systems. It provides additional flexibility in the system which can lower the operation cost of the system, generate additional revenue streams for the DR providers and increase the possibility for RES integration. However, various DR models can have different impacts on the energy system operation. The DR model based on the fluctuations in the day-ahead electricity market is presented with equations (19)-(21). The DR model is integrated into network constrained distribution system model previously described and applied to the distribution grid model of the Kvarner archipelago. The price of electric energy on the day-ahead market is denoted with λ_t and the higher difference between the consecutive prices on the market will result in a higher possibility

for the DR. The model is also considered as a price-taker model, meaning it does not influence the settlement price on the day-ahead electricity market.

$$\varphi_{i,t}^- \begin{cases} \leq \tanh \frac{2(\lambda_t - \lambda_{t-1})}{k(\lambda_t + \lambda_{t-1})}, \lambda_t - \lambda_{t-1} > 0 \\ = 0, \text{ else} \end{cases} \quad (19)$$

$$\varphi_{i,t}^+ \begin{cases} \leq \tanh \frac{2(\lambda_{t-1} - \lambda_t)}{k(\lambda_t + \lambda_{t-1})}, \lambda_t - \lambda_{t-1} \leq 0 \\ = 0, \text{ else} \end{cases} \quad (20)$$

$$\sum_t^T \varphi_{i,t}^+ \cdot L_{i,t}^P = \vartheta \sum_t^T \varphi_{i,t}^- \cdot L_{i,t}^P \quad (21)$$

The expressions define the DR coefficient $\varphi_{i,t}^- \in [0,1]$ and the DR retrieval coefficient $\varphi_{i,t}^+ \in [0,1]$. Sensitivity factor $k \in [0,1]$ is introduced in order to represent the technical possibility for the DR provision. Factor ϑ in equation () describes the DR efficiency where $\vartheta = 1$ means that all reduced demand has to be retrieved and $\vartheta = 0$ means that no demand has to be retrieved (e.g. if the flexible load are lights). In case the flexible load is thermal load factor ϑ can even be higher than 1. Finally, a hyperbolic tangent function $\tanh(x): \mathbb{R} \rightarrow [-1,1]$ is introduced because of its characteristics:

- The function is symmetrical $\tanh(-x) = -\tanh(x)$ which makes it suitable for DR as well as for DR retrieval
- The Taylor series of this hyperbolic tangent is $\tanh(x) \approx x - \frac{x^3}{3} + \frac{2x^5}{15} - \dots$ which means that for small x values, the function is approximately linearized which means that we can write $\tanh \left[\frac{2(\lambda_t - \lambda_{t-1})}{k(\lambda_t + \lambda_{t-1})} \right] \approx \left[\frac{2(\lambda_t - \lambda_{t-1})}{k(\lambda_t + \lambda_{t-1})} \right]$, thus the price differentials are approximately linearized around small x values
- Finally, the limes of the function are $\lim_{x \rightarrow -\infty} (\tanh(x)) = -1$ and $\lim_{x \rightarrow \infty} (\tanh(x)) = 1$ which prevents the DR value to exceed the total flexible demand value as well as limits very high changes in the price to cause significant and sudden operation changes which may cause grid issues.

The DR model is included in the active and reactive power balance constraints detaillly presented in PAPER 4. Additionally, the model includes incentive value μ in the objective function of the problem for rewarding the DR providers. This feature allows the possibility to investigate the impact of different incentive values on the operation of the system for different

RES shares. It also enables the possibility to calculate the breakpoint incentive or the highest incentive value after which the DR is not used in the problem. Although the model has several limitations (e.g. difficult application possibility), it is suitable and intended for the investigation of financial and technical repercussions on the energy system as a result of the DR model inclusion.

2.7. Demand response and energy storage in joint energy and reserve markets

The power system represents a complex structure with many different stakeholders and with many required energy and ancillary services needed. Energy system models should reflect on all of these aspects in order to evaluate the feasibility and business models of different technologies. As more revenue streams are available for particular technology its business case is stronger. This is particularly important for the new technologies entering the market such as DR, ESS and technologies that enable cross-sector integration. The joint network constrained energy and reserve UC model is suitable for evaluating the role of different technologies participating in the joint energy and reserve market. Such formulation is detailly described in PAPER 5 where upgraded models for ESS and DR were presented. The new constraints for the ESS included new variables for the reserve provision are given with (22) – (25).

$$r_{i,t}^{d,UP} \leq \frac{SOC_i^{max} - soc_{i,t-1}}{\Delta t} - \frac{p_{i,t}^d}{\eta_i^d} \quad (22)$$

$$r_{i,t}^{c,DO} \leq \frac{soc_{i,t-1} - SOC_i^{min}}{\Delta t} - \eta_i^c \cdot p_{i,t}^c \quad (23)$$

$$r_{i,t}^{d,UP} \leq P_i^{d-MAX} \quad (24)$$

$$r_{i,t}^{c,DO} \leq P_i^{c-MAX} \quad (25)$$

Variables $r_{i,t}^{d,UP}$ and $r_{i,t}^{c,DO}$ denote the reserve allocation variables by the ESS. The reserve provided by the ESS at period t must be lower than the available battery capacity at time $t - 1$ reduced for discharge (or charge) values at the period t . Additionally, the reserve variables cannot be higher than the maximum charging and discharging values because the ESS must be able to activate the reserve in the case of necessity. Similar constraints were included for DR and DR retrieval (26) and (27):

$$r_{i,t}^{drr,UP} \leq DRR_{i,t}^{max} - p_{i,t}^{drr} \quad (26)$$

$$r_{i,t}^{dr,DO} \leq DR_{i,t}^{max} - p_{i,t}^{dr} \quad (27)$$

Variables $r_{i,t}^{dr,UP}$ and $r_{i,t}^{dr,DO}$ denote the up and down reserve values provided by the flexible loads. These values cannot exceed the difference between the maximum flexible load availability and the activated flexible load. From the presented formulation included in the joint energy and reserve model, it is clear that reserve values can impact also other operation parameters, thus the modelled system operation will differ in comparison to models that include only the energy market. Such a comparison was also conducted and presented in PAPER 5. Finally, in order to calculate revenue streams equations (28) and (29) were also presented. They include the revenues for the ESS and DR on both – the energy and reserve markets. The revenue on the energy market was calculated as the difference between the discharged (or saved energy for flexible loads) and charged or (increased consumption by the flexible loads) multiplied with the dual variable $\lambda_{i,t}$ of the power balance equation. Revenues from the reserve allocation were added to these values and calculated as allocated up and down reserve multiplied with dual variables of up $\mu_{i,t}^{UP}$ and down $\mu_{i,t}^{DO}$ reserve balance equations respectively.

$$R_i^{ESS} = \sum_{t \in \mathcal{T}} \Delta t \cdot [\lambda_{i,t}(p_{i,t}^d - p_{i,t}^c) + \mu_{i,t}^{UP} \cdot r_{i,t}^{d,UP} + \mu_{i,t}^{DO} \cdot r_{i,t}^{c,DO}] \quad (28)$$

$$R_i^{DR} = \sum_{t \in \mathcal{T}} \Delta t \cdot [\lambda_{i,t}(p_{i,t}^{dr} - p_{i,t}^{drr}) + \mu_{i,t}^{UP} \cdot r_{i,t}^{drr,UP} + \mu_{i,t}^{DO} \cdot r_{i,t}^{dr,DO}] \quad (29)$$

Presented models are intended for the evaluation of the DR and ESS participation in various energy services provisions. The models represent general expressions for DR and ESS and can further be enhanced by the inclusion of additional variables for the representation of various flexibility options (e.g. Power-to-X technologies, V2G and other cross-sector integration technologies).

2.8. Maritime transport electrification model

Maritime transport represents a vital issue for the islanders and its decarbonisation is necessary in order for any island to be a carbon-neutral island. For the purpose of maritime electrification and its integration with the rest of the energy system, a mathematical model of an electric ship was developed (30) – (32).

$$\psi_{f,t} = \begin{cases} (1 - \tau_f) \psi_{f,t-1}, & x_{f,t} = 0 \\ \psi_{f,t-1} + q_{i,t}^c \mu_{i,f}^c \Delta t, & x_{f,t} = 1 \\ \psi_{f,t-1} - E_{f,k}^d, & x_{f,t} = 2 \end{cases} \quad (30)$$

$$q_{i,t}^c \begin{cases} \leq Q_i^{c,max}, & x_{f,t} = 1 \\ = 0, & else \end{cases} \quad (31)$$

$$\alpha_f \psi_f^{max} \leq \psi_{f,t} \leq \beta_f \psi_f^{max} \quad (32)$$

The model includes the state of charge of the batteries $\psi_{f,t}$ on ship f , charging value $q_{i,t}^c$ and charging efficiency $\mu_{i,f}^c$. The model foresaw the three operation states of the ship:

- $x_{f,t} = 0$: The ship is in the port not sailing and not charging
- $x_{f,t} = 1$: The ship is in the port and charging
- $x_{f,t} = 2$: The ship is travelling on a route k

Additional parameters such as the reduction of state of charge of the ships' batteries while in the port and not charging τ_f , energy consumption or the reduction of the state of charge in the ships' batteries on the route $E_{f,k}^d$, minimum and maximum state of charge of the ships' batteries determined with coefficients α_f and β_f . These values depend on the characteristics of the ship and route and are determined as described in PAPER 6. Additionally, a method for the evaluation of maritime electrification and its integration was developed and presented in Figure 7.

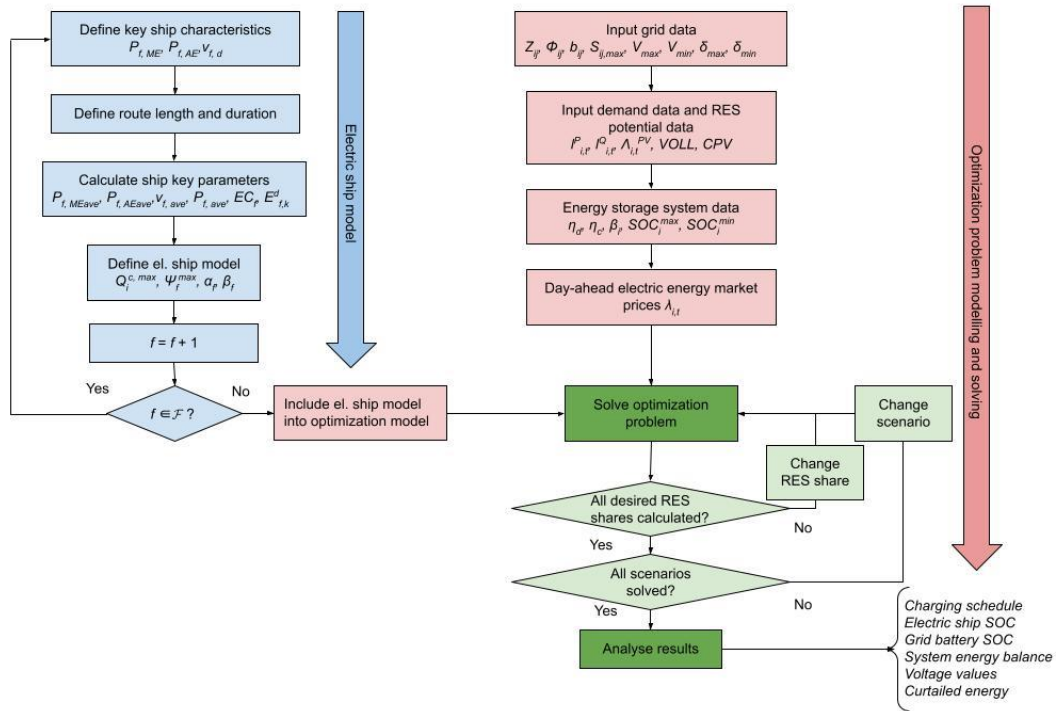


Figure 7 Overview of the method for the impact evaluation of maritime transport electrification and integration with the energy system

The method includes the presented electric ship model into the UC model with detailed distribution grid limitations. The operation of the system is observed for the different RES shares which make it possible to draw conclusions on the connection between maritime electrification and RES penetration. Additionally, the method can integrate other flexible options such as mainland large-scale batteries to evaluate the maritime electrification in such an environment.

3 SELECTED RESULTS AND DISCUSSION

3.1. Meeting islands' needs with local resources

As elaborated in the Methods section, a Smart Islands method was developed in order to find the optimal energy planning scenarios for the islands. The Smart Islands method aims at exploiting islands' resources to meet its needs by proposing technologies that would represent minimum investment cost. The method works in two main steps. In the first step, the method selects all possible technologies for meeting the island's needs with its' resources. In the next step, the method calculates the necessary capacities of the technologies and generates several possible scenarios with different technologies from the technology list generated in the first step.

The Smart Islands method is presented and tested in PAPER 1. The case studies that were used for testing the Smart Islands method were the islands of Krk and Vis. Although both are located in the Adriatic Sea, these islands significantly differentiate one from the other. Krk island is located in the northern part of the Adriatic Sea, while Vis is in the southern part which means that the climatic conditions are different. The difference can be illustrated by observing the HDD (2148 for Krk and 1759 for the Vis island) and CDD (233 for Krk and 381 for the Vis island). The islands also differ in size, where the area of Krk island is 405.8 m² and of the Vis island is 89.72 m². The populations of these islands also significantly differ, being 19374 for the Krk island and 3460 for the Vis island. The full mapping of these islands was performed in PAPER 1.

3.1.1. Krk island

For the case study of the Krk island, the Smart Islands method generated 7 different scenarios. For the electricity generation, the methods' output included different combinations of the wind power plant, PV plant, biomass as well as PHP unit. Four different technologies were generated for meeting the needs of the heating sector – heat pumps, solar thermal, biomass boilers and

heat storage. The electrification of the transport sector is output in all scenarios. The desalination plant, waste fills and wastewater tanks were suggested to be implemented in addition to the water, waste and wastewater infrastructure.

The uncertainty of the input parameters and the robustness of the generated scenarios were considered using the Monte Carlo method. The 200 probabilistic scenarios were conducted in order to test the robustness of the Smart Islands method for two different cases. The scenarios were firstly run considering the uncertainty of the technical input parameters with the uncertainty range being $\pm 5\%$ deviation from the expected value. In the second case, the deviation of the specific investment cost of the technologies was considered with the uncertainty range being $\pm 10\%$ from the expected value. The results shown in Figure 8, represent the electricity generation for different scenarios for the case when the uncertainty of the technical input parameters was considered.

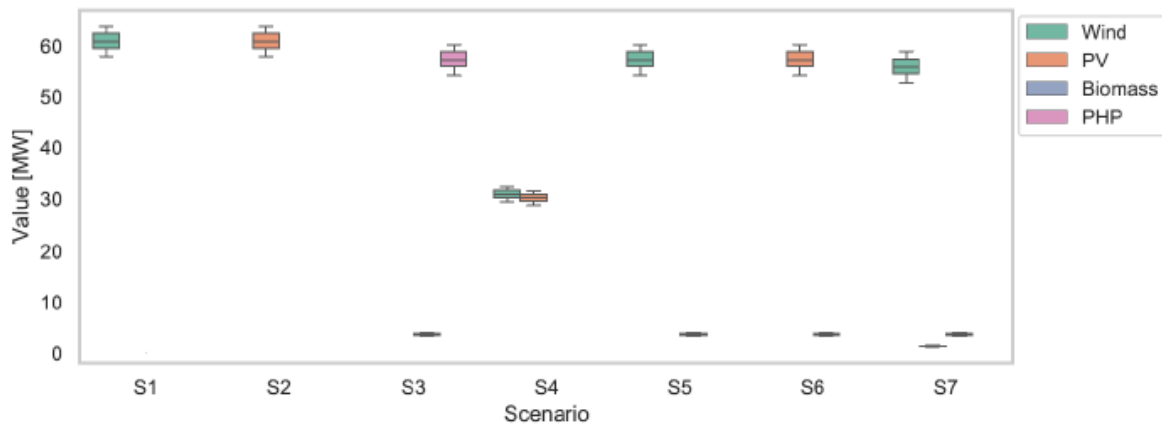


Figure 8 The results of the Krk island case study with the consideration of the uncertainty of technical input parameters

The results of the performed test showed that the results, in this case, the capacity of the electricity generation technologies, remained close to the deterministic values. As the value of technical input parameters such as wind potential, solar potential, electricity demand and similar changes, the Smart Island method adjusted the value of the necessary technology capacities for meeting the needs. All technology sets for each scenario remained the same as in the deterministic calculation. This means that the Smart Islands method is robust with the respect to the uncertainty of the technical input parameters. The considered range of uncertainty of $\pm 5\%$ is considered to be sufficient as the technical parameters (solar potential, wind potential, demand, etc.) can be determined with a high level of accuracy.

Figure 9 shows the output of the Smart Islands method when the uncertainty of the specific investment cost of the technology is considered. Different from the technical input parameters, the specific investment cost of the technology may vary more, especially over a longer period. Because of this, a wider uncertainty range of $\pm 10\%$ was considered.

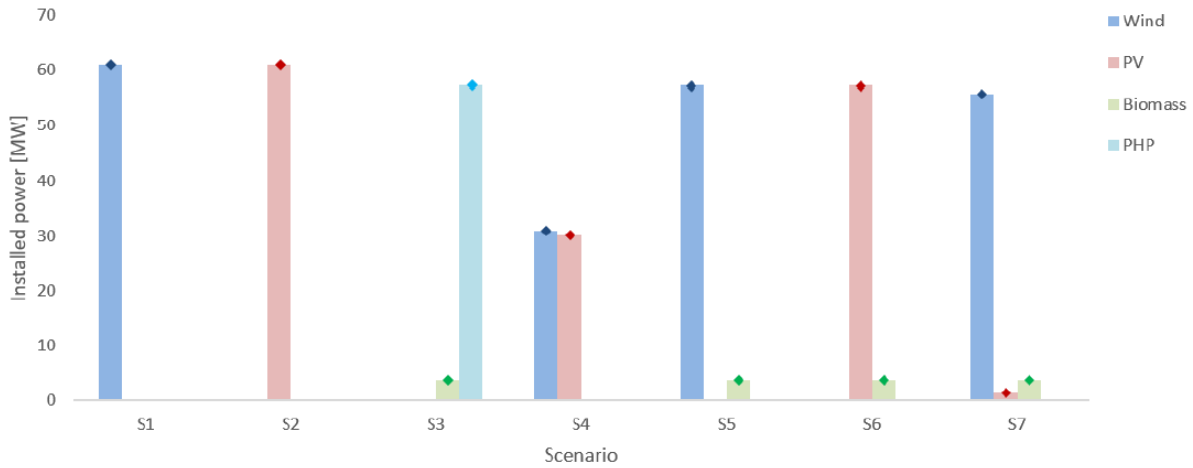


Figure 9 Energy planning scenarios for the electricity generation technologies for Krk island when the uncertainty of the specific investment cost of technologies was considered

The results of the deterministic scenarios are presented with bars in Figure 9, while the mean values of the technology capacities obtained with the Monte Carlo experiments are presented with rhombuses. The combination of the technologies for the scenarios remained the same as in the deterministic scenario for the case of specific investment cost uncertainty as well. The mean values of the technology capacities obtained with the Monte Carlo experiments strongly correspond to the original scenario values. The highest deviation of 0.3% occurred in the S5 scenario for the wind power capacity. The results indicate that the Smart Islands method is robust with respect to the specific investment cost of the technologies, similar to the uncertainty of the technical input parameters.

3.1.2. Vis island

For the case of the Vis island, two possibilities were considered – one with the electrical interconnection with the mainland; and the other – without the electrical interconnection with the mainland. The intention of such an experiment is to observe the difference between the Smart Islands method outputs with respect to the electrical interconnection of the islands. This aspect is particularly important because many islands are significantly dependent on the

interconnection for the power supply and some islands do not have an electrical interconnection with the mainland or other islands. Thus, the Smart Island method should be sensitive to the available interconnection infrastructure and reflect on it in the generated energy planning scenarios for the islands.

Vis island has a 10 kV electrical interconnection with the mainland. The outputs of the Smart Islands method for the cases when the interconnection is considered and when it is not, is presented in Table 1.

Table 1 Results of the case study for the Vis island with and without the interconnection

Interconnection [MW]	16	0
PV [MW]	5.92	5.92
Battery storage [MWh]	0	5.42
HP [MW]	6.85	6.85
EV chargers [MW]	1.96	1.96
Desalination [m ³]	1.13	1.13
Waste fill [tonne]	232	232
Wastewater tanks [m ³]	21.4	21.4

The results show that the difference between the two cases is in the installed battery storage capacity on the island. For the case when there is no interconnection between the Vis island and the mainland, the battery storage with the capacity of 5.42 MWh was included in the output of the Smart Islands method. This indicates that Smart Island recognizes the necessity for the controllable unit in order to maintain the power supply on the island. Additionally, the method calculated that there is 0.3 MW of flexibility potential as a result of cross-sector integration which can further enhance the operation of the island system. It is worth noticing that the scenario generated with the Smart Island is similar to the currently ongoing project on Vis island in the scope of which a PV-battery facility will be installed.

Overall, it was shown and extensively elaborated in PAPER 1 that the Smart Islands method enables the energy transition of the islands with precisely defined capacities of required technologies. The scenarios enable the secure supply of the islands, which is an important aspect as underlined in [97]. The method automatically combines the needs and resources according

to the input indicators and mapping and generates energy planning scenarios for meeting the needs of the island with its' resources. The method values the flexibility potential of the interconnection and DR, similarly as shown in [39]. Although it can be argued that scenarios with lower investment costs can be achieved by removing the constraint of meeting local needs with resources, the islands represent special areas often dependent on the mainland. Thus, the technologies and energy planning scenarios that remove the islands' dependency on the mainland bring additional value to the islands and strongly increase the quality of life of the islands. Moreover, such scenarios increase the reliability and decrease the risk of power supply loss which is strongly connected to the risk analysis conducted in this thesis.

3.2. Risk assessment for island energy planning scenarios

One of the objectives of this thesis was to develop a framework for risk analysis of the islands. Thus, in the scope of PAPER 2, a method for quantifying the risk of different energy planning scenarios on islands was developed. The method models the probability of outage of an element in the power system to create a probability matrix and enters the optimization problem in order to calculate the damage caused by a different outage. By multiplying the probability of outage with the damage caused by the outage it generates a risk matrix with risk values for each energy planning scenario considered. In addition to the deterministic formulation of the method, a robust formulation with respect to the demand uncertainty was developed as well.

The case studies used for the testing of the risk assessment method were conducted on the Croatian island Unije and the Greek island Tilos.

3.2.1. Unije

Four different scenarios were conducted for the Unije island. The first scenario *S0* represented a current situation on the islands with 10 kV electrical interconnection only. Scenario *S1* considered the installation of a 1 MW PV plant and the usage of a 27 kW desalination plant in the demand response mode. In the *S2* scenario, a 1 MWh battery storage and desalination plant in the demand response mode were considered (without the PV). Finally, in the *S3* scenario, a 1 MW PV plant, 0.5 MWh battery storage and a desalination plant in the demand response mode were considered. The calculations were done for the robust optimization model where the conservativeness of the solution was controlled by factor Γ , where the most optimistic result

is achieved for $\Gamma = 0$, and the most pessimistic one for $\Gamma = 1$. The considered demand uncertainty range is presented in Figure 10.

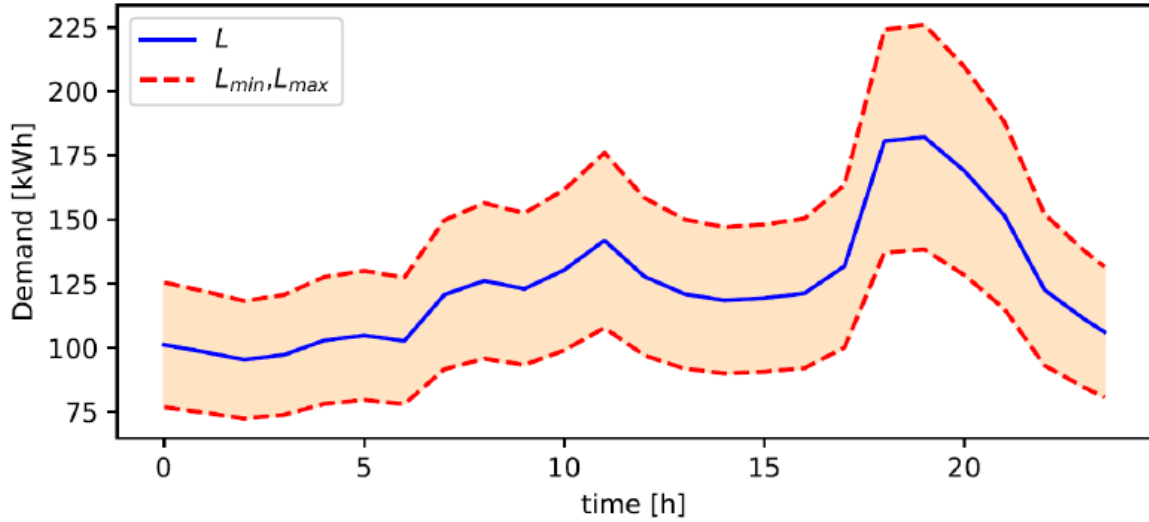


Figure 10 Considered uncertainty range for the Unije island risk assessment calculation

The results of the calculation are provided in Figure 11. It can be seen that the risk values increased according to the increase in the uncertainty budget. It is considered that the island is able to remain in a stable state by the usage of the grid-forming inverters after the outage occurs. When comparing the PV plant and the battery storage system, it can be seen that the lower risk values are obtained for the scenarios with the installed PV system. This was expected as the PV plant reduced the loss of load which is the variable that affects the risk value the most. The lowest risk level was achieved for the scenario with the PV plant battery system which is also an expected result as the battery storage system enables the supply during the hours with the highest electric energy price.

The results of the robustness analysis indicate that the time of the outage is of high importance as well. The summer season is characterized by the highest demand and the results showed that the risk is the highest for this period for all scenarios. The analysis also showed that the scenarios with the PV plant are less exposed to the uncertainty level increase than the scenarios without the PV. The difference in the risk level between the most optimistic and the most pessimistic scenario for the scenarios without the PV was 332.5 €, while for the ones with the PV, the difference was 181.9 €. This further implies the importance of increasing the RES

penetration on the island as they can increase the security of supply during the periods with the highest demand.

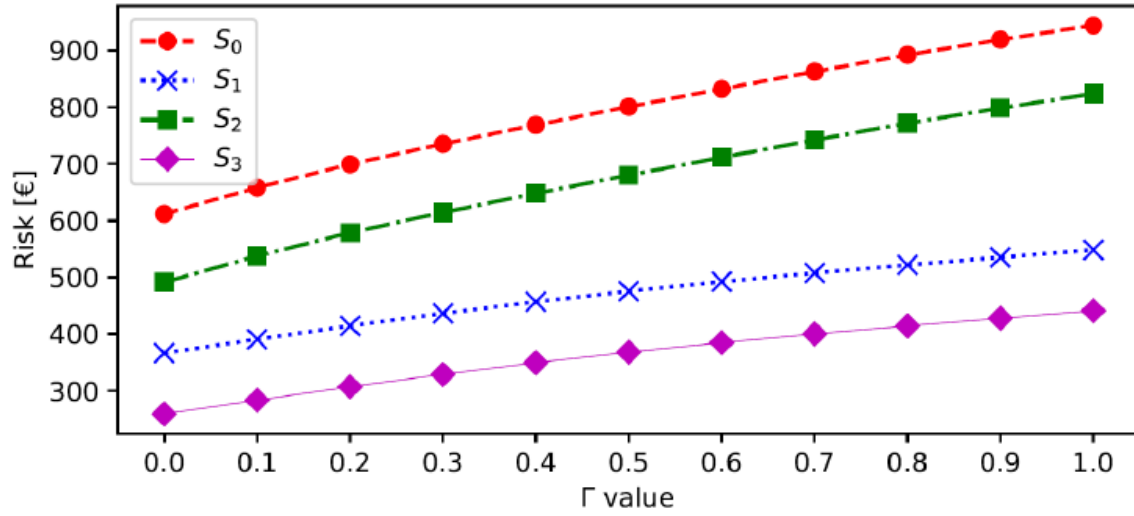


Figure 11 The risk values for different Unije island energy system scenarios considering the uncertainty budget

An additional “zero-import” scenario was also calculated for the Unije island. The objective of this calculation was to find the necessary capacities of PV and the battery storage system in order to achieve an energy planning scenario in which the risk value will be zero. In such a scenario, the island will be able to operate without any loss of load or curtailed energy after the interconnection outage. The calculation was conducted for different PV and battery capacities as well as for the different values of the uncertainty budget. The results are presented in Figure 12 and they showed that the “zero-import” risk scenario was achieved for the scenario with 0.5 MW PV and 3.55 MWh battery. Further increase of the PV capacity would result in the increase of the curtailed energy in the case of the interconnection outage.

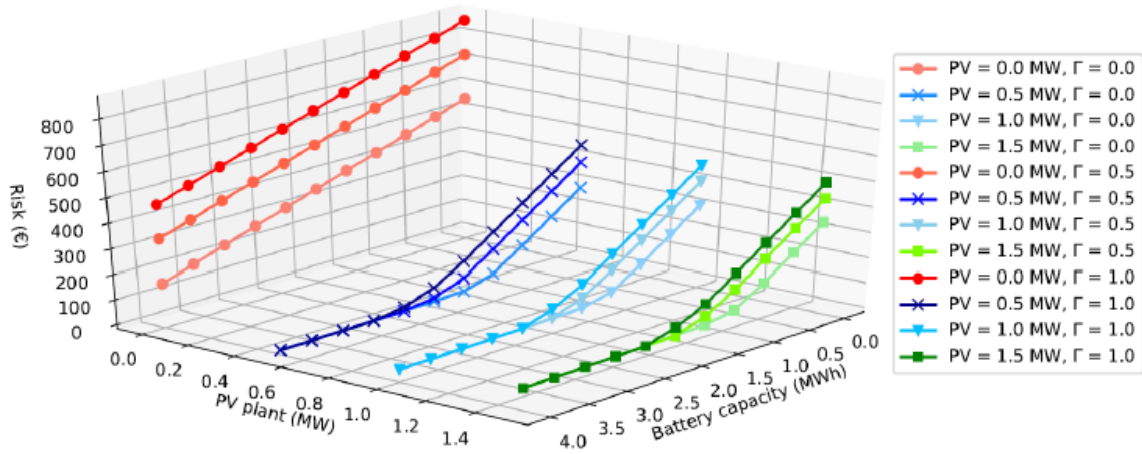


Figure 12 The results of the risk assessment analysis for finding a “zero-import” scenario

3.2.2. Tilos island

Another case study in which the risk assessment method was tested was conducted on Tilos island with topology represented in Figure 13. The case study has two demand centres – Megalo Chorio and Livadia village. The island has also an interconnection, a wind power plant, a PV plant, a battery storage system and backup diesel generators with capacities represented in Figure 13. The case study is more detailly described in the Appendix of PAPER 2. Four different scenarios were analysed for the Tilos case study and are shown in Table 2.

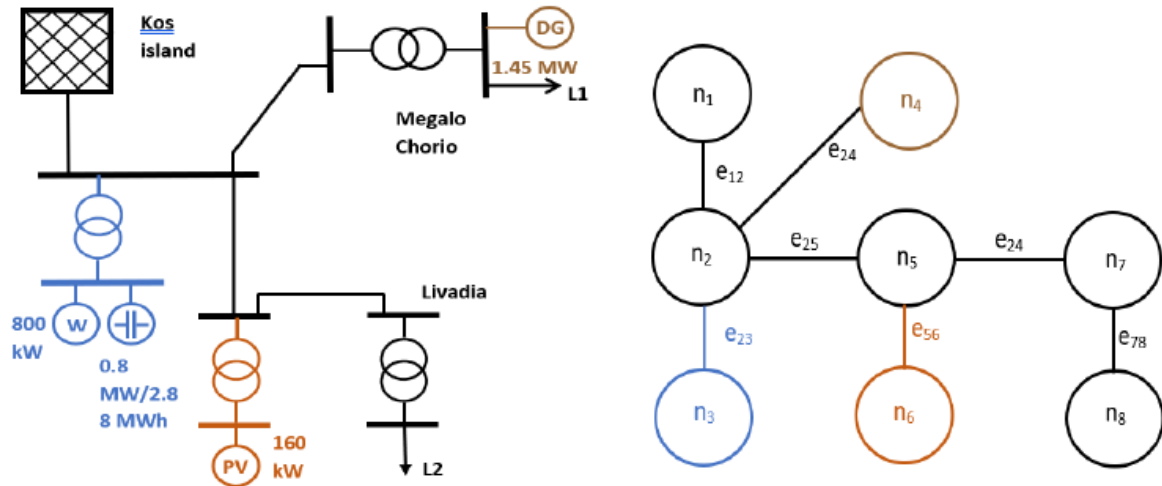
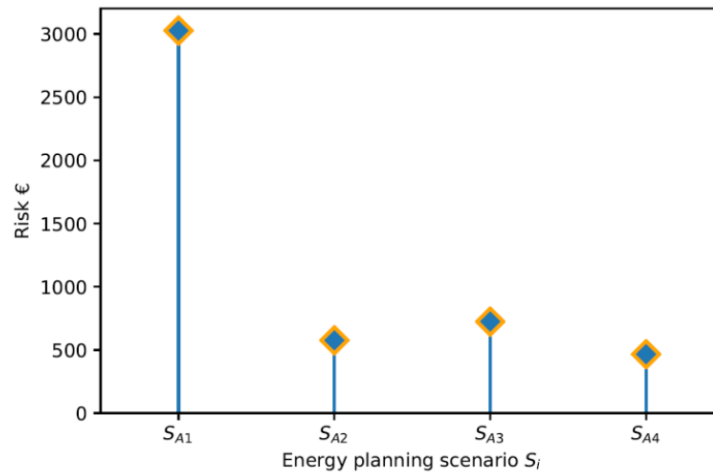


Figure 13 The topology of the Tilos power system and its graph representation

Table 2 Analysed scenarios for the Tilos island

Scenario	Backup diesel genset	Wind power plant and battery storage	Solar power plant
S_{A1}	No	No	No
S_{A2}	Yes	No	No
S_{A3}	No	Yes	No
S_{A4}	No	Yes	Yes

The results of the risk assessment calculations for Tilos island are shown in Figure 14. The highest risk value was achieved for the scenario where the interconnection is the only supply source for the island. With the further installation of the different technologies, the risk value for the island was significantly reduced. The lowest level of risk was achieved for the combination of the wind power plant, PV plant and battery storage system (466.27 €). The lowest risk was achieved for this scenario because there is enough battery capacity to meet the demand at different periods and because of the spatial dispersity of these technologies where part of the island can still be supplied with electricity after the outage. This is different from the scenario with only a diesel generator where the supply is concentrated in one node.

**Figure 14 The results of the deterministic risk assessment analysis for the Tilos island**

The results demonstrated that, by applying the risk assessment method, the risk values of the different energy planning scenarios can be quantified. Moreover, the RES increase led to a lower risk value, which is a similar conclusion as in [98]. It was also shown that it is possible

to use the presented risk assessment method to find the scenario with the RES that will make the island independent from the electrical interconnection to the mainland. The method provides an original approach for the risk assessment of the energy planning on the islands and can provide valuable indicators to the local community and investors when making decisions regarding the energy systems on the islands.

3.3. Advanced energy planning approach for smart islands

The precision of the energy planning scenarios is closely connected to the spatio-temporal level of detail in modelling. Moreover, in order to address the application aspects of energy planning scenarios, a power flow analysis in the current and/or future grid should be conducted. Thus, PAPER 3 provided a method for the analysis of the detailed spatio-temporal approach soft-linked with the power flow analysis. With a soft-linking approach, the problem was computationally relaxed because the simultaneous calculation of energy planning algorithms and power flow would be an extremely complex problem.

The case study for testing the case study was performed on the island of Krk with modelled connections to the mainland and other islands (Figure 15), with a total of eight modelled locations. An overview of modelled technologies and their characteristics are presented in PAPER 3. The model was solved using the CPLEX solver, with a total run time of 1 hour and 24 minutes, maximum RAM usage of 27.5 GB and average RAM usage of 21 GB. Five scenarios were considered in total. The first three scenarios (S1, S2 and S3) analysed different transport options with the described spatial distribution of eight locations and a half-hourly modelling approach. Scenario S3 with half-hourly time resolution and spatial distribution with eight locations is considered to be the reference scenario. The difference between the S3 and S4 scenarios is that S4 considered the hourly resolution, while the difference with the S5 scenario is that S5 considered coarser spatial resolution with all technologies aggregated in one node.

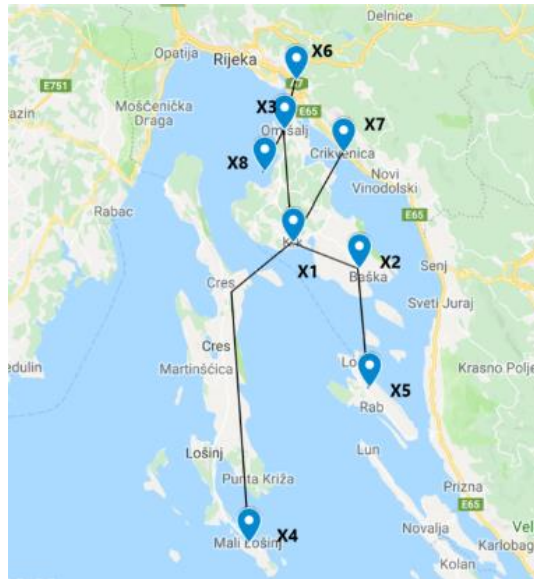


Figure 15 Considered case study with eight locations and interconnections

Figure 16 shows the installed capacities of different renewable sources for different modelling approaches. The figure shows the capacities distribution over the different locations for scenarios S3 and S4, while for scenario S5 only one location was considered. The differences between the different time resolution approaches (S3 and S4) scenarios resulted in different capacity allocations in Dunat (X2) for residential PV plants and in Omišalj (X3) regarding the wind power plant. However, the differences were not significant as the ones between different spatial distributions (S3 and S5). The coarser scenario S5 resulted in a 7 MW lower capacity of installed wind power and 8.5 MW lower residential PV capacity than the referent scenario S3.

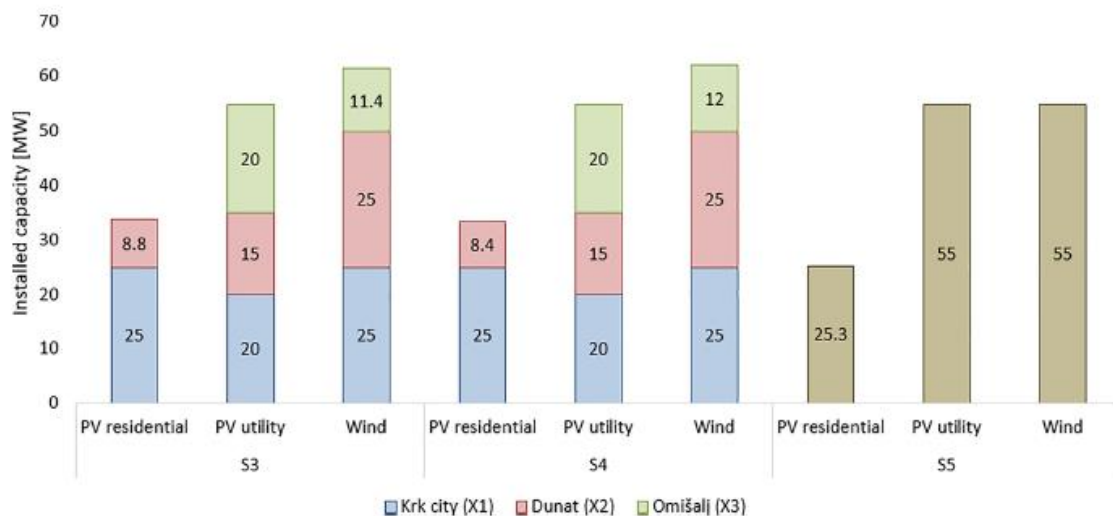


Figure 16 Installed production capacities for different locations and scenarios

Similar can be observed in Figure 17 for the storage technologies. The results showed that the battery capacity significantly differs between the spatially distributed S3 and coarser S5 scenarios. The battery capacity for the coarser scenario was 3.3 times higher than for the spatially distributed scenario. A remarkable reduction in the installed battery capacity in a spatially distributed scenario occurred as the model considered the energy flows between different locations in the modelled energy system.

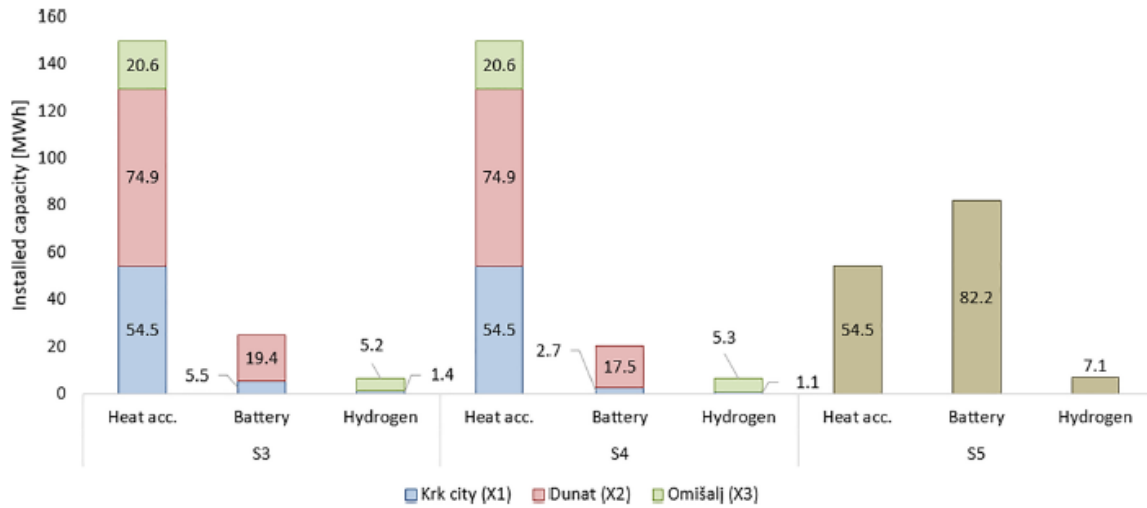


Figure 17 Installed storage technologies for different scenarios and locations

This is reflected in the overall cost of the scenarios (Figure 18). The CAPEX and OPEX costs remained similar for scenarios S1 – S4 but significantly changed for the S5 scenario. This was the direct consequence of different installed capacities for the coarser scenario. The difference in the installed capacities caused the operational differences which were reflected in the operational cost of the scenario. The total cost for the spatially coarser scenario results in a 26.9% cost reduction. A similar study was conducted in [99], where the cost of the spatially coarser scenario was 10%.

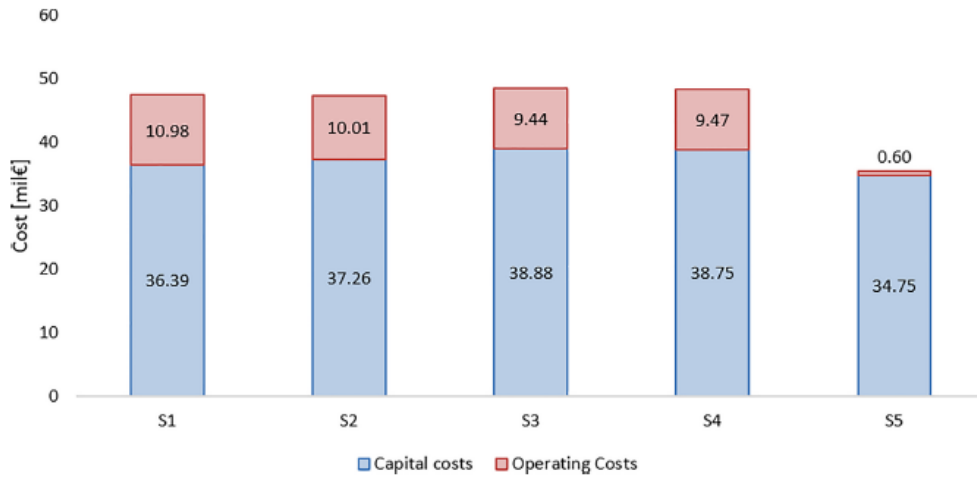


Figure 18 Total costs for different analysed scenarios

Changes in the transport sector and battery operation between the referent S3 and spatially distributed scenario S5 can be observed in Figure 19 and Figure 20. It can be seen that the spatially distributed scenario was able to represent the transport system operation in more detail than the S5 scenario (Figure 19 marked with a red arrow). The difference is even more expressed for the battery system operation, especially in the magnitude of battery SOC which is a direct consequence of the higher installed battery storage capacities in the S5 scenario.

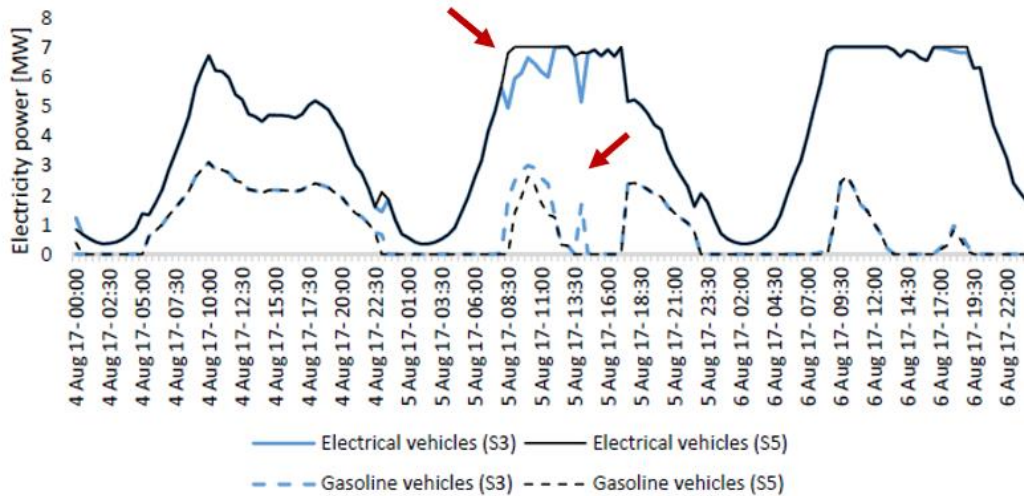


Figure 19 Transport sector operation for S3 and S5 scenarios

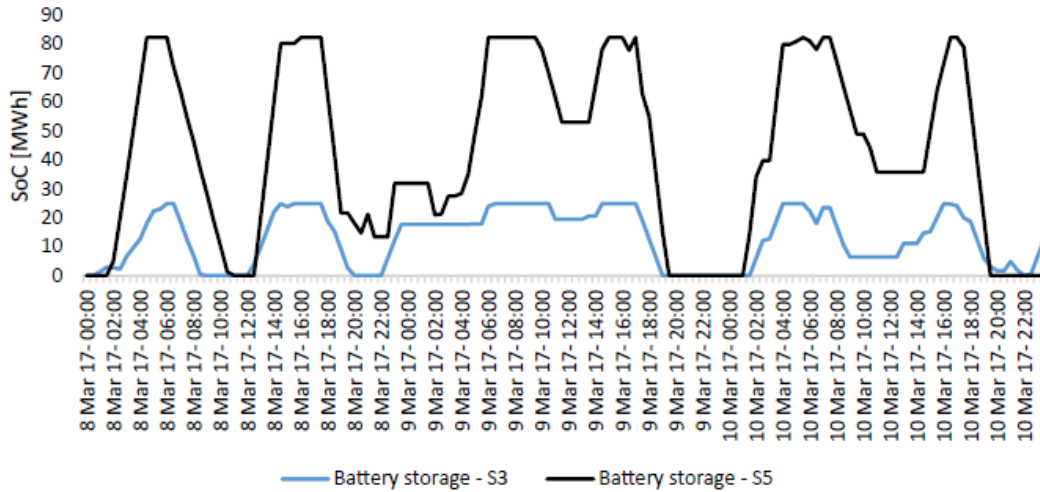


Figure 20 Battery system operation for S3 and S5 scenarios

Similarly, the differences between half-hourly (S3) and hourly (S4) time resolutions in the battery system operation can be observed in Figure 21. The results indicate that differences exist between the different time resolution approaches as well. Overall, it can be concluded that the differences between the different time resolution modelling approaches are not as extreme as the ones for different spatial modelling approaches. However, considering the fact that the half-hourly distributions in this case study were derived from the hourly distributions, the results based on the field devices data may indicate a more expressed difference between the different time resolution modelling. Additionally, Figure 21 shows the benefits of detailed spatio-temporal modelling in terms of result transparency and obtained information. The result further demonstrates the benefits of the presented approach as it provides information about the specific locations and the interactions between them.

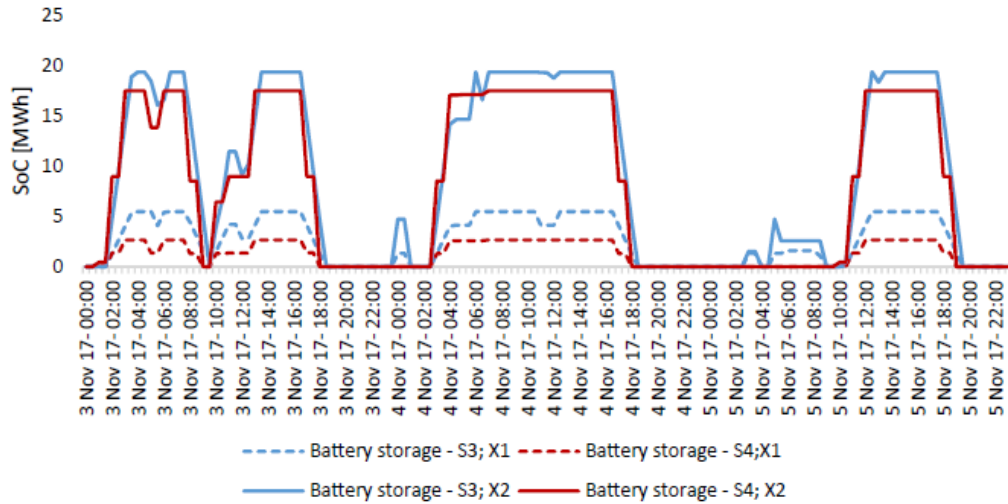


Figure 21 Battery storage operation for X1 and X2 locations and S3 and S4 scenarios

Finally, a power flow analysis for the Krk case study was conducted in order to assess the application possibilities of the analysed energy planning scenarios. The power flow analysis included relevant grid data and considered two states of the grid operation – maximum demand and minimum production state and the minimum demand and maximum production state. The analysis showed that for the maximum demand state, there were no grid code violations. However, as can be seen in Figure 22, for the minimum demand case there were several violations of the voltage limits determined by the grid code. This is mostly due to the increased reactive flows in the transmission grid that caused the voltage limit violation in the 110 kV nodes even before the implementation of analysed energy planning scenarios. The installation of the utility-scale distributed generation caused the upper voltage limit violation in additional nodes in the distribution grid as well. These issues can be solved by different investments in the grid. This means that, in order to have accurate cost estimations of different scenarios, such costs need to be accounted for.

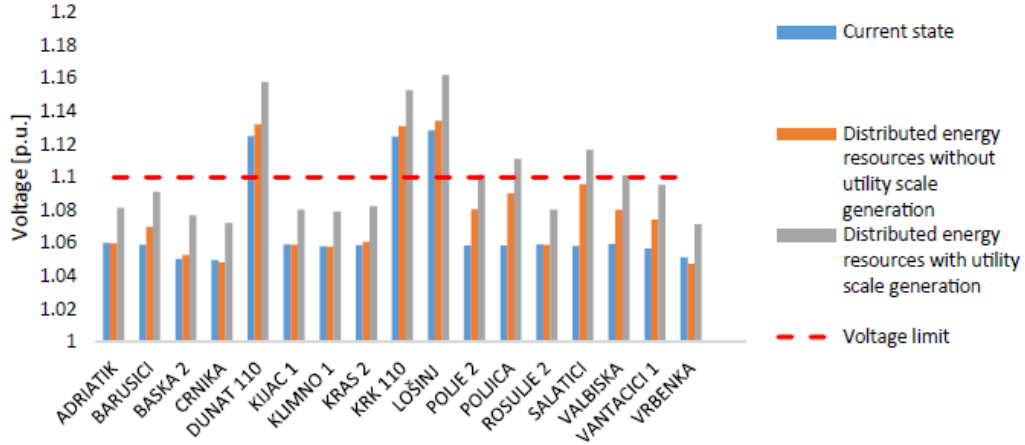


Figure 22 Voltage values for nodes in the power system for minimum demand case

The most important results from the proposed advanced energy planning approach indicate that spatial distribution has a significant impact on the final outcomes of the energy planning models. Further research should focus on this aspect and further address the issue of optimal spatial modelling of energy systems. The approach also proposed the soft-linking approach of the energy planning model and the power flow which made it possible to assess the application possibilities of the proposed energy planning model. Although soft-linking between different models was previously proposed (e.g. PLEXOS and TIMES model in [100], or specifically for the district heating [101]), the proposed approach is the first one that focuses on the detailed spatio-temporal modelling with a significant number of energy vectors soft-linked to the non-linear power flow.

3.4. A novel demand response model for the development of a smart archipelago

Further focus on advanced energy system planning is discussed in this chapter, where an analysis of the creation of the smart archipelago was considered. For this purpose, a mathematical model for the demand response was developed. The developed model is based on the electric energy prices in the day-ahead electric market. The higher the difference between the two consecutive prices, the higher the possibility for the demand response provision. This means that the higher electric price variability will result in an increased possibility for the flexible demand to respond to price differences. However, this does not mean that the flexible demand will influence the price on the day-ahead electric market because the model is

formulated as a price taker. The demand response model was included in the detailed distribution system model which enabled the assessment of technical variables such as voltage in addition to the financial ones.

The case study for the testing of the model was conducted in the Kvarner archipelago, with the distribution system topology as in Figure 23. In this section, only the most interesting results are highlighted, while the detailed description of the case study as well as the detailed analysis of the results is provided in PAPER 2.



Figure 23 The topology of the observed distribution system – red line represents a transmission 110 kV line to Krk island, black lines are the distribution lines and black nodes are the distribution transformers 10(20)/0.4 kV

3.4.1. The impact of the demand response and battery storage system on the financial and technical aspects

The results of the case study were observed for different prices on the day-ahead market obtained according to the historical data and modelled by using the normal probability distribution function. The operation cost reduction in the comparison to the base scenario (Scenario A) and different price values for the scenario with only battery in the system (Scenario B), only demand response model in the system (Scenario C) and battery and demand response model implemented in the system (Scenario D) were observed and presented in Figure 24. The scenarios with the demand response introduce the k parameter that represents the level of

flexibility available in the system (e.g. the technical capability for providing demand response, the number of flexible devices and similar). The lower k level indicates a higher possibility for the demand response provision with two different cases ($k = 1$ and $k = 0.1$) observed in Figure 24.

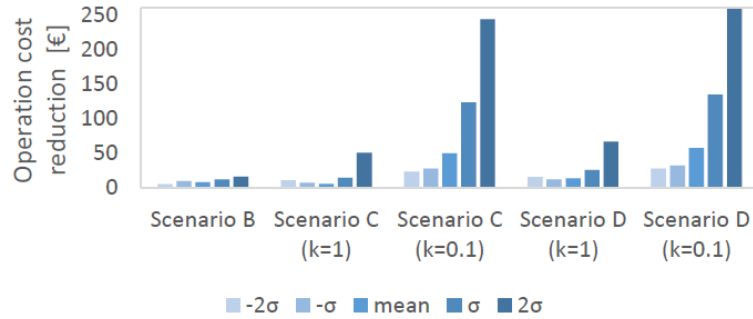


Figure 24 Operation cost reduction for different scenarios in comparison to the base case scenario

It can be observed that the highest impact on the operation cost savings was achieved for the lowest value of the k parameter which is the highest level of flexibility available. It can also be seen that the highest savings as a result of additional flexibility were achieved for the highest prices. For the all scenarios considered, the highest cost reduction was achieved in Scenario D, amounting to 258.7 €.

Since this research conducted in PAPER 4 was completed before the price extremes caused by the increase in gas prices, it would be interesting to observe the results and the effect of flexibility with the new prices. It can be discussed that the benefits of the demand response (and other flexibility options) would significantly increase. It should also be noted that, in addition to the operation cost reduction, the demand response providers were paid incentives included in the objective function. This means that both – the system operator and the demand response provider – benefit from the demand response inclusion in the system.

The inclusion of the demand response model as well as the battery storage system in the detailed distribution grid model enables the evaluation of different flexibility options on technical conditions in the grid. In this context, the voltage magnitude at node 10 for Scenario C and D as well as for different price values of the electric energy are presented in Figure 25. In Scenario C, only the demand response model is included, while, in Scenario D, both demand response and the battery storage system were included in the distribution system model of the Kvarner archipelago.

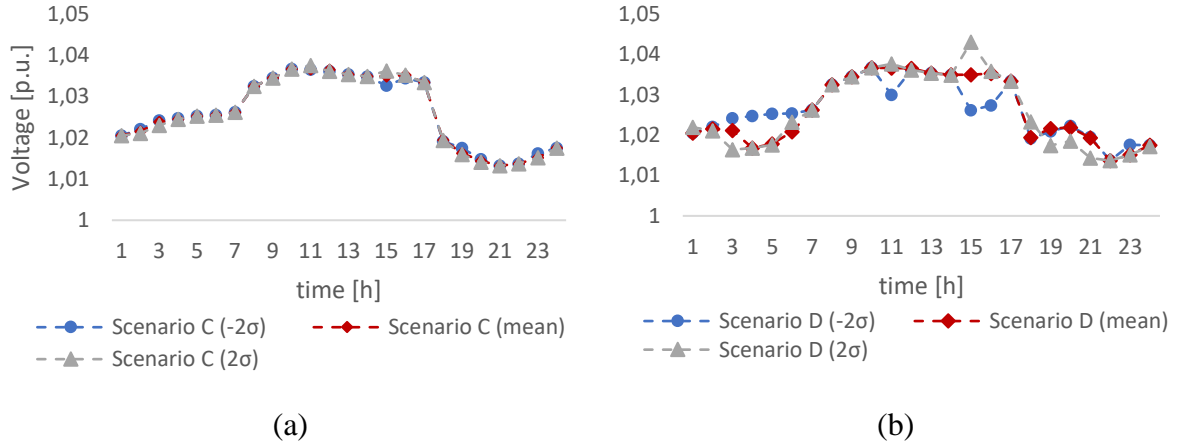


Figure 25 The voltage magnitude at node 10 for different electricity price values for Scenario C (a) and Scenario D (b)

The results showed that the higher impact on the voltage occurred for Scenario D, however, this was expected because the battery storage is connected to the observed node. The local impact of the battery caused voltage fluctuations during the periods of its activation. On the other hand, the demand response model did not cause significant voltage magnitude fluctuations (Figure 25 (a)). Because the flexible loads are dispersed over the observed distribution system, the impact on the voltage magnitude in particular nodes was not significant. Another reason for this result is the mathematical formulation of the demand response model that includes the tangent hyperbolic function. The function prevents significant change in the load which reduces the impact of the flexible load on the voltage magnitude. If the function was not incorporated in the model, in the case of the high number of flexible loads in a particular node, the demand response would more significantly influence the voltage magnitude. With the hyperbolic tangent function included in the model, the model did not affect the voltage magnitude values significantly. This is illustrated in Figure 26, where it can be observed that the available and activated demand response was different for the different values of the electric energy price.

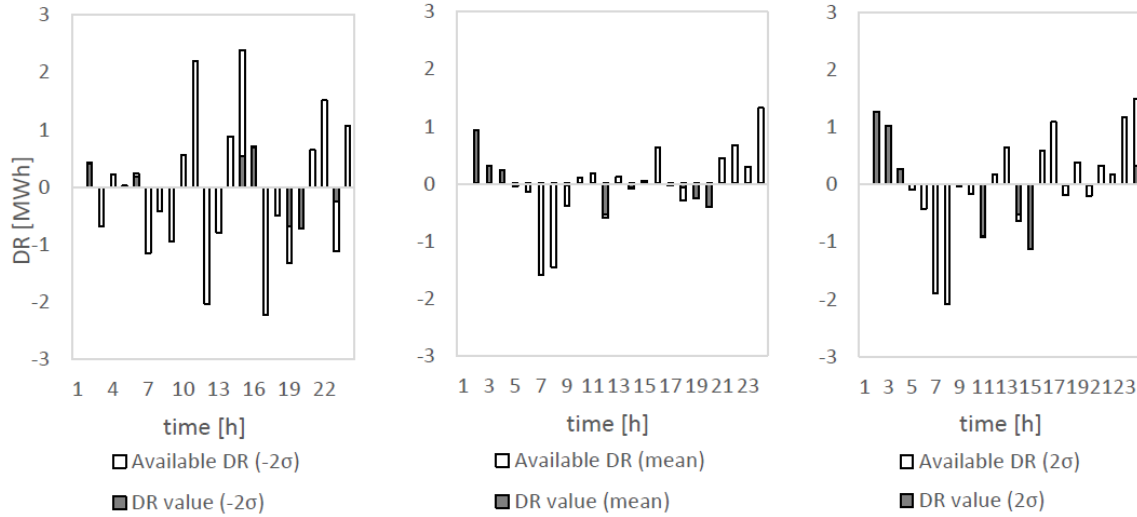


Figure 26 Available and activated demand response for the different price scenarios

This result should be observed in the context of the results presenting the operation cost reduction in Figure 24. The demand response model had a significantly higher effect on the operation cost reduction in comparison with the battery storage system. In addition, by using the demand response the providers received reimbursement in the form of incentives. On the other hand, the battery storage system had a more significant impact on the voltage magnitude. This result illustrates that the suitable implementation of the battery storage system would be in the voltage control mode, while the demand response should be operated in order to reduce the operation cost of the system.

3.4.2. The incentive value for providing the demand response

The value of incentive for providing the demand response services is an important discussion point at this stage of demand response implementation in the EU. Thus, with this thesis, an analysis of the incentive value of the demand response implementation was conducted. The analysis considered that the incentive for the demand response provision is a certain percentage of the electricity price on the day-ahead market. The different levels of available flexible loads controlled with parameter k were also considered in the analysis. Figure 27 presents the impact of the incentive value on the operation cost with different levels of available flexible loads.

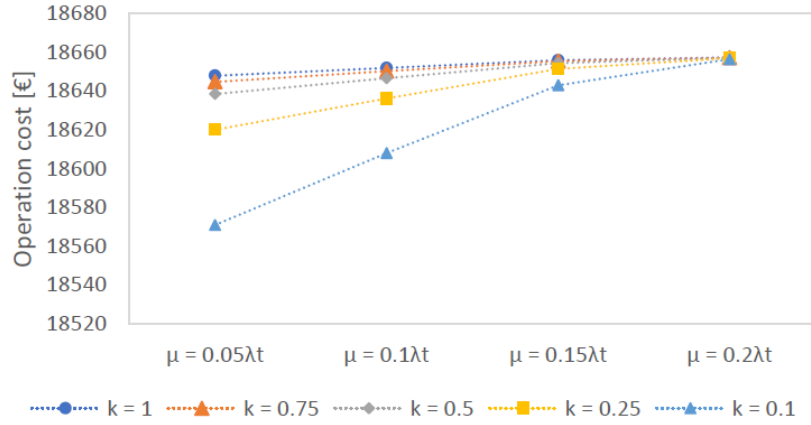


Figure 27 The operation cost for different incentives and available flexible load values

The results showed that the highest savings were achieved for the highest amount of available flexible loads and the lowest incentive equal to 5% of the day ahead of the electricity market price. The higher quantity of available flexibility enables the system to operate more efficiently at a lower cost. At the same time, the reimbursement for the demand response services did not impose significant costs for the system due to the low incentive value. Thus, the operation cost savings are highest in this case.

Another interesting result of this analysis was finding the breakpoint incentive for the demand response model. The breakpoint incentive is the value of the incentive at which the optimization model no longer chooses to use the demand response in the system operation. For the demand response model used in this analysis, the breakpoint incentive was equal to 23% of the day ahead electric energy market price ($0.23 \lambda_t$). This means that the demand response was not activated for that or higher value of the incentive for the demand response services.

The analysis also aimed to observe the correlation between the quantity of flexible load in the system and the incentive value for providing the demand response services. The results of the analysis are presented in Figure 28. Figure 28 (a) presents the value of activated demand response for different quantities of available flexible loads and different incentive values. Figure 28 (b) shows the percentage of the used demand response value (out of total demand response potential achieved with the presented demand response model) for different incentive values and different flexibility values.

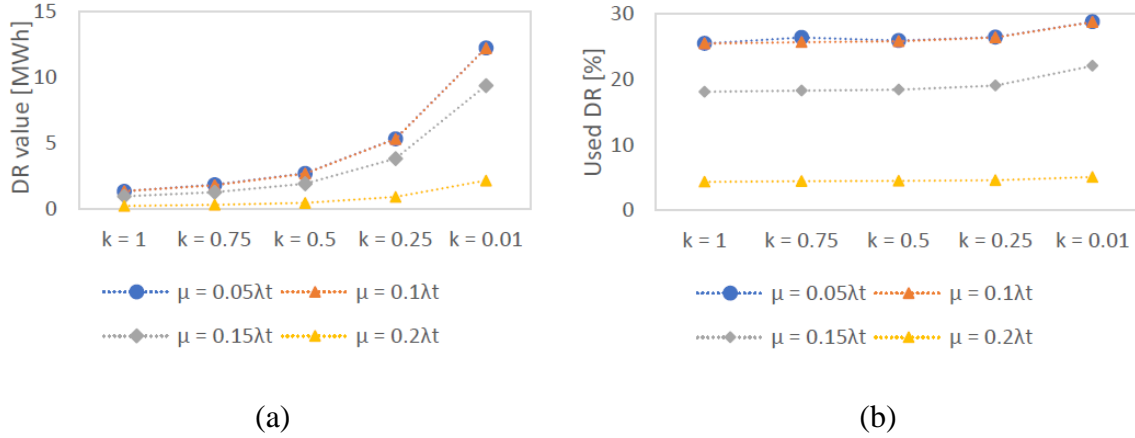


Figure 28 Provided demand response (a) and the percentage of used demand response (b) for different incentive and flexibility values

This analysis provided interesting results as it showed that, for the high available flexibility, the demand response was significantly more activated for the lower flexibility values. The results for the incentives of 5% and 10% of the day-ahead electricity market price did not differ significantly, thus indicating that the incentive of 10% of the day-ahead electricity market price would be the most suitable for the smart archipelago. For the low value of the available flexibility, the provided demand response values did not differ significantly for the different incentive values. This indicates that, for the low flexibility values available in the archipelago, higher values of incentives $0.2\lambda_t$ should be used in order to stimulate the user to install smart devices and join the demand response programme. Proportionally with the increase of the smart devices, thus the demand response providers, the incentive should gradually be decreased to the level of 10% of the day-ahead electricity market prices ($0.1\lambda_t$).

The percentage of the used demand response (Figure 28 (b)) was primarily related to the incentive value. It did not change significantly for the different flexibility values except for the case with the highest flexibility available which resulted in a somewhat higher value of the used demand response. Although for the case with the highest incentive (yellow line in Figure 28 (b)), the level of the used demand response remained practically the same for the highest value of available flexibility as well. The used demand response did not differ significantly for the cases with the $0.1\lambda_t$ and $0.05\lambda_t$ incentive values which is in line with the results in Figure 28 (a).

3.5. Demand response and energy storage system models in a joint network constrained energy and reserve market

The importance of flexibility in power systems is increasing as there is more variable RES penetration in the system. Thus, it is necessary to explore the possibilities for providing flexibility in the systems with high RES share. Historically, the flexibility was provided by the large generators connected to the transmission system that ran on coal or gas. Such generators increased or decreased their production in order to maintain system stability. As they also have a wide capability for reactive power production they were also used for voltage control, in addition to the transformers that contribute to the voltage flexibility. However, with more distributed generators in the distribution grid, more large-scale variable RES in the transmission system and the phase-out of coal and gas plants, it is necessary to find new options for flexibility provision. These options can vary from the Power-to-X concept and smart cross-sector integration to the battery systems integration.

In PAPER 5, the role of battery storage and the demand response was explored in order to evaluate their contribution to flexibility provision. Additionally, their role was also considered in the two different settings. In the first one, only the energy market was considered, while, in the second one, a joint energy and reserve market was considered. Both settings were designed as network-constrained problems. The battery storage and the demand response technology have also another benefit in addition to providing flexibility to the energy system. They include end-users in the form of prosumers in the market which can result in increased overall social welfare and additional revenues for the flexibility providers. For these reasons, it is worthwhile to explore these technologies and propose optimal frameworks for their integration in the energy system.

The consensus regarding the advantages of the joint offering of energy and reserve is widely accepted [102]. The benefits of the co-optimization of these two markets come from the fact that energy supply and reserve provision are strongly connected. Reserve allocation requires that the reserve providers partially dispatch energy which will require more expensive generators to produce more energy to meet demand. This will also limit generators that provide a reserve to produce as much energy as they could if there were no reserve requirements. Thus, the price of electric energy will rise as a result of meeting the reserve requirements. The co-optimization of these markets can secure the minimum operation cost and assure that all

producers are treated equally in the market [103]. The inclusion of flexible technologies such as DR and ESS in such market frameworks can result in viable business cases for these technologies and help the integration of RES as they can generate revenue not only from the energy supply (or savings) but also from the reserve services provision.

The case study that was used in PAPER 5 considered the transmission grid nearby the city of Rijeka that includes mainland consumers and the islands of Krk, Lošinj and Rab. The case study considered aggregated battery and demand response effect in 110 kV nodes of the observed system. It was also considered that this is a 100% RES system with bio-based generators, variable RES, battery storage and the demand response. A detailed description of the case study can be found in PAPER 5. The method implemented in the PAPER 5 used a robust optimization similarly as in PAPER 2 in order to address the impact of the uncertainty on the final results. This means that the budget for uncertainty Γ was included in the model in order to select the conservativeness of the results.

3.5.1. DR and ESS impact on the financial aspects

When observing the operation cost of the modelled system, the results showed the difference between the electricity only and joint electricity and reserve market modelling. For the most optimistic demand scenario, the operation cost of the system with joint electricity and reserve market was 17.9% higher than the system with an electricity-only market. For the most pessimistic scenario, the difference in the operation cost increased to 28.1%. Such a result was expected because the demand is directly connected to the level of the reserve requirements. However, the result strongly underlines the necessity for detailed modelling in order to accurately model the energy systems, especially the ones with high variable RES share. The most pessimistic and optimistic scenarios were determined by utilizing a conservativeness factor and formulating a robust optimization problem similarly as in PAPER 2.

The impact of different modelling approaches on the marginal cost of energy production was also observed (Figure 29). It can be seen that different modelling approaches will result in the different marginal costs of energy production at different periods. However, the marginal cost did not significantly differentiate for different models, which means that the difference between the two models in this aspect exists, but is not significant. The reason behind this result is in the

modelling aspects. Due to the fact that the demand uncertainty was considered only in the reserve requirements equations, the energy balance was affected only by generators, energy storage systems and demand response variables, while the demand (a non-flexible one) was not exposed to the uncertainty. Thus, the difference in the marginal cost of energy production between the two approaches was not significantly expressed. The demand uncertainty was not considered in the energy balance equation in order to better represent the physical aspects of the system. In the real-time applications, the market clearing is performed with the deterministic values, thus the uncertainty was only included in the reserve requirement constraints in order to model the demand fluctuations from the deterministic values.

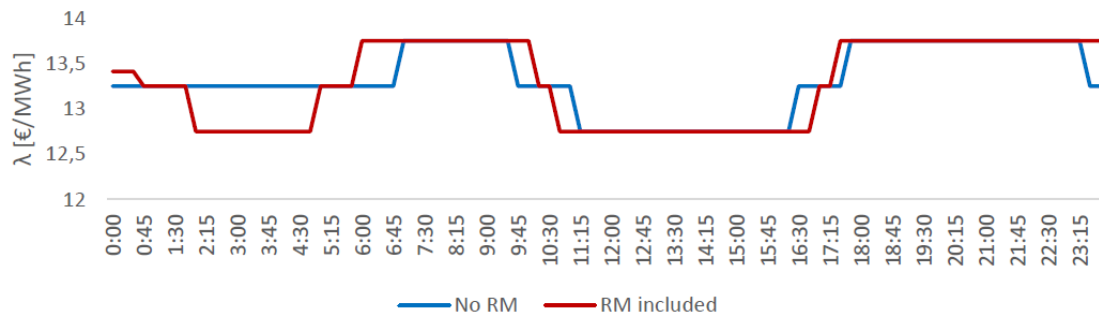


Figure 29 Dual variable of the power balance constraint for energy only and joint energy and reserve market

Another interesting result was achieved for the marginal costs of the reserve provision. The results showed that the marginal costs of up and down reserves differentiated significantly. For the most pessimistic demand scenario, the maximum marginal cost of the up reserve was 36.7 €/MWh, while the marginal cost for the down reserve was 6.05 €/MWh. The reason for such a high difference is in the share of variable RES in the system and the marginal cost of reserve provision of different flexibility providers. Because the modelled system had a high RES share, there is a high excess of produced energy. Thus, the down reserve is required in order to be activated during periods of high electricity production in order to prevent curtailment. A similar finding was presented in [104] where prices for the down reserve were significantly higher than the up reserve.

A similar result can also be observed in Figure 30. The revenues for the ESS and DR were significantly higher when included in the joint energy and reserve market. The revenues gradually increased for the more pessimistic demand scenarios, which is also expected as there

are higher reserve requirements for more pessimistic scenarios. These results indicate that the inclusion of flexibility providers in such markets would create significantly improved business cases for such technologies. This is not limited to battery storage systems and demand response only, but to other technologies such as Power-to-X or different cross-sectoral integration technologies as well. The analysis was done for different variable RES shares as well ($k = 0.5$ being the scenario with the lowest RES share and $k = 1.5$ the highest RES share). It can be observed that the battery storage revenues increase with the increase of the RES share, while the revenue of demand response providers remained similar for different RES shares. Since the battery storage systems have a lower marginal cost of reserve provision, they were prioritized for the reserve provision in comparison to the demand response. This means that the energy storage system was more frequently utilized for the reserve provision which is presented with additional figures and discussions in PAPER 5.

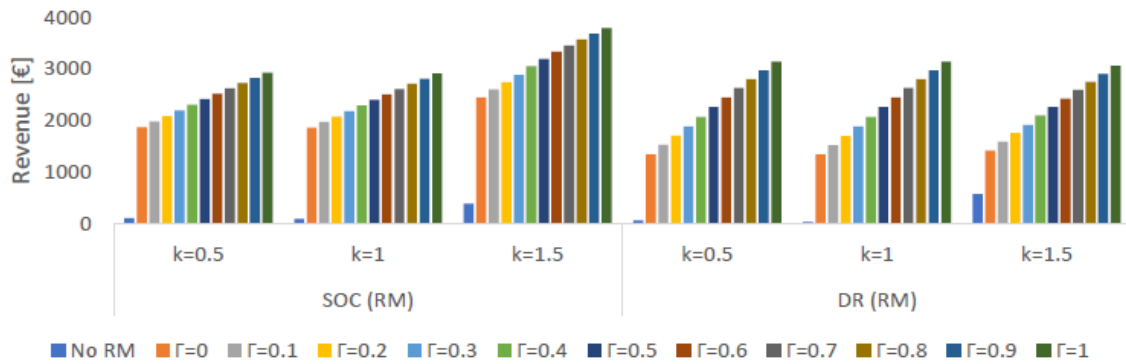


Figure 30 Revenues for the demand response providers and energy storage systems for different RES shares and conservativeness factors

3.5.2. DR and ESS impact on the technical aspects of the system

Besides the financial aspects, technical ones were observed as well. Figure 31 shows the operation of the battery systems in node 2 (Figure 31 (a)) and node 19 (Figure 31 (b)) of the observed system for the two different modelling approaches. As can be seen, the modelling approach highly influences the battery system operation. This is expected because the battery systems participated also as reserve providers in the joint energy and reserve market approach which results in operational differences in comparison with the energy-only market approach. Figure 32 presents the results of the analysis of battery system operation for different VRES shares for the joint energy and reserve market approach only. The figure shows that the impact of VRES share in the system on the battery system operation is significant. The case with high

VRES share (b) results in higher battery system participation in the reserve provision, which caused different battery system operation. This result also indicates the importance of detailed modelling as different approaches result in different outcomes.

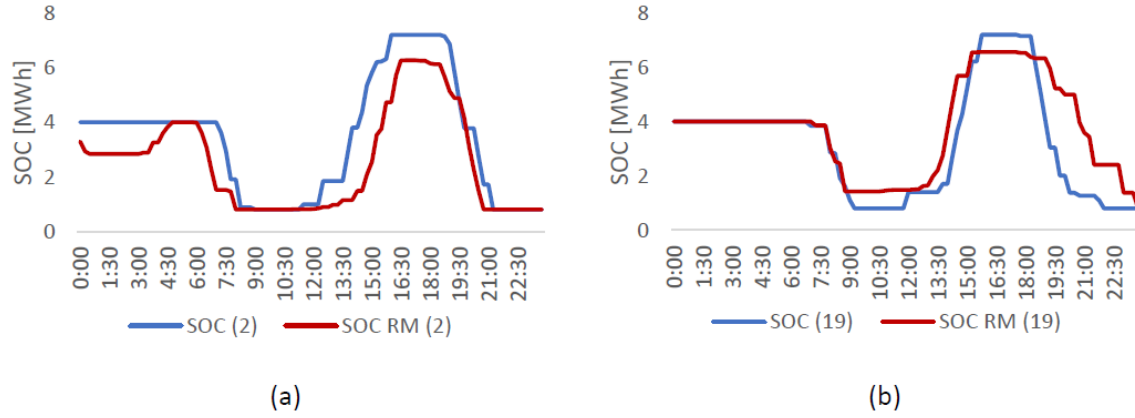


Figure 31 Energy storage operation for two nodes in energy only and joint energy and reserve markets

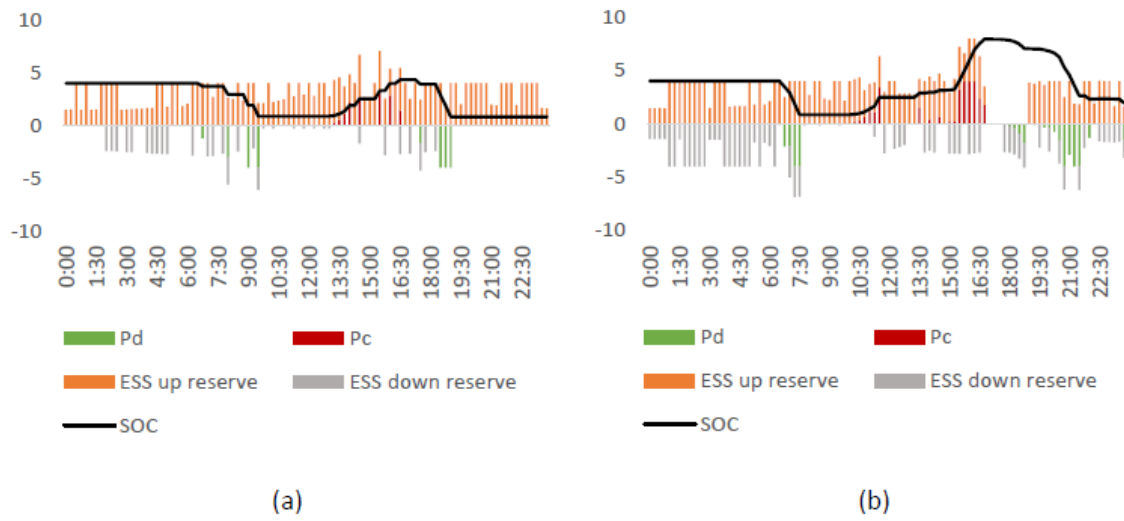


Figure 32 Battery storage operation in node 1 for minimum (a) and maximum (b) VRES share where SOC is measured in MWh and other parameters in MW

More detailed results and discussion on the topic of flexibility and the role of battery storage and demand response can be found in PAPER 5. This research showed that islands with flexible technologies can also contribute to the more efficient operation of the energy systems. The study also emphasised the importance of accurate and detailed modelling for the assessment of the role of flexible technologies in future high VRES energy systems.

3.6. Maritime transport electrification and integration with the energy system

Maritime transport represents one of the key features very specific and important to the island communities. Although the research regarding maritime transportation to and from the islands was not one of the primary objectives of this thesis, it is included in this thesis as it is a topic relevant to islands and as an upgrade to the rest of the research that contributes to the topic of the advanced energy planning on smart islands.

The research regarding maritime transport is conducted in PAPER 6, where a new mathematical model of the electric ship was presented and integrated into the distribution grid model. The case study on which the model was tested was the maritime line from Valbiska (Krk island) to Merag (Cres island). The trip duration between the two ports is 25 minutes and the line length is 3.62 nm. Two ships operate between the ports – Krk (denoted with F1) and Kornati (denoted with F2) according to the defined schedule. It was considered that the existing diesel ships were replaced by electric ones. The charging point was foreseen in the Merag port (node 4 in Figure 33) and the other port, Valbiska, is at node two. The rest of the grid was modelled according to the distribution grid parameters and presented in Figure 33 (a more detailed description and parameter values are provided in PAPER 6).

The research was considered for two base cases – the days with minimum and maximum demand. Three basic scenarios were considered:

- i) S0 – no maritime transport electrification
- ii) S1 – Maritime electrification with 2.4 MW charger at node 4
- iii) S2 – S1 and an additional 1MW/2MWh energy storage system at node 4

All of the scenarios are additionally subjected to sensitivity analysis with respect to the RES share in the distribution grid as described in PAPER 6. This analysis enabled the synergy assessment of maritime transport electrification with the increase of RES share in the distribution grid.

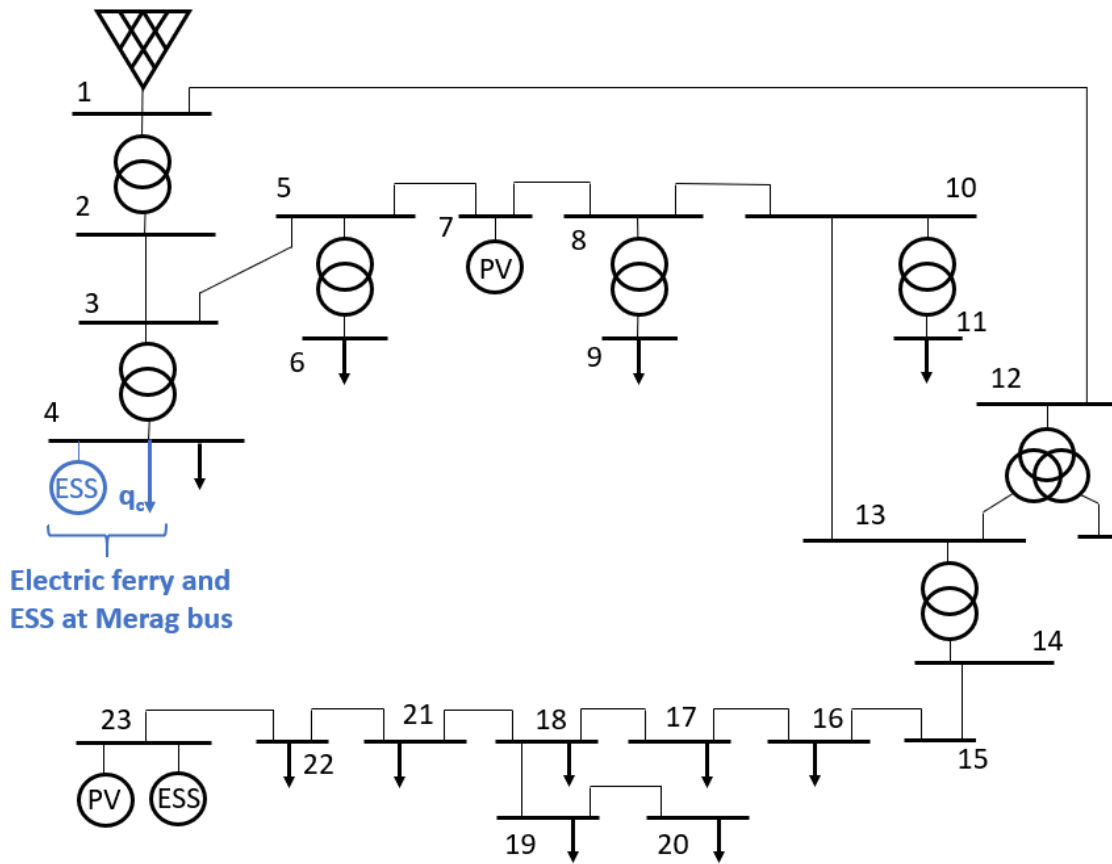


Figure 33 Modelled power system for the maritime transport electrification analysis

For the maximum demand scenario, the charging schedule of the ships was the same for both scenarios S1 and S2 (Figure 34 and Figure 35). Since the ships have to be charged according to the schedule and the operating conditions in the grid are well within the allowed limits (no flexibility is needed at this point in the grid) the addition of the battery storage system did not cause differences in the charging values of the ships. However, with the RES increase in the grid, the results show that differences occurred in the charging values of both ships. An increase in the energy production in the grid enabled less expensive charging at certain periods (changes in the charging marked with red and blue arrows in Figure 34). The state of charge of batteries on ships is presented in Figure 35.

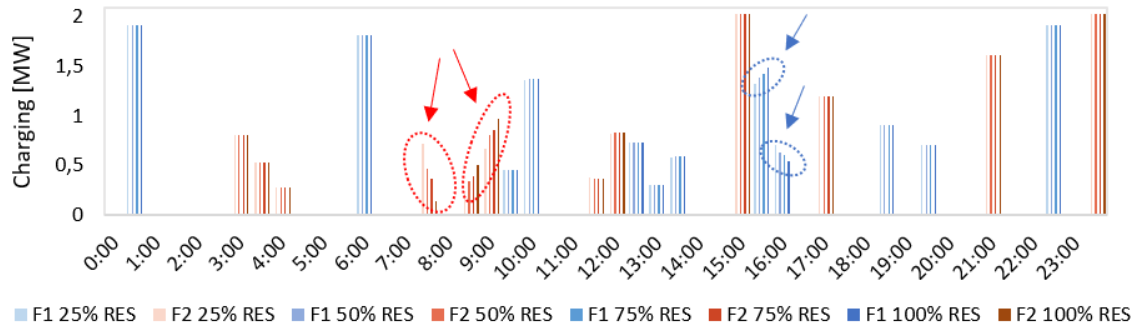


Figure 34 Maximum demand: Charging schedule for Krk and Kornati electric ships for different RES shares

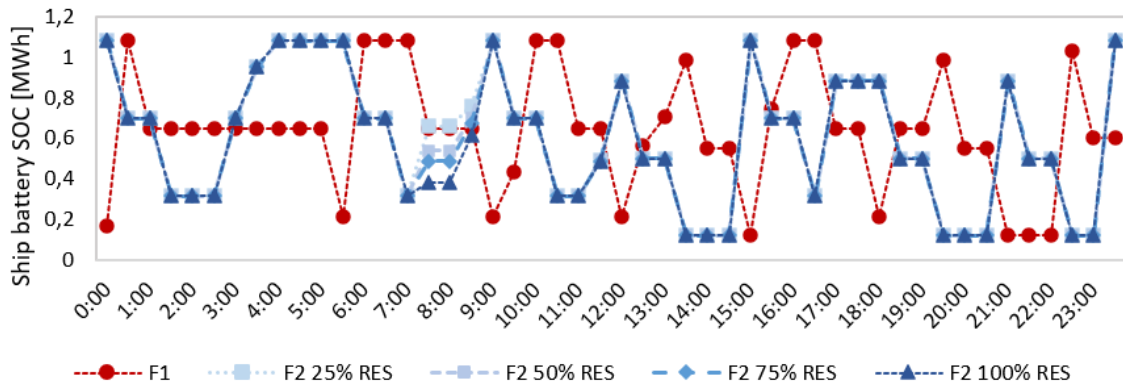


Figure 35 Maximum demand: State of the charge of the Krk and Kornati for different RES shares

The situation is different for the minimum demand case. Figure 36 shows the charging schedule for the Kornati ship. It can be seen that the charging schedule changes significantly depending on whether the battery system is modelled in the Merag node or not (some changes are marked with black arrows in Figure 36). This is the case because voltage magnitude in parts of the distribution grid is near the upper limit (during high RES production). When there is a lack of flexible sources, the system needs to curtail energy from RES, which leads to a higher operation cost of the system. However, when maritime transport is electrified and smartly integrated with the rest of the system, it is possible to provide additional flexibility by managing the charging schedule of the ships. This is in line with Figure 38 which shows the voltage magnitude values at node 4. Figure 37 presents the state of charge of the batteries on the Krk and Kornati ships.

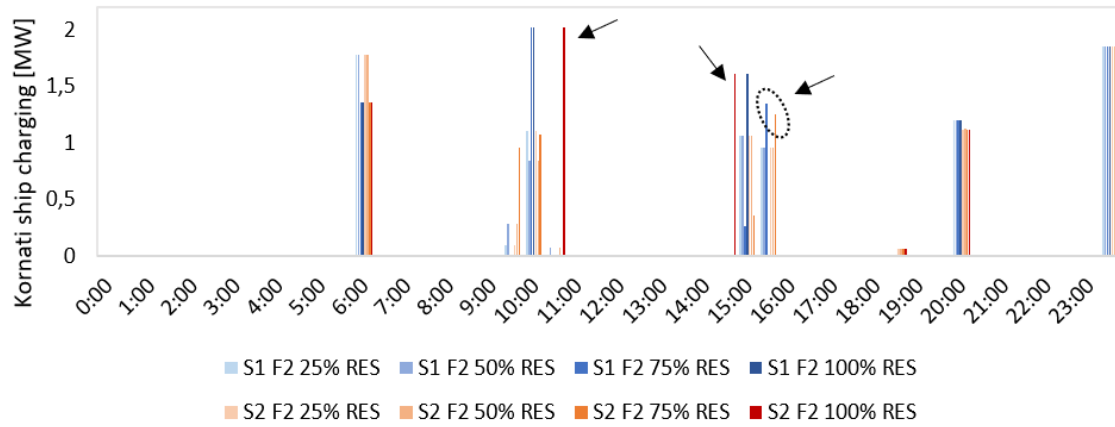


Figure 36 Minimum demand: Charging schedule for Krk and Kornati electric ships for different RES shares

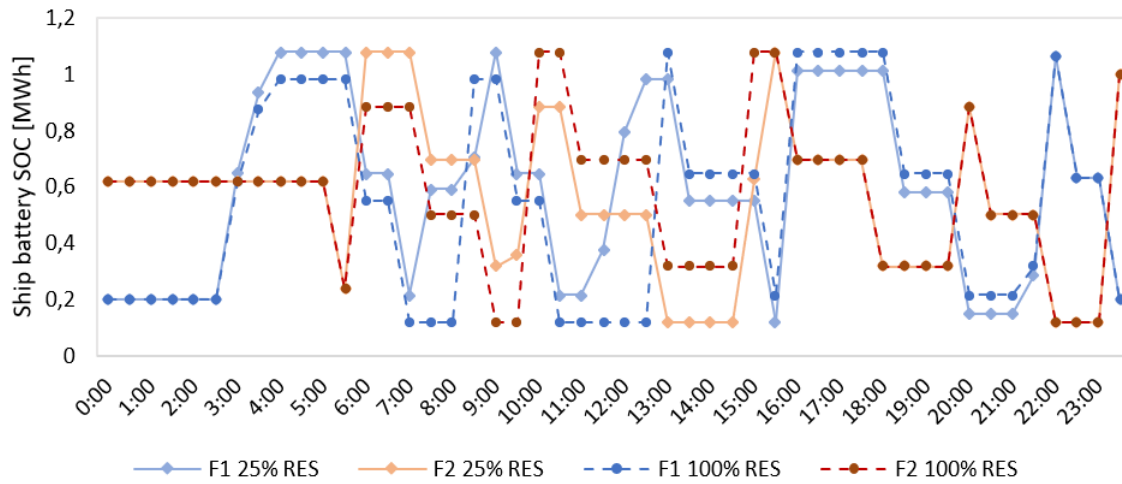


Figure 37 Minimum demand: State of the charge of the Krk and Kornati for different RES shares

Figure 38 shows the voltage magnitude at node 4 for the minimum demand case. It can be seen that the voltage differences between different scenarios are significantly higher for the higher RES shares (marked with dotted circles). Because of the high production from RES, there is the need for additional flexibility in the system which was mostly provided by the battery storage system and smart management of charging in the Merag port. The difference is that, for the S1 scenario, voltage magnitude can only be reduced by charging management, while the battery system can also increase the voltage magnitude by discharging during periods of lower RES production.

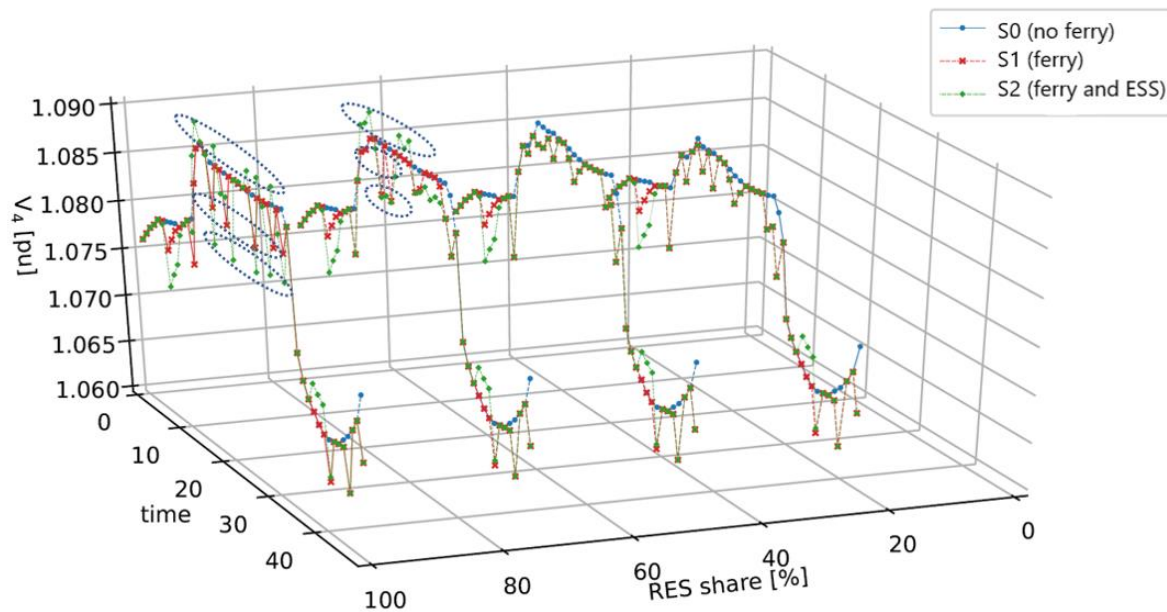


Figure 38 Voltage magnitude at node 4 for different scenarios and RES shares

Table 3 presents the curtailed energy for three scenarios and different RES shares. It can be seen that the electrification of maritime transport can successfully be integrated with the rest of the energy system. Smart cross-sector integration of the maritime and power sector increases the possibility for RES integration and reduces the curtailed energy and overall system operation cost. Additional inclusion of the battery storage system further contributed to the reduction of the curtailed energy and increased efficiency of the system operation.

Table 3 Curtailed energy in the energy system for different scenarios and RES shares

RES share / Scenario	S0	S1	S2
25%	0	0	0
50%	0.234	0	0
75%	5.6	3.68	2.51
100%	25.11	22.65	21.18

The results of this research showed that maritime transport to and from the islands can successfully be electrified and integrated into the island energy system. Smart integration of maritime transport lead to the increased possibility for RES integration as the curtailed energy values were reduced.

4 CONCLUSIONS AND FUTURE WORK

This thesis represents comprehensive research regarding advanced energy planning on smart islands. It includes novel methods with various approaches for the energy planning of islands. It investigates the role and potential of advanced technologies and their optimal integration into the island energy systems. The methods and results presented in the thesis contribute to the objective that is both urgent and complex – the decarbonisation of the energy system.

The main objective of this thesis was to develop methods that support islands in their energy transition. The hypothesis of this thesis stated that it is possible to show that the transformation of island energy systems to renewable energy systems is possible and that it is possible to quantify the risk level for specific energy planning scenarios. The hypothesis of this thesis has been confirmed.

The thesis presented several scientific contributions to the planning of energy systems of islands. The technologies modelled in the thesis include residential and large-scale solar power plants, onshore and offshore wind power plants, combined heat and power units, hydropower plants, batteries, thermal energy storage, hydrogen technologies etc. High importance was given to the investigation of the flexibility options on islands, primarily by sector coupling, storage and demand response integration. There are several key outtakes from the research conducted in this thesis.

First, it was shown that by applying the Smart Islands method it was possible to generate energy planning scenarios that reflect on islands' needs and resources. The method generated scenarios with a defined type and quantity of required technology for meeting islands' needs with resources. The robustness of the method with regard to technical input parameters and specific investment costs of the technology was tested by applying the Monte Carlo method. The capacity of specific technologies adjusted to different scenarios and types of technologies remained the same. The method presents a useful tool for the policymakers that can stimulate

specific technologies in order to help islands locally meet their needs with resources or the investors who can decide on the technology to invest in based on the results.

Second, it was shown that by using the risk assessment method developed in PAPER 2 it was possible to quantify the risk value of specific energy planning scenarios. This represents a suitable comparison indicator when making decisions about the type and capacity of the technologies to be installed on the islands. Moreover, it was shown that this method can also define the necessary capacity and type of technology to be installed to make an island independent of the electrical interconnection. Since islands are often characterised by weak interconnection, this result is even more relevant. Similarly, as the Smart Islands method, the risk assessment method can also be used as a decision-making factor. It can also be used in order to promote the energy transition among islanders as secure supply is one of the priorities for the island communities.

Third, this thesis presented an advanced energy planning approach based on detailed spatio-temporal modelling and soft-linked to the power flow. The application of the method lead to several conclusions. It was shown that differences between spatially distributed modelling and coarser modelling are significant and that energy system topology should be accounted for. It was also shown that power grid aspects should be also considered as island energy planning scenarios may require additional grid investments not considered in the energy planning models.

Fourth, the research regarding the advanced technologies – demand response and energy storage system integration in the energy systems on islands was carried out in PAPER 4 and PAPER 5. The implementation of such technologies in island energy systems is of great importance as they include islanders in the energy systems and make them active participants in the energy transition of islands. The joint conclusion is that the integration of the demand response and energy storage systems lead to the lower operating cost of the energy system, a higher possibility for the integration of renewable energy sources in the island energy systems and additional revenue streams for the flexibility providers. Additionally, the method presented in PAPER 4 also includes an incentive for the demand response providers and is suitable for evaluating the impacts of different incentive values. The results showed that higher incentives should be used with systems with a lower share of the flexible load, while lower incentives should be used in systems with a higher share of the flexible load. The research in PAPER 5

presented a method that modelled demand response providers and energy storage systems as actors in the energy and reserve market in a joint network-constrained energy and reserve market formulation and concluded that business models for these technologies can generate a higher revenue than just participating on the energy market.

Finally, the effect of maritime electrification was analysed in PAPER 6. The results showed that the electrification of maritime transport and its integration into the distribution system can unlock additional flexibility that increases the possibility for the integration of renewable energy sources. Moreover, such smart system is able to more easily control its technical variables and increase the system efficiency by reducing the value of the curtailed energy.

This thesis offered several contributions to the advanced energy planning on islands. However, additional research should be further conducted in order to accelerate the decarbonisation of islands and transfer the solutions from islands to the mainland area. The role of flexibility should be further investigated and it will require detailed models that fully capture the effects of the smart energy systems. Methods and approaches for the inclusion of islanders in energy transition should be also considered in the smart energy system models as their acceptance is crucial for the successful decarbonisation of the islands. Finally, this PhD thesis showed that existing technologies are sufficient for overcoming the challenge of the energy transition. However, there is still a need for the development of markets and policies that will accelerate the transition and fully transform this great challenge into a great opportunity.

5 LITERATURE

- [1] Huang HF, Lo SL. Review and classify the GHGs-related indicators. *Renew Sustain Energy Rev* 2011;15. <https://doi.org/10.1016/j.rser.2010.07.023>.
- [2] United Nations Conference on the Human Environment. *Europhys News* 1972;3. <https://doi.org/10.1051/epn/19720307006>.
- [3] United Nations. A/CONF.151/26/Vol.I: Rio Declaration on Environment and Development. Rep United Nations Conf Environ Dev 1992;I.
- [4] Baste IA, Watson RT. Tackling the climate, biodiversity and pollution emergencies by making peace with nature 50 years after the Stockholm Conference. *Glob Environ Chang* 2022;73. <https://doi.org/10.1016/j.gloenvcha.2022.102466>.
- [5] Abeydeera LHUW, Mesthrige JW, Samarasinghalage TI. Global research on carbon emissions: A scientometric review. *Sustain* 2019;11. <https://doi.org/10.3390/su11143972>.
- [6] Jahn A. Reduced probability of ice-free summers for 1.5 °c compared to 2 °c warming. *Nat Clim Chang* 2018;8. <https://doi.org/10.1038/s41558-018-0127-8>.
- [7] United Nations. Paris Agreement - UNFCCC. 2015.
- [8] Chen X, Yang F, Zhang S, Zakeri B, Chen X, Liu C, et al. Regional emission pathways, energy transition paths and cost analysis under various effort-sharing approaches for meeting Paris Agreement goals. *Energy*, vol. 232, 2021. <https://doi.org/10.1016/j.energy.2021.121024>.
- [9] Bataille C, Åhman M, Neuhoﬀ K, Nilsson LJ, Fischedick M, Lechtenböhmer S, et al. A review of technology and policy deep decarbonization pathway options for making energy-intensive industry production consistent with the Paris Agreement. *J Clean Prod* 2018;187. <https://doi.org/10.1016/j.jclepro.2018.03.107>.
- [10] Kang JN, Wei YM, Liu LC, Han R, Yu BY, Wang JW. Energy systems for climate change mitigation: A systematic review. *Appl Energy* 2020;263. <https://doi.org/10.1016/j.apenergy.2020.114602>.
- [11] Climate Action Tracker. Glasgow's 2030 credibility gap: net zero's lip service to climate action Wave of net zero emission goals not matched by action on the ground. 2021.
- [12] European Commission. 2009/28/EG - The 2020 climate and energy package. *Eur Comm* 2014.

- [13] European Environment Agency. Trends and projections in Europe 2021. 2021.
- [14] European Commission. Communication from the Commission: The European Green Deal. COM(2019) 640 Final 2019.
- [15] European Commission. Sustainable Europe Investment Plan European - European Green Deal Investment Plan. J Chem Inf Model 2019;53.
- [16] European Commission. Annex - REPowerEU: Joint European Action for more affordable, secure and sustainable energy EN 2022.
- [17] European Commission. Clean Energy for EU Islands launch. Eur Comm Energy News 2017.
- [18] European Commission. Clean energy for European Union islands: The memorandum of Split. 2020.
- [19] European Commission. Smart Island Initiative 2017.
- [20] Matschoss K, Fahy F, Rau H, Backhaus J, Goggins G, Grealis E, et al. Challenging practices: experiences from community and individual living lab approaches. Sustain Sci Pract Policy 2021;17. <https://doi.org/10.1080/15487733.2021.1902062>.
- [21] Mimica M, Krajacic G, Medved D, Jardas D. Digitalization and smart islands in the kvarner archipelago. 2020 43rd Int. Conv. Information, Commun. Electron. Technol. MIPRO 2020 - Proc., 2020. <https://doi.org/10.23919/MIPRO48935.2020.9245328>.
- [22] Sperling K. How does a pioneer community energy project succeed in practice? The case of the Samsø Renewable Energy Island. Renew Sustain Energy Rev 2017;71. <https://doi.org/10.1016/j.rser.2016.12.116>.
- [23] Dileep G. A survey on smart grid technologies and applications. Renew Energy 2020;146. <https://doi.org/10.1016/j.renene.2019.08.092>.
- [24] Tosatto A, Martinez Beseler X, Østergaard J, Pinson P, Chatzivasileiadis S. North Sea Energy Islands: Impact on national markets and grids. Energy Policy 2022;167:112907. <https://doi.org/10.1016/j.enpol.2022.112907>.
- [25] IPCC. Summary for Policymakers. 2018.
- [26] Lund H, Østergaard PA, Connolly D, Mathiesen BV. Smart energy and smart energy systems. Energy 2017. <https://doi.org/10.1016/j.energy.2017.05.123>.
- [27] Mancarella P. MES (multi-energy systems): An overview of concepts and evaluation models. Energy 2014;65. <https://doi.org/10.1016/j.energy.2013.10.041>.
- [28] Bogdanov D, Ram M, Aghahosseini A, Gulagi A, Oyewo AS, Child M, et al. Low-cost renewable electricity as the key driver of the global energy transition towards sustainability. Energy 2021;227. <https://doi.org/10.1016/j.energy.2021.120467>.

- [29] Skjølsvold TM, Ryghaug M, Throndsen W. European island imaginaries: Examining the actors, innovations, and renewable energy transitions of 8 islands. *Energy Res Soc Sci* 2020;65. <https://doi.org/10.1016/j.erss.2020.101491>.
- [30] Kotzebue JR, Weissenbacher M. The EU's Clean Energy strategy for islands: A policy perspective on Malta's spatial governance in energy transition. *Energy Policy* 2020;139. <https://doi.org/10.1016/j.enpol.2020.111361>.
- [31] Lee T, Glick MB, Lee JH. Island energy transition: Assessing Hawaii's multi-level, policy-driven approach. *Renew Sustain Energy Rev* 2020;118. <https://doi.org/10.1016/j.rser.2019.109500>.
- [32] Hauer ME, Fussell E, Mueller V, Burkett M, Call M, Abel K, et al. Sea-level rise and human migration. *Nat Rev Earth Environ* 2020;1. <https://doi.org/10.1038/s43017-019-0002-9>.
- [33] McIntyre A, El-Ashram AM, Ronci M, Reynaud J, Che N, Wang K, et al. *Caribbean Energy: Macro-Related Challenges*. 2016.
- [34] M.Supapo KR, Lozano L, F.Tabañag ID, M.Querikiol E. Untangling the impact of socio-demographic factors on energy consumption: Why is energy access difficult to achieve in off-grid island communities? *Energy Sustain Dev* 2022;70:32–44. <https://doi.org/10.1016/j.esd.2022.07.005>.
- [35] Matsumoto K, Matsumura Y. Challenges and economic effects of introducing renewable energy in a remote island: A case study of Tsushima Island, Japan. *Renew Sustain Energy Rev* 2022;162:112456. <https://doi.org/10.1016/j.rser.2022.112456>.
- [36] Duić N, Krajačić G, da Graça Carvalho M. RenewIslands methodology for sustainable energy and resource planning for islands. *Renew Sustain Energy Rev* 2008. <https://doi.org/10.1016/j.rser.2006.10.015>.
- [37] Krajačić G, Martins R, Busuttil A, Duić N, da Graça Carvalho M. Hydrogen as an energy vector in the islands' energy supply. *Int J Hydrogen Energy* 2008. <https://doi.org/10.1016/j.ijhydene.2007.12.025>.
- [38] Petruschke P, Gasparovic G, Voll P, Krajačić G, Duić N, Bardow A. A hybrid approach for the efficient synthesis of renewable energy systems. *Appl Energy* 2014. <https://doi.org/10.1016/j.apenergy.2014.03.051>.
- [39] Pfeifer A, Dobravec V, Pavlinek L, Krajačić G, Duić N. Integration of renewable energy and demand response technologies in interconnected energy systems. *Energy* 2018. <https://doi.org/10.1016/j.energy.2018.07.134>.
- [40] Meschede H, Bertheau P, Khalili S, Breyer C. A review of 100% renewable energy

- scenarios on islands. WIREs Energy Environ 2022. <https://doi.org/10.1002/wene.450>.
- [41] Duić N, Da Graça Carvalho M. Increasing renewable energy sources in island energy supply: Case study Porto Santo. *Renew Sustain Energy Rev* 2004;8. <https://doi.org/10.1016/j.rser.2003.11.004>.
- [42] Gašparović G, Krajačić G, Duić N, Baotić M. New Energy Planning Software for Analysis of Island Energy Systems and Microgrid Operations - H2RES Software as a Tool to 100% Renewable Energy System. *Comput Aided Chem Eng* 2014. <https://doi.org/10.1016/B978-0-444-63455-9.50144-6>.
- [43] Krajačić G, Duić N, Carvalho M da G. H2RES, Energy planning tool for island energy systems - The case of the Island of Mljet. *Int J Hydrogen Energy* 2009;34. <https://doi.org/10.1016/j.ijhydene.2008.12.054>.
- [44] Busuttil A, Krajačić G, Duić N. Energy scenarios for Malta. *Int J Hydrogen Energy* 2008;33. <https://doi.org/10.1016/j.ijhydene.2008.06.010>.
- [45] Segurado R, Krajačić G, Duić N, Alves L. Increasing the penetration of renewable energy resources in S. Vicente, Cape Verde. *Appl Energy* 2011. <https://doi.org/10.1016/j.apenergy.2010.07.005>.
- [46] Lund H, Thellufsen JZ. EnergyPLAN: Advanced energy systems analysis computer model. Documentation Version 16.0. 2021.
- [47] Lund H, Duić N, Krajačić G, Graça Carvalho M da. Two energy system analysis models: A comparison of methodologies and results. *Energy* 2007. <https://doi.org/10.1016/j.energy.2006.10.014>.
- [48] Yue CD, Chen CS, Lee YC. Integration of optimal combinations of renewable energy sources into the energy supply of Wang-An Island. *Renew Energy* 2016. <https://doi.org/10.1016/j.renene.2015.08.073>.
- [49] Calise F, Duić N, Pfeifer A, Vicidomini M, Orlando AM. Moving the system boundaries in decarbonization of large islands. *Energy Convers Manag* 2021;234. <https://doi.org/10.1016/j.enconman.2021.113956>.
- [50] Arévalo P, Cano A, Jurado F. Mitigation of carbon footprint with 100% renewable energy system by 2050: The case of Galapagos islands. *Energy* 2022;245. <https://doi.org/10.1016/j.energy.2022.123247>.
- [51] Østergaard PA, Lund H, Thellufsen JZ, Sorknæs P, Mathiesen B. Review and validation of EnergyPLAN. *Renew Sustain Energy Rev* 2022;168:112724. <https://doi.org/10.1016/j.rser.2022.112724>.
- [52] HOMER Energy LLC. HOMER Pro Version 3.7 User Manual. 2016.

- [53] Uwineza L, Kim HG, Kim CK. Feasibility study of integrating the renewable energy system in Popova Island using the Monte Carlo model and HOMER. *Energy Strateg Rev* 2021;33. <https://doi.org/10.1016/j.esr.2020.100607>.
- [54] Groppi D, Astiaso Garcia D, Lo Basso G, De Santoli L. Synergy between smart energy systems simulation tools for greening small Mediterranean islands. *Renew Energy* 2019;135. <https://doi.org/10.1016/j.renene.2018.12.043>.
- [55] Sadrul Islam AKM, Rahman MM, Mondal MAH, Alam F. Hybrid energy system for St. Martin island, Bangladesh: An optimized model. *Procedia Eng.*, 2012. <https://doi.org/10.1016/j.proeng.2012.10.126>.
- [56] Goldstein G, Kanudia A, Lehtila A, Remme U, Wright E. Documentation for the TIMES Model Part III. 2021.
- [57] Zhou W, Hagos DA, Stikbakke S, Huang L, Cheng X, Onstein E. Assessment of the impacts of different policy instruments on achieving the deep decarbonization targets of island energy systems in Norway – The case of Hinnøya. *Energy* 2022;246. <https://doi.org/10.1016/j.energy.2022.123249>.
- [58] Dominkovic DF, Stark G, Hodge BM, Pedersen AS. Integrated energy planning with a high share of variable renewable energy sources for a Caribbean Island. *Energies* 2018;11. <https://doi.org/10.3390/en11092193>.
- [59] Barone G, Buonomano A, Forzano C, Giuzio GF, Palombo A. Increasing renewable energy penetration and energy independence of island communities: A novel dynamic simulation approach for energy, economic, and environmental analysis, and optimization. *J Clean Prod* 2021;311. <https://doi.org/10.1016/j.jclepro.2021.127558>.
- [60] Wang Z, Lin X, Tong N, Li Z, Sun S, Liu C. Optimal planning of a 100% renewable energy island supply system based on the integration of a concentrating solar power plant and desalination units. *Int J Electr Power Energy Syst* 2020. <https://doi.org/10.1016/j.ijepes.2019.105707>.
- [61] Raveendran V, Alvarez-Bel C, Nair MG. Assessing the ancillary service potential of electric vehicles to support renewable energy integration in touristic islands: A case study from Balearic island of Menorca. *Renew Energy* 2020;161. <https://doi.org/10.1016/j.renene.2020.06.083>.
- [62] Prina MG, Groppi D, Nastasi B, Garcia DA. Bottom-up energy system models applied to sustainable islands. *Renew Sustain Energy Rev* 2021;152. <https://doi.org/10.1016/j.rser.2021.111625>.
- [63] Bueno C, Carta JA. Technical-economic analysis of wind-powered pumped

- hydrostorage systems. Part I: Model development. *Sol Energy* 2005;78.
<https://doi.org/10.1016/j.solener.2004.08.006>.
- [64] Fernández-Muñoz D, Pérez-Díaz JI. Contribution of non-conventional pumped storage hydropower plant configurations in an isolated power system with an increasing share of renewable energy. *IET Renew Power Gener* 2020;14. <https://doi.org/10.1049/iet-rpg.2019.0874>.
- [65] Katsaprakakis D Al, Voumvoulakis M. A hybrid power plant towards 100% energy autonomy for the island of Sifnos, Greece. Perspectives created from energy cooperatives. *Energy* 2018;161. <https://doi.org/10.1016/j.energy.2018.07.198>.
- [66] Groppi D, Pfeifer A, Garcia DA, Krajačić G, Duić N. A review on energy storage and demand side management solutions in smart energy islands. *Renew Sustain Energy Rev* 2021;135. <https://doi.org/10.1016/j.rser.2020.110183>.
- [67] Curto D, Favuzza S, Franzitta V, Guercio A, Amparo Navarro Navia M, Telaretti E, et al. Grid Stability Improvement Using Synthetic Inertia by Battery Energy Storage Systems in Small Islands. *Energy* 2022;254:124456.
<https://doi.org/10.1016/j.energy.2022.124456>.
- [68] Pacheco A, Monteiro J, Santos J, Sequeira C, Nunes J. Energy transition process and community engagement on geographic islands: The case of Culatra Island (Ria Formosa, Portugal). *Renew Energy* 2022;184.
<https://doi.org/10.1016/j.renene.2021.11.115>.
- [69] Masala F, Groppi D, Nastasi B, Piras G, Garcia DA. Techno-economic analysis of biogas production and use scenarios in a small island energy system. *Energy* 2022;258:124831. <https://doi.org/10.1016/j.energy.2022.124831>.
- [70] Almoghayer MA, Woolf DK, Kerr S, Davies G. Integration of tidal energy into an island energy system – A case study of Orkney islands. *Energy* 2022;242.
<https://doi.org/10.1016/j.energy.2021.122547>.
- [71] Nikolaidis G, Karaolia A, Matsikaris A, Nikolaidis A, Nicolaidis M, Georgiou GC. Blue energy potential analysis in the Mediterranean. *Front Energy Res* 2019;7.
<https://doi.org/10.3389/fenrg.2019.00062>.
- [72] Stančin H, Pfeifer A, Perakis C, Stefanatos N, Damasiotis M, Magaouda S, et al. Blue Energy Spearheading the Energy Transition: The Case of Crete. *Front Energy Res* 2022;10:868334. <https://doi.org/10.3389/fenrg.2022.868334>.
- [73] Meschede H. Analysis on the demand response potential in hotels with varying probabilistic influencing time-series for the Canary Islands. *Renew Energy* 2020;160.

- <https://doi.org/10.1016/j.renene.2020.06.024>.
- [74] Fukaume S, Nagasaki Y, Tsuda M. Stable power supply of an independent power source for a remote island using a Hybrid Energy Storage System composed of electric and hydrogen energy storage systems. *Int J Hydrogen Energy* 2022;47. <https://doi.org/10.1016/j.ijhydene.2022.02.142>.
 - [75] Bach H, Bergek A, Bjørgum Ø, Hansen T, Kenzhegaliyeva A, Steen M. Implementing maritime battery-electric and hydrogen solutions: A technological innovation systems analysis. *Transp Res Part D Transp Environ* 2020;87. <https://doi.org/10.1016/j.trd.2020.102492>.
 - [76] Sæther SR, Moe E. A green maritime shift: Lessons from the electrification of ferries in Norway. *Energy Res Soc Sci* 2021;81. <https://doi.org/10.1016/j.erss.2021.102282>.
 - [77] Dorotić H, Doračić B, Dobravec V, Pukšec T, Krajačić G, Duić N. Integration of transport and energy sectors in island communities with 100% intermittent renewable energy sources. *Renew Sustain Energy Rev* 2019;99. <https://doi.org/10.1016/j.rser.2018.09.033>.
 - [78] Pfeifer A, Prebeg P, Duić N. Challenges and opportunities of zero emission shipping in smart islands: A study of zero emission ferry lines. *ETransportation* 2020;3. <https://doi.org/10.1016/j.etrans.2020.100048>.
 - [79] Perčić M, Ančić I, Vladimir N. Life-cycle cost assessments of different power system configurations to reduce the carbon footprint in the Croatian short-sea shipping sector. *Renew Sustain Energy Rev* 2020;131. <https://doi.org/10.1016/j.rser.2020.110028>.
 - [80] Gurobi Optimization L. Gurobi Optimizer Reference Manual. <https://www.gurobi.com/doc> Aufgerufen Am 27.10.2020 2020.
 - [81] GAMS. GAMS GDX facilities and tools. Continuum (Minneapolis Minn) 2012;18.
 - [82] Pfenninger S, Pickering B. Calliope: a multi-scale energy systems modelling framework. *J Open Source Softw* 2018;3. <https://doi.org/10.21105/joss.00825>.
 - [83] Busarello, Cott, Partner Inc., ABB Utilities GmbH. NEPLAN Users' guide Electrical, Version 5. n.d.
 - [84] Jarre F, Vavasis SA. Convex optimization. Algorithms Theory Comput. Handbook, Second Ed. Vol. 1 Gen. Concepts Tech., 2009. <https://doi.org/10.1201/b11399-3>.
 - [85] Matak N, Mimica M, Krajačić G. Optimising the Cost of Reducing the CO₂ Emissions in Sustainable Energy and Climate Action Plans. *Sustain* 2022;14. <https://doi.org/10.3390/su14063462>.
 - [86] Huang Y, Pardalos PM, Zheng QP. Deterministic Unit Commitment Models and

- Algorithms, 2017. https://doi.org/10.1007/978-1-4939-6768-1_2.
- [87] Huang Y, Zheng QP, Wang J. Two-stage stochastic unit commitment model including non-generation resources with conditional value-at-risk constraints. *Electr Power Syst Res* 2014;116. <https://doi.org/10.1016/j.epsr.2014.07.010>.
 - [88] Pandžić H, Bobanac V. An accurate charging model of battery energy storage. *IEEE Trans Power Syst* 2019;34. <https://doi.org/10.1109/TPWRS.2018.2876466>.
 - [89] Christie RD, Wollenberg BF, Wangensteen I. Transmission management in the deregulated environment. *Proc IEEE* 2000;88. <https://doi.org/10.1109/5.823997>.
 - [90] Overbye TJ, Cheng X, Sun Y. A comparison of the AC and DC power flow models for LMP calculations. *Proc. Hawaii Int. Conf. Syst. Sci.*, vol. 37, 2004. <https://doi.org/10.1109/hicss.2004.1265164>.
 - [91] Bolfek M, Capuder T. A practical approach to flexibility provision assessment in an unobservable distribution network. *Electr Power Syst Res* 2022;212:108262. <https://doi.org/10.1016/J.EPSR.2022.108262>.
 - [92] Zimmerman RD, Murillo-Sánchez CE, Thomas RJ. MATPOWER: Steady-state operations, planning, and analysis tools for power systems research and education. *IEEE Trans Power Syst* 2011;26. <https://doi.org/10.1109/TPWRS.2010.2051168>.
 - [93] Pfenninger S. Dealing with multiple decades of hourly wind and PV time series in energy models: A comparison of methods to reduce time resolution and the planning implications of inter-annual variability. *Appl Energy* 2017. <https://doi.org/10.1016/j.apenergy.2017.03.051>.
 - [94] Calliope. Calliope documentation: Mathematical formulation n.d.
 - [95] Verbeke J, Cools R. The newton-raphson method. *Int J Math Educ Sci Technol* 1995;26. <https://doi.org/10.1080/0020739950260202>.
 - [96] Ferroukhi R, Khalid A, Lopez-Peña A, Renner M. “Renewable Energy and Jobs: Annual Review 2014.” *Int Renew Energy Agency* 2014.
 - [97] Meschede H, Esparcia EA, Holzapfel P, Bertheau P, Ang RC, Blanco AC, et al. On the transferability of smart energy systems on off-grid islands using cluster analysis – A case study for the Philippine archipelago. *Appl Energy* 2019;251. <https://doi.org/10.1016/j.apenergy.2019.05.093>.
 - [98] Wang C, Yan C, Li G, Liu S, Bie Z. Risk assessment of integrated electricity and heat system with independent energy operators based on Stackelberg game. *Energy* 2020;198. <https://doi.org/10.1016/j.energy.2020.117349>.
 - [99] Frew BA, Jacobson MZ. Temporal and spatial tradeoffs in power system modeling

- with assumptions about storage: An application of the POWER model. *Energy* 2016;117:198–213. <https://doi.org/10.1016/j.energy.2016.10.074>.
- [100] Deane JP, Chiodi A, Gargiulo M, Ó Gallachóir BP. Soft-linking of a power systems model to an energy systems model. *Energy* 2012;42. <https://doi.org/10.1016/j.energy.2012.03.052>.
- [101] Dominković DF, Junker RG, Lindberg KB, Madsen H. Implementing flexibility into energy planning models: Soft-linking of a high-level energy planning model and a short-term operational model. *Appl Energy* 2020;260. <https://doi.org/10.1016/j.apenergy.2019.114292>.
- [102] Kirschen D, Strbac G. *Fundamentals of Power System Economics*. 2005. <https://doi.org/10.1002/0470020598>.
- [103] Read EG, Drayton-Bright GR, Ring BJ. An Integrated Energy and Reserve Market for New Zealand. *Deregul. Electr. Util.*, 1998. https://doi.org/10.1007/978-1-4615-5729-6_13.
- [104] Pandžić K, Pavić I, Androćec I, Pandžić H. Optimal Battery Storage Participation in European Energy and Reserves Markets. *Energies* 2020;13. <https://doi.org/10.3390/en13246629>.

6 CURRICULUM VITAE

Marko Mimica was born on March 4th 1994 in Split, Croatia where he went to primary school and Fourth gymnasium Marko Marulić. In 2012 he started his study at Faculty of electrical engineering, University of Zagreb where he successfully obtained Masters' Degree in 2017. In 2016/17 he was a president of Electrical Engineering Students' European Association – EESTEC LC Zagreb and he was also a member of the Faculty council of Faculty of electrical engineering and computing. From 2014 to the end of his Masters' Degree he was working for Končar Group d.d. and for Circular Energy Resources Ltd. After his study, from 2017 to 2018 he worked for Siemens d.d.

In 2018 he enrolled a PhD at the Faculty of mechanical engineering and naval architecture, University of Zagreb under the mentorship of prof. Goran Krajačić and was employed as a Research Assistant. His research interest includes advanced energy system planning and optimization with emphasis on the RES integration. He developed methods that support the islands in their energy transition and applied new energy planning approaches on the island energy systems.

During his research work he also worked on several research and innovation projects. He works on the H2020 INSULAE project that deals with the decarbonisation of the geographical islands. He also worked on YENESIS project that deals with the youth employment on the islands. During his research work he also participated in the preparation of several project and studies regarding the maritime electrification and electric grid impact.

He is also a member of the Senate of the University of Zagreb as a representative of the doctoral students of technical and natural sciences from 2019 and he is also a member of the Quality Management Board of the University of Zagreb since 2021. He is a member of the Technical Council of the University of Zagreb since 2020. He was the president of the Student Council of the University of Zagreb in 2021.

During his four years of research he was the author of 7 scientific papers and 8 conference papers. His current h-index is 4 (Scopus).

7 SUMMARY OF PAPERS

PAPER 1

M. Mimica, G. Krajačić, The Smart Islands method for defining energy planning scenarios on islands, *Energy*, 237, 121653, 2021. DOI: 10.1016/j.energy.2021.121653

Islands represent areas where it is possible to have a clear overview of resources and needs over a large number of sectors. Because of this, the developed energy planning scenarios on the islands should reflect the possibility of meeting local needs with available resources of a wide range of sectors. This is often not the case in the current studies that analyse only a limited number of sectors. The developed method automatically combines needs and resources based on the quantitative indicators and generates energy planning scenarios with precisely defined types and the capacities of required technologies. The results show that the Smart Islands method provides 7 energy planning scenarios for Krk island with different technology mixes. The case study for Vis island is considered for cases with and without electrical interconnection. When the interconnection is not considered, the method suggests a 5.42 MWh battery system for maintaining grid stability. The results indicate that the Smart Islands method can be applied to islands with different characteristics as well as suggest optimal energy planning scenarios while meeting needs with local resources.

In this paper, the indexation method for mapping the islands' resources and needs, the optimization model and overall the Smart Islands method was designed by Marko Mimica. Goran Krajačić reviewed the methods and suggested possible interpretations of result. The paper was written by Marko Mimica and reviewed by Goran Krajačić.

PAPER 2

M. Mimica, L.G. De Urtasun, G. Krajačić, A robust risk assessment method for energy planning scenarios on smart islands under the demand uncertainty, *Energy*, 240, 122769, 2022. DOI: 10.1016/j.energy.2021.122769

Energy systems with a high share of variable renewable energy are more vulnerable to sudden changes in the system operation. This is especially emphasized on small systems such as energy systems on geographical islands. Because of these reasons, there is a need for quantifying the risk of energy scenarios of such systems. This paper presents a novel robust risk assessment method under demand uncertainty for energy planning scenarios for the islands. The method uses graph theory for the representation of power system topology. The Poisson distribution is used for calculating the probability of power system element failure. The robust modelling approach is applied by the introduction of auxiliary variables and compared to the deterministic model results. Four energy planning scenarios for Unije island are modelled and subjugated to several power system outages resulting in a risk vector calculated as the product of probability vector and damage matrix. The study also presents a zero-import risk energy planning scenario for Unije island that is achieved for a system of 0.5 MW photovoltaic plant and 3.55 MWh battery storage system.

PAPER 2 was written by Marko Mimica and reviewed by Laura Gimenez de Urtasun and Goran Krajačić. The overall risk assessment method was designed and carried out by Marko Mimica. Laura Gimenez de Urtasun and Goran Krajačić reviewed the results.

PAPER 3

M. Mimica, D.F. Dominković, V. Kirinčić, G. Krajačić, Soft-linking of improved spatiotemporal capacity expansion model with a power flow analysis for increased integration of renewable energy sources into interconnected archipelago, Applied Energy, 305, 117855, 2022. DOI: 10.1016/j.apenergy.2021.117855

This present study offers a novel approach for the improvement of energy planning. This has become increasingly important as higher penetration of variable energy resources and increased interconnection between the different energy sectors require more detailed planning in terms of spatiotemporal modeling in comparison to the presently available approaches. In this study, we present a method that soft-linked the energy planning and power flow models, which enabled fast and reliable solving of optimization problems. A linear continuous optimization model was used for the energy system optimization and the non-linear problem for the power system analysis. The method is used to compare different energy planning scenarios; further, this also offers the possibility for implementation assessment of the proposed scenarios. The method was applied to interconnected islands for five different scenarios. It was determined that the detailed spatial approach resulted in 26.7% higher total system costs, 3.3 times lower battery capacity, and 14.9 MW higher renewable energy generation capacities installed than in the coarser spatial representation. Moreover, the results of the power flow model indicated that the highest voltage deviation was 16% higher than the nominal voltage level. This indicates the need for inclusion of implementation possibility assessments of energy planning scenarios.

Marko Mimica and Dominik Franjo Dominković developed the soft-linking method presented in PAPER 3 and analysed the results. Vedran Kirinčić run the power flow calculation. Goran Krajačić and Marko Mimica provided the input data for the energy planning model. The paper was written by Marko Mimica and Dominik Franjo Dominković and reviewed by Goran Krajačić and Vedran Kirinčić.

PAPER 4

M. Mimica, D.F. Dominković, T. Capuder, G. Krajačić, On the value and potential of demand response in the Smart island archipelago, Renewable Energy, 176, 153-168, 2021. DOI: 10.1016/j.renene.2021.05.043

Existing studies propose different demand response models and often test them on islands that represent test-beds for new technologies. However, proposed models are often simplified and integrated into energy system models that do not consider the existing limitations of the power grid. This study proposes a novel demand response model based on price differentials on the day-ahead electricity market. The model is implemented in the distribution system that considers all relevant grid constraints. The case study is conducted in an archipelago characterised by a medium-voltage distribution system connected to the mainland grid. The obtained results showed that the implementation of the proposed demand response model caused a 0.13 kV voltage deviation which did not cause voltage issues for the observed distribution system. The breakpoint incentive was achieved for an incentive value of 23% of the day-ahead market, and the demand response was not activated for higher values than the breakpoint incentive. The highest savings amounted to 258.7 € for the scenario with the highest flexibility allowed. The results implicate that implementing the demand response model in the grid would benefit all observed stakeholders in the system.

The demand response model and the optimization model were developed by Marko Mimica. Tomislav Capuder and Dominik Franjo Dominković suggested the scenario designs. The paper was written by Marko Mimica and reviewed by Goran Krajačić, Tomislav Capuder and Dominik Franjo Dominković.

PAPER 5

M. Mimica, Z. Sinovčić, A. Jokić, G. Krajačić, The role of the energy storage and the demand response in the robust reserve and network-constrained joint electricity and reserve market, *Electric Power Systems Research*, 204, 107716, 2022. DOI: 10.1016/j.epsr.2021.107716

Increase of the variable renewable energy sources in the power system is causing additional needs for the reserve in the system. On the other hand, the integration of energy storage and the demand response offers additional sources of flexibility in the system. Most of the current studies that model energy systems do not model the reserve market. Because of this, these studies eliminate the possibility to assess the full benefits of energy storage and demand response. The method proposed in this study enables the comparison between the two approaches and evaluates the benefits of energy storage and demand response for both approaches. The case study was conducted on the power system consisted of 13 interconnected nodes. The results showed that the operation cost of the system was 28.1% higher when the reserve constraints were imposed for the most pessimistic scenario. Moreover, the results showed that energy storage and flexible loads achieved significantly higher revenues when they were able to participate in the reserve market. The results indicated the need for the development of the reserve market as well as frameworks that will enable the energy storage and the demand response to participate in the reserve markets.

The optimization model was developed by Marko Mimica. Andrej Jokić contributed to the modelling of robust formulation of optimization problem. Zoran Sinovčić provided the input data for the transmission system. Marko Mimica wrote the paper. Goran Krajačić, Andrej Jokić and Zoran Sinovčić reviewed the paper.

PAPER 6

M. Mimica, M. Perčić, N. Vladimir, G. Krajačić, Cross-sectoral integration for increased penetration of renewable energy sources in the energy system – unlocking the flexibility potential of maritime transport electrification, *Smart Energy*, 2022 (*in review*)

The creation of smart energy systems is essential for the energy transition of the European Union. Electrification and smart integration of maritime transport with the power system is becoming highly important in order to successfully decarbonise maritime transportation and increase the possibility for the integration of renewable energy sources. This study presents a novel method for the analysis of maritime transportation integration with the power system. The method includes a novel model for electric ships that include all relevant engine, ship route and energy storage system aspects. By including the ship charging variable it is possible to connect the model to the distribution grid. The method provides the possibility to analyse the impact of maritime integration for different connection options and with the different shares of renewable energy sources present in the system. The study found that such smart integration can have a positive impact on the overall smart energy system. In particular, the smart integration of maritime transport with the power grid led to the reduction of curtailed energy by 3.9 MWh in the Kvarner archipelago for the maximum analysed penetration of renewable energy sources.

Marko Mimica developed the optimization model and electric ship model. Maja Perčić and Nikola Vladimir contributed to the model by providing maritime specific models and data. Goran Krajačić contributed to the scenario design. Marko Mimica and Maja Perčić wrote the paper. Goran Krajačić and Nikola Vladimir reviewed the paper.

PAPER 1

The Smart Islands method for defining energy planning scenarios on islands

Marko Mimica¹, Goran Krajačić¹

¹Department of Energy, Power Engineering and Ecology, Faculty of Mechanical Engineering and Naval Architecture, University of Zagreb, Ivana Lučića 5, 10002 Zagreb, Croatia

e-mail: mmimica@fsb.hr

Abstract

Islands represent areas where it is possible to have a clear overview of resources and needs over a large number of sectors. Because of this, the developed energy planning scenarios on the islands should reflect the possibility of meeting local needs with available resources of a wide range of sectors. This is often not the case in the current studies that analyse only a limited number of sectors. The developed method automatically combines needs and resources based on the quantitative indicators and generates energy planning scenarios with precisely defined types and the capacities of required technologies. The results show that the Smart Islands method provides 7 energy planning scenarios for Krk island with different technology mixes. The case study for Vis island is considered for cases with and without electrical interconnection. When the interconnection is not considered, the method suggests a 5.42 MWh battery system for maintaining grid stability. The results indicate that the Smart Islands method can be applied to islands with different characteristics as well as suggest optimal energy planning scenarios while meeting needs with local resources.

Keywords: *Energy planning, Smart Islands method, Renewable energy sources, RenewIslands, Energy system modelling, Smart energy systems*

1. Introduction

Energy planning of islands is becoming increasingly important as the European Union (EU) increases its effort to tackle climate change. The idea that islands can be “living labs” for the new technology and projects laid the foundations for islands to take the leading role in the energy transition towards a clean and sustainable environment. Islands are considered to be unique areas because of many disadvantages they are exposed to such as a weak electrical grid connection, higher fuel prices, overall weaker infrastructure etc. On the other hand, the islands are unique areas because they offer a possibility to have a clearer overview of needs and resources available and often have better solar and wind potential than on the mainland. The implementation of the new technology on unique locations such as islands opens the possibility for replication of solutions achieved on the islands in the mainland areas. The role of islands and objectives for the successful process of the energy transition on the islands are framed within the two documents by the EU, the Smart Islands Initiative [1] and the Clean Energy for EU Islands [2].

RenewIslands method presented in [3] focused on meeting island needs by using local resources and presenting the qualitative framework for energy experts for defining energy planning scenarios. RenewIslands method was applied to numerous case studies including S. Vicente [4] where the authors concluded that it is possible to achieve 72% of generation from RES. The authors at [5] used RenewIslands for generating energy planning scenarios and EnergyPLAN for modelling the interconnection and the demand response (DR) between different islands. The method for defining energy planning scenarios for islands was presented in [6], however, this method is also based on the qualitative RenewIslands method and defines one energy planning scenario depending on the objective function of the problem.

Other studies use different approaches for defining energy planning scenarios without a clear indication of why a particular scenario was modelled. A case for 100% renewable island of Wang-An modelled in EnergyPLAN was presented in [7] where the authors used electricity, thermal and transport demand while the RES potential was assessed based on geographical conditions of the island. A RES scenario for the renewable island of Ustica with 324.9 MWh renewable generation was presented in [8], however, it remained unclear why particular technologies were chosen for simulated scenario. Another example of energy transition scenario for islands in the Philippines was presented in [9] where the authors considered only scenarios with the fossil fuel generation. The presented studies proposed different energy planning scenarios for the energy transition of islands, however, it is not clear how did the authors choose the energy planning scenarios that were analysed. It is clear that there is a lack of such approaches that consider islands' needs and resources for devising energy planning scenarios.

The need for quantifying the impact of cross-sector integration is highly recognized by the various authors that analysed many different scenarios and solutions. The possibility for completely renewable Canary Islands was presented in [10] where the authors suggested that integration of transportation and heating sector with electric power system should be implemented. Islands without electrical interconnection were studied in [11] on the case of the Faroe Islands and the authors proposed a combination of wind and hydrogen technology for the development of sustainable energy systems. Lund et al. [12] elaborated on a holistic approach for achieving a cross-sectoral smart energy system that provides flexibility through several different sectors such as heating, synthetic fuels production and transport. Similarly, the study at [13] presented four possibilities for interconnecting electricity generation and transport systems that resulted in a 50% possibility increase for integration of variable RES. The energy planning tool PLEXOS was used in [14] where the authors concluded that it is possible to

reduce oil imports by 46% on Caribbean Islands when integrating different sectors, namely the cooling, water and transport sector with the electricity sector. The possibility for integration of solar concentrated power and desalination on Dongsha island was presented in [15] where the authors conclude that smart integration of these technologies can result in a 100% renewable island. However, it is not clear how the proposed cross-sectoral solutions for flexibility increase reflect the islands' needs and available resources.

Methods for comparisons of different technologies as well as energy storage sizing were also extensively investigated. A recent study [16] provided a review of the latest energy storage and demand response technologies, as well as underlined the importance of sector integration for increasing the flexibility on the islands. A review of methods for microgrid planning was provided in [17] where the authors elaborate on different methods for microgrid power generation planning. However, the study did not consider a broader approach where many sectors would be included. Chen et al [18] concluded that the optimal energy storage size for considered microgrid in island mode is 1.4 MWh, but did not consider possibilities for sector integration for providing additional flexibility that could lower the needs for flexibility from the energy storage system (ESS) and result with the lower optimal value of ESS. Optimal planning of reserve and power generation of microgrids was presented in [19] where the authors compare the microgrid with ESS and microgrid with the DR but without ESS. The authors concluded that the microgrid with ESS has a 31.16% lower energy cost. The study [20] showed that citizens' participation in the demand response management systems leads to energy cost reduction for the users. Another study [21] concluded that the breakpoint incentive for the demand response is 23% of the day-ahead electricity market price, however without specifying how is the level of flexibility determined. The authors in [22] propose a STEEP approach for the assessment of microgrid failure factors in local communities. The bi-level optimization

approach for microgrid planning and operation is presented in [23] where the authors conclude that it is possible to achieve 84.44% savings in comparison to the base case scenario when the presented method is applied. However, these studies focused only on specific sector without examining the impact of sector coupling.

The study in [24] examined the impact of energy policy on dynamics of the energy transition for the case study of Reunion Island where the authors concluded that the current energy policy in France is slowing down the energy transition on Reunion Island.

Energy planning studies on the regional and national level often consider a limited number of sectors without the objective of meeting the needs of an area with its resources. For example, the study [25] considered coupling of heating and power sector and the authors in [26] considered integration of residential heating and transport sector. The study [27] expanded the approach and considered waste and geothermal resources, however, the capacity optimization was not performed and arbitrary scenarios were considered. The possibility to quantify the flexibility would be especially interesting for regional planning, especially for spatially distributed planning as in [28]. Since the islands have a clearer overview of available needs and resources than the areas on the mainland, the solutions and methods developed on the islands can contribute to resolving issues on the mainland.

The method developed in this paper answers the following research questions derived from the analyzed literature:

- How to define the method for defining the exact type and quantity of required technologies for meeting islands' needs with its resources based on quantitative indicators?
- How to automatize the process of defining energy planning scenarios that match islands' needs and resources?

- How to consider electricity, heating, cooling, transport, water, waste and wastewater sectors in such a method?
- How to quantify the available flexibility of energy scenarios obtained with such a method?

The hypothesis of this study is that by using the new method for calculation of energy planning scenarios on islands (Smart Islands method) it can be shown that the transformation of energy systems on islands to systems that can satisfy all their energy demand from renewable energy sources is possible with a precisely defined amount and type of required technology.

Moreover, the research objectives of this study are as follows:

- Automatization of RenewIslands method implemented in Python programming language
- A novel method for defining the type and quantity of required technology
- A development of case studies for Krk and Vis islands that includes electricity, heating, cooling, transport, water, waste and wastewater sector
- Statistical analysis of energy planning scenarios by using Monte Carlo simulation for the two cases of uncertainty

The paper is organized in the following structure: The introduction is given in the first section of the study, the second section of the paper presents the Smart Islands method developed within this study. The case study on which the method has been applied is presented in the third section, while the fourth section presents the results of the study. The fifth section presents the discussion and the final section presents the conclusions of the study.

2. Material and Methods

The Smart Islands method developed in this study is a tool that enables islands' planners to automatically calculate the quantity and type of technology required for meeting islands' needs with resources. The method considers electricity, heating, cooling, transport, water, waste and wastewater sector and is implemented in the programming language Python. The method is based on the RenewIslands method developed by Duić in [3]. There are two main parts of the method that will be further explained in the paper:

- (1) Calculate possible types of technologies that can meet islands' needs with resources by considering the input indicators (chapter 2.1)
- (2) Perform a capacity optimization by considering only technologies calculated from the first part and repeat the optimization procedure for all possible electricity production combinations (chapter 2.2)

The main advantage of the method is that it automates the process from mapping to generating energy planning scenarios. This means that one can in few seconds generate energy planning scenarios that meet islands' needs with resources once the input data is defined.

It should be noted that, although the method considers many operation parameters (e.g. load factor, variability factor), the method itself is not intended to analyse the operation of the system. It is recommended that the scenarios are further analysed with energy planning tools (e.g. EnergyPLAN [29], H2RES [30], Homer [31]). Moreover, if one would want to assess the possibilities for practical implementations of the scenarios, tools for electric power system analysis should be included in the analysis as well (e.g., NEPLAN [32], DigSILENT [33], PSS/E [34]). The additional analyses with mentioned tools may indicate the need to change the capacities or increase investments in the infrastructure because of special operating conditions of the energy system that may occur (e.g. peak demand that lasts for an extended period, voltage problems may occur in the distribution grids etc.).

The scenarios obtained with the Smart Islands method provide an insight into the possibilities for matching needs with resources at the lowest investment cost. This information is valuable to the decision-makers and policymakers and the scenarios should primarily be used for these purposes. It is also suggested that the scenarios are used as input data for previously mentioned energy planning tools, or, in other words, that the Smart Islands method is used as the pre-processing step for the energy planning tools.

Input data for the Smart islands method are indicators presented in [35] that are divided into four areas A_1 to A_4 and summarized in Appendix A. These areas cover islands' needs, resources, infrastructure and water resources for mentioned sectors. The input data can be defined with more indicators (e.g. biomass potential), however, the intent was to achieve an adequate trade-off between the complexity of input indicators and the quality of the results. The Smart Islands method is visually presented in Figures 1 and 2. Figure 1 presents an outline of the method with every step and actors included, while Figure 2 presents what input data is needed for different technology selection.

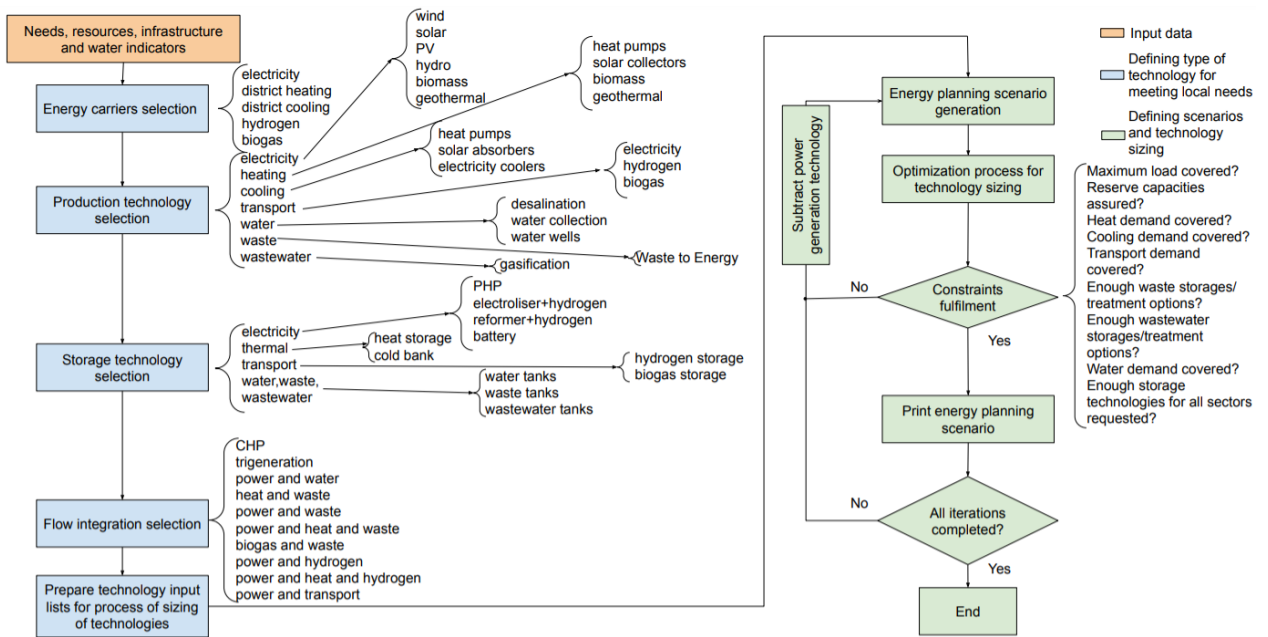


Figure 1. Smart Islands method outline diagram – the blue boxes represent the first part of the method (matching islands' needs with resources), the green boxes present the optimization part of the method, while input data is given in the orange box

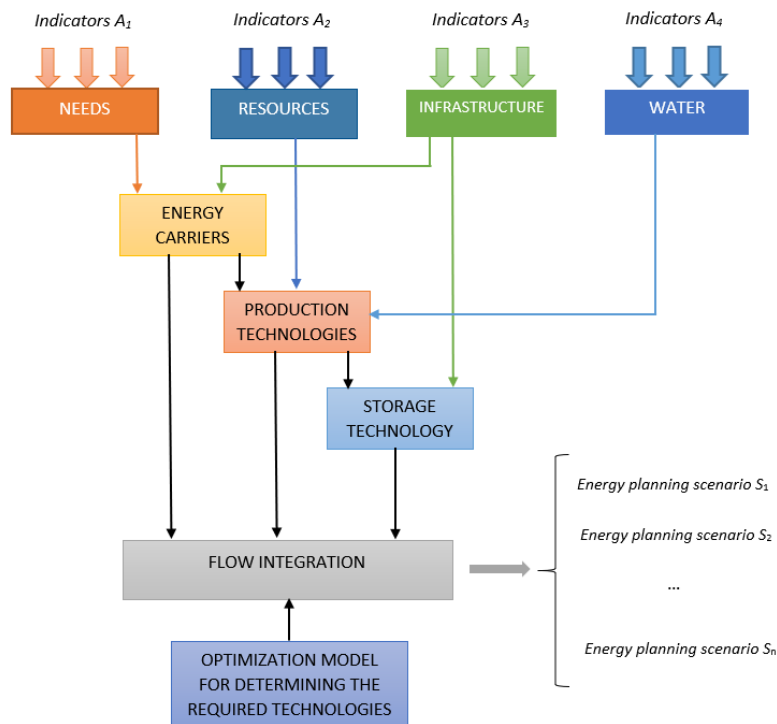


Figure 2. Smart Islands method for defining energy planning scenarios

2.1. Automatized RenewIslands method

The first step of the Smart Islands method is to automatize the RenewIslands method. The RenewIslands is a qualitative method that is used for energy planning of the islands. A novel approach for the automatization of the RenewIslands method is implemented in the Python programming language in the scripts *Modulemethod.py* and *AuthRenewIslands.py*. The input indicators are loaded in the Python script *Modulemethod.py* where the classes for energy carriers, production technologies, storage technologies and flow integration are defined together with the corresponding functions. *AuthRenewIslands.py* is the script that is used for the calculation of scenarios that are defined with several lists as outputs. The software architecture for defining energy planning scenarios by using automatized RenewIslands is presented in Figure 3. The logic implemented in the programming code is available in Appendix B.

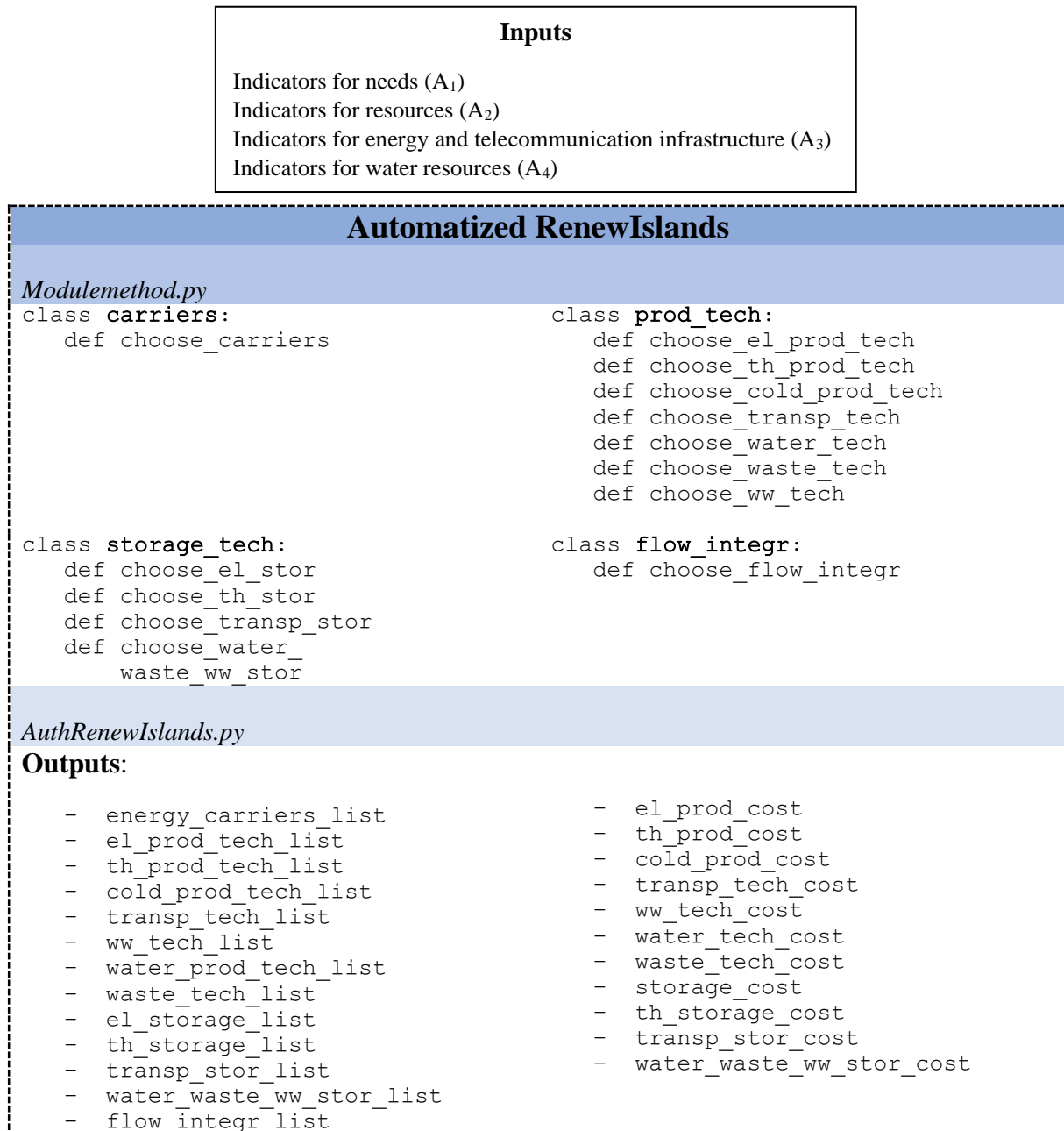


Figure 3. Programming architecture for automatization of RenewIslands method – main output of this part of Smart Islands method is to obtain all possible technologies that match islands' needs with resources based on the input data

2.2. Optimization model

By automatizing the RenewIslands method it is possible to calculate qualitative energy planning scenarios directly from mapping data of the islands. With this contribution, the application of RenewIslands is significantly accelerated and subjected to quantitative indicators. In order to create the Smart Islands method, it is necessary to create the optimization model for calculating

the required quantity of specific technology obtained from the first part of the method. As stated in the introduction, integration of different sectors such as electricity, water, heating, transport etc. is becoming increasingly important in order to achieve sustainable systems. This is due to the fact that the increasing share of variable RES is introducing numerous uncertainties in the electric power systems which are especially highlighted on the islands which are usually characterized by low inertia. By adjusting the operation of other systems such as water or heating system it is possible to improve conditions in the electric power grid and increase the possibility for RES integration. As maintaining the stability of an electric power system is crucial for achieving high RES systems, the optimization model presented in this study is oriented towards energy planning scenarios with different combinations of electricity generation units. This means that the method repeats the optimization procedure until all possible electricity production technologies obtained from the first part of the method are iterated. A complete flow diagram for defining possible energy planning scenarios for islands is provided in Figure 4.

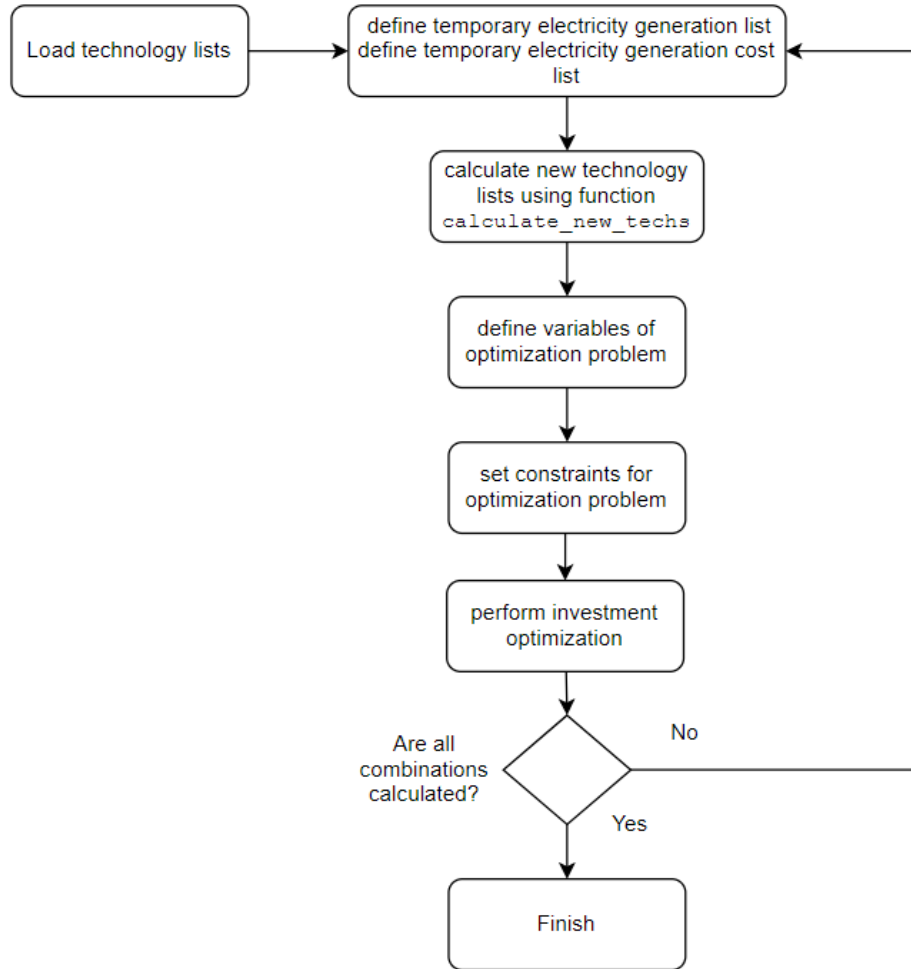


Figure 4. Flow diagram for Smart islands method implementation

2.2.1. Objective function and variables

The objective of the optimization problem is to minimize the specific investment cost of technology for a given energy planning scenario. Although various objectives can be implemented such as minimizing energy dependence of the island or maximizing self-sustainability as elaborated in the introduction, this methods' objective is to minimize the specific investment cost of derived energy planning scenarios on islands. A similar approach can be found in [6] or [36]. The considered assumption is that the operation and maintenance cost would further underline solar and wind as the most affordable technologies. Additionally,

the operation cost depends on the type of technology that is installed (e.g. biomass generator). The Monte Carlo analysis is used to analyse the uncertainty of the cost. Considered uncertainty is +/- 10% from the expected specific cost and it is assumed that such a large uncertainty range is sufficient to observe the results for wide errors in the investment cost of the technologies. The overall objective of the method is to, first, determine all possible technologies for consideration concerning the islands' needs and resources and then calculate all possible energy planning scenarios with a precisely sized quantity of each technology, represented with variables \mathbf{x} of the problem. In this sense, let linear programming optimization problem be defined as equation (1):

$$\min_{\mathbf{x} \in S} \mathbf{c}^T \mathbf{x} \quad (1)$$

$$S = \{ \mathbf{x} | \mathbf{A}^{in} \mathbf{x} \leq \mathbf{b}^{in}, \mathbf{A}^{eq} \mathbf{x} = \mathbf{b}^{eq}, \mathbf{x} \geq 0 \}$$

Where S is a convex set, $\mathbf{A}^{in} \in \mathbb{R}^{p \times n}$ is inequality equation matrix, $\mathbf{A}^{eq} \in \mathbb{R}^{q \times n}$ is equality equation matrix, $\mathbf{c} \in \mathbb{R}^n$ is specific investment cost vector, $\mathbf{b}^{in} \in \mathbb{R}^p$ is inequality vector, $\mathbf{b}^{eq} \in \mathbb{R}^q$ is equality vector and $\mathbf{x} \in \mathbb{R}^n$ are variables of the problem. Sets of variables of the problem are defined with Table 1, each of them having assigned cost. Different relations between the variables are described with equality and inequality constraints. The variables of the problem are considered to be quantitative values of installed electrical power generation of a particular technology, the capacity of storage, thermal generation etc. The specific investment cost vector of different technologies is obtained from data available in the literature [27]–[38].

The product of variable representing the quantity of a specific technology and assigned specific investment cost is implemented with function *calculate_sum* that contains additional check-ups by comparing the size of the list of technologies and list of cost.

After executing function *calculate_new_techs* and defining new lists of different technologies, the model defines variables for the optimization problem. This is implemented with series of *for* loops where one variable is generated for every element of each list of technologies that are generated with function *calculate_new_techs*. The variables in the presented optimization problem represent the required quantity of specific technology. Complete list of variable sets is provided in Table 1, where $X_{eg} = \{x_{eg,1}, \dots, x_{eg,5}\}$, $X_{es} = \{x_{es,1}, \dots, x_{es,4}\}$, $X_{tg} = \{x_{tg,1}, \dots, x_{tg,4}\}$, $X_{cg} = \{x_{cg,1}, \dots, x_{cg,3}\}$, $X_{ts} = \{x_{ts,1}, x_{ts,2}\}$, $X_{tt} = \{x_{tt,1}, \dots, x_{tt,3}\}$, $X_{tts} = \{x_{tts,1}, x_{tts,2}\}$, $X_{wg} = \{x_{wg,1}, \dots, x_{wg,3}\}$, $X_{wt} = \{x_{wt,1}\}$, $X_{wwt} = \{x_{wwt,1}\}$, $X_{ws} = \{x_{ws,1}, \dots, x_{ws,3}\}$. Thus, total number of possible variables is equal to 31. Each of these variables has corresponding cost assigned with vector \mathbf{c}^T .

Table 1. List of variables of Smart islands method

Variables	Mark	Unit	Implementation in programming code
Electricity generation	$x_{eg,i}$	MW	gen
Electricity storage	$x_{es,i}$	MWh	stor
Thermal generation	$x_{tg,i}$	MW	th_prod
Cooling generation	$x_{cg,i}$	MW	cold_prod
Thermal storage	$x_{ts,i}$	MWh	th_stor
Transport technology	$x_{tt,i}$	MW	transp_tech
Transport storage	$x_{tts,i}$	MWh	transp_stor
Water supply technology	$x_{wg,i}$	MW	water_tech
Waste treatment technology	$x_{wt,i}$	MW	waste_tech
Wastewater treatment technology	$x_{wwt,i}$	MW	ww_tech
Water, waste and wastewater storage	$x_{ws,i}$	tonne (waste)	www_stor
		m ³ (else)	

The objective function \mathcal{F} of the observed linear optimization problem can then be written as (2):

$$\begin{aligned} \min \mathcal{F} = \min & \left(\sum_{x_{eg}} x_{eg,i} \cdot c_{eg,i} + \sum_{x_{es}} x_{es,i} \cdot c_{es,i} + \sum_{x_{tg}} x_{tg,i} \cdot c_{tg,i} + \sum_{x_{cg}} x_{cg,i} \cdot \right. \\ & c_{cg,i} + \sum_{x_{ts}} x_{ts,i} \cdot c_{ts,i} + \sum_{x_{tt}} x_{tt,i} \cdot c_{tt,i} + \sum_{x_{tts}} x_{tts,i} \cdot c_{tts,i} + \sum_{x_{wg}} x_{wg,i} \cdot \\ & \left. c_{wg,i} + \sum_{x_{wt}} x_{wt,i} \cdot c_{wt,i} + \sum_{x_{wwt}} x_{wwt,i} \cdot c_{wwt,i} + \sum_{x_{ws}} x_{ws,i} \cdot c_{ws,i} \right) \end{aligned} \quad (2)$$

2.2.2. Constraints

The constraints of the proposed method consist of 13 inequality constraints and 1 equality constraint represented with equations (3) – (16) with bounding condition $\mathbf{x} \geq 0$ for all variables. The proposed Smart Islands method accounts for islands' resources and matches them with islands' needs. Therefore, it is required that the generation of specific technology does not exceed the potentials available on the island. It is also required that islands use technologies for which there is more available potential. This is achieved by loading the list of potentials mapped with the input indicators and setting following constraints (3) and (4) where $E_{\text{pot}} = \{ E_{\text{pot},1}, \dots, E_{\text{pot},5} \}$ represents the potential of each resource:

$$x_{eg,i} \leq E_{\text{pot},i} \quad (3)$$

$$x_{eg,i} \geq x_{eg,j} \cdot \frac{E_{\text{pot},i}}{E_{\text{pot},j}} \quad (4)$$

The constraints regarding minimal electricity, heating and cooling generation are described with equations (5) – (7). The maximum electricity generation capacities must be sufficient to satisfy the maximum electricity load (P_{max}). The Smart Island method sets a 20% higher requirement for generation capacity in order to secure that there will be enough amount of renewable power generation in case of increased demand. The equation also accounts for electricity production

from Waste-to-Energy plants (WtE) and wastewater treatment plants (WWTP) if available. The values for heating production in the case of cogeneration are also accounted for with defined quotients α_1 and α_2 which represent the ratio of heating power and electrical power generation. The required heating and cooling variables were set to satisfy the maximum heating and cooling load which is expressed with the equations (6) and (7). In case there are no available local resources for meeting local needs, the model will be unfeasible and the tool would return the corresponding message. However, such a scenario is unlikely as it would be difficult to find a populated island without any resources.

$$\sum_{x_{eg}} x_{eg,i} + x_{wt} + x_{wwt} \geq 1.2P_{max} \quad (5)$$

$$\sum_{x_{tg}} x_{tg,i} + \alpha_1 x_{wt} + \alpha_2 x_{wwt} \geq L_h \quad (6)$$

$$\sum_{x_{cg}} x_{cg,i} \geq L_c \quad (7)$$

Maximum required power in the transport sector is determined with the quotient of transport demand divided by the load factor available from input indicators. The assumption for the transport sector is that increase in electricity load described with the load factor is enough precise measurement for the increase of the transport sector as well. This assumption can be justified by the fact that the number of residents of the island increases six times during the summer months which corresponds to the increase in electricity consumption [44]. Additionally, a conversion factor β is defined for each specific type of fuel used in the transportation system since the transport demand in input indicators is the energy equivalent for petrol and diesel. This is given with the constraint (8).

$$\beta \sum_{i=1}^n x_{tt,i} \geq \frac{D_t}{m} \quad (8)$$

$$\text{where } \beta = \begin{cases} 1, & \text{for biofuels} \\ 2, & \text{for hydrogen} \\ 3, & \text{for electricity} \end{cases}$$

High amounts of variable RES such as solar and wind generation are the cause of many uncertainties in the electric power system. In order to overcome periods of a substantial change of generated power, the electric power system has to have enough units that can provide a reserve to the system. The reserve can be provided through the interconnection if the island is connected to the mainland, and by using batteries, conventional generators or the DR. For conventional systems without variable RES the minimum required amount of reserve is well investigated. Penetration of variable RES imposes new requirements for available reserve as in [45]. The reserve requirements are determined with factors $\Gamma_1, \Gamma_2, \Gamma_3 \in [0,1]$, and are specific for different case studies. The reserve constraint is defined with equation (9) where I represents the available interconnection capacity.

$$\Gamma_1 \cdot P_{max} + \Gamma_2 \cdot x_{eg,wind} + \Gamma_3 \cdot x_{eg,solar} \leq I + DR + x_{eg,biomass} + x_{eg,geothermal} + \sum_{X_{es}} x_{es,i} \quad (9)$$

For case hydrogen or biofuels are used for transport there is a requirement for transport storage. The required size of storage should be sufficient to satisfy a share of transport demand defined with factor β_1 . This is given with the constraint (10)

$$x_{tts,i} \geq \beta_1 \cdot D_t \quad (10)$$

In case there is a need for heating and cooling storage, their values are defined with equation (11). A condition set for heating and cooling demand is that they are able to cover a share of heating or cooling demand defined with coefficients α_3 and α_4 .

$$x_{ts,i} \geq \begin{cases} \alpha_3 D_h, & i = 1 \\ \alpha_4 D_c, & i = 2 \end{cases} \quad (11)$$

In case that the desalination plant is chosen as a water technology, its power required for operation is calculated using the available load factor. Similarly to the transport sector, it is assumed that the water demand can be approximated with the load factor as well. The specific power consumption of desalination was taken as in [46] and interpreted with coefficient α_5 . The described constraint is given with equation (12).

$$x_{wg,des} \geq \alpha_5 \frac{D_w}{m} \quad (12)$$

If the waste produced on the island is not exported, but the method rather suggests that it should be treated on the island with the WtE, the constraint for the power of such plant is presented with an equation according to specifications taken from [47] and represented with coefficient α_6 . The rated power must be equal to or less than the available yearly amount of waste (13).

$$x_{wt,i} \geq \alpha_6 G_w \quad (13)$$

If the WWTP is proposed, the waste heat produced for the wastewater treatment process can be used for heating. The specifications of wastewater treatment plant are taken from [48] which is represented with coefficient α_7 and the constraint for heat production is given with constraint (14):

$$x_{wwt,i} \geq \alpha_7 G_{ww} \quad (14)$$

Waste, wastewater and water tanks are used in case other technologies are not suitable. Their value is based on coefficient α_8 that is opposite proportional to the number of times the tank is being emptied or filled during the year. The tanks have to have enough volume to ensure the entire demand is met with taking into account the number of times the tanks are being emptied/filled (15).

$$x_{ws,i} \geq \begin{cases} \alpha_8 D_w, & i = 1 \\ \alpha_8 G_w, & i = 2 \\ \alpha_8 G_{ww}, & i = 3 \end{cases} \quad (15)$$

The DR is achieved through the integration of different sectors. The proposed method allows different sectors integration if there is telecommunication infrastructure available on analysed islands. Factor k is introduced in order to quantify the share of power that can participate in the DR for a particular plant. Therefore, if available, the DR constraint is defined with equation (16):

$$DR = k_{des} \cdot x_{wg,des} + k_{WtE} \cdot x_{et,WtE} + k_{tt} \cdot x_{tt,el} + k_{ts} \cdot x_{ts} \quad (16)$$

2.3. Uncertainty management

The results of the method are dependent on the quality of input data. Thus, it is necessary to conduct the sensitivity analysis when the input data is subjugated to the realistic uncertainty ranges. This study uses the Monte Carlo experiments for the probabilistic assessment of the impact of the uncertain parameters, similarly as in [49]. The uncertain input data can be divided into two main categories. The first category is related to the technical input parameters that describe islands needs and resources, while the second input data category is related to the

specific investment cost of the particular technology. The uncertainty for the first category is related primarily to the measurement uncertainties conducted for the particular island, while the uncertainty for the specific cost is related to the projections of the specific investment costs of the technologies. The study does not estimate the possible future load growth as it is considered that this aspect is covered with the Monte Carlo analysis because it is one of the uncertain input parameters. The Monte Carlo experiments are conducted in the following steps:

- Generate random input data for the experiment
- Solve the method for generated input data
- Analyse and synthesize the results after generating a large number of experiments

3. Case study

In order to test the presented method, a case study is conducted on two Croatian islands – Krk in the north part of the Adriatic Sea and Vis in the south part of the Adriatic Sea. The two islands are different in their size, population and geographic conditions which are more discussed in the next chapters for each island.

3.1. Krk island

Krk is located in the Kvarner archipelago in Croatia. Krk is the largest island out of seven islands in total in the Kvarner archipelago. The population of Krk island is 19374 which makes it the most populated island in Croatia. The electricity demand in 2016 was 139.19 GWh and is obtained through the electricity interconnection with the mainland. The electric connection with the mainland is achieved with two interconnection lines with a total capacity of 170 MVA. The heating energy demand on the Krk island was equal to 136.73 GWh, the cooling energy demand was 12.871 GWh while the transport energy demand was 68.55 GWh. Krk island has very good potential for wind energy production, as wind speed is 9.25 m/s at 10 m height, and solar energy

production, as 1.429 MWh/m². There are also two identified locations for pumped hydro plant (PHP) on Krk island. Krk island also has a very good biomass potential of 192.21 MWh/m². The capacity factor for wind, PV and biomass are 0.25, 0.15 and 0.8 respectively. A lot of investments have been made in advancing the water infrastructure on the island resulting in a centre for water control on the island as well as water connection for all residents of the island. Further improvements can be made in wastewater infrastructure although there is a mechanical treatment of wastewater on Krk island. Detailed mapping and the rest of the required input data for the Smart Islands method is presented in an extensive study in [35]. The coefficients that are used in the Smart Islands method for this case study are presented in Table 2.

3.2. Vis island

Vis island is a significantly smaller island in comparison with Krk. The population of Vis is 3637 and its surface is 89.72 km². The yearly electricity demand of Vis island was 16 GWh in 2016. The available electric interconnection is 16 MVA. The heating demand for Vis island was 12 GWh, cooling demand 2.3 GWh and transport demand was 19 GWh. Vis is characterised by high solar radiation equal to 1.555 MWh/m².

Table 2. Smart islands method coefficients value

Factor	Value	Unit	Factor	Value	Unit
α_1	1.6	-	Γ_1	0.05	-
α_2	5.68	-	Γ_2	0.3	-
α_3	0.05	-	Γ_3	0.1	-
α_4	0.1	-	β_1	0.1	-
α_5	0.00675	MW/m ³	k_{des}	0.2	-
α_6	0.000063	MW/tonne	k_{WtE}	0.2	-
α_7	0.00005	MW/m ³	k_{tt}	0.2	-
α_8	0.25	-	k_{ts}	0.0001	1/h

3.3.Monte Carlo experiments

As elaborated previously in the Method part, this study uses the Monte Carlo experiments for analysing the impacts of uncertain input parameters on the energy planning scenarios for the island of Krk. Thus, the Monte Carlo is performed outside of the Smart Islands method. In order to conduct the experiments, 200 probabilistic Monte Carlo experiments are generated for two specific cases:

- Technical input parameters are considered as the uncertain variable – the uncertainty range of input data was considered to be $\pm 5\%$ from the expected value
- Specific investment costs of the technologies are considered as the uncertain variable – the uncertainty range was considered to be $\pm 10\%$ from the expected value

These cases enabled the assessment of errors in measurements and cost predictions on the final results of the case study. It is assumed that the error of measurements is less than the possible error of cost estimation, thus the uncertainty range for the input indicators is shorter than the range for cost uncertainty.

4. Results

4.1. Krk island

The results that are generated with the Smart Islands method are presented in Table 3. The presented results show the installed capacities for each scenario. The method generates 7 possible optimal energy planning scenarios depending on which electric energy sources are used. The technology for electric energy production varies from scenario to scenario aiming to achieve electric energy self-sufficiency of the island with desired technology. Most diversified electric energy sources are achieved for scenario S7 with installed wind, PV and biomass. In the S3 scenario, a PHP is suggested as a possible solution. This is reasonable as there are

remarkable peak and off-peak periods on the Krk island, which can make PHP an effective solution.

The Smart Islands method suggests heat pumps (HP), biomass boilers and heat storage as a technology solution for heating. The dominant technology for all scenarios is HPs as the most affordable solution for heating as well as cooling. However, the method also suggests the sustainable usage of the biomass technology as there is local biomass resource present on the island as well. The method also suggests solar thermal as a possible technology for heating purposes. However, the assigned value to this technology is zero as HPs are a cheaper solution. It should be noted that these technologies are usually incentivized and the Smart Island method did not consider this possibility. However, this can be accounted for by adjusting the investment cost of the technology.

Electrification of the entire transportation system is suggested for all scenarios. The Smart Islands method also proposes the installation of a desalination plant as well as waste fill and wastewater tanks as technology for treating waste and wastewater.

Table 3. Energy planning scenario as result of Smart islands method

Energy planning scenario		S1	S2	S3	S4	S5	S6	S7
Electricity	Wind [MW]	60.95	0	0	30.86	57.28	0	55.88
	PV [MW]	0	60.95	0	30.1	0	57.28	1.4
	Biomass [MW]	0	0	3.67	0	3.67	3.67	3.67
	PHP [MW]	0	0	57.29	0	0	0	0
Heating	HP [MW]	55.35	55.35	48.96	55.35	48.96	48.96	48.96
	Biomass [MW]	0	0	7.34	0	7.34	7.34	7.34
	Heat storage [MWh]	13673	13673	13673	13673	13673	13673	13673
Cooling	HP [MW]	55.35	55.35	48.96	55.35	48.96	48.96	48.96
	Electricity coolers [MW]	0	0	6.18	0	6.18	6.18	6.18
Transport	EV chargers [MW]	4.55	4.55	4.55	4.55	4.55	4.55	4.55
Water	Desalination [m ³]	4.45	4.45	4.45	4.45	4.45	4.45	4.45
Waste	Waste fill [tonne]	116507	116507	116507	116507	116507	116507	116507
Wastewater	Wastewater tanks [m ³]	1745.2	1745.2	1745.2	1745.2	1745.2	1745.2	1745.2

4.1.1. Technical input parameters uncertainty

Moreover, the results are analysed by applying Monte Carlo simulation on the technical input data. 200 probabilistic scenarios are run in order to assess the Smart Islands method performance subjugated to the uncertainty of the technical input parameters. The results are presented in Figures 5-10 as boxplots. The boxplots show mean value, interquartile ranges,

minimum and maximum values. The results do not show significant differences in comparison to the scenarios presented in Table 3. The method adjusts the quantity of all technologies as the indicators change which is expected. The results indicate that the results of the Smart Island method are robust with respect to the uncertainty of the technical input data.

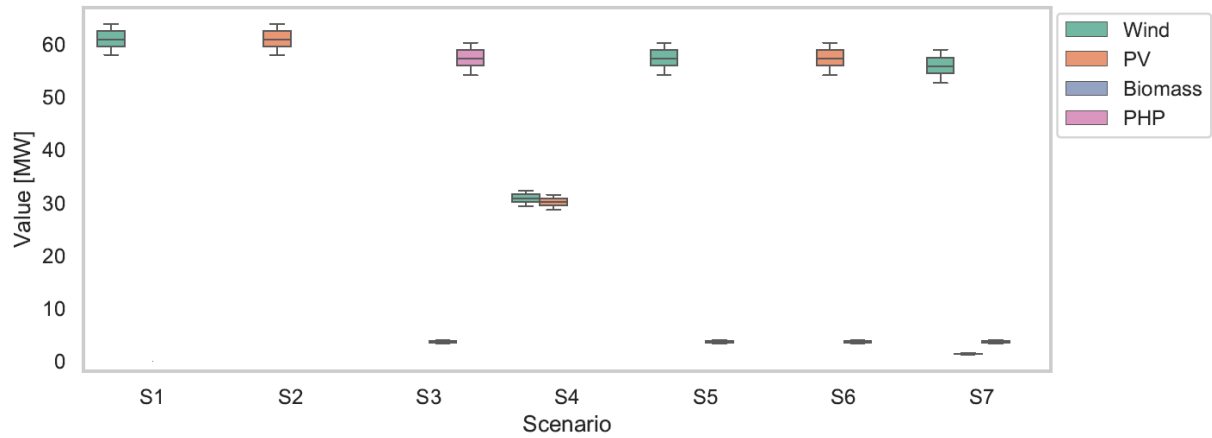


Figure 5. Results of Monte Carlo analysis for electricity generation technologies

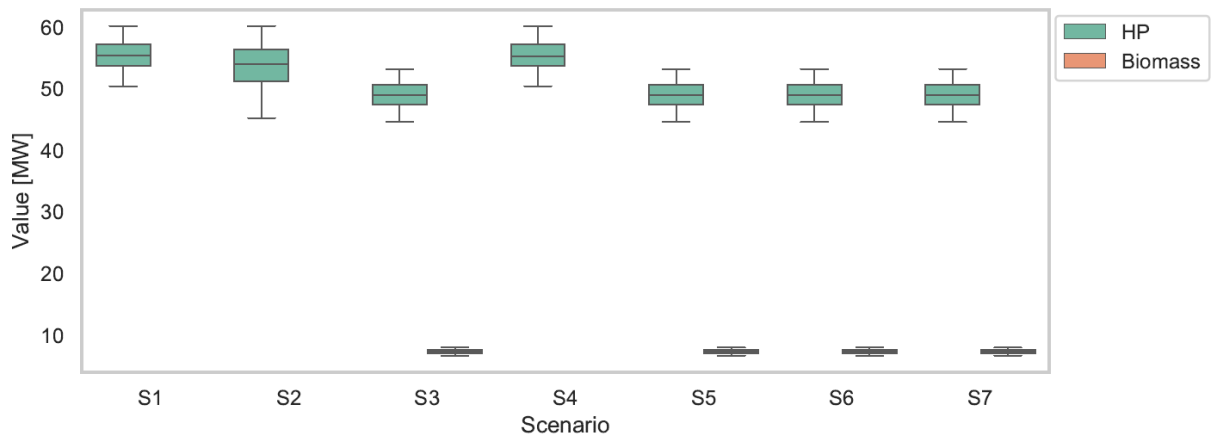


Figure 6. Results of Monte Carlo analysis for heating energy generation technologies

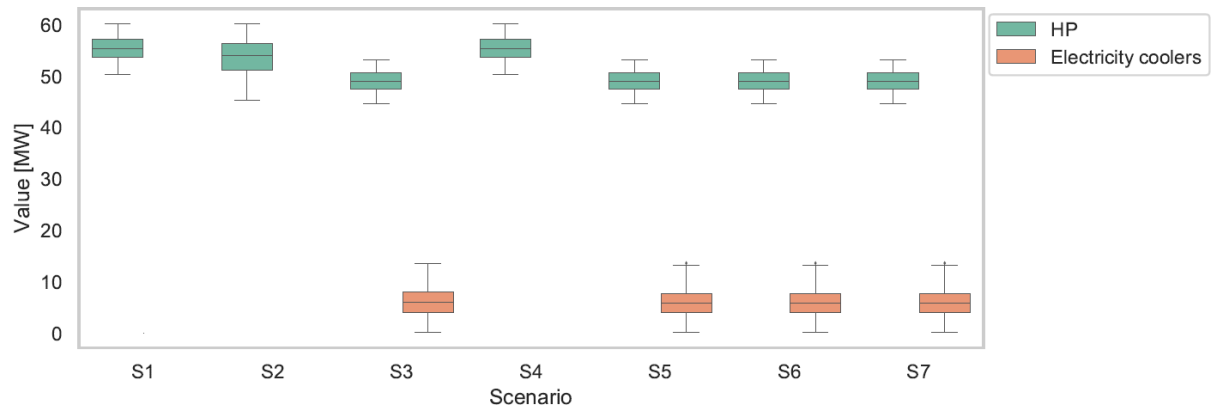


Figure 7. Results of Monte Carlo analysis for cooling energy generation technologies

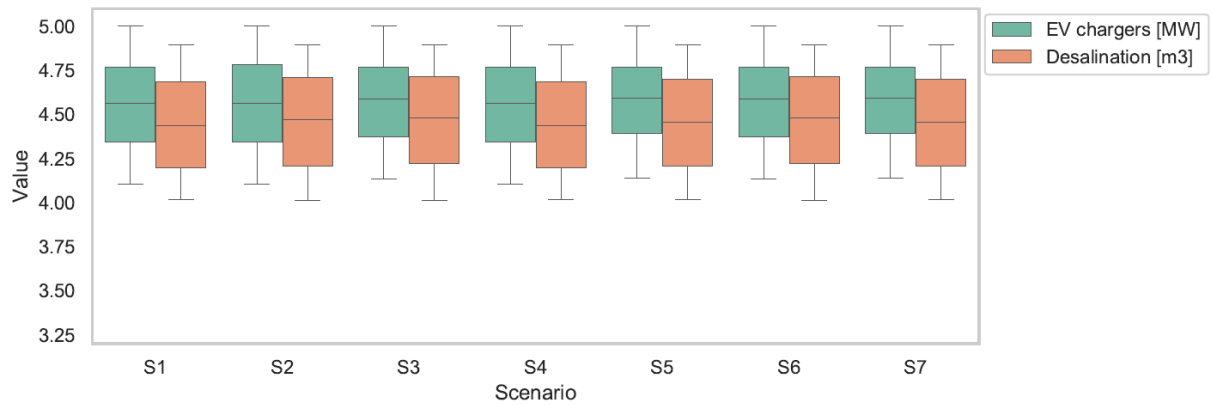


Figure 8. Results of Monte Carlo analysis for transport energy and water technologies

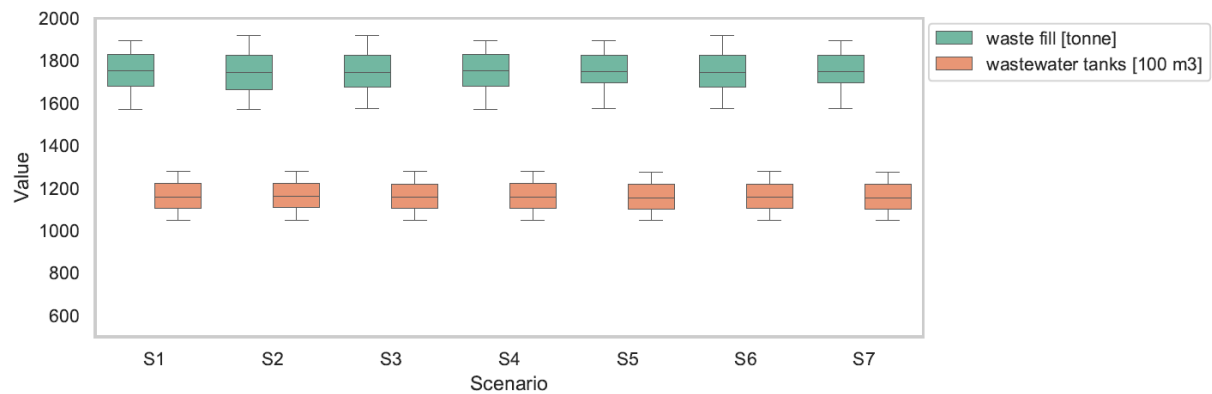


Figure 9. Results of Monte Carlo analysis for waste and wastewater treatment technologies

Additionally, values for the available flexibility are presented in Figure 11 with the DR parameter. As Krk has a satisfactory telecommunication infrastructure, there is a possibility for coordination between different sectors for purpose of their integration. Based on input data, the Smart Islands method proposes three flow integrations:

- Power and transport
- Power and water
- Power to heat technology.

By coordinating the operation between these sectors, the system can provide flexibility when necessary. The values for the DR parameter in the deterministic scenarios amounted to 2.33 MW (12.5% of the average load on the island), while the values after the Monte Carlo simulations are presented in Figure 10. Presented DR values adjust according to different probabilistic scenarios.

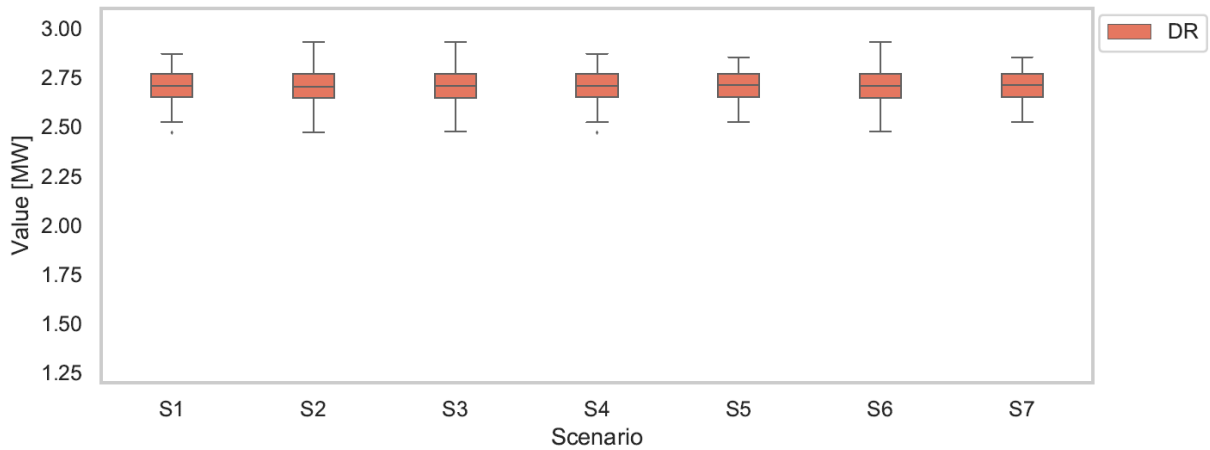


Figure 10. Results of Monte Carlo analysis for the demand response

Figure 11 shows mean values of the quantity of technology for each scenario (represented with rhombuses) and quantities obtained from original results presented in Table 3 (represented with bar plots). It is possible to observe that there are no significant differences between these results and the results obtained after 200 probabilistic scenarios which suggest the same technologies

as in the original case. For example, the highest difference for electricity generation is achieved for S5 where the quantity of suggested installed wind power between the original case and mean value of 200 scenarios differentiated for 0.3%. These results also confirm the robustness of the proposed Smart Island method with the respect to the uncertainty of the technical input parameters.

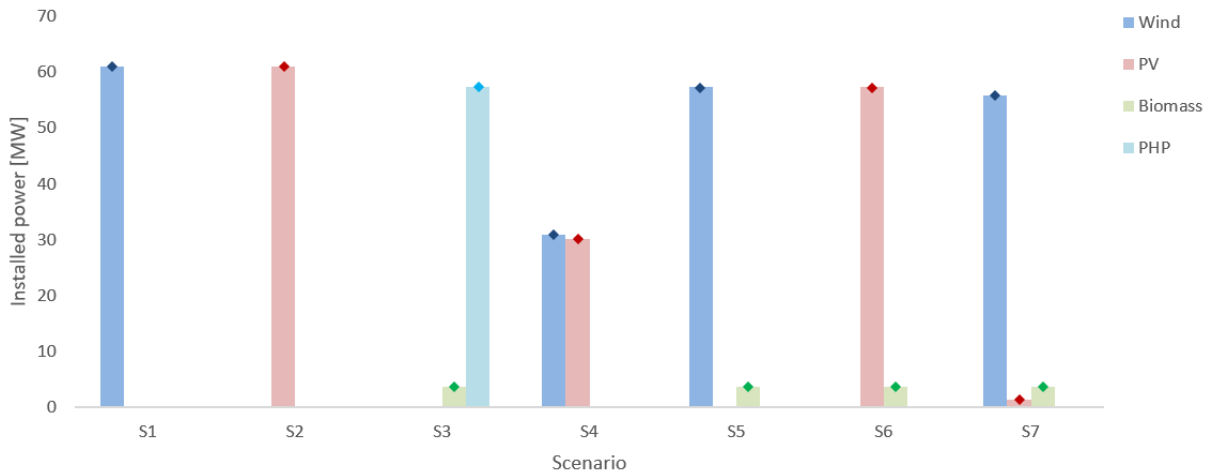


Figure 11. Comparison between original results obtained with Smart islands and mean values of Monte Carlo simulation for electricity generation technologies

4.1.2. Technology specific cost uncertainty

Since the cost of technology changes over time, it is necessary to assess the robustness of the proposed method against the uncertainty of the specific cost. Similarly to the previous Monte Carlo experiment, 200 probabilistic scenarios are run in this case as well. The results show that no deviation from the original scenarios occurs. This result indicates that the possible deviations in the specific investment cost do not influence the type and quantity of the required technology. From this result, it can be concluded that the method is robust with respect to the uncertain technology specific investment cost.

The comparison between each scenario investment cost for the two Monte Carlo experiments was also conducted (Figure 12). Higher investment costs can be seen for scenario S3 where a PHP is proposed as a solution. As the cost of PHP is significantly higher than other technologies, the cost for this scenario is higher as well. This result demonstrates that the Smart Islands method presents all possible solutions that meet island needs with island resources with respect to the cost uncertainty. It is then upon the decision-maker to decide what would be the most suitable solution among the scenarios generated with the Smart Islands method.

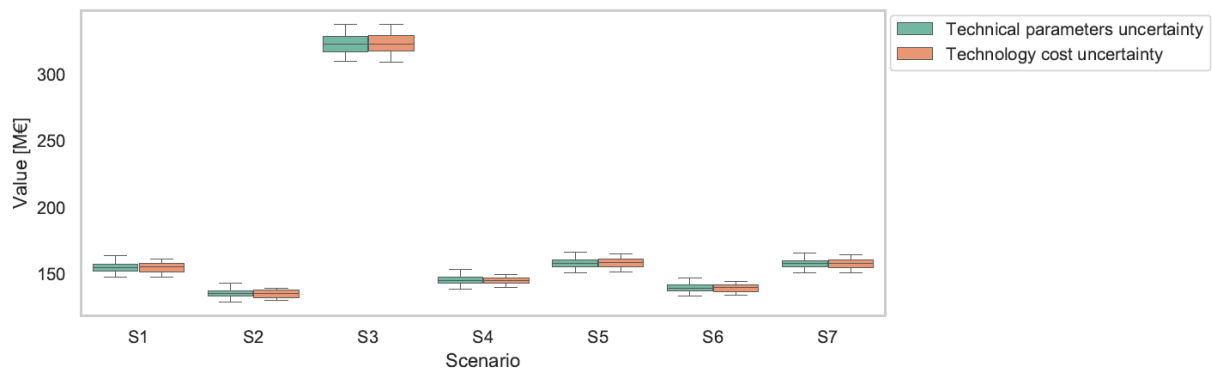


Figure 12. Investment costs of each energy planning scenario for two analysed cases of uncertainty

4.2. Vis island

The results for the Vis case study are presented in Table 4. The table shows scenarios generated with the Smart Islands method for two cases of interconnection availability. The difference between the two scenarios is in the installed battery capacity. For the scenario where there is no interconnection, the installed capacity of the battery storage should be 5.42 MWh. This result indicates that the Smart Islands method can be applied to islands with different interconnection capacities.

Additionally, both scenarios suggest the installation of a 5.92 MW PV plant. This is an expected result as solar potential is the dominant resource on the island. More interestingly, the results of the Vis case study align with the current ongoing projects on Vis. Recently, a 3.5 MW PV plant was installed on the island and a battery storage system is currently under construction [50]. The capacities of the technologies differ, however that is expected as the objective of the method is suitable for local communities, while the objective and possibilities of the investors may not correlate with those of local communities. The Smart Islands method also suggests the integration of the electricity and transport sector which can provide 0.3 MW (9.4% of the average load) of flexibility for the island.

Table 4. Energy planning scenarios for Vis case study for different interconnection value

Interconnection [MW]	16	0
PV [MW]	5.92	5.92
Battery storage [MWh]	0	5.42
HP [MW]	6.85	6.85
EV chargers [MW]	1.96	1.96
Desalination [m ³]	1.13	1.13
Waste fill [tonne]	232	232
Wastewater tanks [m ³]	21.4	21.4

5. Discussion

The results of this study indicate that the proposed Smart Islands method automatically generates the energy planning scenarios for islands with respect to their local needs and resources. The results of the Monte Carlo experiment suggest that the proposed method adjusts

the technologies according to the change in the input data. The technology mix and the installed values remain robust even when the technology costs are considered to be uncertain. In addition, the Smart Islands method proposes possibilities for flow integration depending on the available telecommunication infrastructure on the island. The key finding of the results is that the proposed method automatizes the process of energy planning for the smart islands. The method precisely defines the type and quantity of technology required for meeting local needs with local resources for each analysed sector.

The study [3] presented the RenewIslands method which suggested the type of technology that can be used but without precising the quantity of each technology. The fact that the study [3] did not develop the method for quantifying the required amount of each technology resulted in the research gap where different experts could suggest different amounts of required technologies. The Smart Islands method fills the research gap and improves the RenewIslands method as it provides the experts with the exact values of each technology for different energy planning scenarios that can be analysed. The results of this study are in line with the statement from [51] as every scenario assures the secure energy supply of the island. The results underline the findings of the studies [52] and [53] that defined the smart energy concepts and the flow integration of different sectors for the increase of RES penetration. Concerning the previous studies discussing the potential DR as a result of different sector integration (e.g. [12], [13] for the power and transport sector and [54] for the power and water sector), the flexibility can be increased by interconnecting different flows if the sufficient telecommunication infrastructure is available. Furthermore, the results value the importance of the interconnection as the integration of a high amount of RES would not be possible without it. The value of the interconnection and increased flexibility as a result of strong interconnection was emphasized in [5].

This study uses the Monte Carlo experiments to determine the impact of probabilistic input data on the results and showed that the results remain robust. A similar approach was taken in [55] to determine the optimal operation and sizing of the CHP. The study [56] also applied Monte Carlo experiments for the analysis of RES and energy system demand uncertainty influence.

The findings of the study place the focus on meeting island needs with its' resources, thus enhancing the self-sustainability of the island. One could argue that the objective of meeting local needs with local resources may not be the best possible solution for designing the energy planning scenarios. The other open possibility would be to eliminate the constraints of local needs and local resources and to search only for the lowest cost solutions. This study cannot prove this statement to be false. However, at least two strong arguments can be put forward to disagree with this statement. The first argument is that islands are unique areas with very limited possibilities for the integration of RES which is why local needs and resources should be considered. The second argument is that the cost of the technologies and the fuels is significantly higher on the islands than on the mainland. Consequently, the lowest cost solution on the mainland may not be the lowest cost solution on the islands. From the observed probabilistic analysis, which showed that the installed technologies remain the same even when the error in technology cost is considered, it can be concluded that the method proposed the same solutions whether the statement is adopted or not. Hence, there is no need for further consideration of this statement.

It should be noted that the proposed Smart Islands method is limited to the technologies described in the method section. However, this limitation may be easily mitigated. Further additions of the technologies may be proposed by an expert depending on the needs of the research. If the technology parameters are defined, one can simply implement the technology module in the programming code and account for any technology.

In this study, the Smart Islands method was demonstrated in the cases of the Krk and Vis islands. The methods' features and parameters are universal for all islands which makes it easy to generalize the method. The results of the method are useful for different decision-makers as national and local governments or investors in renewable energy. The Smart Islands method enables them to observe the possibilities for meeting the islands' needs with available resources at the lowest investment cost. In order to analyse the operation of the obtained scenarios, the tools for energy planning should be used. In this sense, the Smart Islands method can serve as a pre-processing method for the simulation of energy system operation and contribute the energy planning experts in the mapping of needs and resources of the island.

The proposed Smart Islands method contributes to the overall understanding of the smart energy system and provides the framework for testing the smart systems on the islands. The method will be further developed as new technologies will emerge with the overall objective of providing useful information for islands on the possibilities of meeting their own needs with local resources.

6. Conclusion

This study presents a novel Smart Islands method for energy planning of islands. The method generates energy planning scenarios based on the input data obtained from islands' mapping. The objective of the method is to propose optimal energy planning scenarios in order to meet the islands' needs by using local resources. Following contributions can be derived from the presented results:

- The results showed that, in addition to defining the type of technology, the Smart Islands method defines the precise quantity of each technology for each scenario. In the

presented case study, the Smart Islands method generated 7 renewable scenarios for Krk island for 7 different sectors

- The results showed that integration of power, heating, transport and water flows resulted in the possibility for the DR of 2.71 MW for Krk island and 0.3 MW for Vis island. This value of the DR represents the available flexibility of the system which leads to the conclusion that the Smart Island quantifies the flexibility of the system
- The results for the Vis case study showed that a 5.42 MWh battery is suggested to be installed for the scenario without the interconnection. This indicates that the method can be applied to islands regardless of their electrical interconnection.
- The Smart Islands method accelerates the process of energy planning of islands because it automatizes the design process of energy scenarios
- The results of 200 probabilistic Monte Carlo experiments for the Krk island indicated that the results of the Smart Islands method were robust under the technical input parameters uncertainty and technology-specific cost uncertainty

Future work of this research will be directed in investigating the possibilities for extending the application of the presented method to mainland areas, especially rural ones with similar characteristics to islands. Moreover, with the development of new technologies in the renewable energy sector, the method will be updated and the impacts of the new technology will be assessed.

Nomenclature

X_{eg}, x_{eg}, c_{eg}	Set, variables [MW] and specific investment costs [M€/MW] for the electricity generation technologies
X_{es}, x_{es}, c_{es}	Set, variables [MWh] and specific investment costs [M€/MWh] for the electricity storage technologies
X_{tg}, x_{tg}, c_{tg}	Set, variables [MW] and specific investment costs [M€/MW] for the thermal generation
$X_{cg}, x_{cg,i}, c_{cg,i}$	Set, variables [MW] and specific investment costs [M€/MW] for the cooling generation
$X_{ts}, x_{ts,i}, c_{ts,i}$	Set, variables [MWh] and specific investment costs [M€/MWh] for the thermal storage
$X_{tt}, x_{tt,i}, c_{tt,i}$	Set, variables [MW] and specific investment costs [M€/MW] for the transport technology
$X_{tts}, x_{tts,i}, c_{tts,i}$	Set, variables [MWh] and specific investment costs [M€/MWh] for the transport storage
$X_{wg}, x_{wg,i}, c_{wg,i}$	Set, variables [MW] and specific investment costs [M€/MW] for the water supply technology
$X_{wt}, x_{wt,i}, c_{wt,i}$	Set, variables [MW] and specific investment costs [M€/MW] for the waste treatment technology
$X_{wwt}, x_{wwt,i}, c_{wwt,i}$	Set, variables [MW] and specific investment costs [M€/MW] for the wastewater treatment technology
$X_{ws}, x_{ws,i}, c_{ws,i}$	Set, variables [tonne or m ³] and specific investment costs [M€/tonne or M€/m ³] for the water, waste and wastewater storage
$E_{pot,i}$	The maximum potential of i technology [MWh]

P_{max}	Maximum electrical load [MW]
L_h, L_c	Maximum heating and cooling load [MW]
D_t	Transport demand [MWh]
D_w	Water demand [m ³]
G_w	Waste generation [tonne]
G_{ww}	Wastewater generation [m ³]
m	Load factor

Appendix A

Table A1. Input data for Smart Islands method [35]

	Component	Indicator	$i_{k,y}$
Needs	Electricity	Electricity consumption [MWh per capita]	$i_{1,1}$
		Load factor	$i_{1,2}$
	Heat	Heating consumption [MWh per capita]	$i_{1,3}$
		HDD	$i_{1,4}$
	Cold	Cooling consumption [MWh per capita]	$i_{1,5}$
		CDD	$i_{1,6}$
	Waste treatment	Generated waste [tonne per capita]	$i_{1,7}$
		Separated waste [%]	$i_{1,8}$
	Wastewater treatment	Generated wastewater [m ³ per capita]	$i_{1,9}$
		Treated wastewater [%]	$i_{1,10}$
	Water	Water consumption [m ³ per capita]	$i_{1,11}$
	Transport	Transport energy consumption [MWh per capita]	$i_{1,12}$
Resources	Wind	Wind speed [m/s]	$i_{2,1}$
		Wind energy in total demand [%]	$i_{2,2}$
		Used wind potential [%]	$i_{2,3}$
	Solar	Solar irradiation [MWh/m ²]	$i_{2,4}$
		Solar energy in total demand [%]	$i_{2,5}$
		Used solar potential [%]	$i_{2,6}$
	Biomass	Biomass potential [MWh/m ²]	$i_{2,7}$
		Biomass energy in total demand [%]	$i_{2,8}$
		Used biomass potential [%]	$i_{2,9}$
	Hydro	Elevation [m]	$i_{2,10}$
		Hydro energy in total demand [%]	$i_{2,11}$
		Used hydro potential [%]	$i_{2,12}$
	Geothermal	Geothermal gradient [°C/100 m]	$i_{2,13}$
		Geothermal energy in total demand [%]	$i_{2,14}$
		Used geothermal potential [%]	$i_{2,15}$
Energy and telecommunication infrastructure	Grid infrastructure	Interconnection [MVA]	$i_{3,1}$
		Reserve [MVA]	$i_{3,2}$
		Variability factor	$i_{3,3}$
	Natural gas pipeline	Yes or No	$i_{3,4}$
	LNG terminal	Yes or No	$i_{3,5}$
	Oil terminal/refinery	Yes or No	$i_{3,6}$
	Oil derivatives terminal	Yes or No	$i_{3,7}$
	Telecommunications	Internet speed [Mbit/s]	$i_{3,8}$
		Mobile network coverage [%]	$i_{3,9}$
Water	Precipitation	Yearly precipitation	$i_{4,1}$
	Groundwater	Yes or No	$i_{4,2}$
	Water pipeline	Percentage of households [%]	$i_{4,3}$
	Desalination	Flow [m ³ /h]	$i_{4,4}$

Appendix B

Table B1. Energy carriers selection

Energy carriers	Energy carriers list
$if(i_{1,1} > 0)$	Electric energy
$if((i_{1,3} > 7) \text{ and } (i_{1,4} > 1500))$	District heating
$if((i_{1,5} > 7) \text{ and } (i_{1,6} > 1500))$	District cooling
$if(i_{1,12} > 10)$	Hydrogen
$if((i_{3,4} == 1) \text{ and } (i_{3,5} == 1))$	Natural gas
$If(((i_{2,7} > 200) \text{ and } (i_{2,8} < 0.3) \text{ and } (i_{2,9} < 0.3)) \text{ or } ((i_{1,7} > 7) \text{ and } (i_{1,8} < 0.5)) \text{ or } ((i_{1,9} > 7) \text{ and } (i_{1,10} < 0.5)) \text{ and } ((i_{3,6} == 1) \text{ or } (i_{3,7} == 1)))$	Biogas

Table B2. Technology selection for all sectors

Electric energy production technology	Electricity production technology list
$if((i_{1,1} > 7) \text{ and } (i_{1,2} > 0.2) \text{ and } (i_{2,1} > 7.5) \text{ and } (i_{2,2} < 0.3) \text{ and } (i_{2,3} < 0.5))$	Wind
$if((i_{1,1} > 1) \text{ and } (i_{1,2} > 0.1) \text{ and } (i_{2,4} > 1000) \text{ and } (i_{2,5} < 0.4) \text{ and } (i_{2,6} < 0.7))$	PV
$If((i_{1,1} > 9) \text{ and } (i_{1,2} > 0.1) \text{ and } (i_{2,4} > 1300) \text{ and } (i_{2,5} < 0.4) \text{ and } (i_{2,6} < 0.7))$	Solar
$If((i_{1,1} > 6) \text{ and } (i_{1,2} < 0.5) \text{ and } (i_{3,3} < 0.4) \text{ and } (i_{2,10} > 500) \text{ and } (i_{2,11} == 0) \text{ and } (i_{2,12} == 0))$	Hydro
$If((i_{1,1} > 4) \text{ and } (i_{2,7} > 150) \text{ and } (i_{2,8} < 0.5) \text{ and } (i_{2,9} < 0.5))$	Biomass
$If((i_{1,1} > 5) \text{ and } (i_{2,13} > 10) \text{ and } (i_{2,14} < 0.5) \text{ and } (i_{2,15} < 0.5))$	Geothermal
Heating production technology	Heating production technology list
$If((i_{1,3} > 1) \text{ and } (i_{2,4} > 1100) \text{ and } (i_{2,5} < 0.50) \text{ and } (i_{2,6} < 0.5))$	Solar collectors
$If((i_{1,3} > 2) \text{ and } \text{“Electric energy” in Energy carriers list})$	Heat pumps
$If(\text{“Geothermal” in Electricity production technology list})$	Geothermal
$If(\text{“Biomass” in Electricity production technology list})$	Biomass
Cooling production technology	Cooling production technology list
$If((i_{1,3} > 2) \text{ and } (i_{1,4} > 200) \text{ and } (i_{2,4} > 1300) \text{ and } (i_{2,5} < 0.50) \text{ and } (i_{2,6} < 0.5))$	Solar absorbers
$If(\text{“Heat pumps” in Heating production technology list})$	Heat pumps
$If((i_{1,3} > 1) \text{ and } (i_{1,4} > 200) \text{ and } \text{“Electricity” in Electricity carriers list})$	Electricity coolers
Transport technology	Transport technology list
$If((i_{1,12} > 6) \text{ and } \text{“Hydrogen” in Energy carriers list})$	Hydrogen
$If((i_{1,12} > 0.5) \text{ and } \text{“Electricity” in Energy carriers list})$	Electricity
$If((i_{1,12} > 6) \text{ and } \text{“Biogas” in energy carriers list})$	Biogas
Water technology	Water technology list
$If((i_{1,11} < 30) \text{ and } (i_{4,1} > 3000) \text{ and } (i_{4,3} == 0))$	Water collection
$If((i_{1,11} < 50) \text{ and } (i_{4,2} == 1))$	Water wells

<i>If($i_{4,2} == 0$) and ($i_{4,4} == 0$) (“Water collection” and “Water wells” not in Water technology list))</i>	Desalination
Waste technology	Waste technology list
<i>If($i_{1,7} > 1.5$) and ($i_{1,8} < 0.4$))</i>	Waste to Energy
Wastewater technology	Wastewater technology list
<i>If($i_{1,9} > 90$) and ($i_{1,10} < 0.4$))</i>	Gasification

Table B3. Storage technology selection

Electricity storage	Electricity storage list
<i>If(“Hydro” in Electricity production technology list)</i>	Hydro
<i>if(“Hydrogen” in Energy carriers list) and (“Hydro” not in Electricity production technology list) and (“PV” in Electricity production technology list) or (“Solar” in Electricity production technology list) or (“Wind” in Electricity production technology list))</i>	Electrolyser + hydrogen
<i>if(“Hydrogen” in Energy carriers list) and (“Hydro” not in Electricity production technology list) and (“Natural gas” or “Biogas”) in Energy carriers list)</i>	Reformer + hydrogen
<i>if(“Hydrogen” and “Hydro” not in Energy carriers list)</i>	Battery
Thermal storage	Thermal storage list
<i>if($i_{1,3} > 5$)</i>	Heat storage
<i>if($i_{1,5} > 7$)</i>	Cold bank
Transport (fuel) storage	Transport storage list
<i>if(“Hydrogen” in Transport technology list)</i>	Hydrogen
<i>if(“Biogas” in Transport technology list)</i>	Biogas
Waste/wastewater storage	Waste/wastewater storage list
<i>if($i_{1,7} > 0$) and (“Waste to Energy” not in Waste technology list))</i>	Waste fill
<i>if($i_{1,9} > 0$) and (“Gasification” not in Wastewater technology list))</i>	Wastewater tanks

Table B4. Flow integration selection

Flow integration	Flow integration list
<i>if($i_{1,1} > 2$) and ($i_{1,3} > 2$) or (“Biomass” or “Solar” or “Geothermal” in Electricity production list))</i>	CHP
<i>if($i_{1,1} > 2$) and ($i_{1,3} > 2$) and ($i_{1,5} > 2$) or (“Biomass” or “Solar” or “Geothermal” in Electricity production list))</i>	Trigeneration
<i>if($i_{3,8} > 40$) and (“Desalination” in Water technology list))</i>	Power and water
<i>if($i_{1,1} < 4$) and (“Waste to Energy” in Waste technology)</i>	Heat and waste
<i>if($i_{1,1} == 4$) and (“Waste to Energy” in Waste technology)</i>	Power and heat and waste
<i>if($i_{1,1} == 4$) and ($i_{1,5} > 5$) and (“Waste to Energy” in Waste technology list)</i>	Power and heat and cold and waste
<i>If(“Gasification” in Wastewater technology list)</i>	Biogas and waste
<i>If(“Wind” or “Solar” or “PV” in Electricity production technology list) and (“Hydrogen” in Energy carriers list))</i>	Power and hydrogen
<i>if($i_{3,8} > 40$) and ($i_{3,9} > 0.5$) and (“Desalination” in Water technology list))</i>	Power and transport

Acknowledgement

This work has been supported by the Young Researchers' Career Development Programme (DOK-01-2018) of Croatian Science Foundation which is financed by the European Union from European Social Fund and Horizon 2020 project INSULAE - Maximizing the impact of innovative energy approaches in the EU islands (Grant number ID: 824433). This support is gratefully acknowledged. The publication was presented at the 4th South East European Conference on Sustainable Development of Energy Water and Environment Systems, Sarajevo, Bosnia and Herzegovina (online), June 28 – July 02 2020.

References

- [1] European Commission, “Smart Island Initiative,” 2017. .
- [2] European Commission, “Clean Energy for EU Islands launch,” *European Commission Energy News*, 2017. .
- [3] N. Duić, G. Krajačić, and M. da Graça Carvalho, “RenewIslands methodology for sustainable energy and resource planning for islands,” *Renewable and Sustainable Energy Reviews*. 2008.
- [4] R. Segurado, G. Krajačić, N. Duić, and L. Alves, “Increasing the penetration of renewable energy resources in S. Vicente, Cape Verde,” *Appl. Energy*, 2011.
- [5] A. Pfeifer, V. Dobravec, L. Pavlinek, G. Krajačić, and N. Duić, “Integration of renewable energy and demand response technologies in interconnected energy systems,” *Energy*, 2018.
- [6] P. Petruschke, G. Gasparovic, P. Voll, G. Krajačić, N. Duić, and A. Bardow, “A hybrid approach for the efficient synthesis of renewable energy systems,” *Appl. Energy*, 2014.
- [7] C. D. Yue, C. S. Chen, and Y. C. Lee, “Integration of optimal combinations of

- renewable energy sources into the energy supply of Wang-An Island,” *Renew. Energy*, 2016.
- [8] D. Curto, V. FRANZITTA, M. Trapanese, and M. Cirrincione, “A Preliminary Energy Assessment to Improve the Energy Sustainability in the Small Islands of the Mediterranean Sea,” *J. Sustain. Dev. Energy, Water Environ. Syst.*, vol. N/A, no. N/A, 2020.
- [9] J. D. Ocon and P. Bertheau, “Energy transition from diesel-based to solar photovoltaics-battery-diesel hybrid system-based island grids in the Philippines – Techno-economic potential and policy implication on missionary electrification,” *J. Sustain. Dev. Energy, Water Environ. Syst.*, vol. 7, no. 1, 2019.
- [10] H. C. Gils and S. Simon, “Carbon neutral archipelago – 100% renewable energy supply for the Canary Islands,” *Appl. Energy*, 2017.
- [11] P. Enevoldsen and B. K. Sovacool, “Integrating power systems for remote island energy supply: Lessons from Mykines, Faroe Islands,” *Renew. Energy*, 2016.
- [12] H. Lund, P. A. Østergaard, D. Connolly, and B. V. Mathiesen, “Smart energy and smart energy systems,” *Energy*, 2017.
- [13] B. V. Mathiesen *et al.*, “Smart Energy Systems for coherent 100% renewable energy and transport solutions,” *Applied Energy*, 2015.
- [14] D. F. Dominkovic, G. Stark, B. M. Hodge, and A. S. Pedersen, “Integrated energy planning with a high share of variable renewable energy sources for a Caribbean Island,” *Energies*, 2018.
- [15] Z. Wang, X. Lin, N. Tong, Z. Li, S. Sun, and C. Liu, “Optimal planning of a 100% renewable energy island supply system based on the integration of a concentrating solar power plant and desalination units,” *Int. J. Electr. Power Energy Syst.*, 2020.
- [16] D. Groppi, A. Pfeifer, D. A. Garcia, G. Krajačić, and N. Duić, “A review on energy

- storage and demand side management solutions in smart energy islands,” *Renew. Sustain. Energy Rev.*, vol. 135, 2021.
- [17] C. Gamarra and J. M. Guerrero, “Computational optimization techniques applied to microgrids planning: A review,” *Renewable and Sustainable Energy Reviews*, vol. 48. Elsevier Ltd, pp. 413–424, 01-Aug-2015.
- [18] S. X. Chen, H. B. Gooi, and M. Q. Wang, “Sizing of energy storage for microgrids,” *IEEE Trans. Smart Grid*, 2012.
- [19] M. Quashie, C. Marnay, F. Bouffard, and G. Joós, “Optimal planning of microgrid power and operating reserve capacity,” *Appl. Energy*, vol. 210, pp. 1229–1236, Jan. 2018.
- [20] S. N. Khan, “Intelligent algorithm for efficient use of energy using tackling the load uncertainty method in smart grid,” *J. Sustain. Dev. Energy, Water Environ. Syst.*, vol. 8, no. 3, 2020.
- [21] M. Mimica, D. F. Dominković, T. Capuder, and G. Krajačić, “On the value and potential of demand response in the smart island archipelago,” *Renew. Energy*, vol. 176, 2021.
- [22] D. Akinyele, J. Belikov, and Y. Levron, “Challenges of microgrids in remote communities: A STEEP model application,” *Energies*, 2018.
- [23] M. Quashie, F. Bouffard, C. Marnay, R. Jassim, and G. Joós, “On bilevel planning of advanced microgrids,” *Int. J. Electr. Power Energy Syst.*, vol. 96, pp. 422–431, Mar. 2018.
- [24] F. Bénard-Sora and J. P. Praene, “Sustainable urban planning for a successful energy transition on Reunion Island: From policy intentions to practical achievement,” *Util. Policy*, 2018.
- [25] J. P. Jimenez-Navarro, K. Kavvadias, F. Filippidou, M. Pavičević, and S. Quoilin,

- “Coupling the heating and power sectors: The role of centralised combined heat and power plants and district heat in a European decarbonised power system,” *Appl. Energy*, vol. 270, 2020.
- [26] S. Bellocchi, M. Manno, M. Noussan, M. G. Prina, and M. Vellini, “Electrification of transport and residential heating sectors in support of renewable penetration: Scenarios for the Italian energy system,” *Energy*, vol. 196, 2020.
- [27] I. Bačeković and P. A. Østergaard, “A smart energy system approach vs a non-integrated renewable energy system approach to designing a future energy system in Zagreb,” *Energy*, vol. 155, 2018.
- [28] M. G. Prina *et al.*, “Multi-objective investment optimization for energy system models in high temporal and spatial resolution,” *Appl. Energy*, vol. 264, 2020.
- [29] H. Lund, J. Z. Thellufsen, P. A. Østergaard, P. Sorknæs, I. R. Skov, and B. V. Mathiesen, “EnergyPLAN – Advanced analysis of smart energy systems,” *Smart Energy*, vol. 1, 2021.
- [30] G. Krajačić, N. Duić, and M. da G. Carvalho, “H2RES, Energy planning tool for island energy systems - The case of the Island of Mljet,” *Int. J. Hydrogen Energy*, vol. 34, no. 16, 2009.
- [31] HOMER Energy LLC, *HOMER Pro Version 3.7 User Manual*, no. August. 2016.
- [32] Busarello, Cott Partner Inc. and ABB Utilities Gmbh, “NEPLAN Users’ guide Electrical, Version 5.”
- [33] DigSILENT Gmbh, “DigSILENT Power Factory,” 2021.
- [34] Siemens, “PSS/E user manual,” 2021.
- [35] M. Mimica and G. Krajačić, “Advanced RenewIslands method with quantitative mapping of islands’ needs and resources,” in *SDEWES Conference*, 2019.
- [36] T. Dragičević, H. Pandžić, D. Škrlec, I. Kuzle, J. M. Guerrero, and D. S. Kirschen,

- “Capacity Optimization of Renewable Energy Sources and Battery Storage in an Autonomous Telecommunication Facility,” *IEEE Trans. Sustain. Energy*, vol. 5, no. 4, 2014.
- [37] IRENA, “Hydrogen: A Renewable Energy Perspective,” 2019.
- [38] IRENA, “Road transport: The cost of renewable solutions,” 2013.
- [39] World Energy Council, “Cost of Energy Technologies,” 2013.
- [40] A. Belderbos, E. Delarue, and W. D’haeseleer, “Calculating the levelized cost of storage?” *Energy Expect. Uncertainty, 39th IAEE Int. Conf.*, 2016.
- [41] A. Ramos, C. A. Teixeira, and A. Rouboa, “Environmental assessment of municipal solid waste by two-stage plasma gasification,” *Energies*, 2019.
- [42] B. Miao and S. H. Chan, “The economic feasibility study of a 100-MW Power-to-Gas plant,” *Int. J. Hydrogen Energy*, 2019.
- [43] D. Thomas, “State of play and developments of power-to-hydrogen technologies,” 2019.
- [44] Republic of Croatia – Central Bureau of Statistics, “Census of Population, Households and Dwellings (in Croatian),” 2011.
- [45] M. D. Sanij, M. Dehghani-Ashkezari, and H. Hashemi-Dezaki, “Optimum reserve estimation in micro-grids containing renewable distributed generation resources,” *Indian J. Sci. Technol.*, 2015.
- [46] A. J. Karabelas, C. P. Koutsou, M. Kostoglou, and D. C. Sioutopoulos, “Analysis of specific energy consumption in reverse osmosis desalination processes,” *Desalination*, 2018.
- [47] D. R. Schneider, D. Lonèar, and Ž. Bogdan, “Cost analysis of waste-to-energy plant,” *Strojarstvo*, 2010.
- [48] X. Yang *et al.*, “The correlations among wastewater internal energy, energy

- consumption and energy recovery/production potentials in wastewater treatment plant: An assessment of the energy balance,” *Sci. Total Environ.*, vol. 714, no. 136655, 2020.
- [49] C. S. B. Gonzaga, O. de Q. F. Araújo, and J. L. de Medeiros, “A Monte Carlo methodology for environmental assessment applied to offshore processing of natural gas with high carbon dioxide content,” *J. Sustain. Dev. Energy, Water Environ. Syst.*, vol. 8, no. 1, 2020.
- [50] Croatian Energy Company HEP, “<https://www.hep.hr/solar-power-plant-vis-the-largest-solar-power-plant-in-croatia-put-into-operation/3550>,” 2021. .
- [51] H. Meschede *et al.*, “On the transferability of smart energy systems on off-grid islands using cluster analysis – A case study for the Philippine archipelago,” *Appl. Energy*, vol. 251, 2019.
- [52] P. Cabrera, H. Lund, and J. A. Carta, “Smart renewable energy penetration strategies on islands: The case of Gran Canaria,” *Energy*, vol. 162, 2018.
- [53] J. Z. Thellufsen *et al.*, “Smart energy cities in a 100% renewable energy context,” *Renew. Sustain. Energy Rev.*, vol. 129, 2020.
- [54] H. Meschede, “Analysis on the demand response potential in hotels with varying probabilistic influencing time-series for the Canary Islands,” *Renew. Energy*, vol. 160, 2020.
- [55] L. Urbanucci and D. Testi, “Optimal integrated sizing and operation of a CHP system with Monte Carlo risk analysis for long-term uncertainty in energy demands,” *Energy Convers. Manag.*, vol. 157, 2018.
- [56] E. Arriagada, E. López, M. López, R. Blasco-Gimenez, C. Roa, and M. Poloujadoff, “A probabilistic economic dispatch model and methodology considering renewable energy, demand and generator uncertainties,” *Electr. Power Syst. Res.*, vol. 121, 2015.

PAPER 2

A robust risk assessment method for energy planning scenarios on smart islands under the demand uncertainty

Marko Mimica^{1}, Laura Giménez De Urtasun², Goran Krajačić¹*

¹Department of Energy, Power and Environmental Engineering, Faculty of Mechanical Engineering and Naval Architecture, University of Zagreb, Ivana Lučića 5, 10002 Zagreb, Croatia

²CIRCE Foundation, Avenida Ranillas 3D, 50018, Zaragoza, Spain

Corresponding author (*) e-mail: mmimica@fsb.hr

Abstract

Energy systems with a high share of variable renewable energy are more vulnerable to sudden changes in the system operation. This is especially emphasized on small systems such as energy systems on geographical islands. Because of these reasons, there is a need for quantifying the risk of energy scenarios of such systems. This paper presents a novel robust risk assessment method under demand uncertainty for energy planning scenarios for the islands. The method uses graph theory for the representation of power system topology. The Poisson distribution is used for calculating the probability of power system element failure. The robust modelling approach is applied by the introduction of auxiliary variables and compared to the deterministic model results. Four energy planning scenarios for Unije island are modelled and subjugated to several power system outages resulting in a risk vector calculated as the product of probability vector and damage matrix. The study also presents a zero-import risk energy planning scenario for Unije island that is achieved for a system of 0.5 MW photovoltaic plant and 3.55 MWh battery storage system.

Keywords

Power system risk assessment; Smart islands; Graph theory; Power system optimization; Energy planning; Robust optimization

1. Introduction

The increasing effort of the European Union (EU) for decarbonization of energy systems imposes new challenges for scientists and engineers [1]. Due to their variability, integration of renewable energy sources (RES) in the energy systems reduce the security of supply and impose a new risk to power system operation. Therefore, it is necessary to implement new technology such as the energy storage systems (ESS) and the demand response (DR) for risk reduction when the power system is subjected to sudden and strong changes. Lately, a new concept of geographical islands as living labs emerges as a beneficial way of testing the new technology on islands as emphasized in [2]. The idea behind this is that, if it is possible to integrate a high amount of variable RES on islands, it will be possible to transfer and scale up the same solutions to similar locations on the mainland.

Methods and tools for energy planning of the islands have been presented in many studies. Duić et al. [3] presented a RenewIslands method for energy planning of the islands with an emphasis on different sector integration. The method was applied to Croatian islands in [4] where the authors analysed the effect of the interconnection between the island and concluded that interconnection can reduce the critical excess electricity power up to 22% when the islands are interconnected. Another study conducted on Cape Verde [5] showed that overall yearly costs of the energy system operation can reduce by 19% in comparison to the business as usual scenario when there is a higher penetration of wind coupled with the desalination plant and the pumped hydro plant. However, the method does not consider the risk assessment of generated scenarios. By applying the presented risk assessment method, these studies could be improved and it would be possible to quantify the risk level of each scenario.

To increase the possibility for RES integration technologies such as batteries and the DR are introduced in the power systems. To determine how flexible or resilient a particular energy scenario is, it is necessary to quantify the risk level of each scenario. Lund et al. [6] emphasizes the importance of energy system flexibility for RES integration. The paper analysed demand and production strategies to increase flexibility. The latest review of flexibility sources was provided in [7] where authors emphasized the importance of energy storage and demand response. The authors in [8] emphasized the importance of the proper pricing mechanism on a battery and PV system and concluded that the arbitrage for the batteries should be enabled in order to maximize the profitability of the investment. One of the possible solutions for

increasing the flexibility of the energy system is to use an integrated approach to energy planning as described in [9]. This research included refrigeration, smart EV charging and reverse osmosis technology to achieve flexibility and the authors conclude that 78.1% of the electricity demand can be met with the RES production by this approach.

The authors in [10] proposed a renewable mix that could produce 324.9 MWh/year and cover the entire demand of the island Ustica, however, the authors do not model the power system elements nor do they examine the failure probability. Similarly, the study [11] presented the approach for the energy transition from the diesel-based to the hybridized systems with a RES share of 50.4% for four analyzed islands. It would be interesting to apply the presented risk assessment approach to assess the trade-off between the risk level and the share of RES in electricity production. The authors in [12] underlined the importance of proper energy policy in the creation of energy planning scenarios, however without the quantification or inclusion of the risk assessment in the study.

A significant amount of energy planning methods and scenarios were proposed in these studies [3-12], however, none of them provided a risk analysis. Because of this, it remained unclear to what risk level are local communities exposed to when a particular energy planning scenario would be utilized. Application of the risk assessment method as an extension to analysed studies would contribute to the understanding of the overall impact on energy security on the islands.

The decision support system is presented in [13], where the expected load loss was taken as a measure of risk, but only larger systems such as Taiwan are considered and the system did not consider the cost that a possible power outage would cause. The authors in [14] presented an algorithm for maximizing the predictability of the electrical power system and the Power Flow Predictability Index. The authors showed that an increase in the 34.5% predictability index is possible with the increased system cost of 1.28%, however, the authors did not include the possibility for the power system elements failure nor the predictability of failures. Risk management in wind energy was analyzed in [15] with the conclusion that the lowest risk for wind energy integration is in the areas where governments have a long-term and clear vision of electricity price policy.

A method for assessing the safety of the electrical power system is presented in [16] where external risks are considered as threats caused by inclement weather, while load loss was considered as a measure of risk. The numerical results of the study [17] show that it is possible to achieve a 13.8% higher microgrid profit when considering the risk of unsafe power system parameters such as electricity price and the production from the variable RES. The study did

not analyze the specific operating conditions of the power system operation that may be a result of element outage. The power system risk assessment method based on the historical data and the predicted stochastic element failure for three scenarios in the power system is presented in [18] where the probability of the load loss and the average load loss was taken as a measure of risk. Besides using different measures of risk, the study did not use the robust approach and did not consider the curtailment of RES production.

The study [19] assessed the impact of different smart grid technologies and concluded that, when the load flexibility level is equal to 25%, it is possible to achieve monthly savings of 11.3 €. However, the study did not provide the impact analysis of different technologies on the risk level. Impact on the financial and technical aspects of running the power system under conditions of financial risk based on the behaviour of other players in the market was given in [20] where it was shown that the greatest financial profit of 10498.98 currency units for the case is achieved when the production of the solar power plants and the wind farms is managed under a single aggregator. Two scenarios for the microgrids with RES and electricity storage under the influence of risk are given in [21] where the author specifically considered the rate of change in solar radiation and wind speed between the two time periods, further examining the system's resistance to sudden changes.

Operation of the virtual power plant consisted of wind power, solar power, battery and diesel power under the conditions of the financial risks affecting its daily profit were explored in [22]. The authors in [23] used Pinch analysis for defining the energy planning scenarios and the calculation of the loss of power supply probability where they presented that it is possible to achieve the loss of power supply probability of 2.57%. Another study [24] presented the stochastic risk-averse approach for the microgrid planning under uncertainty and concluded that the stochastic approach results with 10,732 \$/year in comparison with the deterministic model for the best-case scenario. Multi-objective stochastic risk optimization model was presented in [25] with conclusion that the proposed approach reduced the overall expenditure by 23%. However, these studies did not model the power system elements and did not consider the possibility for the elements outage (e.g. line or transformer).

Quantitative risk analysis of functional failure in the fracturing system of unconventional natural gas was provided in [26]. Multi-objective risk analysis for a reforming reactor system was presented in [27] with the conclusion that P-graph can be used for representation of the process flow diagrams of the power plants. The proposed studies did not analyse energy systems as a whole nor they provided the method for risk assessment reduction when smart technology as energy storage is introduced.

From analysed literature, it is possible to conclude that the development of different energy planning scenarios for small renewable island systems is becoming increasingly important and the authors offer various methods for defining them. However, a risk assessment approach of developed scenarios for small island systems based on the grid elements failure probability, as well as potential damage that would occur as a result of an outage, was not analysed. The novel method developed within this study offers the possibility for such risk analysis and provides important information in the energy planning process. Moreover, this study proposes a robust approach for the risk assessment under the demand uncertainty which enables the evaluation of an entire range of possible scenarios – from most optimistic ones to most pessimistic. As such, the proposed method is beneficial for many different stakeholders such as investors in renewable technology or local island governments where outages occur more often as a result of harsh weather conditions. The method highlights a new aspect of long term development of the islands that is often based on financial parameters while the risk assessment for the islanders is neglected.

The hypothesis of this study is that, by using the presented robust risk assessment method based on graph theory, it is possible to quantify the risk level of energy planning scenarios for islands under the demand uncertainty. Relevant contributions of this paper are:

- A novel robust risk assessment method under the demand uncertainty that underlines the resilience of energy planning scenarios and provides another parameter in decision making for the smart islands
- The risk assessment analysis of the renewable energy planning scenarios conducted for Unije island and can be applied to numerous similar islands
- Comparison of deterministic and robust approach for risk assessment
- The case for a zero-import risk energy planning scenario for Unije island enabled the operation of the power system without any curtailment and any load shedding even when the fault on the interconnection occurs.

After the introduction section with literature review, gap analysis and description of the novelty of the developed method, the second section presents the novel risk assessment method developed within this study. The analysed case study is presented in the third section, while the fourth section presents the results of the study. The final section presents the concluding remarks of the study.

2. Materials and methods

The proposed method enables a risk assessment of the energy planning scenarios for the smart islands. This makes it a suitable decision-making tool for deciding what energy planning scenario or smart solution should be implemented. The method can be divided into several steps as follows:

- Step 1: Generate desired energy planning scenarios of an island.
- Step 2: Construct power system topology and belonging graph G together with probabilities for the failure of power system elements
- Step 3: Create robust optimization models for energy planning scenarios and define inputs for the optimization model
- Step 4: Apply outages on elements of the power system (bring the system to different states) and solve optimization models for every state of every scenario and measure the results
- Step 5: Calculate the risk vector of every energy planning scenario and analyse the results

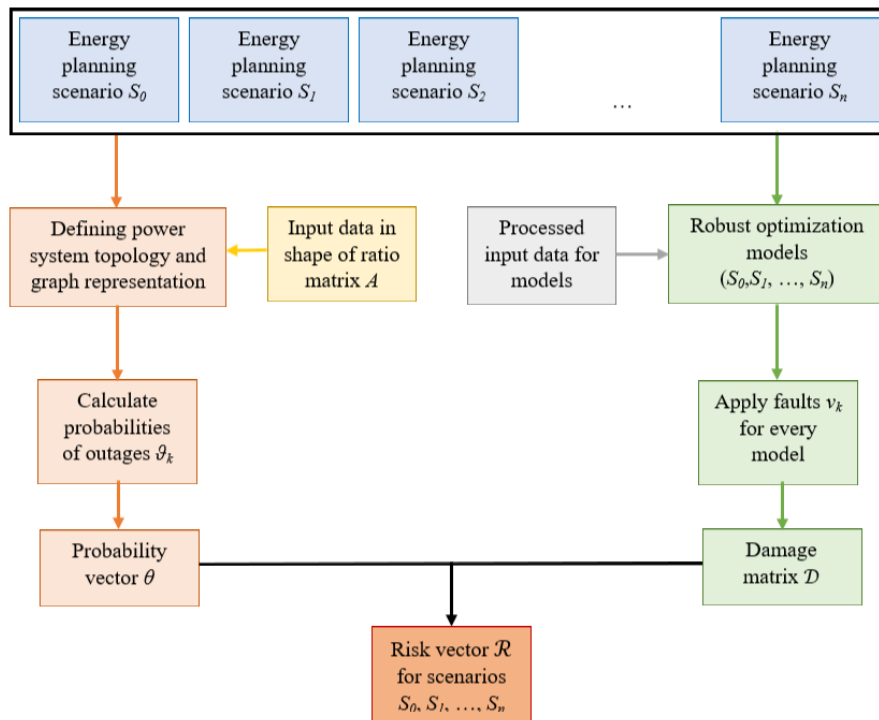


Figure 1. Risk assessment method scheme

2.1. Power system elements outage probability calculation

Let $G = (\mathcal{N}, \mathcal{E}, A)$ be the undirected graph which represents electrical power network of a small island with set of $\mathcal{N} = \{n_1, \dots, n_n\}$ nodes, $\mathcal{E} \subseteq \mathcal{N} \times \mathcal{N}$ edges or links and where A is a matrix of ratios of an event occurring. Undirected edges are denoted as $e_{ij} = (n_i, n_j)$, the cardinality of a set of undirected edges is denoted as $|\mathcal{E}|$ and the matrix A satisfies $[A]_{ij} \neq 0 \Leftrightarrow e_{ij} \in \mathcal{E}$ and $[A]_{ij} = 0 \Leftrightarrow e_{ij} \notin \mathcal{E}$ where $A \in \mathbb{R}^{n \times n}$ and $e_{ii} \notin \mathcal{E}$. Matrix A represents a failure ratio of the elements of the power system. The elements of the matrix are defined as $[A]_{ij} = a_{ij}$ where a_{ij} is a ratio of the outage of the given element of the power system. The importance of the graph theory is clear as there is a necessity for a objective mathematical formulation for connecting the ratio of outage of each particular element in the power system with the connections of different elements (objects) in the power system. Thus, the matrix of ratios A is created based on the graph theory.

A power system is a system of small probabilities and large damages. Small probabilities are described with a Poisson distribution which answers the question of what is the probability that an event occurs and is defined with expression (1). Poisson distribution is often applied in the power system modelling as in [28] for the transmission system or [29] for the distribution system.

$$\vartheta_m(N, \Delta t) = \frac{(a_{ij} \cdot \Delta t)^N \cdot e^{-a_{ij} \cdot \Delta t}}{N!} \quad (1)$$

Where N is the number of times that an event occurs in the given time Δt at a rate of a (events/time) where i and j stand for a particular element of the power system and correspond to e_{ij} . Therefore, a vector of probabilities is defined as $\theta = [\vartheta_1, \dots, \vartheta_{|\mathcal{E}|}]$ where $\vartheta_m \in \langle 0, 1 \rangle$ for all $m = 1, 2, \dots, |\mathcal{E}|$ and represents probabilities for fault at a given element of the power system.

2.2. Deterministic model

Islands' power systems are observed as the microgrids during the set of periods Ω^T , where $|\Omega^T| = 96$. Considered microgrids generally consist of non-flexible and flexible demand, RES and the ESS. The microgrid is subjugated to the dynamic pricing which opens the chance for

the microgrid components to provide flexibility to the system and allows final customers participation in the market on the distribution level. The objective of microgrid optimization is to move the system towards the equilibrium point where social welfare is maximized. Therefore, the objective function of the system is to minimize its operation cost or maximize its profit. It is considered that the buying and selling of electricity take place in the day-ahead electricity market. In this chapter, a general optimization model is presented that can be adjusted for the specific case study. The objective function $F: \mathbb{R} \rightarrow \mathbb{R}$ is defined as convex and derivative at every point of its domain and is represented by the following expression (2):

$$\max F \triangleq \max[\sum_{t \in \Omega^T} \lambda_t (E_t^s - E_t^b) - C_t] \quad (2)$$

Where λ_t is electricity market price at a given period t , E_t^s and E_t^b are sold and purchased energy to and from the electricity market and C_t are microgrid costs at a given period t . Costs of the microgrid are defined as the cost of curtailed energy and the cost of loss of load. A microgrid is subjugated to power balance constraint given with equation (3) for $\forall t \in \Omega^T, \forall pv \in \Omega^{PV}, \forall d, c \in \Omega^{ESS}, \forall w \in \Omega^W, \forall g \in \Omega^G$.

$$p_{g,t} + p_{w,t} + p_{pv,t} + p_{d,t} + p_{imp,t} + DR_t + LS_t = L_t + FL_t + p_{exp,t} + p_{c,t} \quad (3)$$

The left side of the equation presents power inputs to the microgrid and the right side presents power withdrawal elements. The power injections are PV generation ($p_{pv,t}$), wind power plant generation ($p_{w,t}$), conventional generator production ($p_{g,t}$), imported power ($p_{imp,t}$) to the microgrid, discharge from the ESS ($p_{d,t}$), load shedding (LS_t) as well as DR (DR_t) which reduces the need for electricity. The inflexible (L_t) and flexible load (FL_t), exported power ($p_{exp,t}$) and energy storage charging ($p_{c,t}$) represent the withdrawal of the electricity. Imported and exported electricity represent sold and purchased electricity on the day-ahead electricity market.

The total cost of the microgrid is expressed with equation (4) for $\forall t \in \Omega^T, \forall pv \in \Omega^{PV}, \forall w \in \Omega^W, \forall g \in \Omega^G$. $p_{pv,t}^{curt}$ is curtailed solar power from the set of PV plants Ω^{PV} . VPVC is the penalty for the curtailment of the PV production that represents the compensation for the loss of profit of the producer. Value of lost load (VOLL) is the cost of not delivering the electricity

to the customer. It is the estimated value and represents the amount that is a customer willing to pay for avoiding loss of supply.

Thermal generator model in the unit commitment is based on the models presented in [30]. There are several decisions that need to be made regarding the thermal generators in the day-ahead planning. These decisions are represented with the binary variables and include a start-up decision ($x_{g,t}$) and a shut-down decision ($z_{g,t}$) that are related to the start-up and shut-down costs (SU_g and SD_g) as in (4). The cost function (4) also includes a fuel cost function $F_g(p_{g,t})$ for the periods when generator is operating. The fuel cost function is usually in the quadratic form and should be linearized according to the procedure described in [30]. The thermal generator minimum and maximum output should also be constrained (5) and (6) with minimum (P_g^{min}) and maximum values (P_g^{max}). These constraints should be active only when the generator is operating, which is controlled with the binary variable $u_{g,t}$. The binary variable $u_{g,t}$ is equal to 1 if the generator is operating, otherwise it is equal to 0. Ramping up (RU_g) and down (RD_g) capabilities between the two consecutive periods are defined with equation (7).

The thermal generators usually cannot be started immediately nor can they be shut-down immediately. Thus, it is necessary to define minimum start-up (UT_g) and shut-down time (DT_g) of the generator. Equations (8) and (9) enable that the generators cannot be shut down until the shortest on time (UT_g) has passed and cannot be started-up before minimum down time (DT_g). Equation (10) defines the start-up action and equation (11) defines the shut down action. Moreover, equation (12) prevents simultaneous start-up and shut down of the generator.

The PV plant model is represented with equation (14) and the wind plant model with equation (15). The renewable units are designed in a way that the sum of produced energy and curtailed energy has to be equal to the maximum possible production $\Lambda_{pv,t}$ and $\Lambda_{w,t}$. The ESS model is given with equations (16) – (19) where $\mu_t \in \{0, 1\}$, $\xi \in [0, 1]$. The SOC represents the state of charge of the storage, η_c and η_d the efficiency of charge and discharge and μ_t is the binary variable preventing simultaneous charging and discharging of the storage. ξ represents the share of total battery capacity that can be charged or discharged at a given time. The flexible load can provide significant flexibility to the island power system by providing the DR to the system. The most common way of providing flexibility to the power system on the islands is by desalination plants. Other ways for providing the DR is by heating storage, electric vehicles, automatic switching on and off of different house devices etc. A simplified DR model is given

with equation (20) and (21) where $\alpha, \beta \in [0,1]$. α_t and β_t represent the percentages of available flexible load for providing up and down DR services. ω represents the total amount of available DR for the observed period. Import and export power is limited by the capacity of the power line or physical constraints imposed by the power grid. Such constraints are mostly caused because of voltage issues, transient stability issues or other power quality issues. Islands systems are usually at the end of radially connected distribution grid which means that the voltage issues are more expressed in these areas. Thus, to preserve the stable conditions in the observed grid as well as in the surrounding grid, maximum and minimum export and import power constraints are modelled with equations (22) and (23).

$$C_t = \left(\sum_{g \in \Omega^G} (SU_g \cdot x_{g,t} + SD_g \cdot z_{g,t}) + \sum_{g \in \Omega^G} F_g(p_{g,t}) + VWC \cdot \sum_{w \in \Omega^W} P_{w,t}^{curt} + VPVC \cdot \sum_{pv \in \Omega^{PV}} P_{pv,t}^{curt} + VoLL \cdot LS_t \right) \cdot \Delta t, \quad \forall t \in \Omega^T \quad (4)$$

$$P_g^{min} \cdot u_{g,t} \leq p_{g,t} \leq P_g^{max} \cdot u_{g,t}, \quad \forall g \in \Omega^G, \forall t \in \Omega^T \quad (5)$$

$$p_{g,t} \geq 0, \quad \forall g \in \Omega^G, \forall t \in \Omega^T \quad (6)$$

$$-RD_g \leq p_{g,t} - p_{g,t-1} \leq RU_g, \quad \forall g \in \Omega^G, \forall t \in \Omega^T \quad (7)$$

$$u_{g,t} - u_{g,t-1} \leq u_{g,k}, \quad \forall g \in \Omega^G, \forall t \in \Omega^T, k = t, \dots, \min\{t + UT_g - 1, |\Omega^T|\} \quad (8)$$

$$u_{g,t-1} - u_{g,t} \leq 1 - u_{g,k}, \quad \forall g \in \Omega^G, \forall t \in \Omega^T, k = t, \dots, \min\{t + DT_g - 1, |\Omega^T|\} \quad (9)$$

$$x_{g,t} \geq u_{g,t} - u_{g,t-1}, \quad \forall g \in \Omega^G, \forall t \in \Omega^T \quad (10)$$

$$z_{g,t} \geq u_{g,t-1} - u_{g,t}, \quad \forall g \in \Omega^G, \forall t \in \Omega^T \quad (11)$$

$$x_{g,t} + z_{g,t} \leq 1, \quad \forall g \in \Omega^G, \forall t \in \Omega^T \quad (12)$$

$$x_{g,t}, z_{g,t}, u_{g,t} \in \{0,1\}, \quad \forall g \in \Omega^G, \forall t \in \Omega^T \quad (13)$$

$$p_{pv,t} + p_{pv,t}^{crut} = \Lambda_{pv,t}, \quad \forall t \in \Omega^T \quad (14)$$

$$p_{w,t} + p_{w,t}^{crut} = \Lambda_{w,t}, \quad \forall t \in \Omega^T \quad (15)$$

$$SOC_t = SOC_{t-1} + (p_{c,t} \cdot \eta_c - \frac{p_{d,t}}{\eta_d}) \cdot \Delta t, \quad \forall t \in \Omega^T \quad (16)$$

$$SOC^{min} \leq SOC_t \leq SOC^{max}, \quad \forall t \in \Omega^T \quad (17)$$

$$p_{c,t} \cdot \Delta t \leq \xi \cdot SOC^{max} \cdot \mu_t, \quad \forall t \in \Omega^T \quad (18)$$

$$p_{d,t} \cdot \Delta t \leq \xi \cdot SOC^{max} \cdot (1 - \mu_t), \quad \forall t \in \Omega^T \quad (19)$$

$$-\alpha_t \cdot FL_t \leq DR_t \leq \beta_t \cdot FL_t, \quad \forall t \in \Omega^T \quad (20)$$

$$DR_t \cdot \Delta t \leq \omega, \quad \forall t \in \Omega^T \quad (21)$$

$$P_{imp}^{min} \leq p_{imp,t} \leq P_{imp}^{max}, \forall t \in \Omega^T \quad (22)$$

$$P_{eks}^{min} \leq p_{exp,t} \leq P_{eks}^{max}, \forall t \in \Omega^T \quad (23)$$

2.3. Robust model formulation

Loss of load is the variable that has the highest effect on the damage caused by the power system outage. However, this is the uncertain variable that depends on the current demand of the observed system. Thus, equations (2)-(23) are valid only if demand L_t is considered as a deterministic parameter. Several techniques are available for modelling demand as an uncertain parameter. For stochastic scenario modelling [31], a probability density function of the observed parameter should be known. The membership function of the observed parameter should be known when fuzzy modelling is applied [32]. Stochastic scenario and fuzzy modelling are often computationally demanding. In this paper, a robust modelling approach [33] is applied. The robust modelling approach considers the uncertainty set to take the uncertainty parameter into the consideration. The uncertainty set is defined with the upper and lower values over the period that is available from the historic data. The boundaries are set to a 5th and 95th percentile. This approach assures that 95% of scenarios are under the upper boundary, while 5% of scenarios is under the lower boundary. The demand uncertainty interval is defined with expression (24):

$$\tilde{L}_t \in U(\tilde{L}_t) = \{\tilde{L}_t : L_t^{min} \leq \tilde{L}_t \leq L_t^{max}\}, \forall t \in \Omega^T \quad (24)$$

It is assumed that the only known values are minimum and maximum bounds of demand interval (L_t^{min} and L_t^{max}). The robust formulation of proposed MILP optimization problem was achieved by modifying the balance equation according to the [34] and [35].

Equality (3) should be transformed into two inequations as explained in [36]. Then, the robust counterpart of equation (3) of the deterministic problem can be written as (25) and (26):

$$\begin{aligned} & p_{g,t} + p_{w,t} + p_{pv,t} + p_{d,t} + p_{imp,t} + DR_t + LS_t \\ & \geq L_t + \phi_{L,t} \cdot \Gamma + \psi_{L,t} + FL_t + p_{exp,t} + p_{c,t}, \quad \forall t \in \Omega^T \end{aligned} \quad (25)$$

$$\begin{aligned}
& p_{g,t} + p_{w,t} + p_{pv,t} + p_{d,t} + p_{imp,t} + DR_t + LS_t \\
& \leq L_t + \phi_{L,t} \cdot \Gamma + \psi_{L,t} + FL_t + p_{exp,t} + p_{c,t}, \forall t \in \Omega^T
\end{aligned} \tag{26}$$

In order to control the uncertainty interval, a conservativeness factor Γ is introduced. The conservativeness factor can range from 0 to 1 ($\Gamma \in [0,1]$) because there is only one uncertain value observed. The most optimistic result occurs for $\Gamma = 0$, when no deviation is considered. Increase of Γ_L parameter results with more pessimistic cases. The corresponding positive auxiliary variables are $\phi_{L,t}$, and $\psi_{L,t}$, necessary for the robust formulation modelling. Additional constraints (27) and (28) are necessary in order to take into account the uncertainty range.

$$\phi_{L,t} + \psi_{L,t} \geq \delta_{L,t}, \forall t \in \Omega^T \tag{27}$$

$$\phi_{L,t} \geq 0, \psi_{L,t} \geq 0, \forall t \in \Omega^T \tag{28}$$

The summation of auxiliary variables $\phi_{L,t}$ and $\psi_{L,t}$ needs to be greater or equal to the uncertainty range deviation $\delta_{L,t}$. The values of $\phi_{L,t}$ and $\psi_{L,t}$ are determined with the conservativeness factor Γ so that the worst case of uncertainty occurs. The final robust problem is defined with equations (2), (4)-(33) and (25)-(28).

2.4. Risk calculation

Let $S = \{S_1, \dots, S_Y\}$ represent set of energy planning scenarios, $V = \{v_1, \dots, v_{|\mathcal{E}|}\}$ set of modelled electric power system faults and $\mathcal{D} \in \mathbb{R}^{|\mathcal{E}| \times Y}$ damage matrix where $[\mathcal{D}]_{ij}$ is damage for every i energy planning scenario subjugated to fault j . Elements of the damage matrix are calculated with presented optimization models. Risk vector $\mathcal{R} \in \mathbb{R}^{1 \times Y}$ is defined as the product of probability vector $\theta \in \mathbb{R}^{1 \times |\mathcal{E}|}$ and damage matrix \mathcal{D} and is defined as follows with equation (29):

$$\begin{bmatrix} \vartheta_1 \\ \vartheta_2 \\ \vdots \\ \vartheta_m \end{bmatrix}^T \cdot \begin{bmatrix} \mathcal{D}_{11} & \dots & \mathcal{D}_{1Y} \\ \vdots & \ddots & \vdots \\ \mathcal{D}_{|\mathcal{E}|1} & \dots & \mathcal{D}_{|\mathcal{E}|Y} \end{bmatrix} = \begin{bmatrix} \mathcal{R}_1 \\ \mathcal{R}_2 \\ \vdots \\ \mathcal{R}_Y \end{bmatrix}^T \tag{29}$$

3. Case study

Case study for testing presented method is conducted on small island Unije located in Kvarner archipelago in Croatia. Unije island has 16,77 km² of area and 88 inhabitants during winter.

During summer the number of people on the island reaches up to six times more residents than during winter. Unije has a 400 kVA substation that is connected with a 10 kV cable to the nearest island Vele Srkane. All the power for these and other small islands is provided from 4 MVA substation on the island of Lošinj. The power system of Unije is dependent on the availability of 10 kV cables from Unije to Lošinj because it is the only way of importing power to the island. There have been two faults on these cables in the period 2011 – 2018 [37] that caused power loss for residents of Unije island. Because of this, Unije represents an excellent location as a living lab for risk evaluation that can later be transferred to similar locations on the mainland. In order to choose the right energy planning scenario for microgrid, there is a need for risk assessment on each scenario. Therefore, this paper observes several different energy planning scenarios and evaluates risk by implementing the described method for each scenario.

3.1. Observed scenarios

Scenarios are presented in Table 1:

Table 1. Analysed scenarios for Unije island

Scenario	PV [MW]	ESS [MWh]	DR
S_0	0	0	No
S_1	1	0	Yes
S_2	0	1	Yes
S_3	1	0.5	Yes
“Zero-import risk”	TBD	TBD	Yes

It is assumed that the DR is provided by the desalination plant on the island represented with the flexible demand of 25 kW. The desalination plant is capable of providing the DR in the amount of 70% of its occupancy at a given period with a total amount of DR being less or equal to 200 kWh. The flexible load is not taken into account in the business as usual scenario (S_0), because the desalination plant is currently not used for providing the DR.

3.2. Network topology

Network topology of the island Unije is given in Figure 2 where existing elements are presented with the black line and elements that need to be built for implementation of energy planning scenarios are presented with the blue line. Presented elements that will be integrated include the PV plant, PV substation, flexible load and energy storage system. The existing elements are a 10 kV connection to the mainland, a transformer with a ratio of 10/0.4 kV and island load.

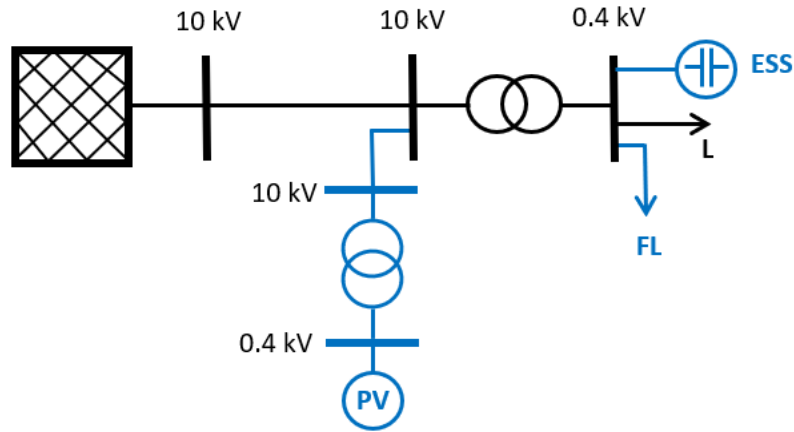


Figure 2. Unije power system with the existing elements marked with the black colour and elements that will be integrated marked with the blue colour

With defined topology and graph representation of topology, it is possible to calculate matrix A . The elements of matrix A are based on the historic data and represent the rate of fault occurrence at a given element of the system. Vector θ consists of the long term failure probabilities of particular elements of the power system network. In the case of Unije, calculated probabilities are the probability of failure of any line from feeder to Unije, which is represented only as one aggregated line in Figure 2, probability of failure of the transformer that connects the loads and the battery with the power line and combined probability of the failure of the line and the transformer that connects the PV plant to the power system. These probabilities correspond with edges e_{12} , e_{23} , e_{24} that connect belonging nodes in Figure 3.

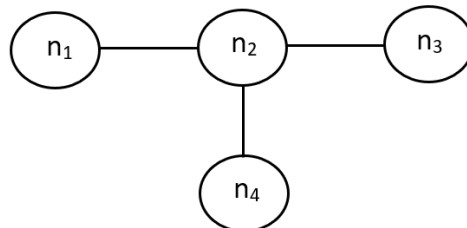


Figure 3. Graph representation of Unije power system

From data available at [37], it is possible to conclude that the failure rate for cables connecting feeder Lošinj and Unije is 0.286 failure per year. The transformer failure happens at a rate of 0.02 failure per year [38] which is significantly rarer than line faults. This is expected because of the high reliability and protection of transformers while cables and lines are vulnerable to outside effects such as weather changes. Cable and transformer that connect PV plant with the power system have to be built and their rate of occurrence can be calculated from the data available from [39] and [40] as the sum of the probabilities of failure of cable or transformer and amounts to 0.041 failures per year. The connection cable of PV and the power grid is significantly shorter (300 m) than cables connecting Unije to the feeder which means a significantly lower probability of failure. Therefore it is possible to construct matrix A for the described power system as:

$$A = \begin{bmatrix} 0 & 0.286 & 0 & 0 \\ 0.286 & 0 & 0.02 & 0.041 \\ 0 & 0.02 & 0 & 0 \\ 0 & 0.041 & 0 & 0 \end{bmatrix}$$

The simulation is considered for two days in august with the highest demand. This period is characterized by the highest demand, thus it is most relevant for the risk calculation. In order to enable the possibility to compare results one to another, the simulation considers that all faults occurred at 10 am and lasted until the end of the simulation.

3.3. Input data and optimization models

Input data for the optimization models is calculated and obtained from known analysis and the available data. The data is represented on a half an hour basis. The data for solar power production is obtained from the Optimal grid connection study [40] conducted for Unije island. The historical demand data is available from the study [41] and presented in Figure 4. The upper and lower boundaries are set in such a way that a two-sigma probability is assured. The data for electric energy prices were obtained from the historical data [42]. The simulation considers the case where values for the demand, solar production and prices occur for two consecutive days.

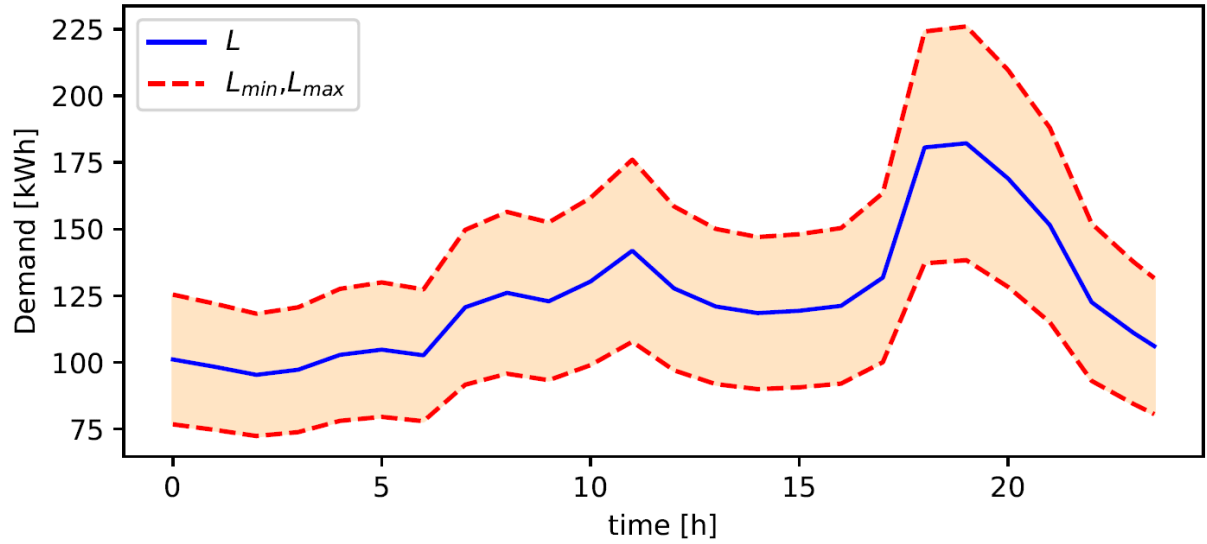


Figure 4. Electric energy demand for a peak summer day

The penalties for the wind and PV curtailment are calculated according to data available at [43] while the value of the lost load is calculated on the national level as the ratio between the gross domestic product and the annual electric energy consumption. The remaining data is given in Table 2.

Table 2. Parameter values for the optimization problem

Parameter	Value	Unit
VPVC/VWC	105.58	€/MWh
VOLL	2840	€/MWh
η_c	0.95	-
η_d	0.9	-
ξ	0.5	-
α	0	-
β	0.7	-
ϑ	0.2	MWh
$p_{imp}^{min}, p_{exp}^{min}$	0	MW
$p_{imp}^{max}, p_{exp}^{max}$	2.0	MW
Δt	0.5	h

Scenario S_0

Scenario S_0 represents the business as usual scenario. This means that island has no newly installed technology and there is no DR available. The objective function of the optimization model for such a scenario is defined with equation (30):

$$\max F^{S_0} \triangleq \max[\sum_{t \in \Omega^T} \lambda_t(-E_t^b) - VoLL \cdot LS_t \cdot \Delta t] \quad (30)$$

Subjected to equations (3), (22) and (23) for the deterministic case and with equations (22), (23), (25)-(28) for the robust model.

Scenario S_1

Scenario with a solar power plant of 1 MW is described by Scenario S_1 . The island is not dependent on power import when the PV plant production is high enough to cover the demand. At the same time, the excess power production is sold on the day-ahead electric energy market and the microgrid is generating profit. At this point, the DR is available from the desalination plant. Scenario S_1 is described with the following objective function (31):

$$\max F^{S_1} \triangleq \max[\sum_{t \in \Omega^T} \lambda_t(E_t^s - E_t^b) - VPVC \cdot P_{pv,t}^{curt} \cdot \Delta t - VoLL \cdot LS_t \cdot \Delta t] \quad (31)$$

Subjected to equations (3), (14), (20)-(23) for the deterministic model and to constraints (14), (20)-(23) and (25)-(28) for the robust optimization model.

Scenario S_2

The conditions in the islands' microgrid with the battery storage of 1 MW are described with scenario S_2 . The battery allows microgrid to arbitrage on the electric energy market by buying the electricity during periods of low price and selling it during periods of high price, thus providing the support for the external electric power system. The optimization model for scenario S_2 is given with equation (32):

$$\max F^{S_2} \triangleq \max[\sum_{t \in \Omega^T} \lambda_t(E_t^s - E_t^b) - VoLL \cdot LS_t \cdot \Delta t] \quad (32)$$

Subjected to equations (3), (16)-(23) for the deterministic case and to equations (16)-(23) and (25)-(28) for the robust case.

Scenario S_3

Final scenario S_3 represents the combination of 1 MW PV plant and 0.5 MW battery. The optimization model balances the microgrid so that its profit is maximized. The objective function of scenario S_3 is given with equation (33):

$$\max F^{S_3} \triangleq \max \left[\sum_{t \in \Omega^T} \lambda_t (E_t^s - E_t^b) - VPVC \cdot P_{pv,t}^{curt} \cdot \Delta t - VoLL \cdot LS_t \cdot \Delta t \right] \quad (33)$$

and is subjected to the constraints given with equations (3), (14), (16)-(23) for the deterministic model and with equations (14), (16)-(13) and (25)-(28) for the robust model.

“Zero-import risk” scenario

Additionally, this paper uses the described method for investigating the possibility for Unije island to become energy self – sufficient. For this purpose, special attention will be given to the scenario S_3 in order to investigate the required amount of installed PV plant power as well as the battery capacity for achieving a zero-import risk level. The scenario is simulated for the case when the fault occurs on Unije connection to the mainland at 10 am and lasts until the end of the simulation.

4. Results

The key outcome of the proposed method is the risk level that is used as a comparison indicator between the different energy planning scenarios. The risk level defined as in this paper may be considered as a reasonable amount of investment that should be made in order to prevent the potential outage of elements. However, the purpose of this method and the risk value as a result of it is to enable comparison between different scenarios. If one would want to calculate the risk value of already existing scenario in order to calculate the necessary periodical investment in order to prevent outages, it would be necessary to modify the proposed method so that it considers wider range of possible outages and their likelihood of occurrence.

4.1.Deterministic results

The risk should be calculated for the worst case which is during maximum demand on the island. Such demand can happen at any time during two summer months July and August, thus it is needed to calculate the probabilities of failure for that period. The probability vector θ is given with (34):

$$\theta = [0.046 \quad 0.0034 \quad 0.0069] \quad (34)$$

The results of optimization problems or caused damage for every scenario subjugated to a series of described faults is presented with damage matrix \mathcal{D} (35):

$$\mathcal{D} = \begin{bmatrix} 15,751.2 & 8,606.7 & 13,308.8 & 6,350.7 \\ 15,751.2 & 15,467.2 & 13,308.8 & 14,388 \\ 0 & 1,683.9 & 0 & 1,683.9 \end{bmatrix} \text{ €} \quad (35)$$

Rows of the matrix represent the energy scenario S_i and columns present fault v_i . For example, when a fault happens on interconnection (v_1) for the energy planning scenario S_2 the damage equals 13,308.8 €. With defined probability vector θ and the damage matrix \mathcal{D} it is possible to calculate the risk vector \mathcal{R} by using expression (29). The results are also visually presented in Figure 5.

$$\mathcal{R} = \begin{bmatrix} 778.1 \\ 460.1 \\ 657.5 \\ 352.7 \end{bmatrix}^T \text{ €} \quad (36)$$

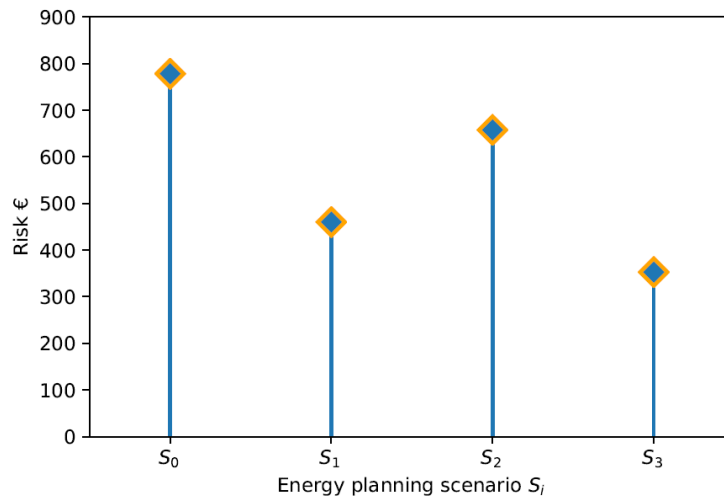


Figure 5. The quantified risk for analysed scenarios

The results indicate that the lowest risk is present in the energy planning scenario S_3 which represents the combination of a 1 MW PV plant and 0.5 MWh battery. Such results were expected because the implementation of different technologies enables easier operation of the system with lower cost in general. Table 3 presents the total cost of the system for two analysed days for different scenarios with applied faults as well as the cost in the normal operation of the system (v_0).

Table 3. Total operation cost in euros [€] for a given scenario and occurred fault for the deterministic model

Scenario	v_0	v_1	v_2	v_3
S_0	-378.9	-15,812	-14,743.4	-378.9
S_1	798	-8,433.6	-14,357.3	-1,822.7
S_2	-354.3	-13,406.9	-13,406.9	-354.3
S_3	807.2	-6,173.7	-13,296.7	-1,813.4

The total cost of the system shows that the system is making a profit only for S_1 and S_3 scenarios which are scenarios with the PV power plant. Other values are in correlation with the calculated energy planning scenario risks.

4.2. Robust model results

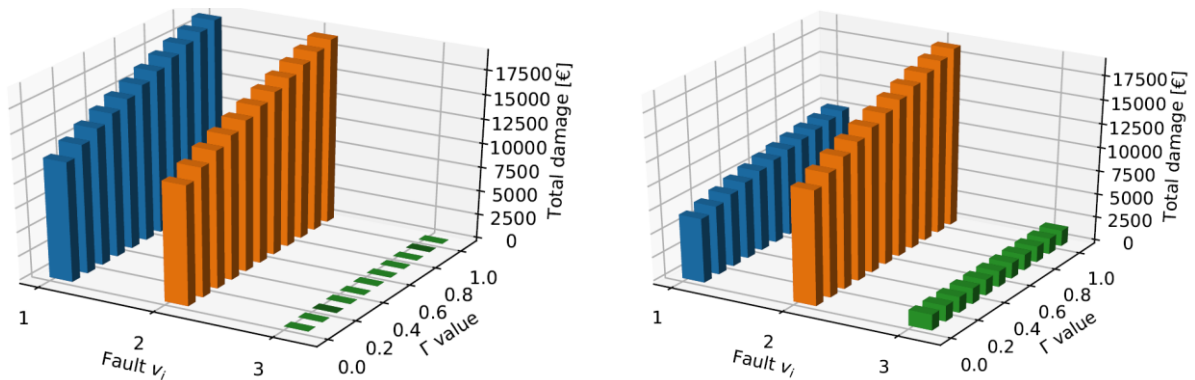
The operation cost of all scenarios under the different budget of uncertainties is summarized in Table 4. The results indicate that the operation cost increases (or the profit reduces) as the conservativeness coefficient increases. Scenario S_3 had the lowest operation cost (or the highest profit) for all faults in the system.

Table 4. The operation cost in euros [€] of all scenarios for a different budget of uncertainty levels

$\Gamma = 0$				
Scenario/Fault	v_1	v_2	v_3	v_4
S_0	-297.9	-12,434.9	-12,434.9	-297.9
S_1	879	-6,633.6	-10,980.2	-1,822.7
S_2	-273.3	-10,029.8	-10,029.8	-273.3

S_3	888.3	-4,374.1	-9,919.6	-1,813.4
$\Gamma = 0.5$				
Scenario/Fault	v_1	v_2	v_3	v_4
S_0	-389.9	-16,274.2	-16,274.2	-389.9
S_1	787	-8,736.5	-14,819.5	-1,914.7
S_2	-365.3	-13,869.1	-13,869.1	-365.3
S_3	796.2	-6,477	-13,758.9	-1,905.5
$\Gamma = 1$				
Scenario/Fault	v_1	v_2	v_3	v_4
S_0	-460	-19,189.2	-19,189.2	-460
S_1	716.9	-10,118	-17,734.4	-1,984.8
S_2	-435.4	-16,784	-16,784	-435.4
S_3	726.1	-7,858.5	-16,673.8	-1,957.6

Figure 6 presents the damage level for four scenarios for different Γ values and different faults v_i . The damage caused by the fault v_3 (loss of PV production) is the lowest for all scenarios. This result is expected as the penalty for the PV curtailment is significantly lower than the penalty for the loss of load. Additionally, scenarios S_0 and S_2 do not have the PV installed which means that there is no damage to these scenarios for the v_3 outage. This is reflected in the green bars in Figure 6. The influence of the PV plant is visible for the fault on the interconnection (v_1), where the presence of the PV plant reduces the damage significantly (Figure 6 (b) and (d)). This is an important result as the fault on interconnection (v_1) is 13 times more likely than the fault on the transformer (v_2). The implementation of the battery storage system leads to the overall damage reduction for faults v_1 and v_2 as can be observed in Figure 6 (c) and (d).



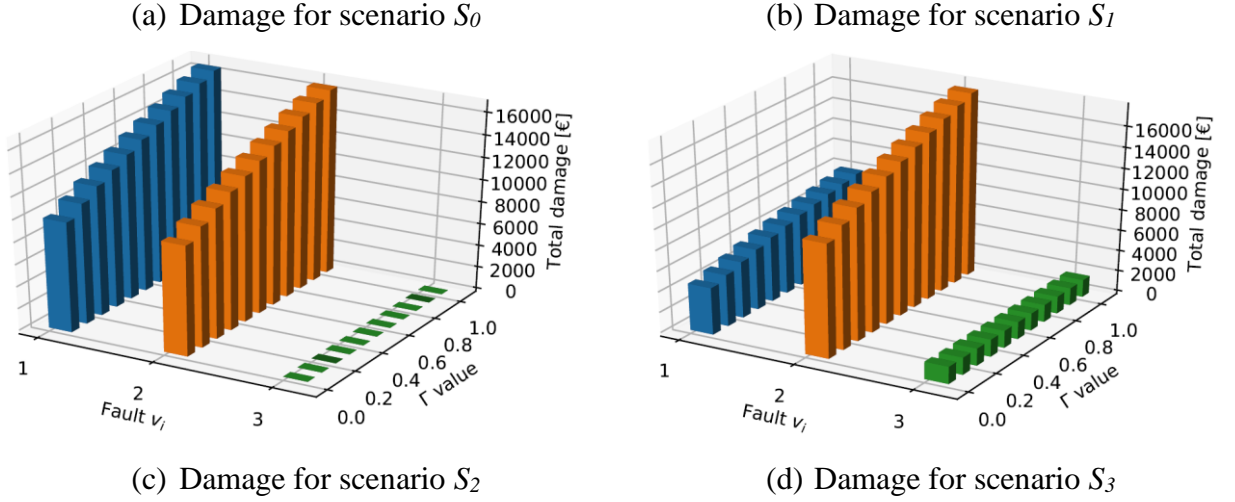


Figure 6. Damage for four scenarios (a), (b), (c) and (d) for different budgets of uncertainty Γ

The risk values for all scenarios for different levels of conservativeness are presented in Figure 7. It is possible to observe that, as the Γ parameter increases, the risk level increases as well. Figure 7 also shows a higher increase of risk level for the scenarios S_0 and S_2 than for the scenarios S_1 and S_3 as the uncertainty increases. The risk level increased for 332.5 € for S_0 and S_2 (when $\Gamma = 0 \rightarrow 1$), while, for S_1 and S_3 , it increases for 181.9 € (when $\Gamma = 0 \rightarrow 1$). This result confirms the importance of the PV plant for risk reduction as the scenarios with the PV had the lowest risk level. Moreover, the risk level for the scenarios with PV (S_1 and S_3) did not increase as rapidly as for scenarios S_0 and S_2 when the uncertainty budget increases, which is another confirmation of the positive PV influence on the risk level.

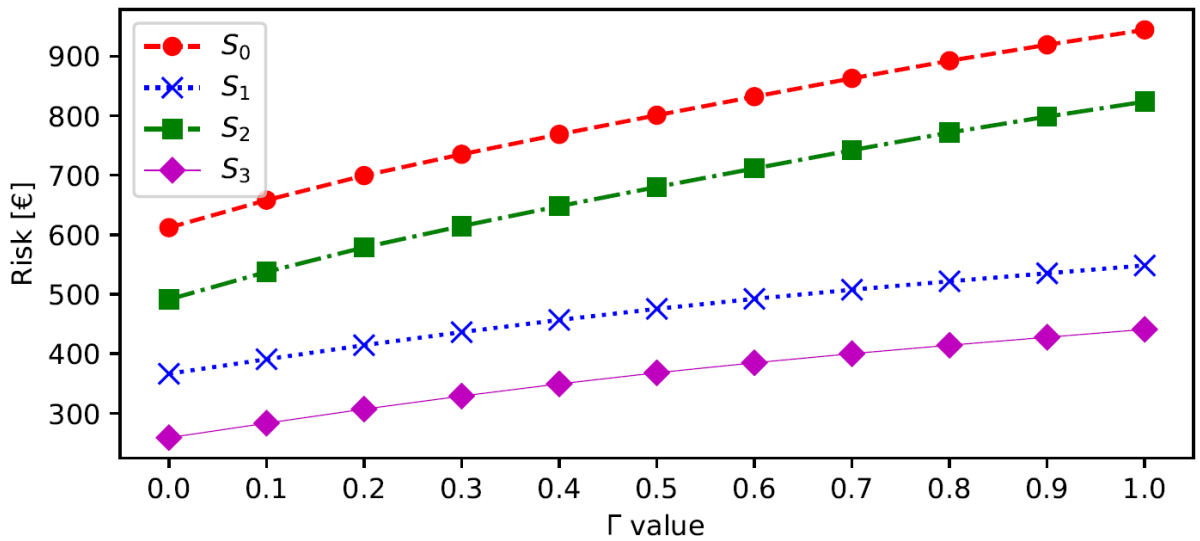


Figure 7. Risk values for all scenarios under different uncertainty budgets Γ

The battery storage influence is also visible in Figure 7. Scenario S_2 has a 120.7 € lower risk level than scenario S_0 , while scenario S_3 has 107.4 € lower risk than scenario S_1 . The consideration of the battery system for scenarios S_2 and S_3 resulted in lower risk in comparison to the scenarios without battery storage. However, the implementation of the battery system resulted in the same value of risk reduction for all uncertainty budget values, while the implementation of the PV plant resulted in higher risk reduction as the uncertainty budget increased.

Mean risk values together with the bar chart of the robust optimization model solutions is presented in Figure 8. The overall order of the scenarios remained the same with scenario S_3 as the lowest risk scenario and S_0 as the highest risk scenario. The obtained mean values were similar to the deterministic model values. The highest difference of risk value occurred for scenario S_2 and amounted to 22.75 € (3.5% increase) in comparison to the deterministic model solution. The results of the robust model confirmed the result of the deterministic model that scenario S_3 is the best-case scenario in terms of the risk assessment.

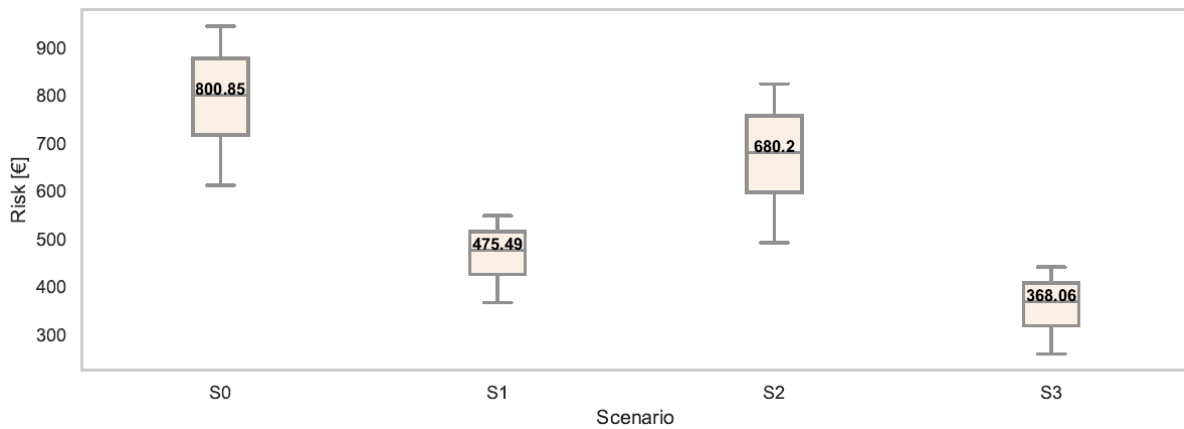


Figure 8. Mean values and quartiles for robust solutions of risk values

4.3. Zero – import risk scenario

The zero-import risk analysis investigated the impact of different PV plant power and battery capacity installations on the risk level under the different budget of uncertainty values when the fault on the interconnection occurs. As previously elaborated, this analysis is important for islands with a weak connection to the mainland such as Unije island. The results of this analysis are presented in Figure 9.

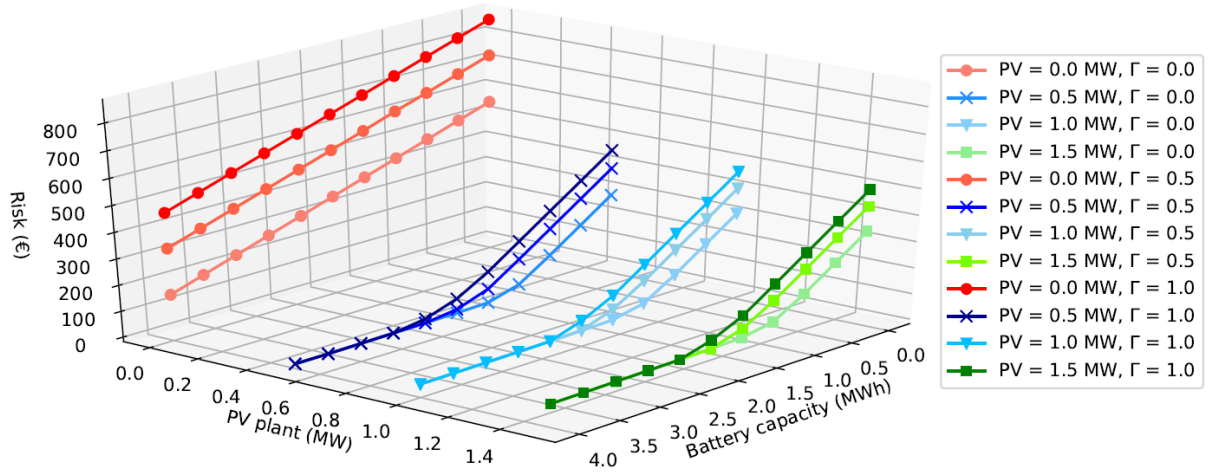


Figure 9. The risk assessment analysis of the S_3 scenario for the different PV, battery and budget of uncertainty values

The analysis was conducted for four cases considering installations of 0, 0.5, 1 and 1.5 MW PV plant, while battery capacity varies from 0 MWh to 4 MWh under three different Γ parameter values (0, 0.5 and 1). When comparing the scenarios with the different installations it is possible to observe that scenario with a 0 MW PV power plant needs a battery with a significantly higher capacity than 4 MWh for securing the supply in case of an outage. The best solution is achieved for the scenario with a 0.5 MW PV power plant and 3.55 MWh battery capacity. These values of installed PV power and battery capacity assure that the risk value is equal to zero and that Unije island is 100% renewable and energy self – sufficient. For this case, after the interconnection fault occurs, Unije successfully transits to the island regime with the secured supply of the island without any curtailed energy.

The scenarios with 1 and 1.5 MW PV power plant can also achieve 100% renewable self – sufficient Unije island but with a battery capacity significantly higher than 4 MWh. This is because the risk is the function of the unsupplied load as well as the curtailed energy. Because of the oversized PV power plant in these two scenarios, there is a need for the battery with much higher capacity than in the scenario with 0.5 MW in order to store all excess power from the PV power plant.

Another interesting analysis is when PV production curtailment is not penalized. Thus, Figure 10 presents the required battery capacity for supplying all the load when a fault on the interconnection occurs for the different PV power and the uncertainty budget values. For battery capacity values presented in Figure 10, there is no load shedding when the interconnection outage occurs and the entire load is supplied but with curtailed production from the PV plant. For the most pessimistic case ($\Gamma = 1$), a 0.2 MWh less battery capacity is needed when the PV power increases from 0.5 MW to 1 MW. However, further increase of the PV power results in

only 0.05 MWh less battery capacity. This result indicates that a further increase of installed PV power would not result in improvement in terms of the lower battery capacity required. This is because PV can only supply load during the day, while, for the other periods of the day, the battery capacity has to be high enough to supply the entire load. For more optimistic cases this relation is less expressed as the overall demand is lower.

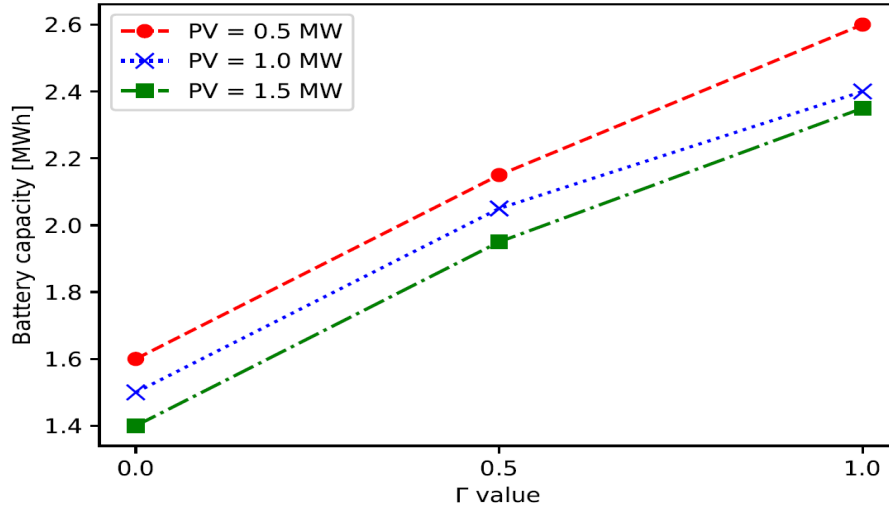


Figure 10. Required battery capacity for the elimination of load shedding when interconnection outage occurs

5. Discussion

This study presented a novel risk assessment approach for energy planning scenarios on islands. The main finding of this study is that the lowest risk value was achieved for the scenarios with joint management of a 1 MW PV plant and 0.5 MWh battery storage. This result was obtained by modelling the outage probability of the power system elements as well as the damage that occurred as a result of the outage.

The study showed that it is possible to determine the capacities of the installed technologies so that they ensure the island operation in the case of interconnection outage. Figure 7 showed that the risk value can significantly differ from the most optimistic case ($\Gamma = 0$) to the most pessimistic case ($\Gamma = 1$). The most optimistic and pessimistic case were observed from the standpoint of the system, meaning that the most favourable case is for $\Gamma = 0$. This result is significant because it indicates that the islands with higher expected demand (e.g. more developed tourist or industry sector) should be more risk-aware.

To the best of the authors' knowledge, the most relevant research of the risk assessment in energy planning was conducted in [44]. The study [44] used the Levelized cost of electricity (LCOE) as a relevant measure of risk. The Monte Carlo analysis was used for modelling of outage history of energy component and proved to be efficient for large systems (e.g. on a country level). This study was designed for smaller systems on the island level, thus it was possible to gather historical data about the outages. Moreover, the study presented in this paper used the risk assessment method for comparison of different energy planning scenarios, while the study [44] used it for different policy recommendations. The results of this study also underlined the findings in [45]. Both studies showed that an increase of RES share in the system resulted in lower risk. However, the method proposed in the study [45] is only applicable to the joint heating and electricity sector.

Many studies consider risk as a means to describe the uncertainty in the energy system operation. Different implementations of risk in the optimization model can be found; the stochastic approach was used in [46], conditional value at risk was considered in [47], a robust approach was implemented in [48] similarly as in this study. However, the studies that analyse the outage possibilities as a part of the energy planning process are rare although they can offer important information. This study utilizes a robust approach in modelling the uncertainty, however, in comparison with previous studies, this study placed the focus on the risk quantization of each energy planning scenario. This allows an island to define the risk level to which it would be exposed in case of an outage which enables additional information while planning renewable energy scenarios.

Another result of this study showed that it is possible to determine the necessary installed capacities of PV and battery storage in order to secure the supply in case of an interconnection outage. As the technology that enables island operation of the power system (e.g. grid forming inverters) is becoming increasingly available, this analysis is becoming more important. Small islands may secure their electricity supply by installing a higher amount of controllable technology (e.g. batteries). This may often be possible without the significant increase in cost and the risk assessment method proposed in this study enables identification of such situations.

There are several limitations to this study. The optimization algorithm presented in the study aims to maximize the social welfare of the observed system. This may not always be the case as different stakeholders with different objectives participate in the power system operation. However, the power system operation in case of an outage is defined with the grid code. Thus,

it would be reasonable that the operation of all stakeholder in the power system would be oriented towards the preservation of the secure operation in case of an outage.

The proposed method will be applied to multi-energy systems in future research. This will include transportation, water, heating and electricity systems. With the proposed method, it will be possible to quantify the risk reduction when different sectors are integrated and jointly operated in comparison to the conventional operation where all sectors operate independently.

6. Conclusion

This paper presented a novel robust method for risk assessment of the energy planning scenarios for islands under the demand uncertainty with a case study conducted on Unije island. The obtained results demonstrated that it is possible to quantify risk levels of analysed energy planning scenarios on the smart islands together with the following conclusions:

- The obtained results showed that the risks for the four analysed scenarios for the deterministic model were equal to 778.1, 460.1, 657.5 and 352.7 € indicating that it is possible to quantify risk and differentiate the energy planning scenarios based on the risk level.
- The energy planning scenario with the lowest risk is S_3 scenario with risk equal to 259.1 € for the most optimistic case ($\Gamma = 0$) and 441 € for the most pessimistic case ($\Gamma = 1$)
- The zero-import risk scenario for the island of Unije is achieved for 0.5 MW PV plant and 3.55 MWh of the battery storage which means that the island can operate without any curtailed energy when the interconnection is lost.
- A case study on Unije shows that it is possible to create completely renewable islands that are energy independent from the mainland
- The presented method provides additional information – risk level of each energy planning scenario – to the experts, investors and decision-makers that are not available in the current studies

Future research will be oriented towards the exploration of additional possibilities for the risk quantification of the energy planning scenarios on the smart islands as well as the other options for uncertainty management.

Acknowledgement

This work has been supported by the Young Researchers' Career Development Programme (DOK-01-2018) of Croatian Science Foundation which is financed by the European Union from European Social Fund and Horizon 2020 project INSULAE - Maximizing the impact of innovative energy approaches in the EU islands (Grant number ID: 824433). This support is gratefully acknowledged.

Appendix A

Case study – Tilos island

In order to illustrate the possible applications of the method, additional example is provided in this Appendix A. In this example, a case of Greek island Tilos is considered. The two main consumption centers on Tilos are Megalo Chorio Village and Livadia Village (represented with L1 and L2 on Figure A1). The Tilos island has a electrical interconnection to the Kos island that can supply the Tilos island with the electric energy with the existing thermal unit. There are several installations on the Tilos island that include a 1.45 MW backup diesel generator, a 0.8 MW wind power plant, a 0.8MW/2.88 MWh battery storage facility and a 0.16 MW PV plant.

In this case study, the effect of installation of these technologies with respect to the risk will be observed according to the scenarios presented in Table A1. Important note regarding the diesel generator is that it is run manually, thus it was assumed that at least 2 hours are necessary to start it up on the grid. The data for the case study can be found in [49] and [50], while the other data relevant for the calculation is provided in Table A2. It is also assumed that the outage happens at 10am of the first day and that the observed period are the two highest demand days. The Tilos power grid topology and the corresponding graph is provided in the Figure A1. Different scenarios are marked in different colors for better visualization.

Table A1. Scenarios for the Tilos island case study

Scenario	Backup diesel genset	Wind power plant and battery storage	Solar power plant
S _{A1}	No	No	No
S _{A2}	Yes	No	No
S _{A3}	No	Yes	No
S _{A4}	No	Yes	Yes

Table A2. Data for the Tilos case study

Parameter	Value	Parameter	Value
VPVC/VWC	105.58 €/MWh	p_g^{min}	0 MW
VOLL	2840 €/MWh	p_g^{max}	1.45 MW
η_c	0.95	UT_g	0 h
η_d	0.9	DT_g	2 h
ξ	0.5	RU_g	1.45 MW
α	0	RD_g	1.45 MW
β	0	ω	0.2 MWh
$p_{imp}^{min}, p_{exp}^{min}$	0	$p_{imp}^{max}, p_{exp}^{max}$	1.6 MW
Δt	0.5 h		

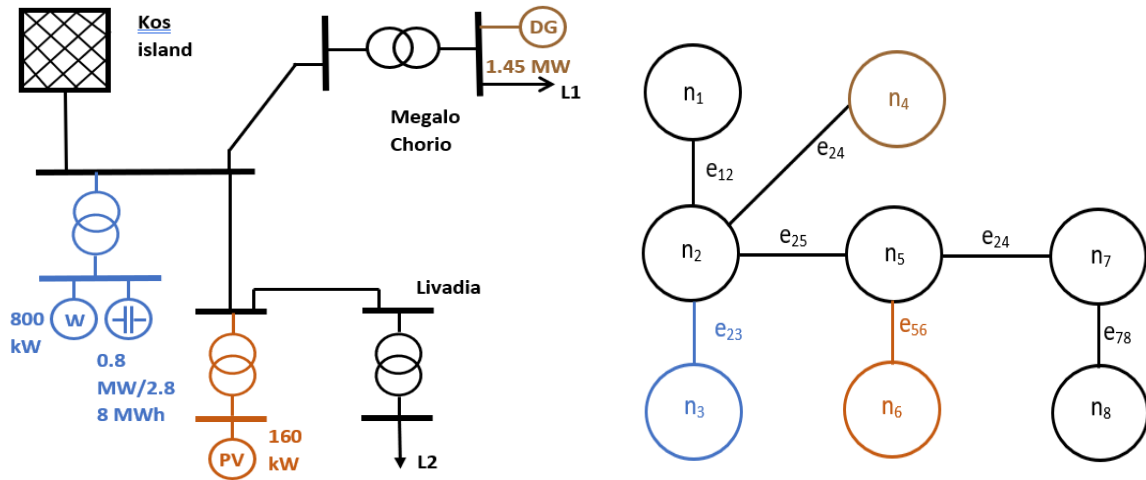


Figure A1. Power system topology for the Tilos island (left) and graph representation of the power system topology for the Tilos island (right)

Results and discussion

The results of the Tilos case study are given with the vector \mathcal{R} and in Figure A2. It can be seen that the scenario with the highest risk is the initial scenario when there is only interconnection available as a power supply. Installation of diesel generator significantly reduces the risk of loss of power supply. However, there is still risk because the generator is operated manually, which means that some load will be lost until the time the diesel generator starts up. The detailed mathematical model presented in the Materials and methods section enables to account for such feature. Installation of 0.8 MW wind power plant and the battery storage system 0.8MW/2.88 MWh reduced the risk in comparison to the original scenario, however the risk is higher than for S_{A2} scenario because there was not enough wind capacity installed. The final, S_{A4} , scenario that included the 0.16 MW solar power plant in addition to the wind power and battery storage system achieved the lowest risk.

There are several reasons why this is the case. First, the battery storage system has a high enough capacity to successfully integrate variable renewables in the system and use the energy produced from these units when necessary. Secondly, in comparison to the diesel generator, the renewable energy units are dispersed across the topology of the grid. This is another benefit of including the graph theory in the method proposed in this paper. Finally, with grid forming inverters, the units connected with the energy electronics on the grid can be run automatically, while backup diesel generators do not have this possibility, thus causing loss of load until the time they are started.

$$A = \begin{bmatrix} 0 & 0.257 & 0 & 0 & 0 & 0 & 0 \\ 0.257 & 0 & 0.02 & 0.02 & 0.037 & 0 & 0 \\ 0 & 0.02 & 0 & 0 & 0 & 0 & 0 \\ 0 & 0.02 & 0 & 0 & 0 & 0 & 0 \\ 0 & 0.037 & 0 & 0 & 0 & 0.02 & 0.01 \\ 0 & 0 & 0 & 0 & 0.02 & 0 & 0.02 \\ 0 & 0 & 0 & 0 & 0.01 & 0.02 & 0 \end{bmatrix}$$

$$\mathcal{R} = \begin{bmatrix} 0.0416 \\ 0.0034 \\ 0.0034 \\ 0.0063 \\ 0.0034 \\ 0.0017 \\ 0.0034 \end{bmatrix}^T \cdot \begin{bmatrix} 60700.74 & 3626.68 & 5276.36 & 0 \\ 0 & 0 & 944.8 & 944.8 \\ 23794.94 & 1326.28 & 23794.94 & 23794.94 \\ 36905.98 & 36905.98 & 36905.8 & 30396.52 \\ 0 & 0 & 0 & 716.25 \\ 36905.98 & 36905.98 & 36905.98 & 36905.98 \\ 36905.98 & 36905.98 & 36905.98 & 36905.98 \end{bmatrix} = \begin{bmatrix} 3026.78 \\ 576.11 \\ 724.34 \\ 466.27 \end{bmatrix}^T \text{ €}$$

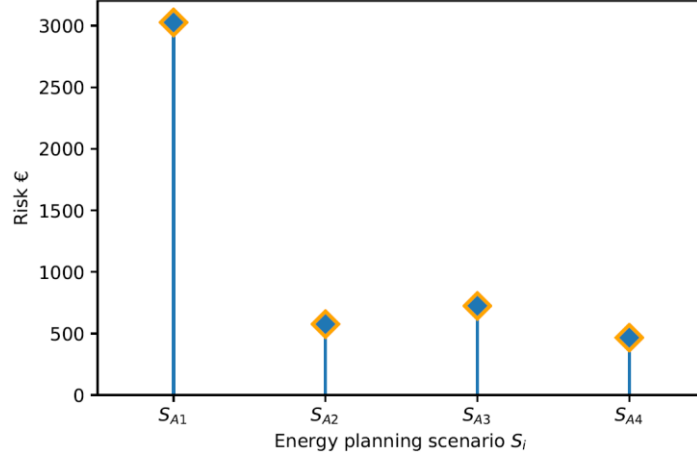


Figure A2. Results of the Tilos case study – highest risk for the scenario without any interventions; lowest risk for the scenario with battery storage system, wind and solar generation

It can be concluded that the proposed method can be universally applied to many different case studies on geographical islands. The results of the method provide a unique and original insight in the risk levels of energy planning scenarios, thus presenting a useful tool for the energy planners, policy makers and local communities.

Nomenclature

Indices and sets

		\tilde{L}_t	Uncertain load at period t [MW]
i, j	Scenario and fault indexes	$P_{imp/exp}^{min/max}$	Minimum and maximum import and export power [MW]
t, k	Time periods	FL_t	Flexible load at time t [MW]
\mathcal{N}	Set of nodes	$\delta_{L,j}$	Deviation of actual load to forecasted load [MW]
\mathcal{E}	Set of lines	Variables and matrixes	
S	Set of scenarios	x	General variable
V	Set of outages	E_t^s, E_t^b	Sold and bought energy on day-ahead market [MWh]

\mathbb{R}	Set of real numbers	C_t	Cost of microgrid operation [€/MWh]
e_{ij}	Undirected edges	$P_{d,t}, P_{c,t}$	Discharging and charging battery power at time t [MW]
Ω^T	Set of time periods	$P_{imp,t}, P_{exp,t}$	Import and export power of observed grid [MW]
Ω^{ESS}	Set of energy storage systems	SOC_t	State of charge of the battery [MWh]
Ω^{PV}	Set of solar power plants	P_t^d, P_t^c	Discharging and charging power of the battery [MW]
Ω^G	Set of conventional generators	$p_{g,t}$	Production from the conventional generator [MW]
Ω^W	Set of wind power plants	$p_{w,t}$	Production from the wind power plant [MW]
Parameters		$P_{pv,t}$	Solar power plant production at time t [MW]
SU_g, SD_g	Start-up and shut down cost of the generator [€/MWh]	$P_{w,t}^{curt}$	Curtailed power from wind power plant at time t [MW]
RU_g, RD_g	Ramp-up and ramp down of the generator [MW]	$F_g(\cdot)$	Quadratic cost function of generator [€/MWh]
UT_g, DT_g	Minimum up and down time of the generator [h]	$x_{g,t}, z_{g,t}, u_{g,t}$	Binary variables for generator operation control
ξ	Factor for limiting battery charge and discharge	$P_{pv,t}^{curt}$	Curtailed power from solar power plant at time t [MW]
$SOC^{min/max}$	Minimum and maximum battery state of charge [MWh]	μ_t	Binary variable for energy storage system

η_c	Charging efficiency	DR_t	Demand response at time t [MW]
η_d	Discharging efficiency	$\phi_L, \psi_{L,t}$	Auxiliary variables
$\Lambda_{i,t}^{PV}$	Maximum available solar power plant generation [MW]	θ	Probability vector
VPVC, VWC	Value of curtailed solar and wind power generation [€/MWh]	\mathcal{D}	Damage matrix
VOLL	Value of lost load [€/MWh]	\mathcal{R}	Risk matrix
λ_t	Electric energy price at period t [€/MWh]	Abbreviations	
α	Factor for downward demand response limitation	EU	European Union
β	Factor for upward demand response limitation	DR	Demand response
Γ	Budget of uncertainty	RES	Renewable energy sources
ϑ	Probability of an event occurring	ESS	Energy storage system
a	Ratio of an event occurring	PHP	Pumped hydro storage
N	Number of times an event occurred	PV	Solar power plant
L_t^{min}, L_t^{max}	Minimum and maximum load at period t [MW]	CVaR	Conditional value at risk

References

- [1] European Commission, “Clean Energy for EU Islands launch,” *European Commission Energy News*, 2017. .
- [2] European Commission, “Smart Island Initiative,” 2017. .
- [3] N. Duić, G. Krajačić, and M. da Graça Carvalho, “RenewIslands methodology for sustainable energy and resource planning for islands,” *Renewable and Sustainable Energy Reviews*. 2008.

- [4] A. Pfeifer, V. Dobravec, L. Pavlinek, G. Krajačić, and N. Duić, "Integration of renewable energy and demand response technologies in interconnected energy systems," *Energy*, 2018.
- [5] R. Segurado, M. Costa, N. Duić, and M. G. Carvalho, "Integrated analysis of energy and water supply in islands. Case study of S. Vicente, Cape Verde," *Energy*, 2014.
- [6] P. D. Lund, J. Lindgren, J. Mikkola, and J. Salpakari, "Review of energy system flexibility measures to enable high levels of variable renewable electricity," *Renewable and Sustainable Energy Reviews*. 2015.
- [7] D. Groppi, A. Pfeifer, D. A. Garcia, G. Krajačić, and N. Duić, "A review on energy storage and demand side management solutions in smart energy islands," *Renew. Sustain. Energy Rev.*, vol. 135, 2021.
- [8] I. Saviuc, K. Milis, H. Peremans, and S. Van Passel, "A cross-european analysis of the impact of electricity pricing on battery uptake in residential microgrids with photovoltaic units," *J. Sustain. Dev. Energy, Water Environ. Syst.*, vol. 9, no. 3, 2021.
- [9] D. F. Dominkovic, G. Stark, B. M. Hodge, and A. S. Pedersen, "Integrated energy planning with a high share of variable renewable energy sources for a Caribbean Island," *Energies*, 2018.
- [10] D. Curto, V. FRANZITTA, M. Trapanese, and M. Cirrincione, "A Preliminary Energy Assessment to Improve the Energy Sustainability in the Small Islands of the Mediterranean Sea," *J. Sustain. Dev. Energy, Water Environ. Syst.*, vol. N/A, no. N/A, 2020.
- [11] J. D. Ocon and P. Bertheau, "Energy transition from diesel-based to solar photovoltaics-battery-diesel hybrid system-based island grids in the Philippines – Techno-economic potential and policy implication on missionary electrification," *J. Sustain. Dev. Energy, Water Environ. Syst.*, vol. 7, no. 1, 2019.
- [12] F. M. Hoffart, E. J. Schmitt, and M. Roos, "Rethinking economic energy policy research-developing qualitative scenarios to identify feasible energy policies," *J. Sustain. Dev. Energy, Water Environ. Syst.*, vol. 9, no. 2, 2021.
- [13] H. H. Yu, K. H. Chang, H. W. Hsu, and R. Cuckler, "A Monte Carlo simulation-based decision support system for reliability analysis of Taiwan's power system: Framework and empirical study," *Energy*, 2019.
- [14] S. Galvani and S. Rezaeian Marjani, "Optimal power flow considering predictability of power systems," *Electr. Power Syst. Res.*, 2019.
- [15] S. Zhou and P. Yang, "Risk management in distributed wind energy implementing

- Analytic Hierarchy Process,” *Renew. Energy*, vol. 150, 2020.
- [16] E. Ciapessoni, D. Cirio, G. Kjølle, S. Massucco, A. Pitto, and M. Sforna, “Probabilistic Risk-Based Security Assessment of Power Systems Considering Incumbent Threats and Uncertainties,” *IEEE Trans. Smart Grid*, 2016.
 - [17] M. Hemmati, B. Mohammadi-Ivatloo, S. Ghasemzadeh, and E. Reihani, “Risk-based optimal scheduling of reconfigurable smart renewable energy based microgrids,” *Int. J. Electr. Power Energy Syst.*, 2018.
 - [18] L. Guo, Q. Qiu, J. Liu, Y. Zhou, and L. Jiang, “Power transmission risk assessment considering component condition,” *J. Mod. Power Syst. Clean Energy*, 2014.
 - [19] L. G. de Urtasun, S. B. Vicente, and N. G. Hernández, “Smart Grid Functionalities Evaluation,” *Smart Grid Renew. Energy*, 2016.
 - [20] T. Ghose, H. W. Pandey, and K. R. Gadham, “Risk assessment of microgrid aggregators considering demand response and uncertain renewable energy sources,” *J. Mod. Power Syst. Clean Energy*, 2019.
 - [21] W. M. Lin, C. Y. Yang, C. S. Tu, and M. T. Tsai, “An optimal scheduling dispatch of a microgrid under risk assessment,” *Energies*, 2018.
 - [22] M. A. Tajeddini, A. Rahimi-Kian, and A. Soroudi, “Risk averse optimal operation of a virtual power plant using two stage stochastic programming,” *Energy*, 2014.
 - [23] H. Zahboune, S. Zouggar, G. Krajacic, P. S. Varbanov, M. Elhafyani, and E. Ziani, “Optimal hybrid renewable energy design in autonomous system using Modified Electric System Cascade Analysis and Homer software,” *Energy Convers. Manag.*, 2016.
 - [24] A. Narayan and K. Ponnambalam, “Risk-averse stochastic programming approach for microgrid planning under uncertainty,” *Renew. Energy*, 2017.
 - [25] T. M. Alabi, L. Lu, and Z. Yang, “A novel multi-objective stochastic risk co-optimization model of a zero-carbon multi-energy system (ZCMES) incorporating energy storage aging model and integrated demand response,” *Energy*, 2021.
 - [26] Q. Wang, X. Diao, Y. Zhao, F. Chen, G. Yang, and C. Smidts, “An expert-based method for the risk analysis of functional failures in the fracturing system of unconventional natural gas,” *Energy*, vol. 220, 2021.
 - [27] Z. Süle, J. Baumgartner, G. Dörgö, and J. Abonyi, “P-graph-based multi-objective risk analysis and redundancy allocation in safety-critical energy systems,” *Energy*, vol. 179, 2019.
 - [28] S. Zolfaghari, G. H. Riahy, M. Abedi, and S. Golshannavaz, “Optimal wind energy

- penetration in power systems: An approach based on spatial distribution of wind speed,” *Energy Convers. Manag.*, vol. 118, 2016.
- [29] J. Martinez-Velasco and G. Guerra, “Reliability Analysis of Distribution Systems with Photovoltaic Generation Using a Power Flow Simulator and a Parallel Monte Carlo Approach,” *Energies*, vol. 9, no. 7, 2016.
- [30] Y. Huang, P. M. Pardalos, and Q. P. Zheng, “Deterministic Unit Commitment Models and Algorithms,” 2017.
- [31] J. M. Wilson, “Introduction to Stochastic Programming,” *J. Oper. Res. Soc.*, vol. 49, no. 8, 1998.
- [32] A. Soroudi, “Possibilistic-scenario model for DG impact assessment on distribution networks in an uncertain environment,” *IEEE Trans. Power Syst.*, vol. 27, no. 3, 2012.
- [33] L. Baringo and A. J. Conejo, “Offering strategy via robust optimization,” *IEEE Trans. Power Syst.*, vol. 26, no. 3, 2011.
- [34] D. Bertsimas and M. Sim, “The price of robustness,” *Oper. Res.*, vol. 52, no. 1, 2004.
- [35] Y. Wang, M. Kazemi, S. Nojavan, and K. Jernsittiparsert, “Robust design of off-grid solar-powered charging station for hydrogen and electric vehicles via robust optimization approach,” *Int. J. Hydrogen Energy*, vol. 45, no. 38, 2020.
- [36] Y. Zhang, L. Fu, W. Zhu, X. Bao, and C. Liu, “Robust model predictive control for optimal energy management of island microgrids with uncertainties,” *Energy*, vol. 164, 2018.
- [37] S. Dubrović, “Experiences in repairing failures on electrodistribution submarine cables in Elektroprimorje Rijeka,” in *6th (12th) Session of CIRED Croatian National Committee*, 2018.
- [38] S. Keitoue, A. Keller, I. Murat, A. Mikulecky, and M. Poljak, “Monitoring system for power transformers in distribution networks,” in *1st Session of CIRED Croatian National Committee*, 2008.
- [39] HEP-ODS, “Ten year (2018. - 2027.) development plan of distribution system network of HEP-ODS,” 2017.
- [40] T. Cerovečki, M. Cvitanović, F. Damjanović, R. Ivković, J. Majcen, and I. Širić, “Optimal technical connection of PV plant on distribution grid.” 2019.
- [41] RINA-C, “INSULAE - Energy Storage System - Conceptual design Unije,” 2019.
- [42] “www.cropex.hr.” .
- [43] M. Joos and I. Staffell, “Short-term integration costs of variable renewable energy: Wind curtailment and balancing in Britain and Germany,” *Renewable and Sustainable*

Energy Reviews. 2018.

- [44] M. R. Quitoras, P. Cabrera, P. E. Campana, P. Rowley, and C. Crawford, "Towards robust investment decisions and policies in integrated energy systems planning: Evaluating trade-offs and risk hedging strategies for remote communities," *Energy Convers. Manag.*, vol. 229, 2021.
- [45] C. Wang, C. Yan, G. Li, S. Liu, and Z. Bie, "Risk assessment of integrated electricity and heat system with independent energy operators based on Stackelberg game," *Energy*, vol. 198, 2020.
- [46] M. Roustaei *et al.*, "A scenario-based approach for the design of Smart Energy and Water Hub," *Energy*, vol. 195, 2020.
- [47] R. A. de Freitas, E. P. Vogel, A. L. Korzenowski, and L. A. Oliveira Rocha, "Stochastic model to aid decision making on investments in renewable energy generation: Portfolio diffusion and investor risk aversion," *Renewable Energy*, vol. 162, 2020.
- [48] A. Soroudi, P. Siano, and A. Keane, "Optimal DR and ESS scheduling for distribution losses payments minimization under electricity price uncertainty," *IEEE Trans. Smart Grid*, 2016.
- [49] G. Notton, M. L. Nivet, D. Zafirakis, F. Motte, C. Voyant, and A. Fouilloy, "Tilos, the first autonomous renewable green island in Mediterranean: A Horizon 2020 project," in *2017 15th International Conference on Electrical Machines, Drives and Power Systems, ELMA 2017 - Proceedings*, 2017.
- [50] J. K. Kaldellis, "Supporting the clean electrification for remote islands: The case of the greek tilos island," *Energies*, vol. 14, no. 5, 2021.

PAPER 3

Soft-linking of improved spatiotemporal capacity expansion model with a power flow analysis for increased integration of renewable energy sources into interconnected archipelago

Marko Mimica^{*a}, Dominik F. Dominković^b, Vedran Kirinčić^c, Goran Krajačić^a

^aDepartment of Energy, Power Engineering and Ecology, Faculty of Mechanical Engineering and Naval Architecture, University of Zagreb, Ivana Lučića 5, 10002 Zagreb, Croatia

^bDepartment of Applied Mathematics and Computer Science, Technical University of Denmark, Matematiktorvet, 2800 Lyngby, Denmark

^cUniversity of Rijeka, Faculty of Engineering, Department of Electric Power Systems, Vukovarska 58, 51000 Rijeka, Croatia

email: mmimica@fsb.hr

Abstract

This present study offers a novel approach for the improvement of energy planning. This has become increasingly important as higher penetration of variable energy resources and increased interconnection between the different energy sectors require more detailed planning in terms of spatiotemporal modeling in comparison to the presently available approaches. In this study, we present a method that soft-linked the energy planning and power flow models, which enabled fast and reliable solving of optimization problems. A linear continuous optimization model was used for the energy system optimization and the non-linear problem for the power system analysis. The method is used to compare different energy planning scenarios; further, this also offers the possibility for implementation assessment of the proposed scenarios. The method was applied to interconnected islands for five different scenarios. It was determined that the detailed spatial approach resulted in 26.7% higher total system costs, 3.3 times lower battery capacity, and 14.9 MW higher renewable energy generation capacities installed than in the coarser spatial representation. Moreover, the results of the power flow model indicated that the highest voltage deviation was 16% higher than the nominal voltage level. This indicates the need for inclusion of implementation possibility assessments of energy planning scenarios.

Keywords: energy planning; soft-linking; Calliope modeling framework; power flow; renewable energy sources; energy system analysis

Nomenclature

Parameters	
i, j	Nodes in the power system
n	Total number of nodes in the power system
g	Total number of generating nodes in the power system
ϕ	The phase angle between current and voltage [rad]
\overline{Y}_{ij}	Phasor value of admittance between nodes i and j
Y_{ij}	The scalar value of admittance between nodes i and j [S]
θ_{ij}	The phase of the admittance between nodes i and j [rad]
Q_{\min}, Q_{\max}	Minimum and maximum values of reactive power [MVar]
ε	Accuracy of the iterative procedure
Variables	
\overline{V}_i	Phasor value of the voltage at node i
V_i	The scalar value of the voltage at node i [kV]
ΔV	Voltage deviation [kV]
δ_i	Voltage angle at node i [rad]
$\Delta\delta$	Voltage angle deviation [rad]
P_i	Active power at node i [MW]
ΔP	Active power deviation [MW]
Q_i	Reactive power at node i [MVar]
ΔQ	Reactive power deviation [MVar]
J_1, J_2, J_3, J_4	Elements of the Jacobian matrix
Additional nomenclature	
$S1, S2, S3, S4, S5$	Analyzed scenarios
$X1, X2, X3, X4, X5, X6, X7, X8$	Modeled locations in the case study

1. Introduction

1.1. Background

Although islands have brought about a negligible impact on the rising issue of climate change, they will be the first ones that will experience its negative consequences [1]. For these reasons, there are two important initiatives in the European Union (EU) in terms of discussing the climate changes on the islands. First is the “Smart Islands Initiative” [2], which represents a bottom-up approach for the development of the islands’ communities. This document presented ten goals for maximizing islands’ potential and transforming them into living labs for testing advanced solutions for the energy transition that can later be transferred to the mainland. Second is a top-down document from the EU Commission [3] that aims to achieve sustainable communities on islands with clean and low-cost energy production.

These efforts need to be matched with the increased accuracy of the energy planning processes developed by the scientific community, especially for systems with the high share of variable renewable energy sources (RES). Moreover, the implementation possibilities of the proposed energy planning scenarios in the power system need to be further researched. The introduction of variable RES often creates voltage difficulties in the power system grid [4]; the latter has been deemed essential as a distribution system operator will deny permits to projects that integrate a large amount of variable RES if grid code is violated. The method proposed in this study enables a finer modeling of the energy planning scenarios and their application possibilities assessment in the existing power system infrastructure.

1.2.Literature review

Energy planning methods for islands have been extensively researched throughout the years. The authors in [5] presented the case study of S. Vicente, Cape Verde, where they analyzed the possibility of creating an energy system based only on wind power and pumped hydro plant. This particular study was further examined in [6] where authors included the water system by considering the desalination plant. The study showed that the integration of these two sectors resulted with a 36% increase in the renewable generation. Likewise, Child et al. [7] presented several energy planning scenarios on an hourly basis for the Åland Islands, which have the similar grid topology as the Krk island, with the conclusion that it is possible to achieve a 100% renewable production. Curto et al. [8] proposed a renewable energy mix based on the monthly time resolution and without application implications of the proposed scenario for the Ustica island. Depending on the investment cost of a battery, the authors in [9] showed that it is possible to achieve renewable energy share from 35.1% to 58.8%, but the study did not show the detailed operation of such system. Evidence from the study in [10] showed that a 100% renewable island such as La Gomera is economically and technically feasible. The application of the finer energy planning approach would enable a more detailed overview of the flexibility technologies (e.g., batteries) operation in this study [10]. A comparative study [11] indicated that the renewable energy mix can satisfy 87% of annual electrical energy demand on Fiji and 46% on the Balearic Islands. Comparison analyses based on rough time and spatial resolution can also provide somewhat more information; however, the results would be more significant if a finer approach would be considered. These analyzed studies had several similar research gaps. Most of these studies [5-11] considered the rough time resolution (hourly resolution or higher); they did not consider spatial distribution nor did they propose an approach for the implementation possibilities of considered energy planning scenarios in the power system grid.

Thus, the approach presented in this study proposed solution for all three research gaps. Moreover, this paper analyzed four different sectors, which is a significant advancement in comparison with the studies [5-11] that focused only on one or two sectors.

The following studies have focused either on a fine temporal resolution or fine spatial resolution. Mixed-integer linear programming was expanded with receding horizon model predictive control (RH-MPC) in [12] for the integration of different energy vectors on a half-hourly temporal resolution. In the case study for the carbon-neutral Canary Islands [13], it was determined that it is possible to completely cover local electricity and heating and transport demands with just utilizing local resources. The importance of islands' interconnection and the demand response was presented in [14] where the share of the renewable generation reached 85% in the final energy consumption of the interconnected system. Flexibility options were extensively discussed in these studies [12-14] by applying the coarser time resolution. The approach presented in this study offers a significantly finer overview of the operation of the flexibility providers such as batteries.

Spatially distributed modeling is necessary for the modeling of advanced technologies that are being introduced in the energy system. For example, spatial distribution was considered in [15] where the authors observed prosumer behavior. The study [16] used the spatially distributed model for measurement of network energy efficiency exchange. The soft-linking approach between different models was applied in several studies in order to reduce the computational time of the simulations. For example, soft-linking between the unit commitment model and the multi-sectoral model was used in the [17], whereas the energy planning model was soft-linked with the transport behavioral model in [18]. The aforementioned studies [12-18] did not provide a comparative analysis that would analyze the benefits of more detailed spatial and time modeling. Moreover, the current state-of-the-art analysis revealed that none of the analyzed papers, which focus on high RES energy system planning, has provided detailed electrical power grid analysis. The approach proposed in this study enabled a detailed comparison that clearly illustrated the pros and cons of different modeling approaches, highlighting the importance of electric power grid analysis.

The authors in [19] conducted the analysis on a 5-minute temporal resolution; however, the application possibilities were not analyzed. Load flow is a commonly used method for power system state assessment [20] and can be used for the assessment of the application possibilities of the energy planning scenarios. Since load flow is a non-linear and non-convex problem, several algorithms such as Gauss-Seidel or, the more common, Newton-Raphson method are

used for solving them. Although novel methods based on neural networks such as in [21] have emerged, Newton-Raphson method has proved to be sufficient for the power grids with the low ratio between the resistance and the reactance. The study [22] used the power flow to assess the impact of different strategies for the sizing the energy communities with battery and photovoltaics, however no capacity expansion model was considered. This paper proposed a joint approach with coupling of capacity expansion model and the power flow method, which enables precise estimation of the application possibilities of the energy planning scenarios.

1.3. Contributions

The aforementioned studies indicate that most of the simulations of energy systems on the islands are conducted on hourly time resolution and mostly do not consider the geographical distribution of energy resources and demands. Analyzed studies focus either on higher temporal or spatial distribution, but they do not consider them jointly. Analyzed studies failed to examine the technical changes in the power system steady state, which makes it hard to assess whether the proposed scenarios can be implemented in the electric power system or not. To the best of our knowledge, this is the first study that has analyzed island energy systems with high spatial and temporal resolution and with coupling of four sectors and has modeled and performed analysis of the power system on islands. This present study offers a solution to the gaps observed in current studies, thus representing a comprehensive approach in examining energy systems as summarized below:

- A detailed spatial coupled with a half-hourly temporal resolution analysis was performed by applying an electrical capacity expansion model
- Results obtained from the application of the energy system model were validated by conducting a power system analysis that provided insights about the energy system voltage and power flows
- The power transmission and distribution systems were modeled, thus enabling the checking of the power flows along the grid

To allow other researchers to repeat calculations and achieve the same results or improve them, the study also follows Open Energy Modelling Initiative for open energy modeling, with the entire model and code available at GitHub (link is provided in the acknowledgments).

This paper is organized as follows: the introduction and literature review are followed by the materials and methods section. The third section describes the case study; the results and

discussion are provided in the fourth section; and, in the fifth section, conclusions of this study are provided. The general overview of the presented approach is given in Figure 1.

2. Methods

2.1. Energy planning model

The Calliope modeling framework was used to develop the energy planning model. Calliope is a multi-scale energy systems modeling framework [23]. It is a free and open-source tool, which makes it easily accessible to everyone. The latter is in line with the push-in academia for radical transparency of the model assumptions, as well of the model implementation itself [24]. All of the code, as well as its documentation, are freely available online. The Calliope modeling tool is very versatile as it allows the modeler to create models with the user-defined temporal and spatial resolution as well as pre-model any technology that is relevant for the chosen case study. Hence, it is possible to use the tool for creating models at different scales, from urban districts to entire continents. The modeling tool was used, among others, for case studies of Bangalore, Cambridge, South Africa, and the United Kingdom [25].

The Calliope model used in this study was a linear continuous optimization model. The created model was a capacity expansion one, which included optimizing the operation of the system, as well as optimizing the capacities technologies to be installed. Its objective function was to minimize the total socio-economic costs throughout the target year. In the specific model developed in this paper, the objective function included annualized investment costs, fixed and variable operating and maintenance costs, as well as fuel and CO₂ costs. CO₂ costs were internalized in the form of CO₂ tax for the transport fuels, while a more complicated calculation was used for the import of electricity from outside of the system boundaries. To account for the CO₂ cost, it was taken into consideration that the EU Emissions Trading System (ETS) price was already included in the price of electricity that was settled on a day-ahead market in the reference year (e.g., the year 2017). To take into account a higher ETS cost in the target year (e.g., the year 2030), a difference between the projected ETS cost in the target year and the achieved ETS price in the reference year was added to the electricity cost in a form of the fixed carbon tax.

Constraints of the model were set to meet the half-hourly heating demand, cooling demand, electricity, as well as transport demand in each of the location. Satisfying the heating, cooling,

and electricity demands in each of the time-steps can be done by a wide range of technologies and storage solutions that are partly specific for a certain case study. The predefined technologies for the case study used in this paper are discussed in detail in the Case Study section. Meeting the transport demand could be done by gasoline, electric, and/or hydrogen vehicles. It was taken into account that for the same vehicle type, electric vehicles are 3.5 times more efficient compared to the gasoline vehicles and two times more efficient than the hydrogen vehicles, expressed as energy consumed per kilometer traveled [26]. The transport demand for electric and hydrogen vehicles was defined as the energy demand for charging/fueling of vehicles at specific time-steps, while for gasoline vehicles, it was considered that they can be fueled at any point of time without any capacity constraint. The electricity demand for transport was modeled as on-demand charge, while smart charging and vehicle-to-grid options were not modeled.

Furthermore, several factors in relation to location as well as scenario were imposed, as described in the Case Study section in more details.

The full mathematical model of the Calliope modeling framework can be read directly in [27]. The stated reference presents detailed documentation with well-explained system equations, as well as their implementation. The Calliope version 0.6.4 was used for the modeling presented in this paper.

Socio-economic costs were optimized in this paper. The socio-economic costs have been considered as a good representation of the costs of an energy system that are imposed on society. As opposed to the business-economic costs, they do not include different taxes and subsidies, as those are considered to be only internal redistributions within the society [28]. However, the costs of CO₂ were taken into calculation, as the CO₂ costs present internalization of the negative externalities that are imposed on the society through climate change.

The socio-economic analysis was further enhanced with the job-potential analysis of different technologies, in order to assess the impact of the energy transition on the local economy and community. This is an important segment necessary for the successful implementation of energy projects, which are often perceived negatively within the local community. Therefore, this study also calculated the job-years and permanent jobs created, as a result of proposed energy planning scenarios. The report [29] stated that the 1 MW of onshore wind power installed has resulted in 8.6 job-years and 1 MW of photovoltaic plants (PV) in 17.9 job-years related to maintenance, production, and installation of these technologies. Moreover, additional

0.2 and 0.3 local permanent jobs per MW of installed PV and onshore wind respectively will be created in relation to the maintenance of these installed plants. The same job creation potential was used in this study. However, it is also important to note that this study elaborates on the impact on the local and global economy. Only O&M jobs contribute to the local economy, while other jobs are related to the production and the development of the technology and contribute on the global scale. The obtained results were also put in the perspective of the local community where the proposed scenarios were located.

2.2. Power system analysis

High penetration of variable RES in the system often creates voltage problems in the grid, which can limit the potential capacity of variable RES that can be integrated to the grid, especially in the distribution grid [4]. Thus, to validate the results of the capacity expansion energy planning model, a more detailed transmission and distribution grid analysis was carried out in NEPLAN [30]. The method has included the modeling of 20 kV and 110 kV grid and included lines, transformers, nodes, loads, variable RES installations, and replacement model for the external grid. The data needed to model the power system is provided in Table 1. The required data include electrical parameters for lines, transformers, generation, and loads. Additionally, it is necessary to define the node type that can be one of the following:

- Referent node (slack or swing node)—the node for which voltage and voltage angle values are known
- Generation nodes (“PV” nodes)—the nodes for which the active power and voltage are known (these nodes have the regulation possibility)
- Load nodes (“PQ” nodes)—the nodes for which active and reactive power is known

To model the rest of the grid that is connected to the observed grid, the active grid model was defined with its electrical parameters.

Table 1. Necessary data for the load flow calculation

An element of the power system	Required data for modeling
Nodes	Nominal voltage; type of node (slack, generator, node)
Lines	Direct resistance; direct reactance; direct capacitance; length; current
Transformers	Nominal power; short circuit voltage; vector group; primary and secondary voltage ratio; losses; tap regulation
Active grid	Short circuit; short circuit three-phase apparent power; direct resistance and reactance ratio
Loads	Active power, $\cos(\phi)$
Renewable generators	Connection voltage; active power; reactive power; $\cos(\phi)$; regulation (PQ for renewables)

Moreover, power flow was performed to obtain all-electric power grid vectors. In addition to active power, power flow also considers reactive power flows in order to represent the exact model. As power flow is a non-linear and non-convex problem, a Newton-Raphson algorithm (described in Appendix A) was used to obtain its solutions. Grid modeling and power flow analysis were necessary to validate energy planning scenarios, as well as to assess whether it is possible to implement developed energy planning scenarios. If the latter is not the case, the analysis will indicate where are the problems in the grid that need to be resolved. In case of unfavorable conditions in the power system grid, another solution could be to change constraints of the energy system model and obtain different results that could then be validated in the power system analysis.

2.3. The soft-linking approach and the overview of the method

The definition of soft-linking in this paper is as follows: soft-linking combines the output of one model as an input to the second model. By using the term "soft", we denote that the models are not run in parallel, but one after another. In this way, we do not increase the complexity of the models, as would be the case when hard-linking the two models. Hard-linking would combine both models together and result in one very complex model [31]. The reason for the application of the soft-linking approach is that running both models simultaneously would present a complex computational problem, especially because the power flow model is non-linear and non-convex. Thus, outputs from the energy planning model (installed capacity and energy production) are used in the power flow model in order to assess the implementation possibilities of the proposed scenarios. A soft-linked model can implement a feedback loop

between them if needed. For the case of this paper, this feedback loop was not needed and thus, it was not implemented.

The proposed method does not prescribe any specific procedure for the data collection. The input data for the model should be collected according to the available data sources. This proposed model offers a wide range of possibilities for the inclusion of different energy sectors, the definition of various technical parameters, and the definition of the arbitrary topology of the model. The proposition of a specific data collection method would limit the possibilities of the model; thus, this study aims to avoid such scenario. The Case Study section of this paper offers an example of what data can be used for the model.

The methods used in this paper can be summarized in eight steps. These steps included the creation of a specific integrated energy model for the selected case study, the usage of detailed temporal and spatial resolution, the linkage of the output of the energy planning model to the input of the power flow analysis, and the analysis of the results. The steps of the proposed method are stated below and the proposed soft-linking method is presented in Figure 1.

Step 1: Data inventory: Collect, check, and organize the data input for the model

Step 2: Topology of the analyzed Case Study: Definition of the locations and connections of the analyzed energy system as well as the types of technologies at each location following available spatial plans and data

Step 3: Energy system optimization procedure: Run the optimization model, extract results, and identify energy conversion and energy storage technologies to be installed, their combination, and capacity for every single node of the system

Step 4: Socio-economic analysis: Analyze the impacts of the obtained results on the local economy and society

Step 5: Soft-linking between the energy optimization model and the power flow model: Transform and prepare the output results from energy planning results into input data for the power flow model

Step 6: Define the power system grid parameters: Nodes, lines, transformers, generators, loads, and active grid

Step 7: Load flow analysis procedure: Solve non-linear equations using iteration methods and obtain voltage vector and power flows

Step 8: Results analysis: Installed capacities and operation of all technologies, impact on the power system grid, implementation possibilities of the proposed energy planning scenarios

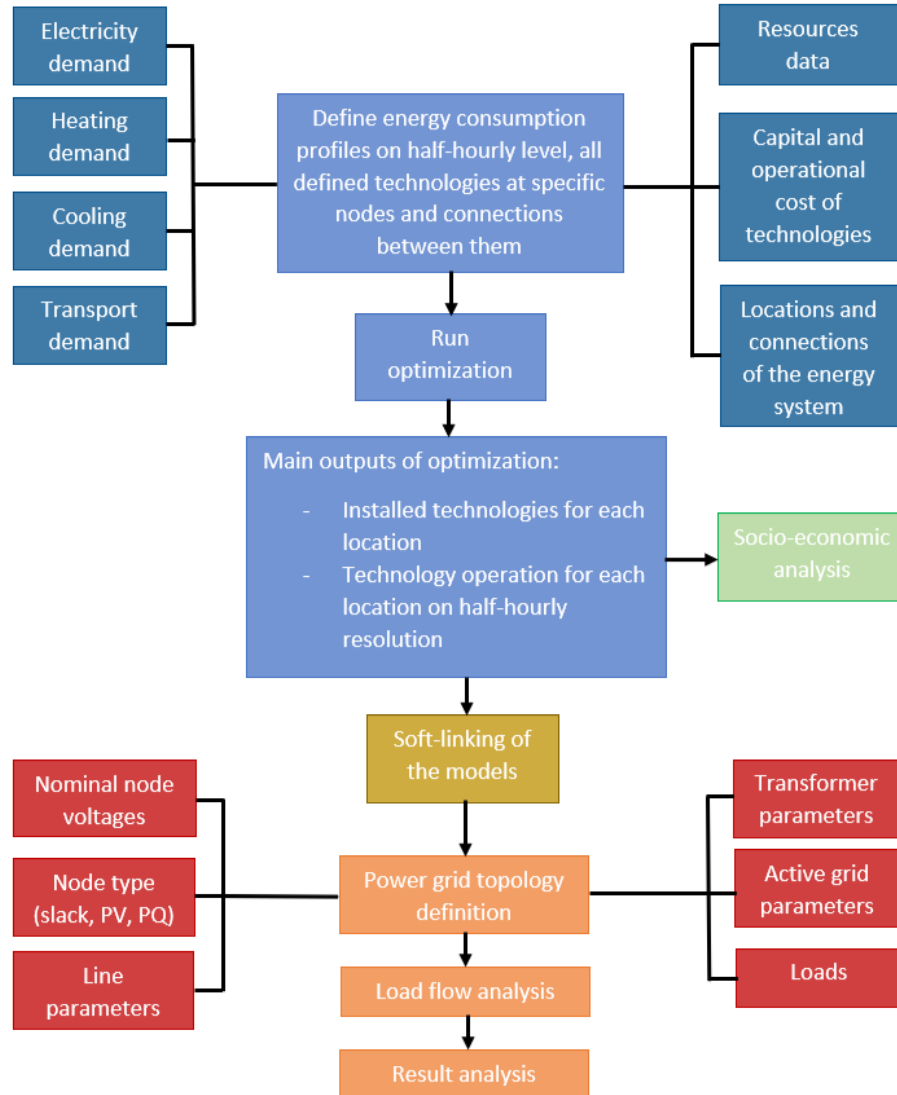


Figure 1. Presented energy planning framework. The data from the Calliope modeling framework that was used as inputs to the load flow model were as follows: the installation power of utility and residential generating technologies, electrified transport demand, and electricity demand for all locations.

3. Case Study

3.1. Geographical location

To test the proposed approach, a case study was conducted on the islands of the Kvarner archipelago, located in the north-west part of Croatia. The places are the island of Krk, Lošinj, Cres, Rab, Unije, Ilovik, and Sušak. Their location is part of the Mediterranean climate characteristic for Italy, France, Greece, and Spain. The total population of all islands has been determined to be 42 503 [32]. Krk is the largest island in Kvarner archipelago, with a population of 19 374 residents and is divided into three parts—the cities of Krk, Dunat, and Omišalj.

A half-hourly temporal resolution was used, and the model was run consecutively, meaning that no slicing and/or decomposition was applied. This approach allowed a detailed representation of the behavior of different storage types during different time scales, such as diurnal, weekly, monthly, and seasonal [33]. A proper spatial resolution was defined following the assessment of the current power grid and the population centers within the island. In total, eight different geographical locations were modeled. Three different locations were considered on the island of Krk (X1, X2, and X3), while two locations were considered for the nearby remote islands wherein their electricity demand need to be met through the island of Krk (X4 and X5). Furthermore, two locations were considered for the import/export interconnectors to the national (mainland) electricity grid (X6 and X7), whereas one location was considered for the potential wind offshore wind turbine (X8).

Two substations 110/20 kV are located in the cities of Krk (X1) and Dunat (X2) that are supplying electric energy to all islands of Kvarner archipelago. Substations in the cities of Krk and Dunat, as well as cities of Krk and Omišalj (X3), are connected with 110 kV line. The connection between Krk and mainland consists two underwater cables, one connecting Omišalj and Melina (X6) with a maximum capacity of 100 MW and another connecting the substation in city of Krk directly to Crikvenica (X7) on the mainland with a total capacity of 70 MW. Islands of Lošinj, Cres, Unije, Ilovik, and Sušak were considered as one location Lošinj (X4), while the island of Rab (X5) was considered as one location. Rab (X5) is connected to Dunat (X2) and Lošinj (X4) to Krk (X1), both with a 100 MW transmission line. All transmission capacities were fixed since there is no indication that they should be changed in the future. Additionally, potential offshore wind turbine plant (X8) near Omišalj was considered. The list

of the considered locations is provided in Table 2, while Figure 2 visually presents the locations of the case study with all connections between different locations [34]:

Table 2. List of the geographical locations, energy function, and reciprocal connections as designed in the Calliope model

Location	Name	Type	Connection to	Distributed generation
X1	City of Krk	Demand	X2; X3; X4; X7	Yes
X2	Dunat	Demand	X1; X5	Yes
X3	Omišalj	Demand	X1; X6; X8	Yes
X4	Lošinj	Demand	X1	No
X5	Rab	Demand	X2	No
X6	Melina	Import/export	X3	No
X7	Crikvenica	Import/export	X1	No
X8	Offshore wind turbine	Generation	X3	No

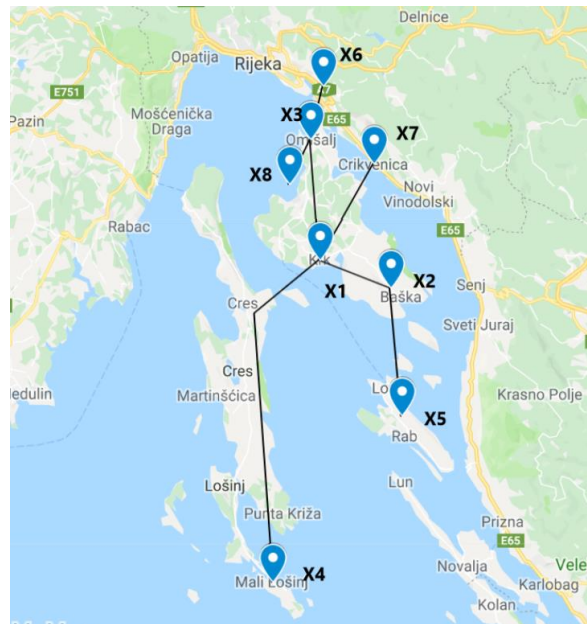


Figure 2. Geographic map showing nodes and their connecting network considered in the energy system modeling

3.2. Considered technologies and energy system related data

Different technology options were considered in this model. The following electricity technologies were included in this model: wind onshore, wind offshore, PV residential, utility-

scale PV, biogas engines (and gasification plants), a waste incineration plant, concentrated solar power, hydrogen electrolyzers and fuel cells (proton-exchange membrane technology), and a biomass power plant. In the heating and cooling sectors, the following technologies were considered: air-to-water heat pumps, ground-source heat pumps, electric boilers, biomass boilers, and solar thermal coupled with storage. Moreover, the following storage solutions were defined: Li-ion batteries, hydrogen storage, and heat accumulators for individual use. Finally, the transport sector included the following options: gasoline, electric, and hydrogen vehicles. The use of electric and hydrogen vehicles was modeled as energy storage satisfying the transport demand. A diverse range of technologies modeled for this case study included all the technologies that are suitable for distributed energy generation. Although there is a liquefied natural gas terminal under construction that will be connected to the gas grid and exported to the mainland, gas-fueled boilers and cogeneration plants were not modeled because of the EU bans on this carrier for household heating (e.g. [35], [36]). Nuclear power plants were not predefined, as their usually large capacities were considered as significantly too large for the collection of islands of the population and size considered in this case study.

Distributed generation was modeled on locations X1, X2, and X3. There have already been plans for the development of PV plants on the islands surrounding Krk; however, they are not considered because the development of these projects still needs to take place. Required input data were obtained from detailed measurements and reports that are available. Annual data for electricity, heating, cooling, transport, solar irradiation, and wind speed are provided in Table 3. All the data inputs are referred for the year 2017. The annual time course of energy demands and imports, as well as energy generation and export, was arranged with respect to the different energy sectors and referring to the entire energy system of Krk Island. The wind generation normalized pattern and the half-hourly cooling and heating curves were created using the data acquired from [37]. Moreover, the hourly PV generation pattern was acquired from the PV GIS database for different locations and interpolated to achieve half-hourly time resolution [38]. Thanks to the availability of detailed data on permanent and temporary occupied housings in Krk in [32], it was possible to estimate upper capacities for individual boilers and residential PVs. Half-hourly data of all the locations are openly available on the GitHub website, together with the applied model [39].

Table 3. Summarized input data for the case study. Full dataset available at [39]

Demand type	Location	Demand quantity	Maximum load [MW]	References
Electricity	X1	49 GWh	17	[40], [41], [42], [43]
	X2	68 GWh	20	
	X3	19 GWh	6	
Heating	X1	40 GWh	20.8	[40], [41], [42]
	X2	22 GWh	11.2	
	X3	11 GWh	5.8	
Cooling	X1	6 GWh	13.4	[40], [41], [42]
	X2	3 GWh	7.2	
	X3	2 GWh	3.8	
Transport	X1	12 GWh*	4.7	[44]
	X2	12 GWh*	4.9	
	X3	5 GWh*	1.5	
Resources	Location	Capacity factor	Max capacity factor	References
Solar	X1	0.162	0.9	[45]
	X2	0.15	0.88	
	X3	0.154	0.88	
Onshore wind	X1, X2, X3	0.254	1.0	[46]
Offshore wind	X8	0.35	1.0	[46]

* *Transport equivalent electricity demand. If all the demand was to be covered by gasoline vehicles, the value would be 3.5 times higher, e.g., 42 GWh of gasoline for X1 location. If all the demand was to be covered by hydrogen, the resulting demand would be two times higher, e.g., 24 GWh for X1. This assumption allowed a resulting transport demand to be met by a mix of all three technologies.*

Table 4 presents the investment and O&M costs, as well as the main technical parameters for the modeled technologies. It is assumed that the prices reflect the 2030 technology prices. The interest rate applied in the model was assumed to equal to 10%, except for residential PV, which had a discount rate of 5%. The fixed O&M costs are dependable on the installed capacity, but this cost is the same for each year of the operation.

Table 4. Investment, technical, and O&M parameters of technologies considered by the model. The full list of parameters and technical constraints can be seen in [39]

Technology	Investment cost	O&M fixed cost [€/kW]	O&M variable cost [€/MWh]	Efficiency	Lifetime [years]	Ref.
Fuel cell (PEM)	1900 €/kW	95	-	50%	10	[47]
Electrolyzer (PEM)	1896 €/kW	163	-	58%	15	[47]
Hydrogen storage	11 €/kW	-	-	95%	25	[47]
Residential PV	1070 €/kW	12.8	-	100%**	30	[48]
Utility-scale PV	620 €/kW	8.1	-	100%**	35	[48]
Onshore wind	1120 €/kW	14	-	100%**	27	[48]
Offshore wind	2130 €/kW	40	-	100%**	27	[48]
CSP	2295 €/kW	-	2	100%**	25	[49]
Battery	143 €/kWh	-	-	95%	25	[47]
Heat accumulator	0.55 €/kWh	-	-	90%	25	[47]
Biogas Gasification	1810 €/kW	198		100%**	25	[50]
Biogas engine	950 €/kW	9.75		45%	25	[48]
Waste incinerator	10 500 €/kW	96	5.8	23.5% el	25	[48]
Biomass PP	6000 €/kW	288.9	7.8	29%	25	[48]
BIOboiler	680 €/kW	-	13.88	80%	20	[51]
Air source heat pump	1750 €/kW	-	0.5	COP 3.5 heating; 2.5 cooling	18	[51]
Ground-source heat pump	2750 €/kW		0.5	COP 5.5 heating; 3.5 cooling	20	[51]
Electric boiler individual	1000 €/kW	-	0.1	95%	20	[52]
Solar thermal individual	857 €/kW	16.2		100%**	25	[48]
Electricity grid*	0.01 €/kW/meter	-	-	96%	25	[53]

* Wind offshore site does not have a connection to the island grid; thus, if deemed optimal, this link needed to be built on top of the offshore wind turbine.

** Assumed 100% because the costs are related to the output power of those sources

3.3. Considered scenarios

Three scenarios were modeled; further, two were included in the sensitivity analysis. The electricity prices for all the scenarios were taken for the year 2017 from CROPEX, a Croatian day-ahead power market [54], with the assumption that the same level of electricity prices can be expected for the period relevant for this study (the year 2030), except the expected cost increase of CO₂. The average ETS price of allowances in 2017 was 5.8 €/ton of CO₂ [55], while the projected ETS price in 2030 is 55 €/ton of CO₂, according to [56]. Thus, to account for the difference in the ETS price that was considered in the price of electricity in 2017 and the expected price in 2030, an additional carbon tax of 49.2 €/ton of CO₂ was added to the system. The carbon emission intensity of the Croatian mainland electricity was 250 kgCO₂/MWh. Only the annual average carbon intensity of electricity was available; thus, the same carbon intensity was assumed in all the time-steps of the modeled year. Furthermore, none of the scenarios included any form of subsidies, as socio-economic costs were modeled in this case study.

The first scenario considered all the energy technologies without constraints. The second scenario allowed the electrification of transport by at least 25%, while the third by at least 65%. The third scenario also envisaged a minimum 5% hydrogen share in the transport sector, which was utilized for heavy transport modes. The share of the directly electrified transport sector (65%) was taken based on [44], which has shown that 72% of the transport sector could be directly electrified with the currently known technologies. The third scenario was also the basis for the two sensitivity analysis scenarios, in which the impact of the coarser temporal and spatial resolutions was considered.

To directly assess the differences between the detailed spatial and temporal resolution, a sensitivity analysis was performed by comparing the scenario with the highest share of renewable energy generation with completely the same case study (the same energy system) but using a coarser time resolution, as well as a coarser spatial resolution. The sensitivity analysis was run separately for the case of coarser time resolution from the case of the coarser spatial resolution. These analyses allowed for explicit comparison of the impact of time resolution and the spatial resolution on the capacity expansion modeling problems.

Export of electricity generated on the island was allowed in all the scenarios, and the income for those exports was determined to be equal to the matching hourly CROPEX price. Hence, the income from exporting electricity could lower the total socio-economic costs of the system. Scenarios are summarized in Table 5. However, it is important to note that islands remained

connected to the mainland in all the scenarios and that grid provided ancillary support to islands when needed.

Table 5. Scenarios applied to the model

Scenario	Transport constraint	Temporal resolution
S1	No constraint	Detailed spatial and half-hourly modelling
S2	A minimum 25% of electrified transport	Detailed spatial and half-hourly modelling
S3	A minimum 65% of electrified transport and minimum of 5% hydrogen for transport	Detailed spatial and half-hourly modelling
S4	A minimum 65% of electrified transport and minimum of 5% hydrogen for transport	Detailed spatial and hourly modelling
S5	A minimum 65% of electrified transport and minimum of 5% hydrogen for transport	Single geographic location and half-hourly modelling

S1 was chosen as a reference scenario. Meanwhile, S2 and S3 were chosen to explore the impacts of the introduction of different shares of different transportation types. Thereafter, S4 and S5 were compared to S3 and were chosen to demonstrate the improvements related to a finer resolution in time (S4) and space (S5). Indeed, S4 considered a coarser time resolution of 1 hour, while S5 applied just a single node to the simulated energy system.

3.4. Electric power grid analysis and solution algorithm

Power grid analysis was carried out for the highest RES penetration, as this should be considered the most challenging condition in keeping the voltage within the allowed limits. Two sub-scenarios were considered for this case as well: the first one, in which only distributed energy resources are considered without utility-scale production; and the second one, which includes utility-scale production connected to high voltage buses at substations Krk and Dunat. The analysis was conducted for two cases, i.e., minimum and maximum load, as is usually the case in grid connection projects [57]. It is considered that all loads work with $\cos(\varphi) = 0.95$ in order to include reactive power flow effects as well. The slack node is chosen to be Melina 400/220/110 kV substation (X6) because it has the highest regulation possibilities in the observed area. The measured voltage was obtained from the distribution system operator and it was equal to 115.5 kV for the maximum load and 121.22 kV for the minimum load. The

inclusion of the slack bus voltage data assured that the model is equivalent to a currently existing state.

The largest optimization problem was Scenario 3, and the following parameters have been determined to be associated with that scenario run. The model was run using the CPLEX optimization solver, using on average 4 cores. The average RAM utilization was 21 GB, while the max RAM use was 27.5 GB. The total run time was 1h 24 min, the optimization problem consisted of 6.92 million variables, and there were 1.12 million objective non-zeros.

4. Results

4.1. Installed technologies for S1, S2, and S3

As per the results of the case studies, it was determined that there is a high possibility for the integration of RES on the Krk island by 2030. The results were obtained for electricity, heating, cooling, and transport system for all analyzed scenarios. Figure 3 presents the power of installed technologies for electricity and thermal production. It can be observed that an increased share of electrified transport has led to higher installed capacities of renewable electricity generation. Moreover, the increased share of electrified transport without smart charging resulted in an increased power requirement of the battery storage system.

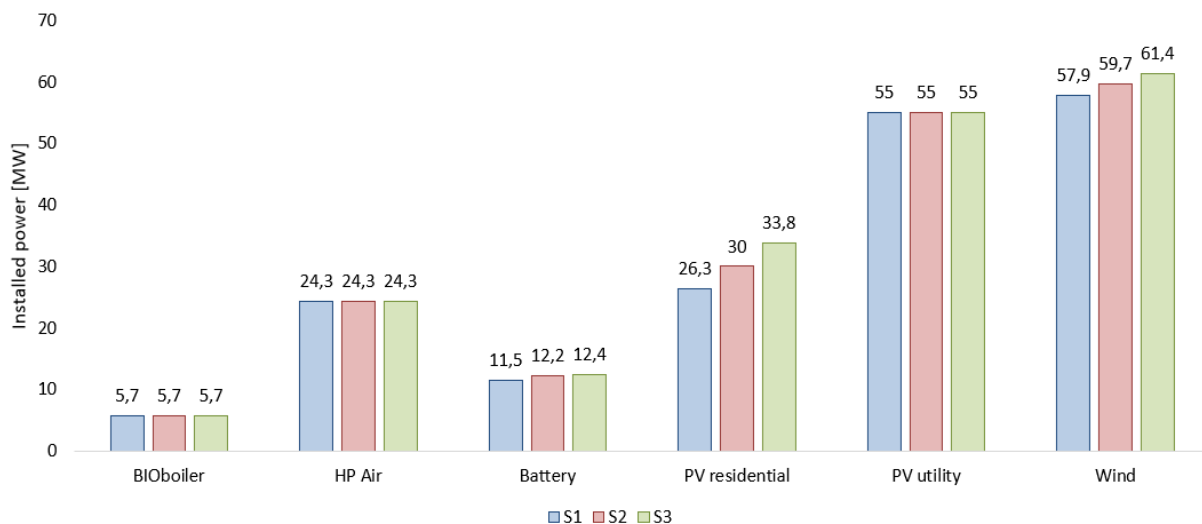


Figure 3. Installed power of electricity, thermal, and battery storage technology

Figure 4 presents the installed electricity generation capacities for all locations on the Krk Island for the S1, S2, and S3. Increase in the electrification of transportation has resulted in an increase

of 1.7 MW wind on the location X3 and an increase of 3.8 MW of residential PV on the location X2 in comparison with S2.

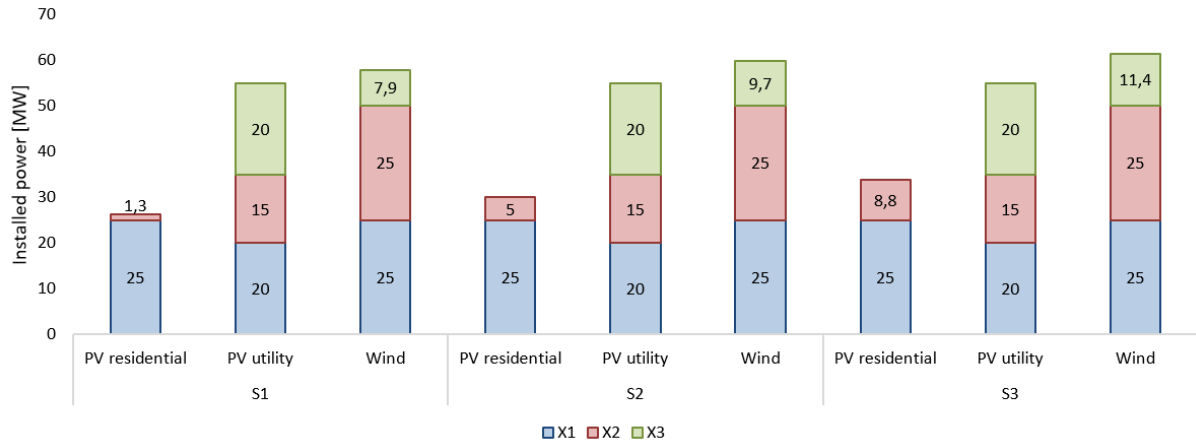


Figure 4. Distribution of installed electricity generation capacities for three scenarios

Different storage technologies and their capacities for the three modeled locations on the Krk Island are presented in Figure 5. In line with the previous results, the increase on electrified transport has also lead to the increase in the required battery capacity. The difference is visible in S2 where the battery capacity increased for 0.6 MWh, 0.7 MWh, and 0.1 MWh for three locations X1, X2, and X3, respectively, in comparison to the S1. Introduction of hydrogen in the transportation sector resulted in the requirements for hydrogen storage for S3. The hydrogen storage requirements were also present for different locations, namely, 1.4 MWh for X1 location and 5.2 MWh for X3 location.

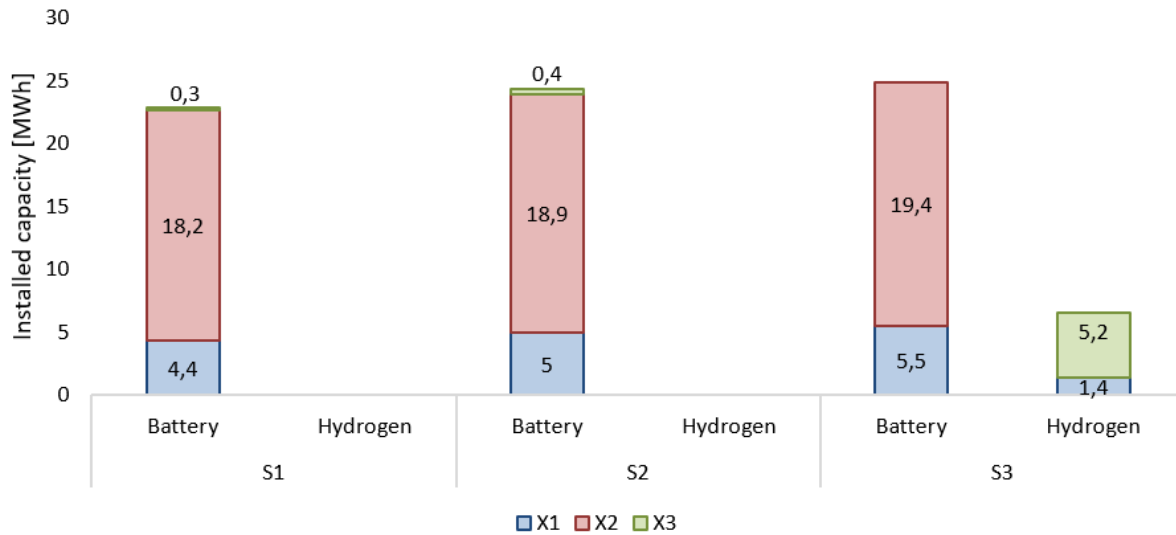


Figure 5. Storage capacity by considered technologies with reference to the Krk island locations and the three compared modeling scenarios. Heat accumulator value remained the same for all three scenarios (150 MWh)

The share of a particular transport type is presented in Table 6. The results showed that the minimum share of certain transport type constraints was activated in the optimization. Thus, the transport shares of different technologies were a result of the constraints of each particular scenario. Contrary to on-demand charging approach used in this paper, modeling smart charging or vehicle-to-grid could change the optimal mix of the transport sector [58]. However, this was left outside of the scope of this paper.

Table 6. Share of transportation type for S1, S2, and S3

Scenario	S1			S2			S3		
Transport type	EVs	Gasoline vehicles	Hydrogen vehicles	EVs	Gasoline vehicles	Hydrogen vehicles	EVs	Gasoline vehicles	Hydrogen vehicles
Share [%]	2	98	0	25	75	0	65	30	5

4.2. Sensitivity analysis between the S3, S4, and S5

As per the results of the sensitivity analysis, the approach used in this study showed significant improvements. Figure 6 presents the installed capacities of different technologies for S3, S4, and S5 scenarios. The comparison between half-hourly and hourly scenarios (S3 and S4) revealed a slight difference in the installed capacities. For example, S4 resulted in 1.2% less

installed power of residential PV in comparison to the S3. Installed wind capacities increased from 61.4 MW for S3 to 62 MW for S4. The difference between the two scenarios can also be observed for the installed battery storage power, which differentiates by 2.3 MW for the two scenarios. Meanwhile, the comparison between the spatially dispersed approach (S3) and the aggregated approach (S5) showed significant differences. The results of the S5 suggested significantly lower amounts of installed electricity generation power than for the case of S3. In this sense, the installed wind power reduced by 7 MW, while the installed power for the residential PV decreased by 8.1 MW. These results represent a change of 11.3% in the installed wind capacity and 24.3% in the installed residential PV capacity for the S5 in comparison to the S3.

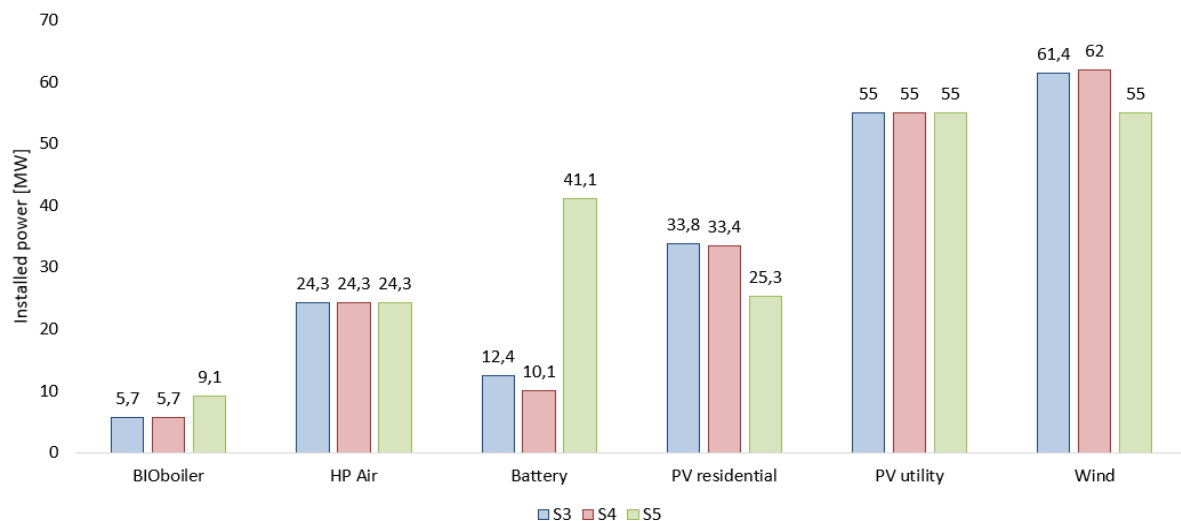


Figure 6. Installed capacities of different technologies for S3 and sensitivity scenarios

More detailed representation of the results for electricity generation technologies is provided in Figure 7. The results of S3, S4, and S5 for all Krk locations were compared. The difference between S3 and S4 was observed in the residential PV on location X2 (4.5% lower value for the S4) and the wind generation on the location X3 (5.3% higher value for the S4). The difference between S3 and S5 is more visible as the results of S5 indicated lower capacities of the installed technologies. Moreover, spatially distributed scenario contained a significantly larger amount of information as it is possible to observe capacities for several locations.

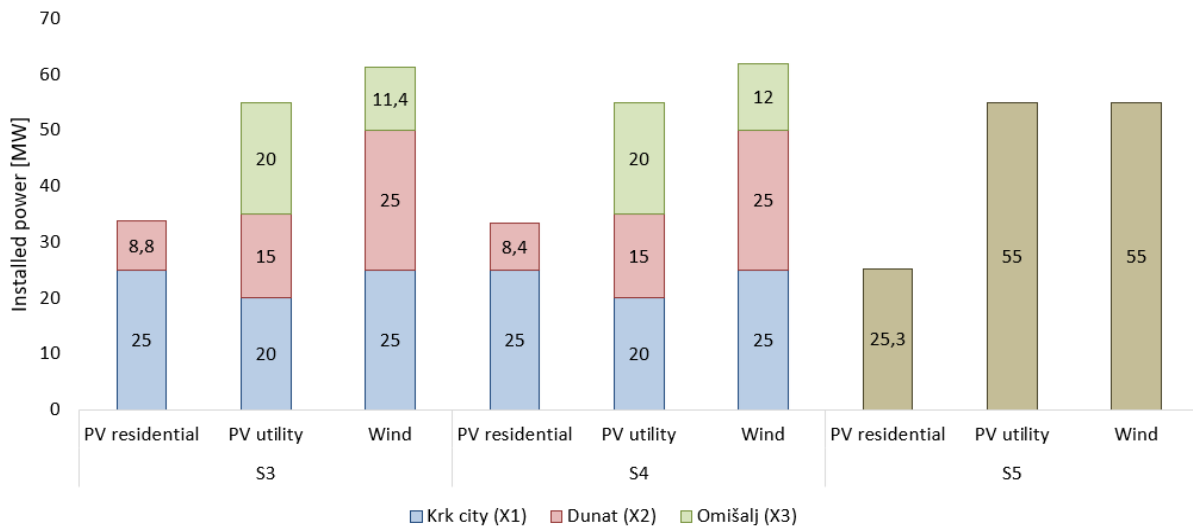


Figure 7. Distribution of installed electricity generation capacities for sensitivity scenarios. In S5, all the technologies were considered to be installed in the same location; thus, they are represented with another color.

Similar results can be observed for the energy storage capacity presented in Figure 8. The differences between S3 and S4 are visible primarily in terms of installed battery storage capacity. Meanwhile, the results of S4 indicated that its installed battery capacity was at 20.2 MWh, while for S3, the battery storage capacity was 24.9 MWh. The reduction of battery capacity is visible for different locations as well. Following the results presented in Figure 7, the difference in spatial modeling between S3 and S5 was significant. Figure 8 shows that the battery storage capacity for S5 was equal to 82.2 MWh, which is 3.3 times higher than the battery capacity for S3. This result indicates the need for spatial distribution modeling in energy planning. Considering S3 as compared to S5, the dispersed energy flows along the entire electrical network allowed a remarkable reduction in the battery storage capacity of the whole energy system. Hydrogen storage also deviated for all three analyzed scenarios, with the highest deviation of 0.5 MWh (between S5 and S3).

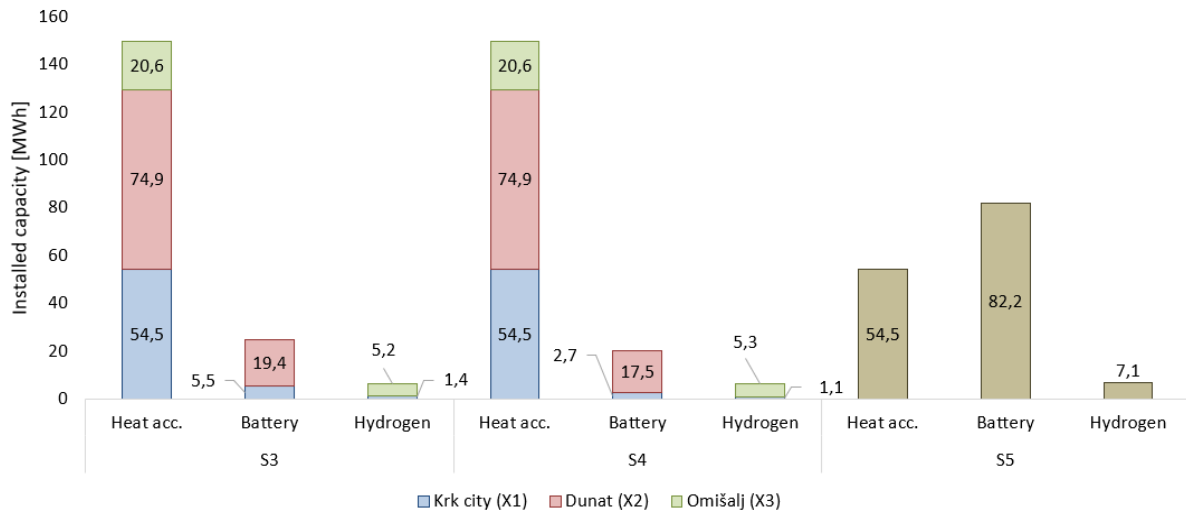


Figure 8. Installed capacities of different storage types in MWh. In S5, all the technologies were considered to be installed in the same location; thus, they are represented with another color.

Capital and operating costs of the five assumed scenarios were then examined. As per the results, similar values were determined for all scenarios except for S5 as can be observed in Figure 9. This result was also in line with the previous findings of the study that showed a significant difference between scenarios that applied different spatial modeling. It should be noted that one of the main reasons for the significant change in S5 is that the scenario does not model the grid connection cost for the potential offshore wind turbine, which is included for S1–S4. In S5, the optimization resulted in the installation of offshore wind turbines instead of onshore ones, as the increased capacity factor has offset the increased capital costs of the technology (Table 7). This result indicated that the cost representation for the spatially distributed scenarios had more realistic value. S3 and S4 also resulted in different total socio-economic costs of the system. The capital system costs of S4 were found to be 0.4% lower than that for S3. Thus, it can be concluded that the half-hourly resolution did not significantly improve the representation of the costs, compared to the hourly temporal resolution.

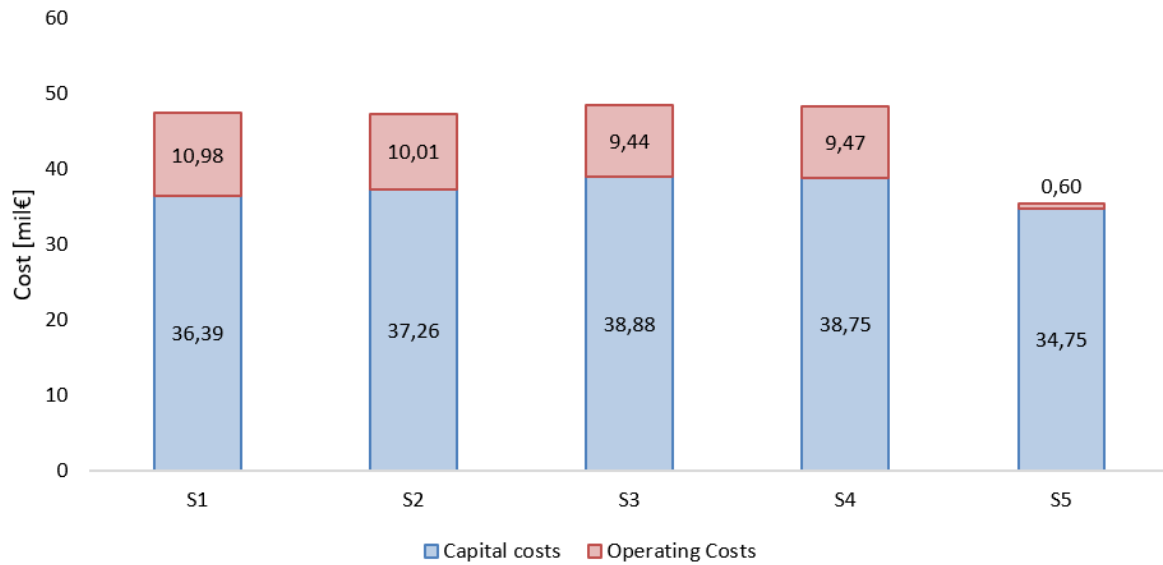


Figure 9. Capital and operating costs for all five scenarios. Internalized costs of CO₂ emissions are included as operating costs.

The following paragraphs focus on the difference in results achieved using different temporal and spatial resolutions. Figure 10 presents the battery storage operation for S3 and S4. Moreover, Figure 10 distinguishes battery storages for two locations—X1 and X2. First, the difference between the different temporal modeling can be observed. This can best be observed for November 4 between midnight and 8:00. The results of the half-hourly scenario (S3) showed the more volatile operation of the battery system storage during this period than for the case of the hourly scenario (S4). On November 5 between 2:00 and 10:00 is also a good example of the benefits of the proposed approach, where charging and discharging of the battery storages occurred only for half-hourly S3. Second, the possibility of observing the operation of different locations for the same scenario allowed more accuracy in energy planning as well. A good example of this is also November 5 where, at 05:00, a sudden 4.72 MWh battery storage system charging occurred at the X2 location. Similar patterns can be observed for the entire period.

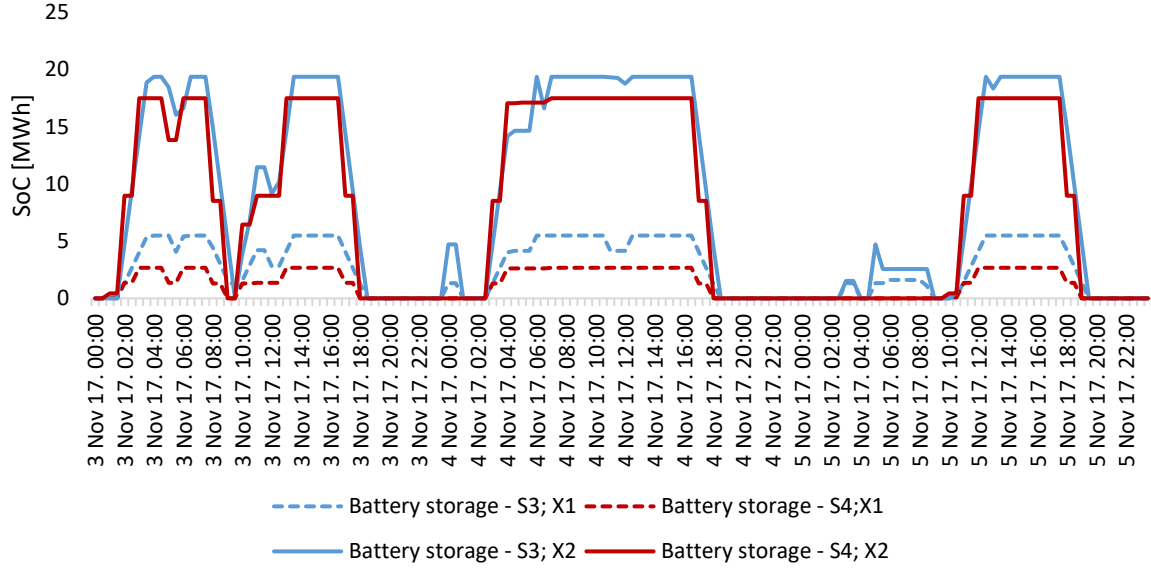


Figure 10. Battery storage operation for S3 and S4 for locations X1 and X2

In Figure 11, the summed battery storage system operation can be observed during May. The results were in line with the findings provided in Figure 10. It can be observed that both scenarios had similar patterns most of the time. However, differences can be observed, for example, on May 20 in the period 4:30–9:00.

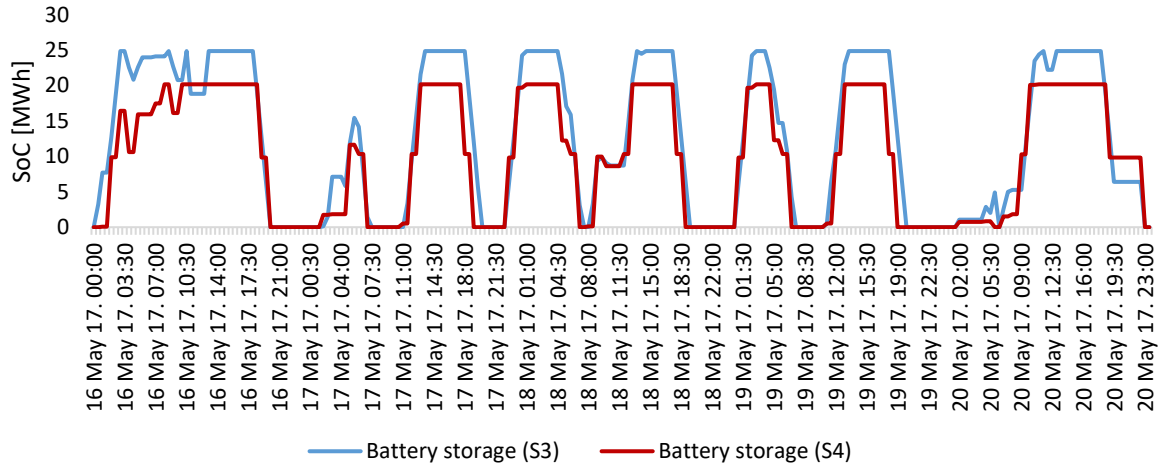


Figure 11. Battery storage operation for the entire Krk Island for S3 and S4

The differences between the two scenarios with different time resolutions were examined for the transport sector as well. Figure 12 presents the end-use power required for the transport sector, namely, the gasoline vehicles and electric vehicles. The end-use power is defined as the power available at wheels of vehicles, meaning that different efficiencies of gasoline and

electric motors cannot be observed in this representation. More detailed representation of the energy system operation was achieved for S3. As shown in Figure 12, the most visible example can be observed on August 5 at 14:00. At this hour, a sudden increase in gasoline demand and a decrease in electricity demand occurred. This change is visible for S3, but not for the hourly scenario S4.

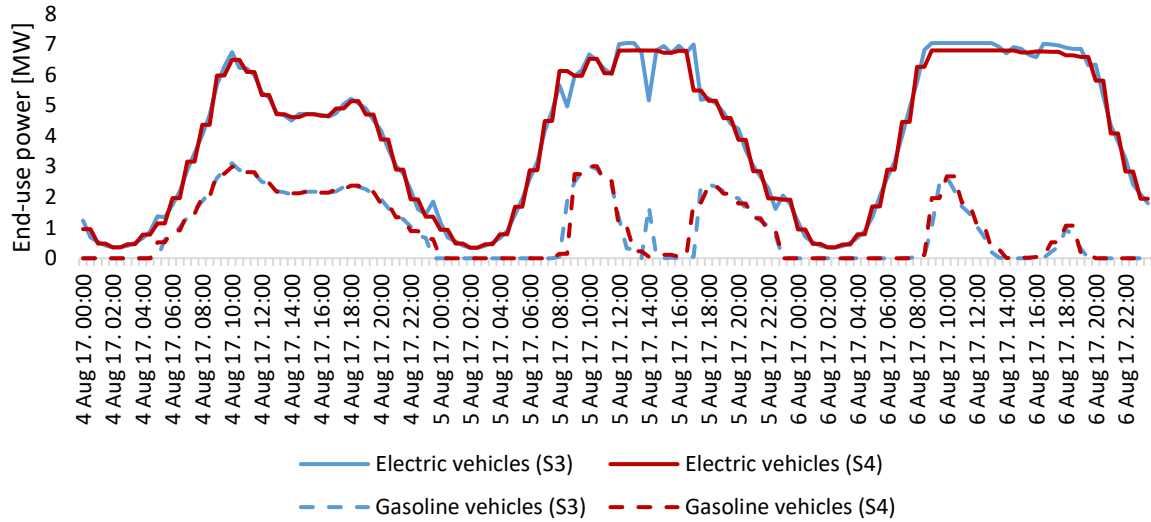


Figure 12. Transport load for S3 and S4 for summer months

The difference in the total SoC of the battery storage system for both scenarios for March is provided in Figure 13. The main difference was in the size of the battery storage systems. The results of S5 with one location modeled indicated several times higher battery storage capacity than the results of S3. Besides the difference in the size of the storages, Figure 13 shows that the trends in the battery system operation are mostly misaligned, especially during charging and discharging periods.

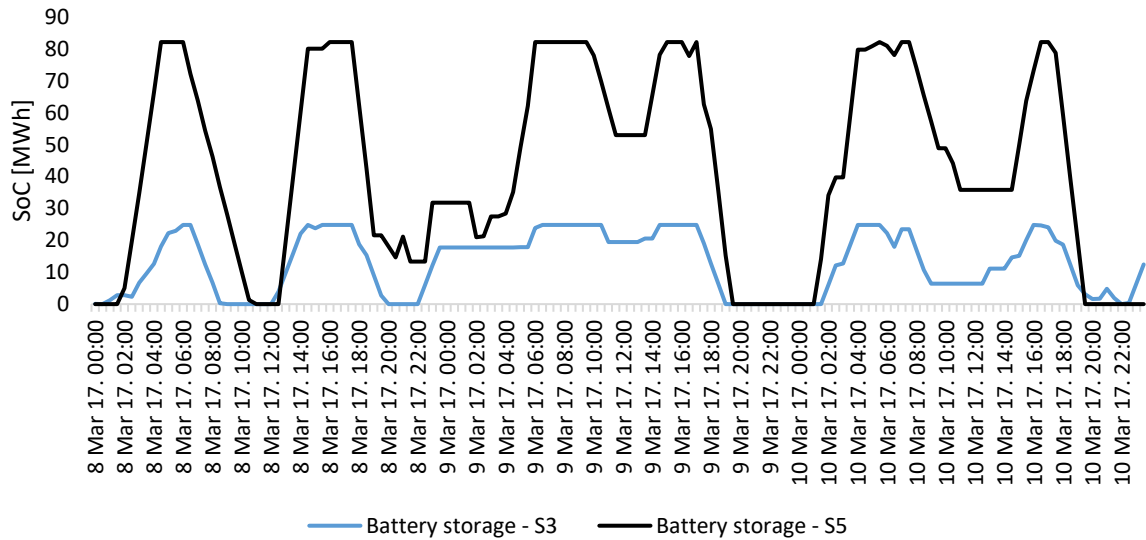


Figure 13. Battery storage operation comparison for S3 and S5

The impact of dispersed spatial modeling was also noted for the transport sector, as shown in Figure 14. The same period was taken as in the scenario analysis of S3 and S4. As per the results, it was determined that S3 and S5 had the same trend for most of the observed period. However, differences occurred for more sudden changes like the one on August 5 at 14:00. Similar to the analysis conducted between S3 and S4, S5 also did not represent this change. The required transport power over time remained approximately the same.

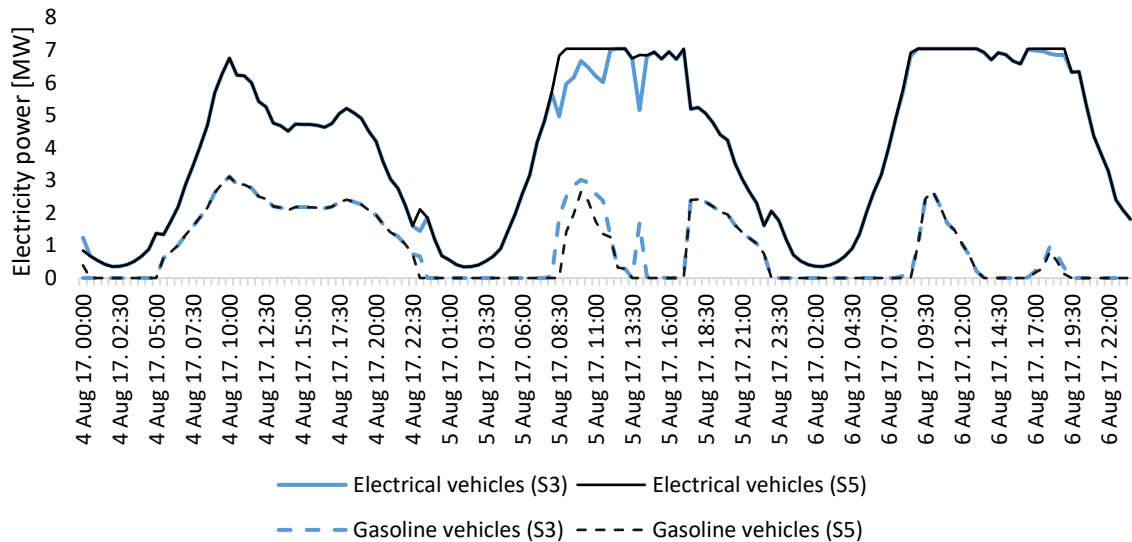


Figure 14. Transport load for S3 and S5 for summer months

4.3. Energy system operation

This chapter presents the key data on the energy system operation of the observed case study. Table 7 presents the overall annual energy production. The results were in line with the previous findings. Slight change in relation to the change in the wind and residential PV production was noted for S1, S2, and S3. The increased level of electrified transport increased the production of these two technologies. Differences are visible for S3 and S4, which could be attributed to the different temporal modeling used for these scenarios. However, the most significant change was noted for S5. The energy system utilized its connection to the mainland grid, resulting in significant export of excess electricity generated on the island. For example, in scenario S3, 16% of the electricity generated by onshore wind, residential, and utility-scale PV were exported. A more detailed figure with exports per locations and technologies can be seen in Appendix B.

Table 7. Annual electricity and thermal energy production

Technology [GWh]	S1	S2	S3	S4	S5
Residential PV	37.3	42.3	47.3	46.7	36.1
Utility PV	75.4	75.4	75.4	75.4	78.5
Wind **	128.9	132.9	136.6	137.9	265.5
Import	169.9	176	182.5	181.8	100.8
Export	41	40.9	41.6	42.1	96.7
Air HP*	62.5	62.5	62.5	62.5	58.1
BIOboilers*	12.5	12.6	12.5	12.5	16.1

*Thermal energy production

**In S1–S4, the numbers represent onshore wind production only, while in S5, the number represents offshore and onshore wind production

Figures 15 and 16 present the operation of the energy system on the Krk Island for winter and summer for S3. The figures provide an insight into the overall operation of the system and the diversity of the installed technologies. It is worth noting that the results have considered the losses in the transmission lines.

Figure 15 presents the operation of the energy system for one day in January. The results showed the dominant influence of wind electricity production for the observed period. Because of this and the lower energy demand during the winter, the export values were determined to be high. As the energy flows were lower during winter months, the corresponding grid losses were also lower. The results showed that the PV generation is less expressed during winter, but

it still provides some of the energy. Grid batteries were mostly charged at night, as a consequence of high wind energy generation in those periods and low electricity prices from the mainland. As the PV generation almost disappeared in this winter day after 13:00, due to overcast, batteries and grid import have helped meeting the demand. This shows the importance of flexibility in the grid such as storage and transmission links. The end of the day was again dominated by wind generation and grid import, while the import increased when the price was low to charge the battery again. During the chosen winter day, the share of PEM electrolyzer consumption in the total final electricity consumption was 1.7%, while the share of final electricity consumed by heat pumps was 39.5%.

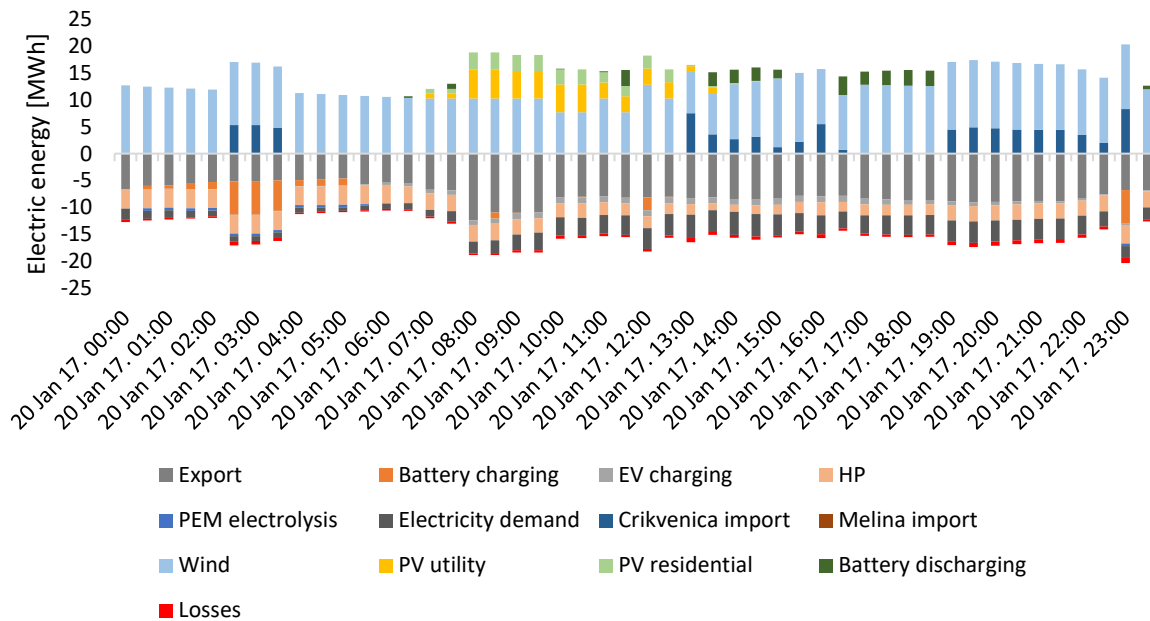


Figure 15. Electricity system operation for two winter days in S3. Export designates the electricity demand of the nearby islands Lošinj (location X4) and Rab (location X5) that have to be supplied through the Krk power grid.

The system operation for summer has been illustrated in Figure 16. With the detailed spatial distribution, it was possible to determine the exact import values from Crikvenica and from Melina, as illustrated in Figure 16. This is expected as the population of Krk can increase up to six times in comparison to the winter period [32]. It was not only the electricity consumption of Krk island that has increased significantly as the same rise in consumption was observed in the nearby islands of Lošinj and Rab. As this consumption needed to be met using the grid of the island of Krk, the total electricity demand in the chosen summer day was 2.5 times higher

than in the chosen winter day. During the night periods, imports from the mainland grid satisfied up to 80% of the consumption. On the other hand, during the day, wind, residential, and utility PV, together with the grid batteries satisfied 100% of the demand in some of the periods (10:00–11:00). It can be observed that much higher grid imports occurred from Crikvenica link (location X7), as this link is connected with the city of Krk consumption point, which has been identified to have the largest electricity demand. The wind production was significantly lower in comparison to the winter period. During the chosen winter day, the share of PEM electrolyzer consumption in the total final electricity consumption was 3%, while the share of final electricity consumed by heat pumps was 15%. The losses in the transmission lines in absolute terms increased as the overall energy flows increased. Batteries were still charged mostly during the night, except for the period from 12:00 to 12:30 as this corresponded with lower mainland grid electricity prices. This representation of the summer day is especially useful to notice wide oscillations between the daily and night operation of the grid. Almost no self-generation during the night is replaced by almost complete self-generation during the day. Thus, it can be seen that for the energy systems of this size, maintaining the link to a larger energy system brings important flexibility to the system, keeping the overall system costs low.

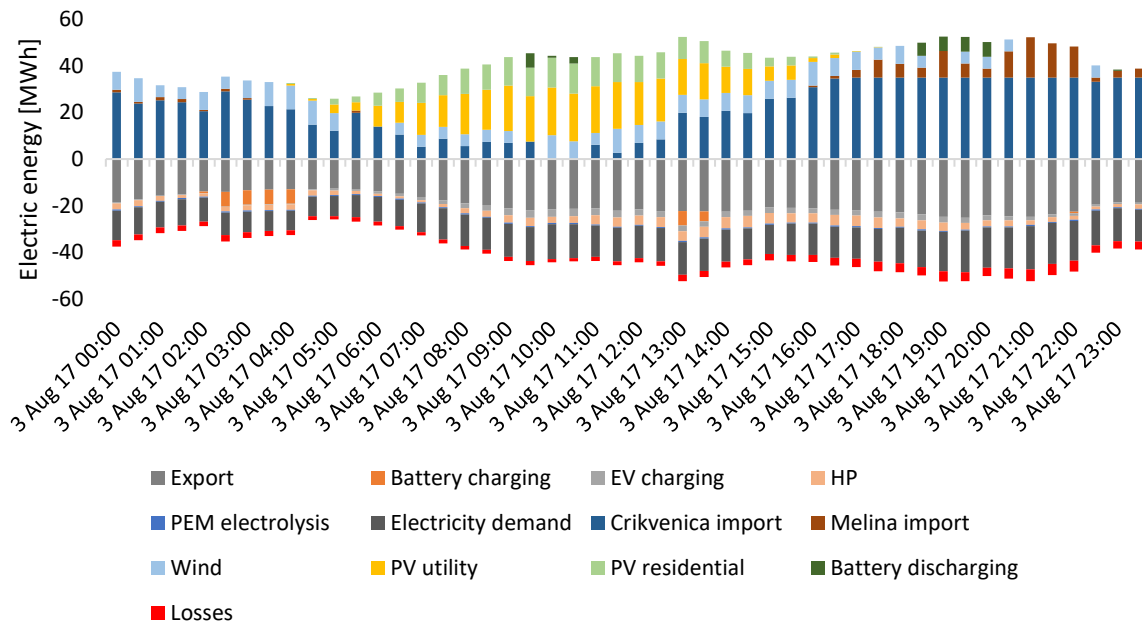


Figure 16. Electricity system operation for two summer days in S3. Export designates the electricity demand of the nearby islands of Lošinj (location X4) and Rab (location X5) that have to be supplied through the Krk power grid.

4.4. Power flow calculation

To assess the impact and evaluate the possibility for the installation of a high amount of variable RES, a power flow calculation has been performed. The calculation was completed for minimum and maximum load and three scenarios. The first scenario is with the state of the currently existing grid at the Krk island, second with the distributed energy resources but without the utility-scale power generations, and, the third scenario, with the utility-scale power generators included at the high voltage bus on the Krk and the Dunat substations. Figures 17 and 18 present the results for the chosen nodes that represent a specific part of the Krk grid. For the case of maximum demand (Figure 17) that occurs during the summer months, it is possible to observe that neither scenario created voltage problems in the grid. Installation of distributed energy resources in the second scenario was determined to have caused an increase in the voltage for all observed nodes, which is already expected. The highest increase of 6.05% was achieved for the Baska 2 node, while the highest voltage value of 1.058 p.u. is recorded for Klimno 1 node. When the utility-scale generations are connected, the highest voltage increase (5.95%) and the highest voltage amount (1.057 p.u.) were recorded for the Dunat substation. As allowed voltage limits range from 0.9 to 1.1 p.u., it can be stated that, for the case of maximum demand, installation of a high amount of variable RES caused the voltage increase but with no threats of violating the voltage limits and without the needed interventions in the electric power grid.

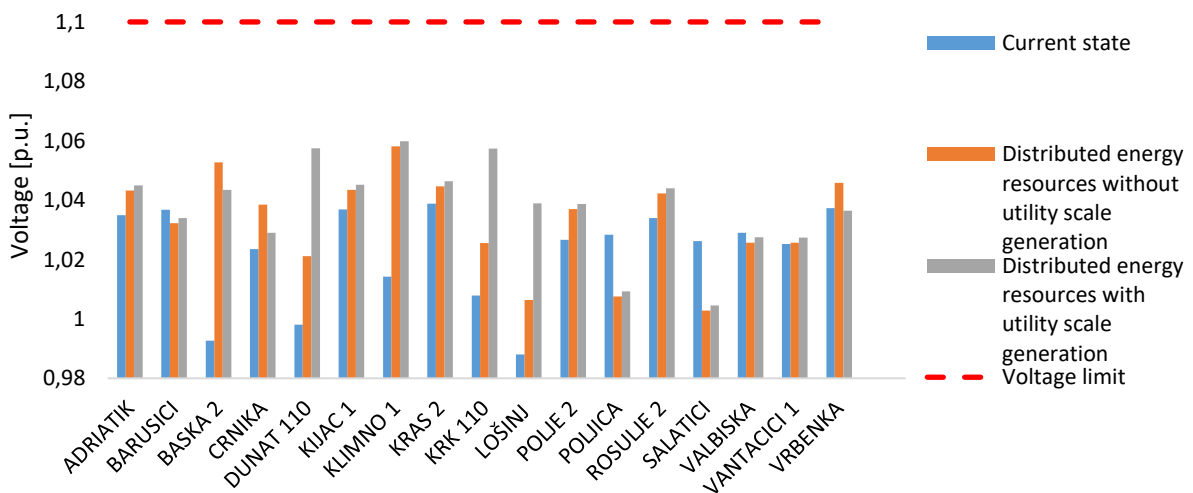


Figure 17. Voltage values for three scenarios at observed nodes for maximum demand case

The results for minimum demand are presented in Figure 18, where it was demonstrated that there was a possible voltage violation on the high voltage buses on Krk, Dunat, and Lošinj substations as well as some distribution transformers located near the high voltage grid (e.g., Poljica and Salatici in Figure 18). This was evident even for the current state of the grid without the connection of the distributed energy resources. The voltage for the current state of the grid was the highest for the Lošinj substation and is equal to 1.128 p.u., but the voltage violations were recorded for Krk (1.125 p.u.) and Dunat (1.125 p.u.). High voltages appeared as a result of low system load during the winter months and the increased reactive power flows in 110 kV grid. Substations Krk and Dunat can be possibly automatically regulated in order to prevent voltage violations in most of the 20 kV grids. However, the voltages were at the higher limit, and some of the nodes violated the limit of 1.1 p.u. (Figure 18). Installation of the distributed energy resources in the medium voltage grid has resulted in voltage increase (the highest increase on Salatica bus of 3.54%, with the voltage value of 1.096 p.u.). The voltages on 110 kV buses also increased by 0.63% at the Dunat substation. When the utility-scale generation was connected as well, the voltage values continued to increase. The voltage at Salatica bus increased by 5.5% and was equal to 1.12 p.u. which is above the limit of 1.1 p.u. Although the medium voltage values remained within the allowed limits for most of the nodes, they were very high and close to the upper limit. It should also be stated that the high voltage values in the medium voltage grid represent the regulation issue at low voltage level as the distribution transformers 20/0.42 kV are required to regulate low voltage values, which may only impose an issue.

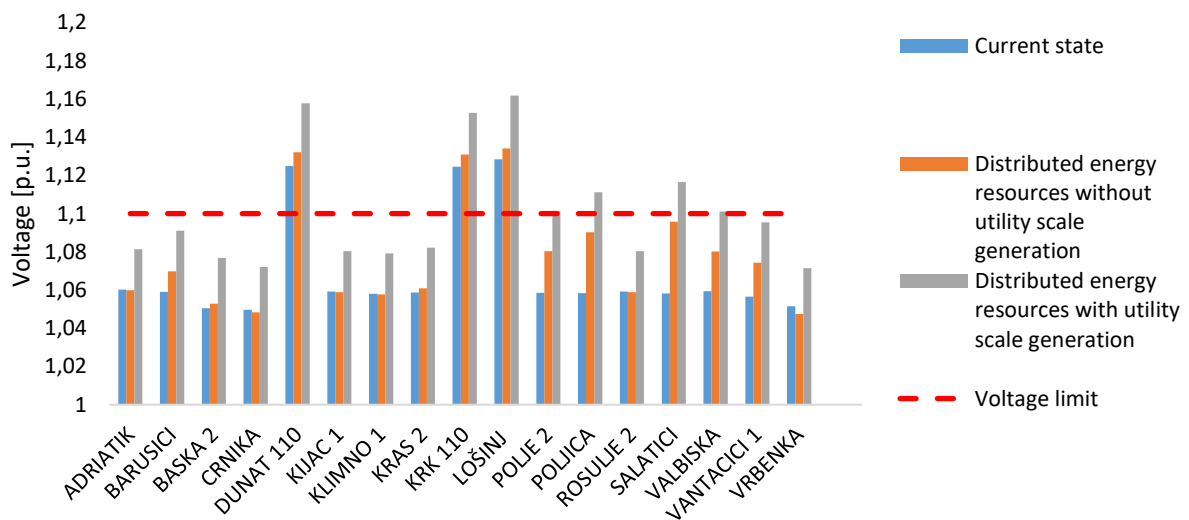


Figure 18. Voltage values for three scenarios at observed nodes for minimum demand case

Although voltage increase is evident for all cases during minimum load, the issue could be resolved by the installation of a 300 Mvar coil in high voltage substation Melina [59]. Installation of this coil would significantly reduce reactive power flows during periods of lower load, thus reducing voltage to its nominal limits. Such installation would also enable installation of proposed energy planning scenarios in this study as well.

4.5. Socio-economic analysis

Using the explained job creation method, the proposed energy scenarios would result in 2435 created job-years on the global scale as well as 45 permanent local jobs. Since these are high-profile green jobs, the proposed energy planning scenarios would have a significant positive impact on the economy that is currently heavily dependent on seasonal tourism. For example, when considering the Krk island population, this would mean that 2.3 permanent local jobs for 1000 residents would be created as a result of decarbonization of the island energy system. It should also be noted that these numbers are obtained without consideration of transport electrification and energy storage systems as there is still no unique approach on how to calculate created jobs as a result of the installation of these technologies.

5. Discussion

The main findings of this paper are related to both detailed spatial and temporal modeling of the capacity expansion problem of the island energy system. This research was enhanced by modeling both the transmission and distribution systems of the island and the validation of the capacity expansion modeling results via power flow analysis.

This study showed that the detailed spatial resolution is more important than the very detailed temporal resolution. However, one has to take into account that hourly resolution is already considered a detailed one for the capacity expansion problems. This study has further showed that a more detailed spatial representation has a significant impact on the calculation of the total system costs and optimal technology mix, it does not underestimate the import needs for electricity from the mainland grid, and it does not overestimate the potential for exporting the electricity to the mainland grid. Furthermore, a coarser spatial representation significantly underestimates the capacity needs for storage technologies that are needed in the energy system.

To the best of our knowledge, the most detailed research on temporal and spatial trade-offs so far has been carried out in [60]. The authors concluded that the most trade-offs between temporal and spatial resolution have yielded up to 15% of cost differences. Concerning the spatial resolution, the authors showed that the uniform buildout case resulted in a 10% reduction in cost compared to the site-by-site buildout case. Focusing on temporal resolution, the authors showed that the total cost is significantly lower with a coarser temporal resolution. In this paper, a fine (hourly) and a very fine (half-hourly) temporal resolution yielded a rather small cost difference, i.e., 0.4%. However, a difference between a detailed and coarse spatial representation yielded a difference in costs of 26.7%, which is significantly higher than that in [60].

Detailed transmission and distribution representation realistically captured possible congestions and resulted in a realistic representation of optimal capacities of distributed energy systems. With the application of the power flow analysis, it was possible to validate the results from the detailed spatiotemporal model. A detailed flow analysis has showed that the voltage levels would violate the allowed values in the scenario with the largest share of grid loading and the variable renewable energy generation (S3), which would result in a distribution system operator's ban on the development before the necessary actions would be taken into account. For this specific case study, an installation of 300 Mvar coils would solve these grid issues. This shows that the usual capacity expansion planning models with a high share of variable renewable energy generation, and a higher share of electric transport, are potentially underestimating grid constraints that cannot be simply evaluated just by modeling simple grid capacity constraints. The soft-linking of PLEXOS and TIMES model was presented in [61]. However, the PLEXOS model was run as a unit commitment and the power flow calculation was not performed. The study in this paper used a more detailed Calliope and power flow model with focus on the feasibility of the problem and the detailed spatiotemporal modeling which was not the case in [61]. An approach to soft-link capacity expansion models and more detailed operational once has been recently proposed for a specific sector, such as district heating [62]. However, this paper expands the same approach to the integrated energy system capacity expansion model, which takes into account a number of different energy sectors including heating and cooling system. This approach enables to analyze the interconnection between different energy vectors in detail which was not the case in [62]. This study [63] analyzed a similar case study with lower electricity consumption and suggested the energy planning system with 30 MW of installed PV and 22 MW of installed wind. The results from the power flow

analysis conducted in this paper indicated that a similar analysis should be constructed in the study [63] in order to assess the implementation possibilities for the proposed scenario.

This paper has also introduced simple job analysis potential modeling as part of the socio-economic analysis. This is the consequence of the rising resistance of the local communities toward installing large amounts of distributed energy systems in their vicinity [64]. If a successfully high local job creation potential can be achieved, it is expected that the local resistance toward the implementation of the renewable energy projects will subside. On top of the local job creation potential, an additional economic benefit could be gained if local residents would be involved as stakeholders in the investments in energy sector facilities. Such inclusion would have social benefits as well, as residents would become more involved in the energy sector, thus leading to the creation of an energy community. Example of such successful small-scale project is given in [65] where citizens were involved in a crowdfunding campaign for the financing of a rooftop solar power plant. In another initiative [66] on the island in Denmark, 650 local citizens became the owners of 6 wind turbines.

Although the methods were applied for a specific case, the methods applied in this case study did not have many case-specific site constraints, creating a higher potential to apply the developed methods to other case studies. It is expected that the developed methods are applicable to many different regions, especially islands connected to the main grid. Most especially, islands in the Mediterranean and tropical belt have a high potential for variable RES. However, the methods developed in this paper showed that islands' power grids could be severely impacted by the large renewable energy capacities and, thus, should follow a more detailed capacity expansion and power flow grid analysis. Moreover, the presented method is especially beneficial for the areas with weaker grids where the integration of RES may be more difficult. It is estimated that there are 11,000 inhabited islands in the world [67], providing many opportunities to test the developed method.

There are several limitations to this study. The goal of the capacity expansion model was on minimizing the total socio-economic costs of the system. Although those are the true costs imposed on the society, the business-economic case for specific investments can significantly vary depending on the risks, regulations, and laws that influence investment decisions. Moreover, an approach of the first-mover into a rapid increase in the share of variable renewable energy capacity was assumed in this paper. It was shown that the island can benefit also from exporting access to the energy generated (Appendix B). If the whole country would undertake a similar transition, there would be fewer opportunities to export excess electricity generated

for good prices, as well as fewer opportunities to use its batteries for price arbitrage. Furthermore, on-demand charging strategy for vehicles was adopted in all the scenarios. Although left outside of the scope of this study, considerations on smart charging and vehicle-to-grid options could significantly influence grid conditions. It is recommended that for future studies, the same methods developed in this paper be expanded to account for more detailed representation of the transport sector strategies.

Finally, this paper was developed fully adopting the open-access goals, using a fully open-source modeling tool, as well as publishing all the data, coding scripts, and results via a public site [42], documenting the steps needed to rerun the model. This will allow for better and faster exchange of ideas within the scientific community, resulting in more rapid improvements in the methods developed in this paper.

6. Conclusions

This paper presented a novel approach for energy planning of interconnected islands. As per our findings, it was determined that taking spatial distribution and the half-hourly distribution into account has resulted in more accurate results in comparison with the previous similar studies that have analyzed the energy systems on the islands. The main conclusions of the study were as follows:

- The results indicated that the total cost for the spatially distributed scenario was 26.7% higher than the scenario with the technologies aggregated in one location. Additionally, the results showed that 3.3 times higher battery capacity was required for the coarser scenario, which leads to the conclusion that detailed spatial modeling significantly improves the energy planning process.
- The comparison between the half-hourly and hourly time resolution modeling resulted in a 0.2% lower total cost for the half-hourly scenario and an 18.9% higher battery storage capacity for the half-hourly scenario. It is possible to conclude that the half-hourly time resolution also improves the energy planning process; however, the improvement is less expressed than for the case of spatial modeling application.
- The presented approach validated the results of the energy system analysis by conducting the power system analysis as the latter provided insights into the voltage and power flows of the analyzed island system. These results showed that several nodes had voltage values higher than 1.1 p.u. and did not satisfy the grid code regulations, which

indicates the need for the power system analysis of the energy planning scenarios for the assessment of the implementation possibilities.

Future research should be geared toward the inclusion of other sectors, such as the water sector, in the model in order to quantify the flexibility of the proposed energy planning scenarios. The use of the ICT for smart charging and the usage of batteries for ancillary service management are examples of the features that will need to be considered in the future models. The soft-linking between the energy planning model and the power flow analysis model will also be further investigated in order to improve the approximation of the grid constraints in the energy planning models. This would result in higher application potential of the energy planning scenarios.

Appendix A

Newton-Raphson method is an iterative method used for solving power flow problem in the electric power grid and it is used in this study. Appendix A provides insight into how the method is defined.

Let voltage and admittance matrix Y elements be defined as:

$$\bar{V}_i = V_i \angle \delta_i, \bar{V}_j = V_j \angle \delta_j \quad (\text{A.1})$$

$$\bar{Y}_{ij} = Y_{ij} \angle \theta_{ij} \quad (\text{A.2})$$

Where i and j represent the nodes in the system, V is the voltage amount at a node, δ is the voltage angle, Y is the value of admittance matrix element and θ is the admittance matrix element angle. Active (P) and reactive power (Q) at power system nodes can be expressed as:

$$P_i = \sum_{j=1}^n V_i Y_{ij} V_j \cos(\delta_i - \theta_{ij} - \delta_j) \quad (\text{A.3})$$

$$Q_i = \sum_{j=1}^n V_i Y_{ij} V_j \sin(\delta_i - \theta_{ij} - \delta_j) \quad (\text{A.4})$$

The fundamental matrix equation for the Newton-Raphson procedure can be expressed as (A.5):

$$\begin{bmatrix} \Delta P \\ \Delta Q \end{bmatrix} = \begin{bmatrix} J_1 & J_2 \\ J_3 & J_4 \end{bmatrix} \cdot \begin{bmatrix} \Delta \delta \\ \Delta V \end{bmatrix} \quad (\text{A.5})$$

Where J_1, \dots, J_4 represent sub-matrix of the Jacobian matrix and their elements are calculated by deriving equations (A.3) and (A.4). From these expressions it is possible to obtain full expression of (A.5) equation:

$$\begin{bmatrix} \Delta P_1 \\ \vdots \\ \Delta P_{n-1} \\ \Delta Q_1 \\ \vdots \\ \Delta Q_{n-1-g} \end{bmatrix} = \begin{bmatrix} \frac{\partial P_1}{\partial \delta_1} & \dots & \frac{\partial P_1}{\partial \delta_{n-1}} & \frac{\partial P_1}{\partial V_1} & \dots & \frac{\partial P_1}{\partial V_{n-1-g}} \\ \vdots & \ddots & \vdots & \vdots & \ddots & \vdots \\ \frac{\partial P_{n-1}}{\partial \delta_1} & \dots & \frac{\partial P_{n-1}}{\partial \delta_{n-1}} & \frac{\partial P_{n-1}}{\partial V_1} & \dots & \frac{\partial P_{n-1}}{\partial V_{n-1-g}} \\ \frac{\partial Q_1}{\partial \delta_1} & \dots & \frac{\partial Q_1}{\partial \delta_{n-1}} & \frac{\partial Q_1}{\partial V_1} & \dots & \frac{\partial Q_1}{\partial V_{n-1-g}} \\ \vdots & \ddots & \vdots & \vdots & \ddots & \vdots \\ \frac{\partial Q_{n-1-g}}{\partial \delta_1} & \dots & \frac{\partial Q_{n-1-g}}{\partial \delta_{n-1}} & \frac{\partial Q_{n-1-g}}{\partial V_1} & \dots & \frac{\partial Q_{n-1-g}}{\partial V_{n-1-g}} \end{bmatrix} \cdot \begin{bmatrix} \Delta \delta_1 \\ \vdots \\ \Delta \delta_{n-1} \\ \Delta V_1 \\ \vdots \\ \Delta V_{n-1-g} \end{bmatrix} \quad (A.6)$$

Where g is the number of generating nodes that can control voltage at the desired value. Therefore, in these nodes, it is not necessary to calculate voltage, but only reactive power according to (A.4) and check if the reactive power is within the allowed limits $Q \in [Q_{\min}, Q_{\max}]$. If the reactive power is not within these limits, the observed node becomes PQ node (where active and reactive power is known) with reactive power at its limit (Q_{\min} or Q_{\max}).

Since voltage amount change to active power change can be neglected and voltage angle change to reactive power change can be neglected as well, it is possible to apply some relaxations and assign zero value to elements of sub-matrix J_2 and J_3 . For this case, it is possible to separately observe equations of active power change to voltage angle change and reactive power change to voltage amount change. Equation (A.5) can then be written as (A.7):

$$\begin{bmatrix} \Delta P \\ \Delta Q \end{bmatrix} = \begin{bmatrix} J_1 & 0 \\ 0 & J_4 \end{bmatrix} \cdot \begin{bmatrix} \Delta \delta \\ \Delta V \end{bmatrix} \quad (A.5)$$

By solving the system of equations stated in (A.5) with iterative Newton-Raphson procedure it is possible to calculate voltages and reactive and active power flow in the electric power grid. The difference between power production and demand is covered from the slack node that is connected to an external grid. Simplified Newton-Raphson procedure is described in a diagram presented in Figure A.1.

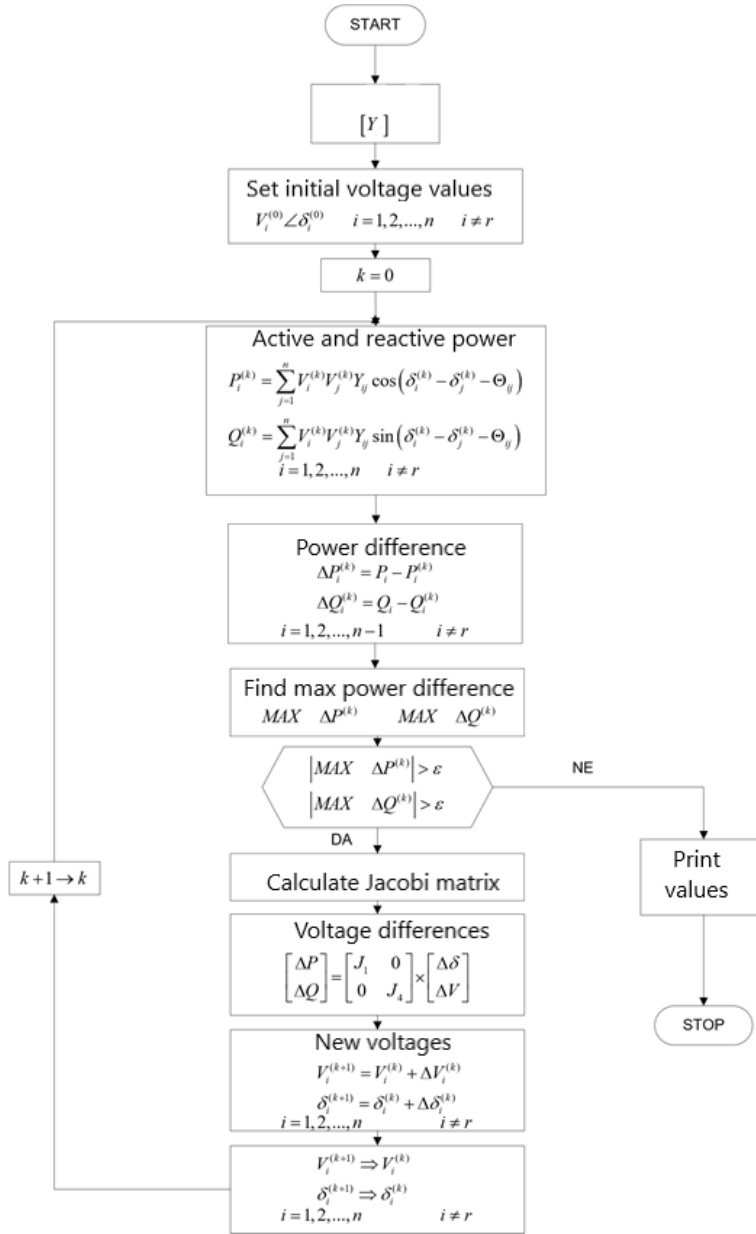


Figure A.1. Diagram for power flow calculation using Newton-Raphson

Appendix B

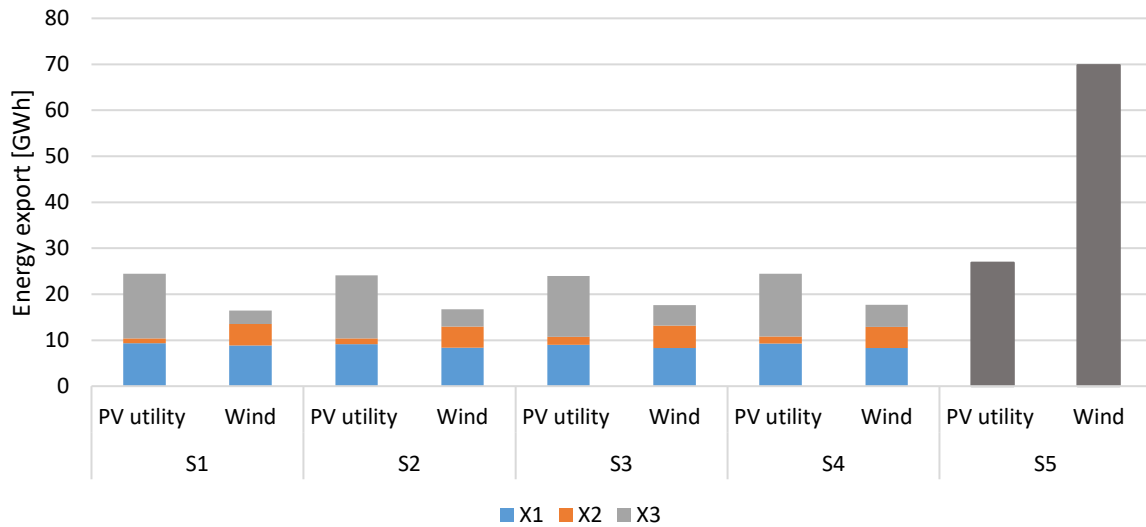


Figure B.1. Energy export values for analysed scenarios and different locations – the scenario S5 is presented with different colour as only one location is considered for S5

Acknowledgement

This work has been supported by the Young Researchers' Career Development Programme (DOK-01-2018) of Croatian Science Foundation which is financed by European Union from European Social Fund and Horizon 2020 project INSULAE - Maximizing the impact of innovative energy approaches in the EU islands (Grant number ID: 824433). Moreover, this project was also funded by CITIES project nr. DSF1305-00027B, funded by the Danish Innovationsfonden. The stated support is gratefully acknowledged. The link with detailed energy system model is provided at https://github.com/CROdominik/Krk_Calliope_energy_model.

References

- [1] Hauer ME, Fussell E, Mueller V, Burkett M, Call M, Abel K, et al. Sea-level rise and human migration. Nat Rev Earth Environ 2020;1. <https://doi.org/10.1038/s43017-019->

0002-9.

- [2] DAFNI. Smart Island Initiative. Netw Sustain Greek Islands 2017.
- [3] European Commission. Clean Energy for EU Islands launch. Eur Comm Energy News 2017.
- [4] Chandran CV, Basu M, Sunderland K, Pukhrem S, Catalão JPS. Application of demand response to improve voltage regulation with high DG penetration. *Electr Power Syst Res* 2020;189. <https://doi.org/10.1016/j.epsr.2020.106722>.
- [5] Segurado R, Krajačić G, Duić N, Alves L. Increasing the penetration of renewable energy resources in S. Vicente, Cape Verde. *Appl Energy* 2011. <https://doi.org/10.1016/j.apenergy.2010.07.005>.
- [6] Segurado R, Costa M, Duić N, Carvalho MG. Integrated analysis of energy and water supply in islands. Case study of S. Vicente, Cape Verde. *Energy* 2014. <https://doi.org/10.1016/j.energy.2015.02.013>.
- [7] Child M, Nordling A, Breyer C. Scenarios for a sustainable energy system in the Åland Islands in 2030. *Energy Convers Manag* 2017. <https://doi.org/10.1016/j.enconman.2017.01.039>.
- [8] Curto D, FRANZITTA V, Trapanese M, Cirrincione M. A Preliminary Energy Assessment to Improve the Energy Sustainability in the Small Islands of the Mediterranean Sea. *J Sustain Dev Energy, Water Environ Syst* 2020; <https://doi.org/10.13044/j.sdewes.d7.0314>.
- [9] Ocon JD, Bertheau P. Energy transition from diesel-based to solar photovoltaics-battery-diesel hybrid system-based island grids in the Philippines – Techno-economic potential and policy implication on missionary electrification. *J Sustain Dev Energy, Water Environ Syst* 2019;7. <https://doi.org/10.13044/j.sdewes.d6.0230>.
- [10] Meschede H, Child M, Breyer C. Assessment of sustainable energy system configuration for a small Canary island in 2030. *Energy Convers Manag* 2018. <https://doi.org/10.1016/j.enconman.2018.03.061>.
- [11] Curto D, Franzitta V, Viola A, Cirrincione M, Mohammadi A, Kumar A. A renewable energy mix to supply small islands. A comparative study applied to Balearic Islands and Fiji. *J Clean Prod* 2019;241. <https://doi.org/10.1016/j.jclepro.2019.118356>.

- [12] Holjevac N, Capuder T, Zhang N, Kuzle I, Kang C. Corrective receding horizon scheduling of flexible distributed multi-energy microgrids. *Appl Energy* 2017. <https://doi.org/10.1016/j.apenergy.2017.06.045>.
- [13] Gils HC, Simon S. Carbon neutral archipelago – 100% renewable energy supply for the Canary Islands. *Appl Energy* 2017. <https://doi.org/10.1016/j.apenergy.2016.12.023>.
- [14] Pfeifer A, Dobravec V, Pavlinek L, Krajačić G, Duić N. Integration of renewable energy and demand response technologies in interconnected energy systems. *Energy* 2018. <https://doi.org/10.1016/j.energy.2018.07.134>.
- [15] Fichera A, Pluchino A, Volpe R. From self-consumption to decentralized distribution among prosumers: A model including technological, operational and spatial issues. *Energy Convers Manag* 2020;217. <https://doi.org/10.1016/j.enconman.2020.112932>.
- [16] Fichera A, Frasca M, Palermo V, Volpe R. An optimization tool for the assessment of urban energy scenarios. *Energy* 2018;156. <https://doi.org/10.1016/j.energy.2018.05.114>.
- [17] Pavičević M, Mangipinto A, Nijs W, Lombardi F, Kavvadias K, Jiménez Navarro JP, et al. The potential of sector coupling in future European energy systems: Soft linking between the Dispa-SET and JRC-EU-TIMES models. *Appl Energy* 2020;267. <https://doi.org/10.1016/j.apenergy.2020.115100>.
- [18] Blanco H, Gómez Vilchez JJ, Nijs W, Thiel C, Faaij A. Soft-linking of a behavioral model for transport with energy system cost optimization applied to hydrogen in EU. *Renew Sustain Energy Rev* 2019;115. <https://doi.org/10.1016/j.rser.2019.109349>.
- [19] Dominkovic DF, Stark G, Hodge BM, Pedersen AS. Integrated energy planning with a high share of variable renewable energy sources for a Caribbean Island. *Energies* 2018. <https://doi.org/10.3390/en11092193>.
- [20] Milano F. Power system modelling and scripting. *Power Syst* 2010. <https://doi.org/10.1007/978-3-642-13669-6>.
- [21] Imen L, Djamel L, Hassiba S, Abdellah D, Selwa F. Optimal power flow study using conventional and neural networks methods. 2015 Int. Conf. Renew. Energy Res. Appl. ICRERA 2015, 2015. <https://doi.org/10.1109/ICRERA.2015.7418642>.
- [22] Weckesser T, Dominković DF, Blomgren EMV, Schledorn A, Madsen H. Renewable Energy Communities: Optimal sizing and distribution grid impact of photo-voltaics and

- p battery storage. Appl Energy 2021;301:117408.
-
- <https://doi.org/10.1016/J.APENERGY.2021.117408>
- .
- [23] Pfenninger S, Pickering B. Calliope: a multi-scale energy systems modelling framework. J Open Source Softw 2018;3. <https://doi.org/10.21105/joss.00825>.
- [24] Hilpert S, Kaldemeyer C, Krien U, Günther S, Wingenbach C, Plessmann G. The Open Energy Modelling Framework (oemof) - A new approach to facilitate open science in energy system modelling. Energy Strateg Rev 2018;22:16–25. <https://doi.org/10.1016/j.esr.2018.07.001>.
- [25] Pfenninger S. Calliope - case studies 2019. <https://www.callio.pe/model-gallery/> (accessed 23rd September 2019).
- [26] Dominković DF, Bačeković I, Pedersen AS, Krajačić G. The future of transportation in sustainable energy systems: Opportunities and barriers in a clean energy transition. Renew Sustain Energy Rev 2018. <https://doi.org/10.1016/j.rser.2017.06.117>.
- [27] Calliope. Calliope documentation: Mathematical formulation, https://calliope.readthedocs.io/en/stable/user/ref_formulation.html (accessed 19th August 2021) n.d.
- [28] Dominković DF, Bačeković I, Sveinbjörnsson D, Pedersen AS, Krajačić G. On the way towards smart energy supply in cities: The impact of interconnecting geographically distributed district heating grids on the energy system. Energy 2017;137:941–60. <https://doi.org/10.1016/j.energy.2017.02.162>.
- [29] Ferroukhi R, Khalid A, Lopez-Peña A, Renner M. “Renewable Energy and Jobs: Annual Review 2014.” Int Renew Energy Agency 2014.
- [30] Busarello, Cott, Partner Inc., ABB Utilities Gmbh. NEPLAN Users’ guide Electrical, 2015; Version 5.
- [31] Bauer N, Edenhofer O, Kypreos S. Linking energy system and macroeconomic growth models. Comput Manag Sci 2008;5. <https://doi.org/10.1007/s10287-007-0042-3>.
- [32] Republic of Croatia – Central Bureau of Statistics. Census of Population, Households and Dwellings 2011; (in Croatian)
- [33] Dominković DF, Dobravec V, Jiang Y, Nielsen PS, Krajačić G. Modelling smart energy

- systems in tropical regions. *Energy* 2018;155:592–609.
<https://doi.org/10.1016/j.energy.2018.05.007>.
- [34] <https://www.google.com/maps> n.d. (accessed 10th November 2020)
- [35] BEIS, UK Government, The Clean Growth Strategy: Leading the way to a low carbon future, 2017.
- [36] <https://www.amsterdam.nl/en/policy/sustainability/policy-phasing-out/> (accessed 7th February 2021) n.d.
- [37] rp5 weather archive. rp5.ru weather forecast. Online Arch 2020.
- [38] European Commission. EU Science Hub: pvgis. Online Database 2020.
- [39] Dominkovic DF, Mimica M. Krk (Croatia) Calliope Energy model - https://github.com/CROdominik/Krk_Calliope_energy_model. Github 2020. (accessed 19th August 2021)
- [40] Rosenthal P, Sišul Jurković S, Josipović S, Goreta D. Zero emission interdisciplinary strategy for sustainable development of Krk island. 2012.
- [41] Čotar A, Hunjak S, Jardas D. Sustainable energy action plan of Krk city. 2016.
- [42] Radulović D, Klanac A. Sustainable energy action plan of Vrbnik municipality. 2015. (in Croatian)
- [43] Variola D. Electric power system modeling of Krk island. University of Rijeka, 2017 (in Croatian)
- [44] Božić M, Kopic D, Mihoci F, Marold N, Gršetić J. Traffic count report for Republic of Croatia 2017. 2018. (in Croatian)
- [45] DHMZ. Krk solar irradiation measurements. 2016.
- [46] <http://rp5.ru/metar.php?metar=LDRI&lang=en> (accessed 9th September 2020) n.d.
- [47] Danish Energy Agency, Energinet. Technology data - Energy storage. 2018.
- [48] Danish Energy Agency, Energinet. Technology data - Energy plants for Electricity and District heating generation. 2016.
- [49] IRENA. Renewable Power Generation Costs in 2017. 2018.

- [50] Danish Energy Agency, Energinet. Technology data - Renewable fuels. 2017.
- [51] Danish Energy Agency, Energinet. Technology data for heating installations. 2016.
- [52] Danish Energy Agency. Technology datasheet - Industrial process heat and cc. 2020.
- [53] Danish Energy Agency, Energinet. Technology data - Energy transport. 2017.
- [54] www.cropex.hr (accessed 11th February 2020) n.d.
- [55] EMBER. EUA Price. Database 2020.
- [56] Lewis M. Carbon Clampdown - Closing the Gap to a Paris-compliant EU-ETS 2018;1–76.
- [57] Cerovečki T, Cvitanović M, Damjanović F, Ivković R, Majcen J, Širić I. Optimal technical connection of PV plant on distribution grid 2019. (in Croatian)
- [58] Dominković DF, Bačeković I, Ćosić B, Krajačić G, Pukšec T, Duić N, et al. Zero carbon energy system of South East Europe in 2050. *Appl Energy* 2016;184. <https://doi.org/10.1016/j.apenergy.2016.03.046>.
- [59] <https://www.sincrogrid.eu/en> (accessed 11th May 2020) n.d.
- [60] Frew BA, Jacobson MZ. Temporal and spatial tradeoffs in power system modeling with assumptions about storage: An application of the POWER model. *Energy* 2016;117:198–213. <https://doi.org/10.1016/j.energy.2016.10.074>.
- [61] Deane JP, Chiodi A, Gargiulo M, Ó Gallachóir BP. Soft-linking of a power systems model to an energy systems model. *Energy* 2012;42. <https://doi.org/10.1016/j.energy.2012.03.052>.
- [62] Dominković DF, Junker RG, Lindberg KB, Madsen H. Implementing flexibility into energy planning models: Soft-linking of a high-level energy planning model and a short-term operational model. *Appl Energy* 2020;260. <https://doi.org/10.1016/j.apenergy.2019.114292>.
- [63] Dorotić H, Doračić B, Dobravec V, Pukšec T, Krajačić G, Duić N. Integration of transport and energy sectors in island communities with 100% intermittent renewable energy sources. *Renew Sustain Energy Rev* 2019. <https://doi.org/10.1016/j.rser.2018.09.033>.

- [64] McKenna R, Ryberg DS, Staffell I, Hahmann AN, Schmidt J, Heinrichs H, et al. On the socio-technical potential for onshore wind in Europe: A response to Enevoldsen et al. (2019), *Energy Policy*, 132, 1092-1100. *Energy Policy* 2020;145:1–6. <https://doi.org/10.1016/j.enpol.2020.111693>.
- [65] <https://www.zez.coop/ulaganja/> (accessed 7th September 2020) n.d.
- [66] <https://www.euislands.eu/aero-finance> (accessed 24th November 2020) n.d.
- [67] Meschede H, Holzapfel P, Kadelbach F, Hesselbach J. Classification of global island regarding the opportunity of using RES. *Appl Energy* 2016. <https://doi.org/10.1016/j.apenergy.2016.05.018>.

PAPER 4

On the value and potential of demand response in the Smart island archipelago

Marko Mimica^{a}, Dominik Franjo Dominković^b, Tomislav Capuder^c, Goran Krajačić^a*

^aDepartment of Energy, Power Engineering and Ecology, Faculty of Mechanical Engineering and Naval Architecture, University of Zagreb, Ivana Lučića 5, 10002 Zagreb, Croatia

^bDepartment of Applied Mathematics and Computer Science, Technical University of Denmark, Matematiktorvet, 2800 Lyngby, Denmark

^cDepartment of Energy and Power Systems, Faculty of Electrical Engineering and Computing, University of Zagreb, Unska 3, 10000 Zagreb, Croatia

*Corresponding author: mmimica@fsb.hr

Abstract

Existing studies propose different demand response models and often test them on islands that represent test-beds for new technologies. However, proposed models are often simplified and integrated into energy system models that do not consider the existing limitations of the power grid. This study proposes a novel demand response model based on price differentials on the day-ahead electricity market. The model is implemented in the distribution system that considers all relevant grid constraints. The case study is conducted in an archipelago characterised by a medium-voltage distribution system connected to the mainland grid. The obtained results showed that the implementation of the proposed demand response model caused a 0.13 kV voltage deviation which did not cause voltage issues for the observed distribution system. The breakpoint incentive was achieved for an incentive value of 23% of the day-ahead market, and the demand response was not activated for higher values than the breakpoint incentive. The highest savings amounted to 258.7 € for the scenario with the highest flexibility allowed. The results implicate that implementing the demand response model in the grid would benefit all observed stakeholders in the system.

Keywords

Smart islands, Demand response, Renewable energy sources, energy system analysis, energy flexibility, Integrated energy system

1. Introduction

The objectives set by the European Union for a rapid increase of renewable energy sources (RES) pose new challenges for the existing power systems. Variable RES such as solar and wind power constantly change their power output that depends on the weather conditions. Such changes create the potential for introducing new technologies such as energy storage and demand response. These technologies can tackle the variability issue and assure the highest possibility for RES integration with generated benefit for the consumers in the energy system. Testing mentioned technologies is increasingly conducted on geographical islands through a concept known as “living labs” based on the idea that successful integration of demand response on the islands can effectively be implemented on the mainland as well [1].

Successful cross-system integration represents a necessity in order to achieve local smart energy systems [2]. In this context, local action is necessary in order to successfully transit to decarbonised energy systems, as stated in [3]. Several studies presented smart energy system concepts on islands. For example, the authors in [4] analysed the energy transition possibilities of Madeira island by investigating the market flexibility requirements with the conclusion that the inclusion of customers in the market is necessary for a successful energy transition. Another example is a generation expansion planning for Santiago Island, Cape Verde [5], where the importance of sector integration for a 100% renewable island was also highlighted. Hybrid solutions consisted of hydrogen, batteries, and RES also present a solution for the islanded microgrids [6]. Battery storage systems can represent another flexibility source and can provide ancillary services by applying concepts such as in [7].

Recent studies focus their research on demand-side management strategies for two main reasons. Firstly, the development of the electric energy markets is starting to enable broader possibilities for demand-side management. Secondly, increased efforts are being invested by the EU to enable customer participation in the electricity market [8]. Thus, as the DR is

becoming more critical in the field of energy research, authors debate about the benefits and the drawbacks of different DR implementations.

A review of the DR model is provided in [9]. The author has explained different DR models with emphasis on different incentive and pricing models for its optimal integration. In order to implement the DR, it is necessary to integrate smart technology such as smart meters, sensors and control units in the grid and at the DR providers. Such technology is available today, and the study [10] presents an overview of different DR possibilities and devices necessary for its implementation. Blockchain platforms that enable DR service were also recently developed [11].

The DR potential assessment is provided in [12], where the author concluded that the hourly average for demand reduction in Europe amounts to 93 GW. In comparison, the average for demand retrieval (an increase of the demand) has amounted to 247 GW. These studies [10] and [12] do not consider any specific mathematical model of the DR implementation. Residential customers' acceptance of the DR technology is one of the main necessities for implementing the DR programs, as highlighted in [13]. Authors found that, on average, a single customer would be willing to invest 150 € in devices that would enable the DR.

Authors in [14] applied the DR at a Dutch case study. They concluded that the DR cuts electricity system costs between 2.4 and 6.3 billion euros, where the electricity market cost, as well as the grid development costs, were considered. However, the grid constraints were modelled only as maximum active power allowed, and the DR model did not impose the constraints that consider the DR feedback effect. Priority banking incentive mechanism was presented in [15], and it showed that savings of 1.57\$ for a particular load during one day are possible; however, the study did not conduct sensitivity analysis of more flexibility levels as well as technical impacts on the observed grid.

A detailed review of battery storage and DR solutions was provided in a recent study [16]. The authors stated several demand-side management implementation possibilities with an emphasis on the integration of electricity, water and transport sector as well as power-to-heat technologies. The authors in particular mentioned the cooling sector as a flexibility provider for the islands. Moreover, the locations with high hydropower resource can use district heating systems as a flexibility provider [17]. The heat storage models presented in [18] can also increase the flexibility if they would be connected to the grid and DR programme.

Dorotić et al. [19] presented a possibility for providing the DR by using smart charging of EV and suggested that it is possible to reduce the energy import from 11 GWh to 6.5 GWh on the island of Korčula. However, this study used the simulation approach and did not consider the conditions in the existing distribution grid. Another study was conducted on Dongfushan Island [20], where authors showed that an 81.98\$ fuel saving is possible when the DR is implemented, but the study does not analyse the DR impact on technical conditions in the grid, nor it defines different levels of flexibility.

A multi-energy microgrid with flexible demand was modelled in [21], where authors underlined that the curtailment of variable RES is 3.25% lower when different sectors are coupled together with flexible demand. The study [21], however, does not consider compensation for the customers that provide flexible demand, nor it considers distribution system grid. Meschede, H. et al. [22] analysed the case for Canary islands and introduced a self-sufficiency indicator that increases by 1.8% when the DR is introduced; however, this study also did not model technical grid characteristics. The parameters that are used for distribution system modelling are voltage amount and angle, current, resistance, reactance, susceptance, and bus type, together with all limitation parameters. Another study conducted on islands used the domestic hot water for providing the DR in the [23], and authors showed that total dispatch cost reduces from 0% to 0.8% when DR is used in comparison to a scenario without the DR. However, the DR modelling in [23] is limited to domestic hot water and the economic dispatch model that neglects the distribution system constraints.

A novel soft-linking approach of the models where flexibility was represented based on temperature values in the district heating system was presented in [24] with the conclusion that it is possible to achieve a 5.4% savings in the district heating system for the best-case scenario, but the study focuses only on district heating system. A similar study [25] with a non-linear DR model was conducted on a case study where water towers are used for supplying the three cities with enough water and with high enough temperature with the conclusion that it is possible to reduce the operation cost of towers for 4.1% when the DR model is introduced. Authors of [26] presented a cost-benefit analysis of applying the DR in the energy system; however, without consideration of the power grid parameters and concluded that the operation cost reduces by 1.17% for the scenario with the DR in comparison to the scenario without DR. Zhang et al. [27] present a DR model considering elasticity of the market and states that, for real-time pricing scheme, total revenue during 24h from the DR is 88 € for observed region although this study does not consider technical characteristics of the grid.

In [28], customer and utility benefit functions were introduced for the DR with the conclusion that possible revenue can amount to 371\$ for three customers for 24 hours when the DR is included in the system operation. However, the study does not define the DR retrieval but only the load shedding. The authors in [29] presented the energy system model of several interconnected islands with an integrated DR model in the form of V2G and showed that the DR could enable the integration of variable RES up to 85.6% of the primary energy supply. However, the result of this study was based on the simulation model, not an optimisation one. Overview of the simulation strategies for enabling the DR is provided in [30] with the remark that the structure of the presented models could be improved with properties of the optimisation models. The main advantage of the optimisation model over simulation one is that it finds the best possible values of decision variables for minimising or maximising the given objective function. The simulation model observes specific case and does not minimise or maximise the objective function.

The study [31] emphasises the need for a more detailed representation of the DR and the energy system models, as many current studies include only simplistic models. Most of the DR is provided by the users connected to the low-voltage (LV) and medium-voltage (MV) distribution network. Thus, it is necessary to include distribution system elements and limitations in order to observe the complete influence of the DR model. An example of such representation of a distribution system is provided in [32]. The application of non-linear programming (NLP) is one of the possibilities for solving DR optimisation problems where every node in the electricity grid has the option of controlling its load, as stated in [33]. However, the authors do not emphasise the limitations of such an approach. The main limitation is that such a model would be computationally complex for large systems and would not guarantee the global optimum. Ghasemi, A. et al. [34] concluded that PHP has better performance than the DR as the economic performance index is higher by 1.6% for the PHP. However, the study used a simple DR model and did not include the DR cost in the objective function. Ajoulabadi et al. [35] presented an optimisation framework that includes the DR program for four cases of user participation and achieves the reduction of operation cost by 1.2% for the case when all customers are part of the DR program. The study, however, does not include the cost of DR in the objective function that minimises the total operation cost. Implementation of the DR in [36] resulted in the system operating cost reduction of 62\$, but the study introduces a simplified DR model, without the DR retrieval constraints, that is based only on estimated DR potential.

Analysed studies mostly used simplified DR models that consider only load curtailment without energy retrieval, or the models did not impose constraints between the curtailed and retrieved energy. This assumption can be valid if analysed loads are lights, for example. However, the biggest DR potential lies with the heating and cooling devices, and their inclusion in DR programs results in higher energy consumption. This study introduces a novel DR model formulation based on price differential on the day-ahead electricity market with modelled constraints for the DR retrieval that assures energy preservation in the system. Secondly, most studies use simulations or simple optimisation formulations that neglect the realistic constraints that exist in the grid and limitations that are imposed by the DSO. These approaches cannot observe the technical impact that is provoked by the DR event. The present study includes the proposed DR model in the energy system with all relevant grid parameters, as well as the limitations set by the DSO. Thus, the proposed approach allows the research of technical parameters as well. To the best of the authors' knowledge, there is no reference to such a DR model implemented in the distribution system grid.

The hypothesis of this paper is that, by using the presented mathematical model of the DR incorporated in the small radial distribution system with modelled all steady-state grid parameters, it is possible to generate revenue for nodal stakeholders and reduce operating costs as well as assess the impact of the DR on the technical parameters of the power system. The contributions of this paper are listed below:

- A novel mathematical model of DR that includes customers in the day-ahead electricity market and aims at operation cost reduction as well as revenue generation for customers
- Energy system optimisation model that considers technical grid parameters and includes the proposed DR model. The model reflects the technical changes in the system operation and ensures that the limitations set by the DSO are not violated.
- Sensitivity analysis of the DR model when the model is placed in the uncertain market conditions for different flexibility levels and different DR incentive values
- The impact assessment of different flexibility levels and incentive values on the energy system operation parameters
- The study contributes to the overall investigation and unlocking of the power system flexibility by proposing a novel DR model

The rest of the paper is organised as follows: the second section presents a method with the DR model and the energy system in which it is included. The third section describes the case study, after which follows results and discussion. The conclusion is provided in the fifth section.

2. Methods and materials

This paper presents a novel DR mathematical model integrated into an energy system model that is described with grid parameters where constraints that are imposed by the DSO are implemented. The DR model is designed in such a way that it uses the price differential between the two consecutive hours on the electricity day-ahead market as a basis for determining the quantity of provided DR. The model aims at exploiting the price changes on the electricity market in order to minimise operational cost and generate revenue for the consumers. It is assumed that the DR model is used within the small radial distribution system. As stated in the literature review, many studies do not analyse grid conditions when new technology is implemented, which can significantly limit the model.

Since the DR model was implemented in the radial distribution system, there is a possibility for voltage deviation because of a change in the power flows. Thus, the new voltage values, that will occur as a result of a DR, should be calculated so that it can be determined whether there was a voltage violation or not. For example, if there is a high VRES production and high market prices at the same time, the algorithm may optimize the operation so that it shifts demand from those periods which would cause additional voltage increase. This is particularly important for the radial distribution systems that already have significant voltage deviations as a result of a high VRES share.

The study assumes that the distribution system operator (DSO) is responsible for system operation. The DSO can control the demand at each node to the extent that model permits. The DR providers are consumers that have the possibility and technical conditions for providing the DR, while the DR users are all consumers in the archipelago.

2.1. System modelling

The energy system is defined as a feasible non-linear optimisation problem with objective function f . The objective function is represented with equation (1):

$$\min f \triangleq \min[\sum_{t \in \Omega_T} (\lambda_t \cdot E_{slack,t} + \mu \cdot \varphi_{i,t}^- \cdot L_{i,t}^P + CPV \cdot E_{CPV,t})], \quad \forall i \in \Omega_N \quad (1)$$

Where μ represents the incentive that is paid by the operator to the DR provider. DR providers are households with their appliances as well as other facilities such as desalination plants which are often present on the islands. The incentive for providing the DR can be expressed as a function or constant value. For implementation reasons, the most straightforward possibility would be to choose a constant value or simple linear function for the representation of the DR incentive.

However, more complex functions can also be modelled in order to determine the incentive. $\varphi_{i,t}^-$ is the DR function (16) and $L_{i,t}^P$ is the load at bus i at time t . CPV is the penalty for the curtailed PV energy and $E_{CPV,t}$ is the actual curtailed energy from PV. λ_t represents the current price of electric energy on the day-ahead market. $E_{slack,t}$ is the amount of electricity that is imported or exported to or from the observed grid through the point of common coupling with the remainder of the system.

The constraints for this optimisation problem are based on real limitations imposed by the distribution grid and the DR providers. They form the NLP model which is solved in GAMS with a CONOPT solver suited for non-linear problems, especially small-scale problems. Active power flow $P_{ij,t}$ between busses i and j are given with equation (2). Reactive power flow $Q_{ij,t}$ between busses i and j is given with equation (3). Apparent power flow $S_{ij,t}$ is defined according to equation (4). It is worth noting that the power transmitted from bus $i \in \Omega_N$ through the line $ij \in \Omega_\epsilon$ will not equal the power transmitted to the bus $j \in \Omega_N$ which corresponds with existing physical conditions in the grid. That is to say, that $P_{ij,t} \neq -P_{ji,t}$ and $Q_{ij,t} \neq -Q_{ji,t}$ for $\forall t \in \Omega_T$, $\forall i \in \Omega_N$ and $\forall ij \in \Omega_\epsilon$.

Apparent power flow is limited with upper and lower values, presented with equation (5) and is a characteristic of the maximum allowable current for a specific line or cable. Current $I_{ij,t}$ is defined with voltages between busses i and j and the impedance of the line connecting these two busses (6). Active and reactive power balance must be assured in every timestep t . These constraints are expressed with equations (7) and (8). It is worth noting that the DR model is

considered in the equations for active and reactive power and has an influence on both parameters. The voltage on a particular node is denoted with $V_{i,t}$ for voltage level and $\delta_{i,t}$ for voltage angle, while the line parameters are given with the impedance parameters Z_{ij} , θ_{ij} and susceptance b . Voltage $V_{i,t}$ and voltage angle $\delta_{i,t}$ are limited with their upper and lower values (9) and (10). Equations (2) – (10) are valid for $\forall t \in \Omega_T$, $\forall i \in \Omega_N$ and $\forall ij \in \Omega_\varepsilon$.

$$P_{ij,t} = \frac{V_{i,t}^2}{Z_{ij}} \cos(\theta_{ij}) - \frac{V_{i,t}V_{j,t}}{Z_{ij}} \cos(\delta_{i,t} - \delta_{j,t} + \theta_{ij}) \quad (2)$$

$$Q_{ij,t} = \frac{V_{i,t}^2}{Z_{ij}} \sin(\theta_{ij}) - \frac{V_{i,t}V_{j,t}}{Z_{ij}} \sin(\delta_{i,t} - \delta_{j,t} + \theta_{ij}) - \frac{bV_{i,t}^2}{2} \quad (3)$$

$$S_{ij,t} = (V_{i,t} \angle \delta_{i,t}) I_{ij,t}^* \quad (4)$$

$$-S_{ij,max} < S_{ij,t} < S_{ij,max} \quad (5)$$

$$I_{ij,t} = \frac{V_{i,t} \angle \delta_{i,t} - V_{j,t} \angle \delta_{j,t}}{Z_{ij} \angle \theta_{ij}} + \frac{bV_{i,t}}{2} \angle \left(\delta_{i,t} + \frac{\pi}{2} \right) \quad (6)$$

$$P_{slack,t} + P_{i,t}^{PV} + P_{i,t}^d + P_{i,t}^c - (1 + \varphi_t^+ - \varphi_t^-) L_{i,t}^P = \sum_{j \in \Omega_i^l} P_{ij,t} \quad (7)$$

$$Q_{slack,t} + Q_{i,t}^{PV} + Q_{i,t}^d + Q_{i,t}^c - (1 + \varphi_t^+ - \varphi_t^-) L_{i,t}^Q = \sum_{j \in \Omega_i^l} Q_{ij,t} \quad (8)$$

$$V_{min} \leq V_{i,t} \leq V_{max} \quad (9)$$

$$\delta_{min} \leq \delta_{i,t} \leq \delta_{max} \quad (10)$$

A constraint for the PV plant is provided with equation (9) for $\forall t \in \Omega_T$ and $\forall i \in \Omega_{PV}$. The sum of the PV production and the curtailed production from PV should be equal to the total possible PV production $\Lambda_{i,t}^{PV}$. It is assumed that the PV plant operates with $\cos\phi = 1$.

$$P_{i,t}^{PV} + P_{i,t}^{CPV} = \Lambda_{i,t}^{PV} \quad (11)$$

The electrical energy storage system (ESS) is provided with a standard model consisted of SOC equation and limits as well as maximum charging and discharging possibility in a given period. Similarly to the PV plant, it is assumed that the ESS can only discharge and charge active power. The battery model is given with equations (12) – (15) for $\forall t \in \Omega_T$ and $\forall i \in \Omega_{ESS}$.

$$SOC_{i,t} = SOC_{i,t-1} + (P_{i,t}^c \cdot \eta_c - \frac{P_{i,t}^d}{\eta_d}) \cdot \Delta t \quad (12)$$

$$SOC_i^{min} \leq SOC_{i,t} \leq SOC_i^{max} \quad (13)$$

$$P_{i,t}^c \cdot \Delta t \leq \beta_i \cdot SOC_i^{max}, \beta_i \in [0,1] \quad (14)$$

$$P_{i,t}^d \cdot \Delta t \leq \beta_i \cdot SOC_i^{min}, \beta_i \in [0,1] \quad (15)$$

2.2. Demand response model

The DR model is based on the price difference between two consecutive hours. The higher the differential of these two values, the higher value of the DR is achieved. This is implemented by defining function $\varphi(\lambda_t, \lambda_{t-1})$. Mathematical expression for the defined function is given with (16) – (18) for $\forall t \in \Omega_T$ and $\forall i \in \Omega_{DR}$.

$$\varphi_{i,t}^- \begin{cases} \leq \tanh \frac{2(\lambda_t - \lambda_{t-1})}{k(\lambda_t + \lambda_{t-1})}, \lambda_t - \lambda_{t-1} > 0 \\ = 0, \text{ else} \end{cases} \quad (16)$$

$$\varphi_{i,t}^+ \begin{cases} \leq \tanh \frac{2(\lambda_{t-1} - \lambda_t)}{k(\lambda_t + \lambda_{t-1})}, \lambda_t - \lambda_{t-1} \leq 0 \\ = 0, \text{ else} \end{cases} \quad (17)$$

$$\sum_t^T \varphi_{i,t}^+ \cdot L_{i,t}^P = \vartheta \sum_t^T \varphi_{i,t}^- \cdot L_{i,t}^P \quad (18)$$

where $k \in [0,1]$ is a coefficient that enables more or less flexibility. The value of factor k is dependent on the number of loads that are used for providing the DR in the distribution grid. More flexible heating or cooling devices, desalination plants, etc. would result in a higher possibility for providing the DR. An exact method for defining a single value of factor k is out of the scope of this paper; however, a detailed sensitivity analysis of the impact its value as will be further elaborated in the Results and discussion section.

$\varphi_{i,t}^- \in [0,1]$ represents the DR coefficient at each node in a particular time, while the $\varphi_{i,t}^+ \in [0,1]$ represents the DR retrieval coefficient. Multiplication of coefficients with the load at each node in the given time results with the exact DR and DR retrieval values. Factor ϑ is used as a representation of the efficiency of the DR. It depends on the types of loads that are present in the distribution grid. For example, the value for heating or cooling devices can be over 1, while for the lights, this value is 0. The zero value of ϑ would also result in a one-way DR or only load shedding.

The DR model aims at reflecting the differential between two consecutive day-ahead market prices. If price differential was divided only with the current market price, the model would be asymmetrical as the values for $\varphi_{i,t}^-$ and $\varphi_{i,t}^+$ would be different for the same price difference. Thus, the price difference is divided with their summation in order to achieve symmetry between $\varphi_{i,t}^-$ and $\varphi_{i,t}^+$ values.

As factor k is introduced, for small values of k there is a possibility that the value of $\varphi_{i,t}^-$ and $\varphi_{i,t}^+$ exceeds available demand. Thus, there is a need for limitation of $\varphi_{i,t}^-$ and $\varphi_{i,t}^+$ values which is one of the reasons why the hyperbolic tangent is used.

The first suitable characteristic of this function is that it is continuous and symmetric within its domain, meaning that $\tanh(-x) = -\tanh(x)$. Such characteristic allows DR in two directions, increasing and decreasing power in times when required. Another characteristic of this function is $\lim_{x \rightarrow -\infty} (\tanh(x)) = -1$ and $\lim_{x \rightarrow \infty} (\tanh(x)) = 1$ meaning that hyperbolic tangent limits values to a range or $\tanh(x): \mathbb{R} \rightarrow [-1,1]$. Because of this characteristic, high positive or negative values of the price differential value do not result in high DR or DR retrieval that may cause financial, technical or social repercussions that may occur as it is assumed that the DR is mandatory for all observed nodes i . For example, too high a request for an increase in the power issued as a result of a significant negative differential of price may cause grid issues, and result in high costs for the operator or cause overloads of devices and utilities that provide the DR service. By limiting their values with $\tanh(x)$ function, this is avoided.

On the other hand, as Taylor series of a hyperbolic tangent is expressed with $\tanh(x) \approx x - \frac{x^3}{3} + \frac{2x^5}{15} - \dots$, the values of the small price differentials are linearised and the value of the functions $\varphi_{i,t}^-$ and $\varphi_{i,t}^+$ is proportional to the price differential. This means that, for small price changes, it is possible to write $\tanh\left[\frac{2(\lambda_t - \lambda_{t-1})}{k(\lambda_t + \lambda_{t-1})}\right] \approx \left[\frac{2(\lambda_t - \lambda_{t-1})}{k(\lambda_t + \lambda_{t-1})}\right]$. The DR model presented in this paper is a price-taker model, meaning that it does not participate in price forming on the market.

Following decision variables (X), parameters (P) and sets (S) are defined:

$$X = \left\{ \begin{array}{l} E_{slack,t}, \varphi_{i,t}^-, \varphi_{i,t}^+, E_{i,t}^{CPV}, \\ Q_{slack,t}, V_{i,t}, \delta_{i,t}, I_{ij,t}, P_{i,t}^d, P_{i,t}^c, SOC_{i,t}, \\ P_{i,t}^{PV}, Q_{i,t}^{PV}, Q_{i,t}^c, Q_{i,t}^d \end{array} \right\}$$

$$P = \left\{ \begin{array}{l} \mu, CPV, SOC_i^{min/max}, Z_{ij}, \\ \theta_{ij}, \eta_c, \eta_d, L_{i,t}^P, L_{i,t}^Q, \\ \lambda_t, \beta_i, \Lambda_i^{PV}, S_{ij,max} \end{array} \right\}$$

$$S = \{\Omega_T, \Omega_N, \Omega_\varepsilon, \Omega_{ESS}, \Omega_{DR}, \Omega_{PV}\}$$

Prices on the day-ahead electricity market are uncertain for many reasons such as variability of the demand, PV and wind power plant installations, price-makers competitions, grid losses etc. Since the proposed DR model is dependent on market prices, this study investigated the model operation under different market scenarios. Operation cost over time, DR model operation, voltage vector and ESS operation with DR model are parameters examined under the different price scenarios. The complete overview of the proposed method is provided in Figure 1.

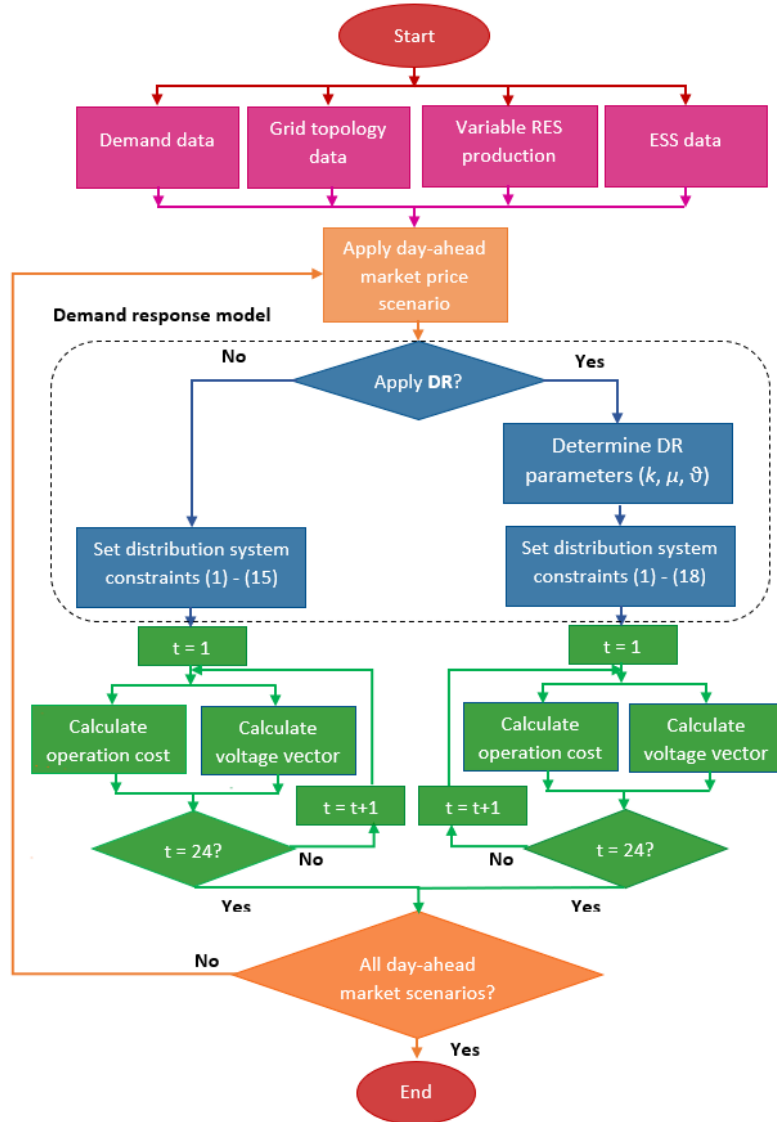


Figure 1. The proposed method for implementation of the DR model

3. Case study

3.1. Analysed scenarios

The proposed method is applied to the case of the Kvarner archipelago in Croatia. The considered islands are Lošinj, Cres with three locations Osor, Hrasta and PV plant Orlec, Male Srkane, Vele Srkane, Susak and Unije. The complete topology of the system with the names of the bus is presented in Figure 2. The number of the bus is represented by the number by the name of the bus. A geographical overview of the archipelago is provided in Figure 3.

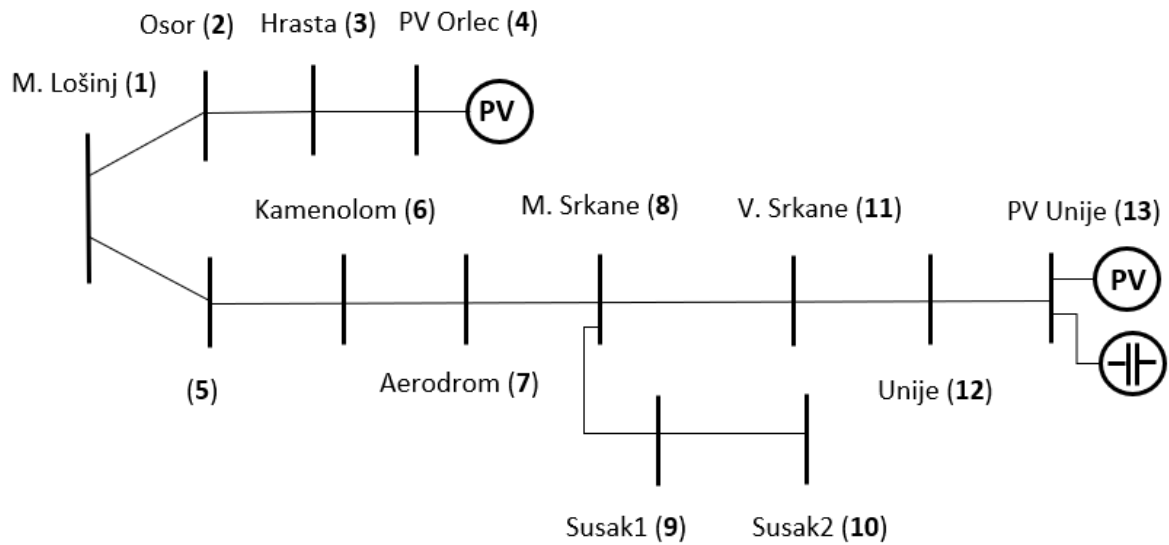


Figure 2. The topology of the power system of the Kvarner archipelago

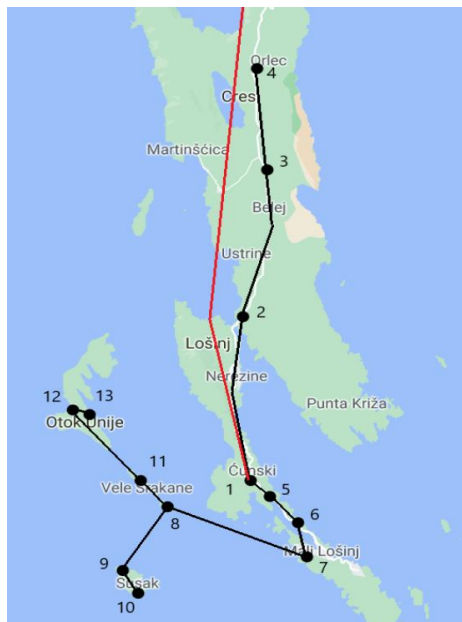


Figure 3. A geographical overview of the analysed archipelago - red line represents a 110 kV line to the mainland grid

The data for grid modelling is provided in [37]. Substation (1) was modelled as a slack bus connecting the archipelago with the rest of the grid. This is possible because this substation is equipped with an automatic transformer 110/35/10 kV and has a 110 kV connection to the Melina substation 400/220/110 kV on the mainland (over the Krk substation). Hydropower plants Senj (216 MW) and Vinodol (90 MW) are connected to Melina 220 kV buses and are able to provide the required spinning reserve and regulation necessary to maintain the grid stability. However, they cannot ensure that voltage in the radial distribution grid is within the allowed limits; thus, voltage values were calculated in this study.

Data about the active and reactive load is available from measurements at the main substation for every hour on the summer day when the maximum load is present. Demand on smaller substations is obtained by scaling measured load values from the main substation. Demand values are given in Figure 4 as a ratio of the load at time t and the maximum load. Prices of electric energy are obtained from CROPEX day-ahead market for the day of maximum load.

Values of all parameters are given in Table 1. This study considered only PV as a VRES according to the existing plans and projects for the observed case study. As mentioned in the method section, incentive μ can be represented as a function or a constant value. This study analysed several possibilities for incentive value. Such implementation would be simple enough for realisation once the EU directive [8], which sets the objective that every retail buyer has access to the hourly prices, is implemented. Energy efficiency is specific for a given case study, and it depends on types of the loads that are present in the observed system. Detailed mapping of different load types was not part of this study, but there are no special industries or larger facilities in the archipelago. However, it can be assumed that there is a larger amount of heating and cooling devices due to warmer climate conditions. Thus it was assumed that the factor ϑ is equal to 1.1. ESS parameters values are specific for the examined case study as foreseen in [38].

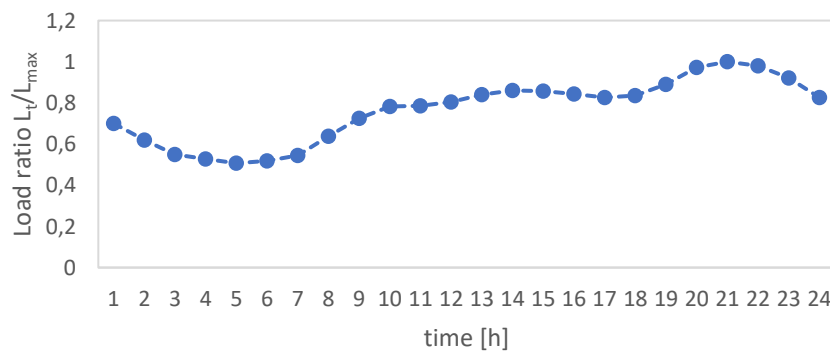


Figure 4. Load at every hour of a summer day

Table 1. The values of parameters used in the model

Name	Value	Name	Value
μ [€/MWh]	$0.1\lambda_t$	η_c	0.95
CPV [€/MWh]	150	η_d	0.9
β	0.25	ϑ	1.1
SOC_i^{min} [€/MWh]	0.16	SOC_i^{max} [€/MWh]	1.44
P_{max} [MW]	20.77		

It is considered that the PV and ESS operate with $\cos \varphi = 1$, thus only active power from PV and ESS is considered while the reactive power values are equal to zero. The maximum PV output on Unije is equal to 1 MW, and on Orlec, it is equal to 4.14. The ESS capacity is equal to 1.6 MWh. In this study, several scenarios were considered:

- 1) *Scenario A*: This scenario represents the base case with the PV plants and without the possibility for DR and ESS. This scenario is subject to load flow constraints and is used as a benchmark case. It also represents a simpler problem as the objective function is to minimise the cost of system operation without consideration of DR. The decision variables are $X_A = \{E_{slack,t}, E_{i,t}^{CPV}, Q_{slack,t}, V_{i,t}, \delta_{i,t}, I_{ij,t}, P_{i,t}^{PV}\}$
- 2) *Scenario B*: This scenario considers the same conditions as in scenario A but with added ESS. Scenario B was used for the assessment of ESS on the power system and also for comparison purposes to DR. The decision variables considered for this scenario are $X_B = X_A \cup \{P_{i,t}^d, P_{i,t}^c, SOC_{i,t}\}$.
- 3) *Scenario C*: Scenario C considers the base scenario with the possibility for DR in the archipelago. Comparison of scenario C to scenario B was conducted in order to assess the benefits of both technologies. The decision variables for this scenario are $X_C = X_A \cup \{\varphi_{i,t}^+, \varphi_{i,t}^-\}$
- 4) *Scenario D*: Final scenario considered the inclusion of both ESS and DR. This scenario was used to assess the joint impact of both technologies and considers all presented decision variables $X_D = X_B \cup X_C$.

3.2. PV share influence

Within this case study, the impact of different PV share will be assessed in order to observe the overall system operation when the different level of variable production is present. In order to conduct this analysis, buses 3 and 7 were also modelled as the buses with the PV plant. This approach is taken in order to avoid high PV curtailment values that would occur if all the production would be placed in buses 4 and 13. Operation cost, curtailed PV production values, voltage, ESS and DR operation were observed under different flexibility and PV share values.

3.3. Market price modelling

In order to model prices on the electricity market, data from the Croatian power market [39] was used. The probabilistic behaviour of electricity market prices was modelled by using the normal probability distribution function (PDF) given with equation (17). The objective of this approach is to assess the DR model behaviour when placed in different market price scenarios as the level of future market prices is highly uncertain.

$$PDF(x) = \frac{1}{\sigma\sqrt{2\pi}} e^{\left(-\frac{(x-\bar{z})^2}{2\sigma^2}\right)} \quad (17)$$

In equation (17), σ represents the standard deviation and \bar{z} mean value of observed data. Similarly, as in referenced studies, a discretised normal distribution was used by considering five scenarios. This simplification was used in order to reduce computation time that can be extensive when a continuous normal distribution is used. With the proposed approach, all scenario values fall into the 95.44% probability range or two-sigma probability. Prices were modelled according to price values during peak demand that occurs in July and August.

4. Results and discussion

4.1. Scenarios overview

1) *Scenario A*: Total operating cost amounted to 18,665.2 € (mean), with the total amount of imported electricity equal to 333.95 MWh (mean). The total operating cost for this scenario varies from 14,081.91 € (-2σ) to 23,247.56 € (2σ).

2) *Scenario B*: This scenario assumes that the ESS is connected to a bus 13 without the

possibility for the DR in the system and the operating costs for this scenario are 18,657.2 € (mean) with the total imported electricity equal to 334.13 MWh (mean). Figure 5 shows the operation of the ESS from which it can be seen that the ESS is active during the night hours when it is charging and in the evening when it is discharging.

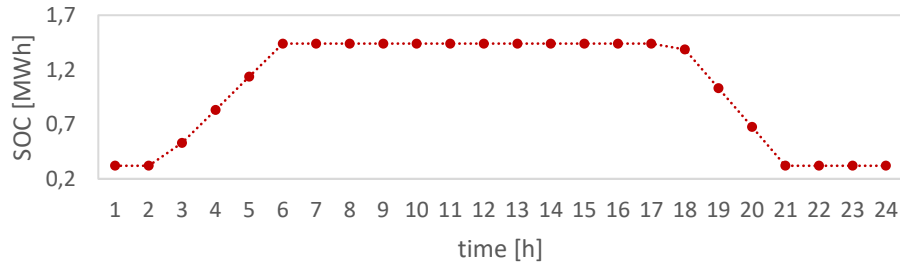


Figure 5. Operation of the ESS in scenario B

It can be observed in Figure 6 that the ESS can have an impact on the technical aspects of the system, such as voltage. In this case, where the ESS operation is determined by the market price, the ESS lowers the voltage toward nominal value during the night hours and increases it in the evening hours.

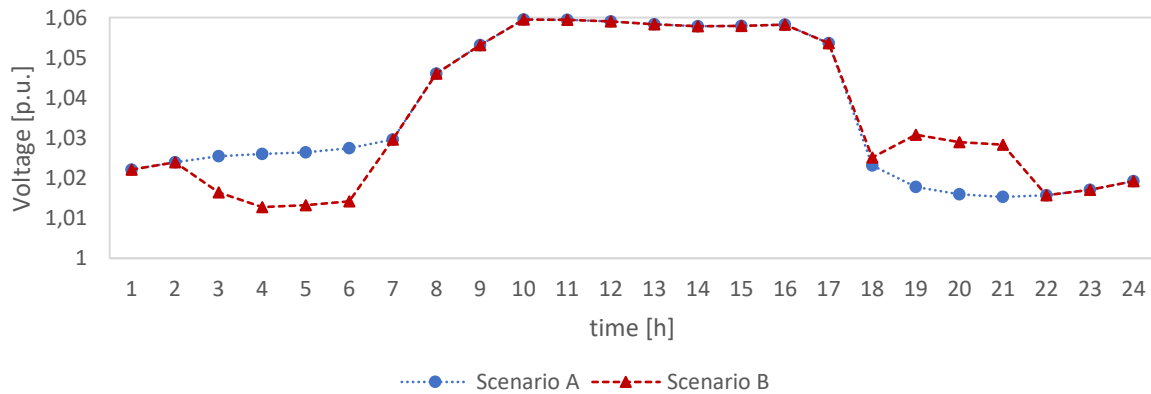


Figure 6. The voltage at node 13 for scenario A and B

- 3) *Scenario C*: Scenario C considers the possibility for the DR in the analysed system without ESS. The results showed that the operating cost for this scenario is 18,659.75 € (mean) with 333.08 MWh of imported electricity. Figure 7 presents the DR operation for scenario C and ESS charge and discharge for scenario B for lowest flexibility ($k = 1$). It is obvious that the DR model is operating differently than the ESS, which is a consequence of the fact that the DR is dependent on consecutive price differences on the day-ahead market while the ESS operation is dependent on low and high prices.

Thus, it is possible to observe a prolonged ESS operation during the night and evening hours, while the DR is active during several periods over the day as well.

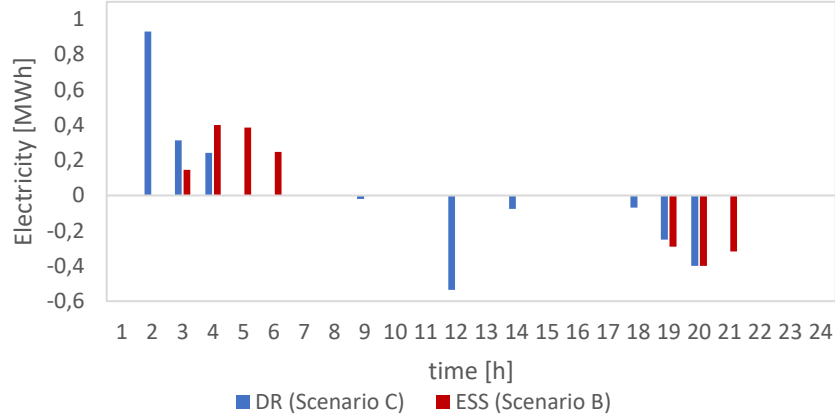


Figure 7. The operation of the DR in scenario C and ESS in scenario B – the charging of the ESS is represented with the positive sign while the discharging is represented with a negative sign as the objective of the figure is to show the values about their impact on the demand of the system

- 4) *Scenario D*: Final scenario considers the operation of both the ESS and the DR. Total operating cost of scenario D is 18,651.8 € (mean), and the total imported electricity is equal to 334.27 MWh (mean). The operation cost for this scenario varies from 14,066.46 € (-2σ) to 23,181.21 € (2σ). Additional analysis was conducted for this scenario by changing the flexibility parameter k . The lower value of the k parameter allows more possibility for higher amounts of DR. Regardless of the difference in consecutive prices on the market, and the hyperbolic tangent function prevents that possible DR amount exceeds node demand, as explained previously.

The total cost of the scenario varies from 18,651.8 € ($k = 1$) to 18,607.78 € ($k = 0.1$). The total cost does not change significantly for the lowest levels of flexibility, but it decreases as more flexibility is introduced in the system. Imported electricity increases from 334.27 MWh in original scenario D ($k = 1$) to 335.8 MWh ($k = 0.1$). The imported electricity for all scenarios and flexibility levels does not change for more than 0.56% of initial scenario A achieved for scenario D and the highest modelled flexibility. This result is expected as it was modelled with equations (17) and (18) that demand has to be retrieved. Moreover, the operation cost with implemented DR does not change significantly in comparison to the original scenario A, which is also expected due to the demand retrieval, as well as, in the D scenario, the additional cost is revenue for DR providers. Nevertheless, the overall benefit is increased as cost reduces for all DR

scenarios and the revenue of DR providers increase. Changes in savings and imported electricity are illustrated in Figures 8 and 9, where the impact of DR model behaviour can be observed over the entire time.

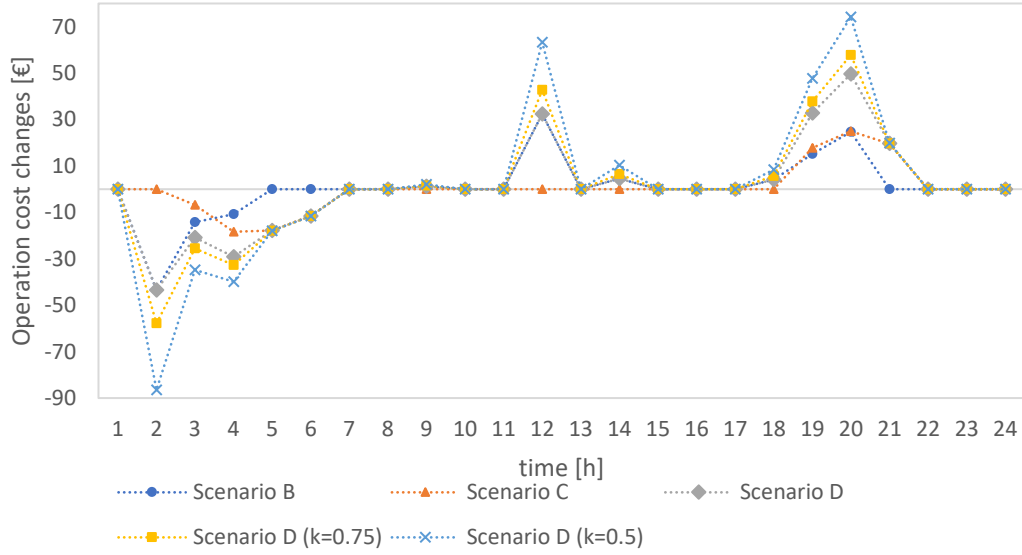


Figure 8. Operation cost for different flexibility levels

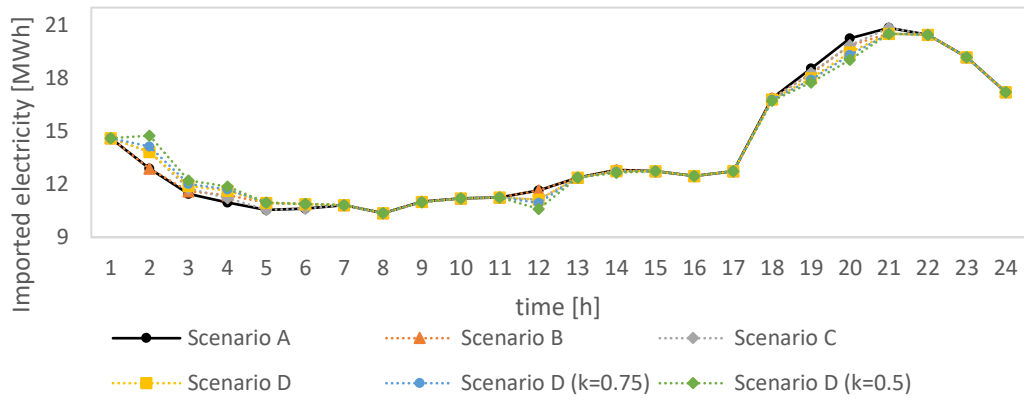


Figure 9. Electricity import for different flexibility levels

The DR operation is presented in Figure 10. It is possible to observe that the demand is reduced during evening hours and during the day, while it is retrieved during night hours. The lowest total demand reduction amounts to 1.35 MWh ($k=1$) and the highest 12.19 MWh ($k=0.1$). The demand retrieval ranges from 1.49 MWh ($k=1$) to 13.41 MWh ($k=0.1$).

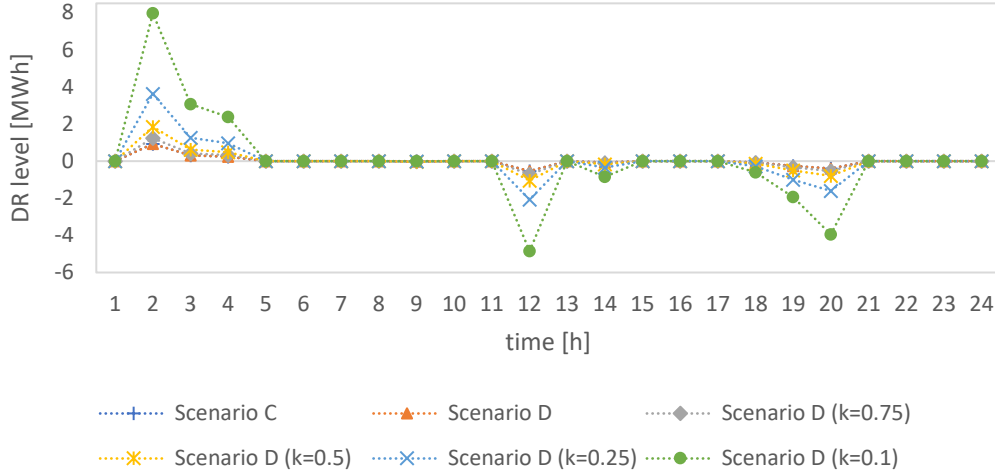


Figure 10. DR operation for different levels of parameter k

4.2. Different PV share influence

The influence of RES share in the archipelago for different levels of flexibility was also part of the study. The PV share is observed as relevant to the total maximum load in the system. Thus, 25% of PV corresponds to the original share of PV (1 MW on bus 13 and 4.14 MW on bus 4). For purposes of this analysis, it was considered that buses 3 and 7 also have PV plants in order to avoid large amounts of curtailed PV production that would occur if all PV production is concentrated. In Figure 11 (a), it is possible to observe the cost reduction of the system operation as a function of the PV penetration compared to the original scenario A (with operation cost of 18,655.2 €). Increasing the share of PV in the system significantly decreases the operation cost.

Further savings are achieved for an increased level of flexibility; however, these savings are significantly lower than when more RES is introduced in the system. This result is justifiable because the assumed cost of PV generation is zero and an increase of DR level with the proposed model allows a better demand schedule depending on the market price. Moreover, Figure 11 (b) presents total curtailed electricity from PV that starts to occur in the case with 75% of PV share. Increased share of PV causes voltage issues (Figure 12 (a)). Thus, it is necessary to curtail PV production in order to maintain a stable operation of the system.

Flexibility increase results with the lower amount of curtailed electricity (Figure 11 (b)), which is expected as the demand can be increased during the periods of PV production.

Minimum and maximum voltage changes are presented in Figure 12 (a) and (b). Minimum voltage isn't significantly influenced by the increase of PV, while the maximum voltage increases from 1.06 p.u. to the maximum allowed value of 1.1 p.u. It is important to note that Figure 12 suggests that the voltage change is caused because of the PV share change in the system, while the flexibility does not have a significant influence on voltage change.

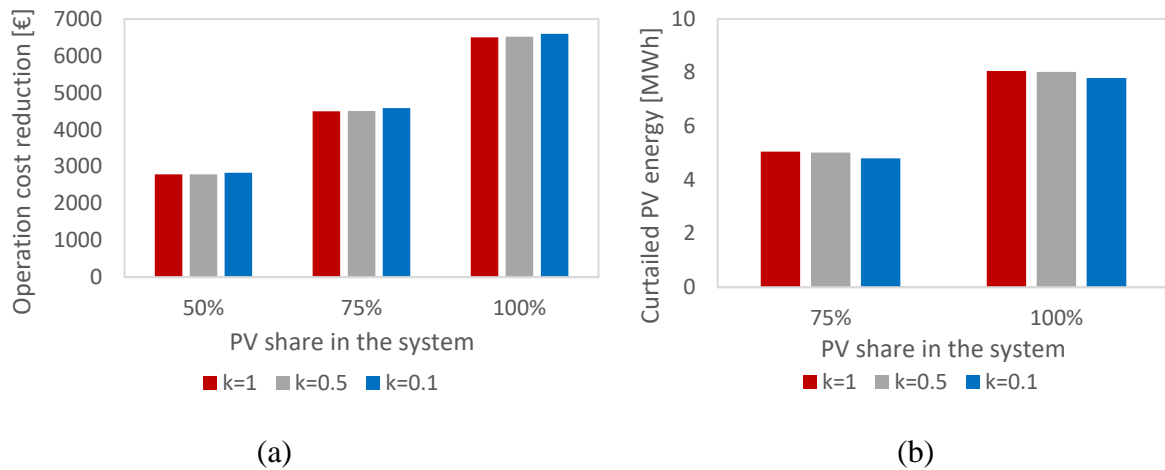


Figure 11. Operation cost reductions in comparison to the original scenario A (a) and total curtailed electricity from the PV (b)

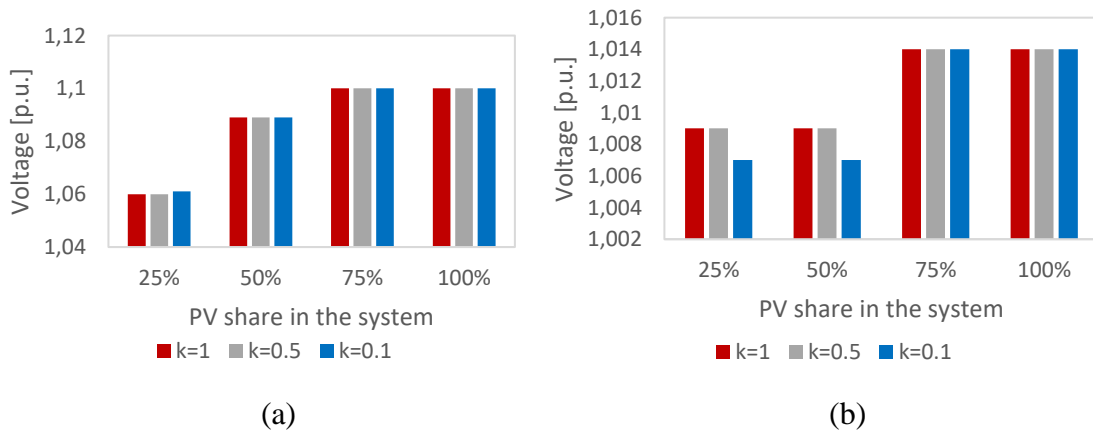


Figure 12. Maximum (a) and minimum voltage (b) in the system

Moreover, the ESS and DR operation was more closely observed in Figure 13 for fixed $k = 0.5$ and different PV share in the system. The first observation is that the ESS operation for 25% and 50% of PV share does not differentiate, while it changes for 75% and 100% of PV share.

As PV share increases, the need for flexibility increases as well. Thus, the ESS, for scenarios with high PV share, adjusts its operation to prioritise the minimisation of PV production curtailment. The DR operation changes according to the day-ahead market prices. Thus its pattern remains approximately the same as in Figure 7.

However, between period 10 and 16, the DR model increases load when possible, which results in 138 kW of increased load. It is interesting to note that the increase of load (DR retrieval) occurs on buses 7 to 13, while the reduction (DR) at period 12 occurs for busses 1 and 2. In other words, the model increases the load on buses with the highest voltage, while it decreases the load on buses where voltage is less affected by the increased RES share. This result shows the benefits of the integration of the DR model in the distribution system grid is not visible in studies that aggregate all distribution system elements.

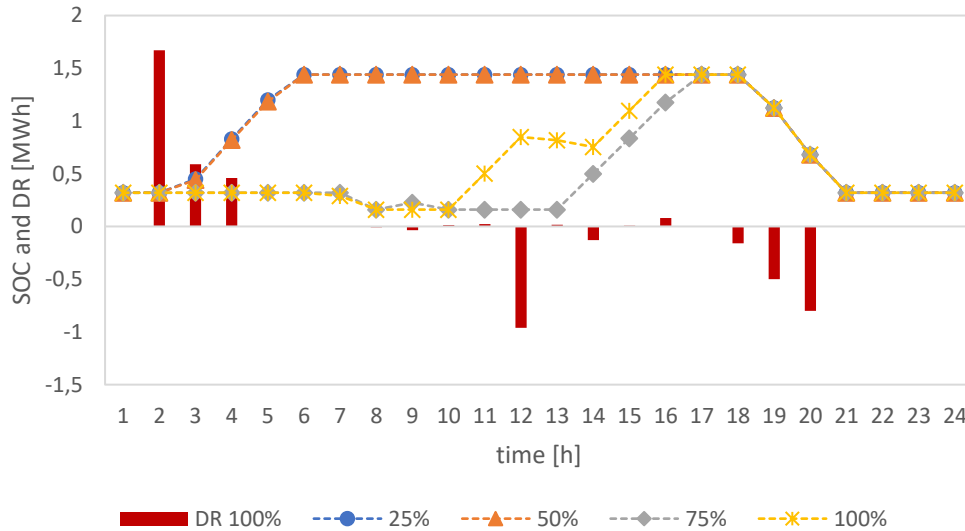


Figure 13. ESS and DR operation for $k = 0.5$

4.3. Price scenario analysis

In order to assess the sensitivity of the model, different market price scenarios have been modelled as described previously in the study. Modelled price values are presented in Figure 14.

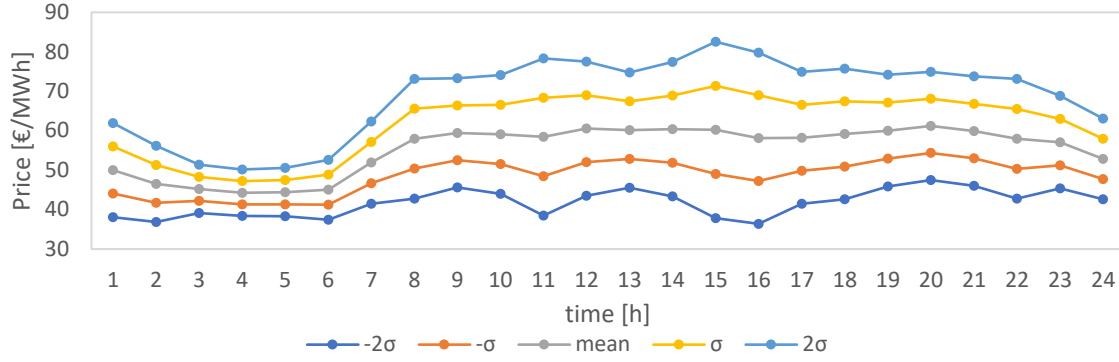


Figure 14. Modelled prices on the day-ahead electricity market

With an increase or decrease of market prices, the total operation cost of every scenario increases or decreases which is expected as higher prices on the market will result in higher electricity import costs and the opposite for lower prices. Figure 15 presents operation cost changes over time for different prices on the electricity market and the lowest flexibility level. Greater changes in operation cost are visible only for the highest price scenarios, which are in correlation with results presented in Table 3 that show that the highest amount of DR occurs for that particular scenario.

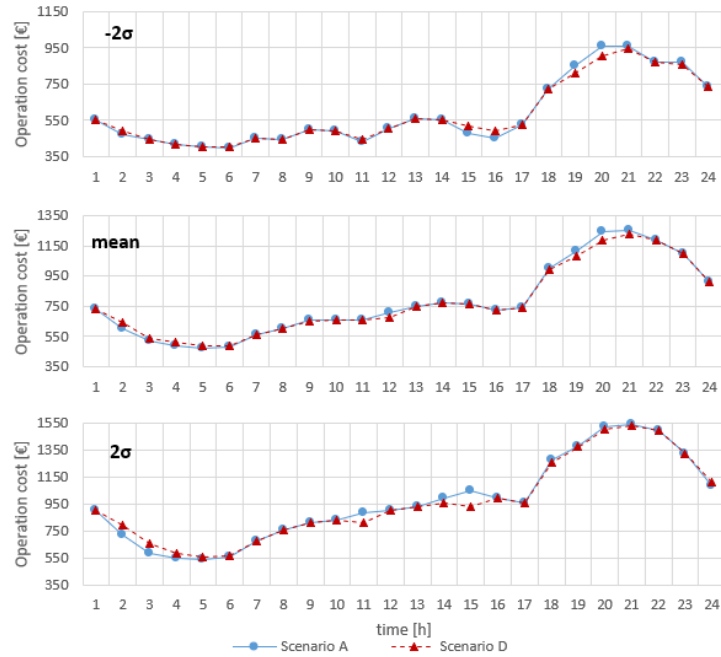


Figure 15. The operation cost of scenario A and D for three different price scenarios

Table 2 presents total operation cost for all scenarios (A – D) and for lowest ($k = 1$) and highest flexibility scenario ($k = 0.1$). The operation cost increased as day-ahead market prices were higher. Scenario B and scenario C for the lowest introduced level of flexibility $k = 1$ do not

present significant operating cost reduction. However, for increased flexibilities, the operation cost reduces more significantly, especially for high electricity prices on the day-ahead market.

It can also be observed that the difference between scenario C and scenario D for the high level of flexibility does not differ significantly for any scenario of market prices. The highest difference occurs for the highest market prices amounting to 15.1 €. This indicates that the ESS does not have a significant effect on the operation cost of the system regardless of the modelled market prices, while the DR model enables higher savings, especially for the increased flexibility.

This result can be explained with the local impact of the ESS, while the DR is available in all buses of the observed distribution grid. Operating cost reductions are illustrated in Figure 16 as well, where it can be seen that the highest reduction occurs for scenario D and is equal to 258.67 €. The technical impacts of analysed cases are further investigated in the study.

Table 2. Operation cost for different scenarios under different flexibility levels in euros [€]

	Scenario A	Scenario B	Scenario C		Scenario D	
k	-	-	1	0.1	1	0.1
-2σ	14,081.9	14,076.9	14,071.2	14,058.5	14,066.5	14,054.2
$-\sigma$	16,378.2	16,369	16,371.3	16,350.9	16,366.6	16,346.5
mean	18,665.2	18,657.2	18,659.8	18,615.4	18,651.8	18,607.8
σ	20,956.7	20,945.3	20,942.7	20,833	20,931.3	20,821.9
2σ	23,247.6	23,231.6	23,197.1	23,004	23,181.2	22,988.9

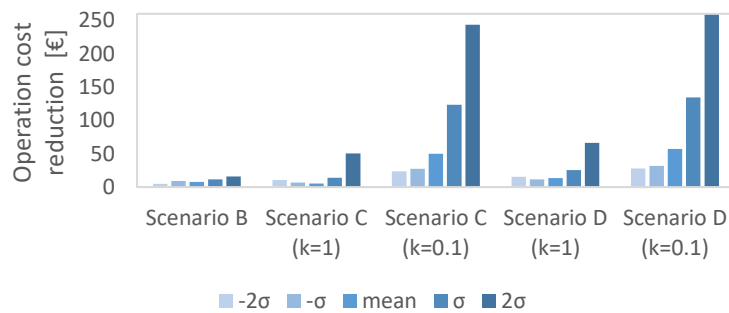


Figure 16. Savings for different scenarios under different flexibility levels

The technical impacts of different market price scenarios can be observed in Figure 17 and Figure 18. The figures present voltage values for scenario C and D for three different market price scenarios. Figure 17 presents voltage changes at bus 10 for scenario C under the influence of different market price scenarios, while Figure 18 presents voltage changes at bus 10 for scenario D under different market price scenarios.

The results indicate that market uncertainty has a more significant impact on the distribution network technical constraints in scenario D in contrast to scenario C. The difference between the two scenarios is that, in scenario D, ESS is connected at bus 13. ESS operation is presented in Figure 19, from which it is possible to observe that the ESS operation changes under different price scenarios, which influences the voltage vector in the system. These results confirm previous results where it was shown that the ESS has a larger impact on bus voltages in contrast to the DR.

The comparison between scenario C and D observed in Figures 17 and 18 confirm this statement as it is obvious that higher voltage fluctuations occur for scenario D. Namely, maximum voltage deviation between lowest (-2σ) and highest market price scenario (-2σ) is 0.02 p.u. (0.2 kV) for scenario D, while, for scenario C, the maximum voltage deviation at node 10 is 0.004 p.u. (0.04 kV). Presented results indicate that the DR model can be implemented in the system without causing significant voltage changes in the distribution grid.

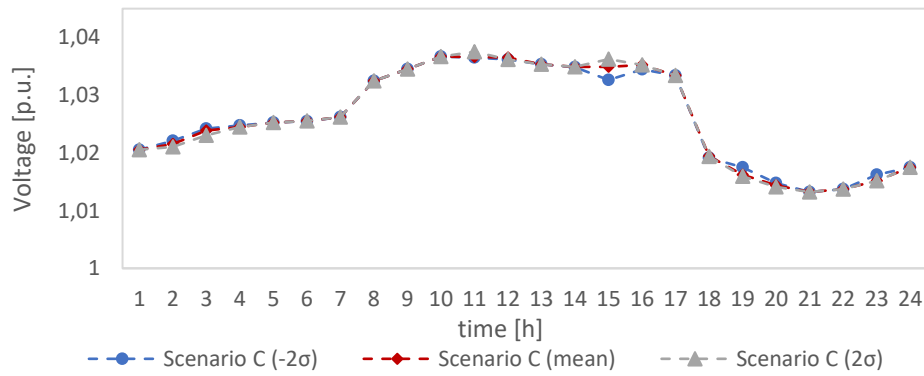


Figure 17. The voltage at node 10 for scenario C under market uncertainty scenarios

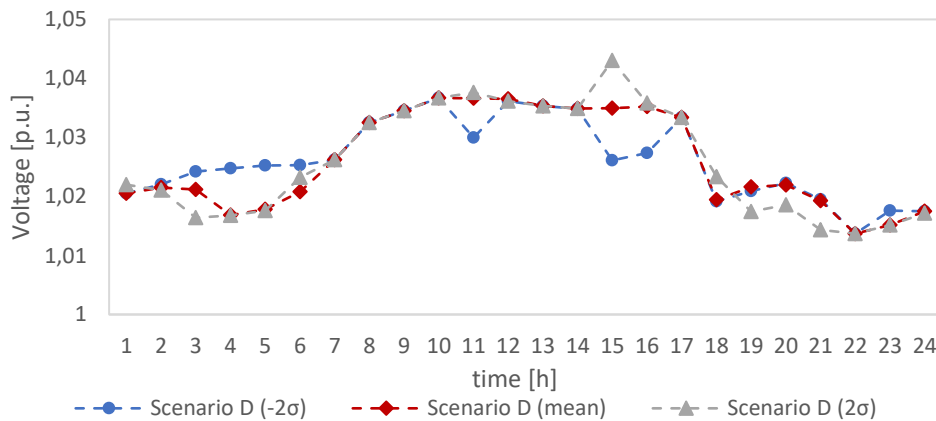


Figure 18. The voltage at node 10 for scenario D under market uncertainty

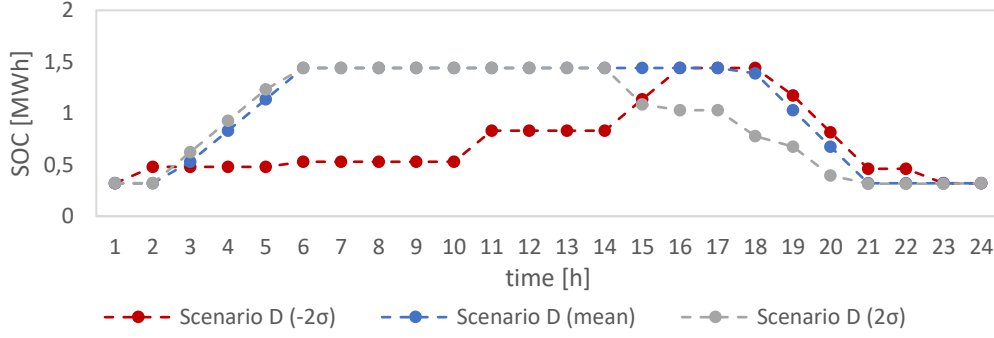


Figure 19. Battery operation for scenario D under market uncertainty

Table 3 illustrates the percentage of total DR used for each price scenario as well as the total available DR. The results indicate that different market prices influence different amounts of available DR, although the model does not decide on using the entire available DR at all periods. The results show that the activation of DR reduces by 0.31 MWh for the mean price scenario in comparison to the low-cost scenario and then again increases by 1.24 MWh for the high price scenario.

The maximum amount of DR is mostly determined with differences between the minimum and maximum price on the day-ahead market. Although used DR in the mean scenario is lower than in -2σ , this can be explained with the fact that the maximum DR possible is more than two times higher for -2σ prices than for mean prices, so the percentage of used DR significantly increases for mean prices in comparison with -2σ prices and continues to increase for 2σ prices.

Table 3. Available and used demand response for different prices for scenario D

	-2σ	mean	2σ
Used DR [MWh] (% of the maximum DR)	1.66 (13.96%)	1.35 (25.66%)	2.59 (33.26%)
Maximum DR [MWh] (% of the total demand)	11.9 (3.12%)	5.27 (1.38%)	7.79 (2.05%)

Figure 20 presents a detailed DR operation for different price scenarios. Figure 20 is in correlation with Table 3 as it can be observed that the available DR is least used for the lowest market prices scenario (a). The highest exploitation occurred for the highest market prices scenario and amounted to 33.26% of used available DR.

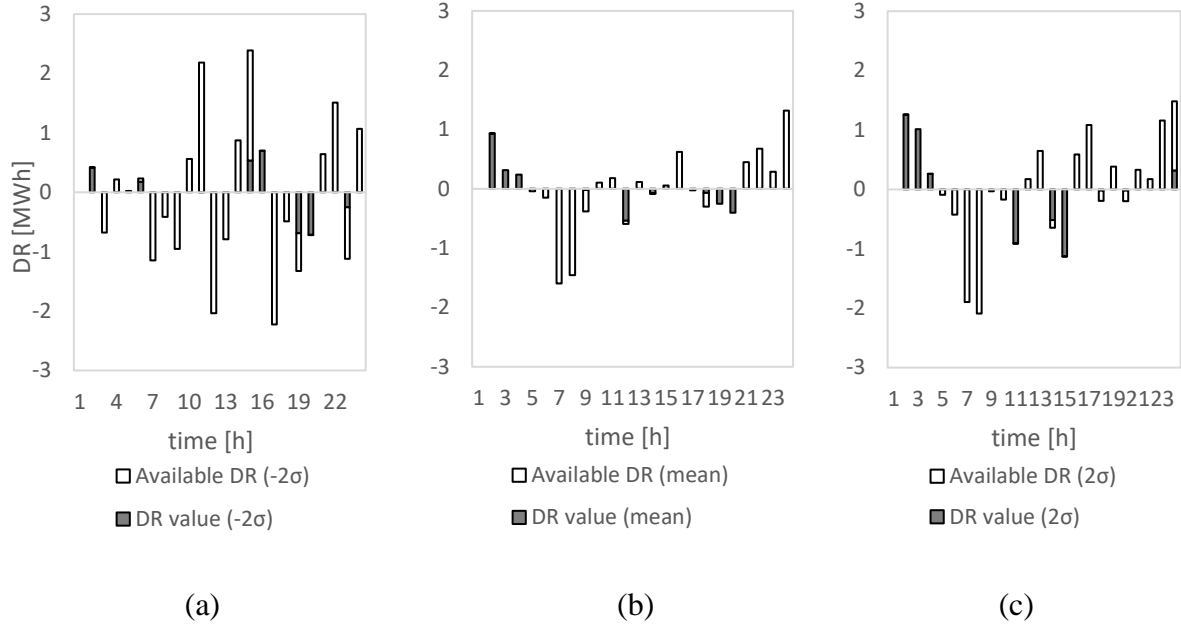


Figure 20. DR value for different price scenarios

Similarities between DR operation and battery operation can be observed in Figure 19 and Figure 20. At periods when DR and ESS can be used for cost reduction, the model is prioritising the DR as ESS is always available if there is a required amount for SOC available for a particular action. For example, Figure 20 (c) shows that the demand retrieval is active for hours 2, 3 and 4, or during the periods with the lowest prices, while the ESS starts charging in the third hour, which allows it to exploit the entire range of lower prices.

Similar can be observed for DR value at hour 11. The DR is fully active during hour 11, while the ESS is not, which saves the electricity for the ESS to discharge once the highest prices occur during night hours while the ESS operation. Without DR model, the ESS may or may not discharge at the given hour, but in either case, this would result in a higher cost because, or the potential to exploit higher price at hour 11 is not used, or the ESS will have less electricity in the evening hours during high prices. The prioritisation of the DR over the ESS occurs due to the losses of ESS cycling represented with efficiencies in the model in the equation (12). The utilisation of the DR model enables additional cost reductions, as well as profit generation for consumers as a result of the exploitation of exceptional electricity prices that occur on the day-ahead market.

4.4. Impact of different incentives μ

Several different values of DR incentives μ were considered for testing the sensitivity of the proposed model. The DR incentives vary from 5% of the market price to 20% of the market price. Each incentive value was considered under a different flexibility level. Figure 21 presents the operation cost of the system for different incentive and flexibility values. The results showed that when the incentive is set to 20% of the market price, the operation cost did not differ for different flexibility values, which means that incentive value should be lower for DR to influence system operation cost.

Flexibility factor values from 1 to 0.5 have no significant influence on the operation cost as it changes only for 9.4 € (from $k = 1$ to $k = 0.5$) with the incentive value of 5% of the market price. It can also be observed that as incentive value decreases, the influence of flexibility level on the operation cost is increasing. The model uses the DR service up to the point of $0.23 \lambda_t$ incentive value, which means that this is the breakpoint incentive for the analysed case. At this point, the total operation cost is equal to the cost of scenario B.

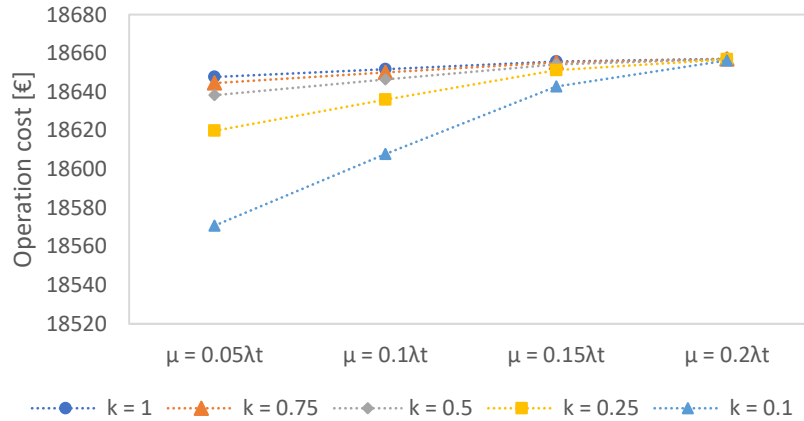


Figure 21. Operation cost for different incentive and flexibility values

Figure 22 presents the DR values (a) and percentage of used DR values (b) (percentage of total available DR) for the different flexibility and incentive values. The total DR values increase as the flexibility level increases and the incentive value decreases. Figure 22 confirms results from previous Figure 21 as incentive value has a more significant impact on the system operation than the flexibility level when k is higher than 0.25.

For example, for the 0.5 value of k factor, a decrease of incentive value from $0.15\lambda_t$ to $0.1\lambda_t$ resulted in 7.37% of increased used DR value, while the change of flexibility level from 0.5 to 0.25 for $0.15\lambda_t$ resulted with 0.61% increase of the same parameter. This result shows that, for

lower levels of available flexibility (higher k parameter value), incentive parameter μ should be used for increasing the DR value in the system. Increased μ would result in higher revenue for the consumers, which would further motivate them for investments in DR technologies.

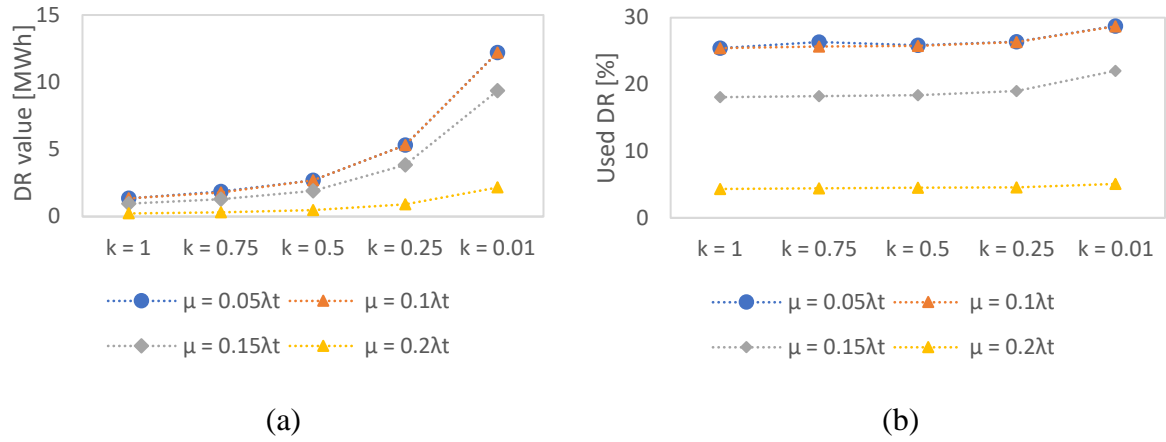


Figure 22. DR value (a) and percentage of used DR (b) for different incentive and flexibility values

Furthermore, the results show that the DR values and used DR do not differentiate for cases when DR incentive is set to 10% and 5%. This result implies that the operation of DR does not change significantly when the DR incentive is reduced below $0.1\lambda_t$. Figure 21 also confirms this result as total operation cost does not increase significantly for the case when the incentive is set to $0.1\lambda_t$ in comparison to $0.05\lambda_t$, especially for higher flexibility levels.

The influence of different flexibility and incentive values on the minimum and maximum voltage in the distribution system was also observed. Figure 23 presents voltage values for observed cases.

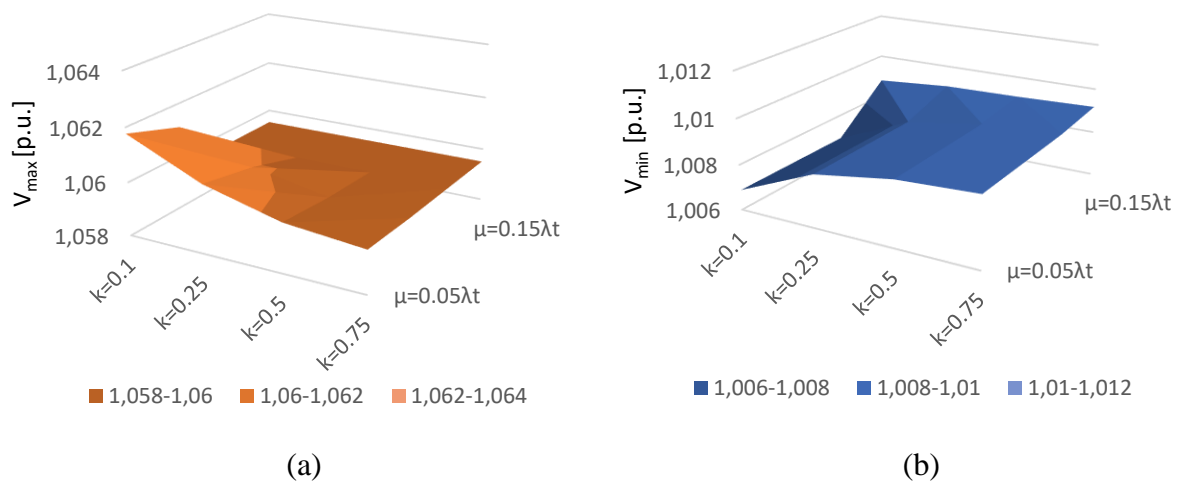


Figure 23. Maximum (a) and minimum (b) voltage values in the observed energy system for different incentive and flexibility values

The results indicate that the presented DR model causes no problems for the DSO as both voltage values – maximum (a) and minimum (b) do not change significantly for different flexibility and incentive values. Changes can be observed when flexibility values increases and reaches a k value of 0.25 and incentive value μ reaches $0.1 \lambda_t$. Voltage value further changed when flexibility increased for k value of 0.1 and incentive value μ of $0.05 \lambda_t$, but this resulted in a maximum voltage change of 0.002 p.u. for both cases (a) and (b). This result suggests that the implementation of the proposed DR model wouldn't result in operational problems in the distribution grid for any flexibility and incentive level, which would result in the continuation of the distribution system stable operation.

Current study opens space for future research that will enable finding of the optimum incentive value. This value would depend on the objective function of the problem. One possibility would be to determine what would be the optimum incentive if the objective would be to maximise the DR providers' profit. Another possibility, particularly in high VRES distribution systems, would be to determine the optimum incentive if the objective would be to use DR for ancillary service provision.

This study observed the impact of different flexibility levels; however, it did not propose the method for determining the flexibility potential of the smart archipelago. Moreover, the study did not foresee the possibility for reactive power control, which will likely be necessary for future energy systems. . It should also be noted that the observed system was not designed as a microgrid, thus it requires the support from the mainland to preserve the stability. These remarks should be considered in future research.

5. Conclusion

This paper presented a novel DR mathematical model. The model was implemented in the small radial distribution. The DR model is a price-taker model based on the price differential between two consecutive hours and represents the increased or decreased share of the load in a specific hour. Providing a DR service to the grid results in revenue for the DR provider. This is also incorporated in the objective function of the optimisation problem. The model includes all grid parameters relevant for the distribution grid as well as the ESS model and two PV plants models.

- Even for the lowest levels of flexibility, the implementation of DR in the system results in a reduction of the operation cost and revenue for the DR provider. The

implementation of the ESS in combination with the DR model resulted in further savings increase.

- An increase in PV share in the system results in a lower cost of the system. When PV is at the 75% value of the maximum load, the PV production curtailment occurs. The curtailment reduces as the flexibility increases.
- The results showed that the market price has an impact on the total operating cost of the system as cost reduced as the market prices increased. The highest reduction of 258.7 € occurred for the highest market prices when the highest amount of flexibility was present in the system.
- It is necessary to observe both parameters – DR incentive μ and flexibility level k in order to optimally utilise the DR model. It was shown that there is no significant increase in DR value in the system when the DR incentive is lower than $0.1\lambda_t$, which leads to the conclusion that this should be the minimum value of the incentive. The breakpoint incentive occurs for an incentive value of $0.23\lambda_t$, after which the DR operation is not active. At the breakpoint incentive value, the total operation cost of scenario D is equal to scenario B.
- The implementation of the proposed DR model wouldn't result in significant voltage changes in the observed energy system, which leads to the conclusion that the DR model does not influence the safe operation of the distribution system run by the DSO.

Future research will be directed in investigating the possibilities of the DR and ESS combined operation when ancillary services are considered together with consideration of other grid management possibilities. Different possibilities for incentive parameters definition will be examined as well. The incentive can be defined as a function of production and realistic conditions in the electricity distribution grid, which would result in a more dynamic DR model.

Nomenclature

Indices and sets

i, j	Grid buses indexes
t	Time period
$\Omega_{\mathcal{T}}$	Set of periods
$\Omega_{\mathcal{N}}$	Set of grid buses

σ

z

\bar{z}

$L_{i,t}^P, L_{i,t}^Q$

Variables

Standard deviation

Observed data segment

Mean value of observed data

Active and reactive load at node i and time t

Ω_{ε}	Set of lines	$\varphi_{i,t}^-, \varphi_{i,t}^+$	DR and DR retrieval values
Ω_{ESS}	Set of energy storage systems buses	$P_{i,t}^{PV}, Q_{i,t}^{PV}$	Active and reactive power from the solar power plant [MW/Mvar]
Ω_{DR}	Set of demand response buses	$E_{slack,t}$	Imported and exported electricity on the slack bus [MWh]
Ω_{PV}	Set of solar power plant buses	$P_{slack,t}, Q_{slack,t}$	Active and reactive power at the slack bus at time t [MW/Mvar]
Parameters		$E_{i,t}^{CPV}$	Curtailed electricity from the solar power plant [MWh]
β_i	Factor for limiting battery charge and discharge	$SOC_{i,t}$	State of charge of the battery [MWh]
$SOC_i^{min/max}$	Minimum and maximum battery state of charge [MWh]	$P_{i,t}^d, P_{i,t}^c$	Discharging and charging active power of the battery [MW]
η_c	Charging efficiency	$Q_{i,t}^d, Q_{i,t}^c$	Discharging and charging reactive power of the battery [Mvar]
η_d	Discharging efficiency	$V_{i,t}$	Voltage at node i at time t [kV]
$\Lambda_{i,t}^{PV}$	Maximum available solar power plant generation [MW]	$\delta_{i,t}$	Voltage angle at node i at time t [rad]
CPV	Value of curtailed solar power generation [€/MWh]	$I_{ij,t}$	Current from node over line ij at time t [A]
k	Flexibility coefficient	Abbreviations	
μ	Incentive for providing demand response [€/MWh]	EU	European Union
ϑ	DR retrieval coefficient	DR	Demand response
Z_{ij}	Impedance between nodes i and j [Ω]	RES	Renewable energy sources
θ_{ij}	Impedance angle between nodes i and j [rad]	ESS	Energy storage system
b	Line susceptance [μS]	PHP	Pumped hydro storage
$V_{min/max}$	Minimum and maximum allowed voltage [kV]	PV	Solar power plant
$\delta_{min/max}$	Minimum and maximum allowed voltage angle [rad]	DSO	Distribution system operator
$S_{ij,max}$	Maximum apparent power through line ij [MVA]	CPV	Curtailed power value
λ_t	Electric energy price at period t [€/MWh]	NLP	Non-linear programming

Acknowledgement

This work has been supported by the Young Researchers' Career Development Programme (DOK-01-2018) of Croatian Science Foundation, which is financed by the European Union from European Social Fund and Horizon 2020 project INSULAE - Maximising the impact of innovative energy approaches in the EU islands (Grant number ID: 824433). This support is gratefully acknowledged. The work was also co-financed by the CITIES project No. DSF1305-00027B funded by the Danish Innovationsfonden. The publication was presented at the 1st Asia Pacific Conference on Sustainable Development of Energy Water and Environment Systems, Gold Coast, Australia (online), 6 – 9 April 2020.

References

- [1] DAFNI, “Smart Island Initiative,” 2017. .
- [2] I. Baččković and P. A. Østergaard, “Local smart energy systems and cross-system integration,” *Energy*, vol. 151, 2018.
- [3] J. Z. Thellufsen *et al.*, “Smart energy cities in a 100% renewable energy context,” *Renew. Sustain. Energy Rev.*, vol. 129, 2020.
- [4] H. M. Marczinkowski and L. Barros, “Technical approaches and institutional alignment to 100% renewable energy system transition of madeira island-electrification, smart energy and the required flexible market conditions,” *Energies*, vol. 13, no. 17, 2020.
- [5] P. Ferreira, A. Lopes, G. G. Dranka, and J. Cunha, “Planning for a 100% renewable energy system for the Santiago Island, Cape Verde,” *Int. J. Sustain. Energy Plan. Manag.*, vol. 29, 2020.
- [6] M. A. Hannan, M. Faisal, P. Jern Ker, R. A. Begum, Z. Y. Dong, and C. Zhang, “Review of optimal methods and algorithms for sizing energy storage systems to achieve decarbonization in microgrid applications,” *Renewable and Sustainable Energy Reviews*, vol. 131, 2020.
- [7] J. Boyle, T. Littler, and A. Foley, “Battery energy storage system state-of-charge

- management to ensure availability of frequency regulating services from wind farms,” *Renew. Energy*, vol. 160, 2020.
- [8] European Parliament, *Directive (EU) 2018/2001 of the European Parliament and of the Council of 11 December 2018 on the promotion of the use of energy from renewable sources*. THE EUROPEAN PARLIAMENT AND THE COUNCIL OF THE EUROPEAN UNION, 2018, pp. 82–209.
 - [9] Q. Wang, C. Zhang, Y. Ding, G. Xydis, J. Wang, and J. Østergaard, “Review of real-time electricity markets for integrating Distributed Energy Resources and Demand Response,” *Applied Energy*. 2015.
 - [10] G. Dileep, “A survey on smart grid technologies and applications,” *Renew. Energy*, vol. 146, 2020.
 - [11] A. Hrga, T. Capuder, and I. P. Zarko, “Demystifying Distributed Ledger Technologies: Limits, Challenges, and Potentials in the Energy Sector,” *IEEE Access*, vol. 8, 2020.
 - [12] H. C. Gils, “Assessment of the theoretical demand response potential in Europe,” *Energy*, 2014.
 - [13] S. Annala, S. Viljainen, J. Tuunanen, and S. Honkapuro, “Does knowledge contribute to the acceptance of demand response?,” *J. Sustain. Dev. Energy, Water Environ. Syst.*, vol. 2, no. 1, 2014.
 - [14] E. A. M. Klaassen, R. J. F. van Gerwen, J. Frunt, and J. G. Slootweg, “A methodology to assess demand response benefits from a system perspective: A Dutch case study,” *Util. Policy*, 2017.
 - [15] H. S. V. S. K. Nunna, A. M. Saklani, A. Sesetti, S. Battula, S. Doolla, and D. Srinivasan, “Multi-agent based Demand Response management system for combined operation of smart microgrids,” *Sustain. Energy, Grids Networks*, 2016.
 - [16] D. Groppi, A. Pfeifer, D. A. Garcia, G. Krajačić, and N. Duić, “A review on energy storage and demand side management solutions in smart energy islands,” *Renew. Sustain. Energy Rev.*, vol. 135, 2021.
 - [17] K. Askeland, K. N. Bozhkova, and P. Sorknæs, “Balancing Europe: Can district heating affect the flexibility potential of Norwegian hydropower resources?,” *Renew. Energy*, vol. 141, 2019.
 - [18] D. Taler, P. Dzierwa, M. Trojan, J. Sacharczuk, K. Kaczmariski, and J. Taler, “Mathematical modeling of heat storage unit for air heating of the building,” *Renew. Energy*, vol. 141, 2019.
 - [19] H. Dorotić, B. Doračić, V. Dobravec, T. Pukšec, G. Krajačić, and N. Duić, “Integration

- of transport and energy sectors in island communities with 100% intermittent renewable energy sources,” *Renewable and Sustainable Energy Reviews*. 2019.
- [20] X. Wu, W. Cao, D. Wang, M. Ding, L. Yu, and Y. Nakanishi, “Demand response model based on improved Pareto optimum considering seasonal electricity prices for Dongfushan Island,” *Renew. Energy*, vol. 164, pp. 926–936, 2021.
 - [21] N. Holjevac, T. Capuder, N. Zhang, I. Kuzle, and C. Kang, “Corrective receding horizon scheduling of flexible distributed multi-energy microgrids,” *Appl. Energy*, 2017.
 - [22] H. Meschede, “Analysis on the demand response potential in hotels with varying probabilistic influencing time-series for the Canary Islands,” *Renew. Energy*, vol. 160, 2020.
 - [23] D. Neves, A. Pina, and C. A. Silva, “Assessment of the potential use of demand response in DHW systems on isolated microgrids,” *Renew. Energy*, vol. 115, 2018.
 - [24] D. F. Dominković, R. G. Junker, K. B. Lindberg, and H. Madsen, “Implementing flexibility into energy planning models: Soft-linking of a high-level energy planning model and a short-term operational model,” *Appl. Energy*, vol. 260, 2020.
 - [25] R. G. Junker, C. S. Kallesøe, J. P. Real, B. Howard, R. A. Lopes, and H. Madsen, “Stochastic nonlinear modelling and application of price-based energy flexibility,” *Appl. Energy*, vol. 275, 2020.
 - [26] Y. Xiang, H. Cai, C. Gu, and X. Shen, “Cost-benefit analysis of integrated energy system planning considering demand response,” *Energy*, 2020.
 - [27] P. Zhang, X. Dou, W. Zhao, M. Hu, and X. Zhang, “Analysis of power sales strategies considering price-based demand response,” in *Energy Procedia*, 2019.
 - [28] N. I. Nwulu and X. Xia, “Optimal dispatch for a microgrid incorporating renewables and demand response,” *Renew. Energy*, vol. 101, 2017.
 - [29] A. Pfeifer, V. Dobravec, L. Pavlinek, G. Krajačić, and N. Duić, “Integration of renewable energy and demand response technologies in interconnected energy systems,” *Energy*, 2018.
 - [30] I. Leobner *et al.*, “Simulation-based strategies for smart demand response,” *J. Sustain. Dev. Energy, Water Environ. Syst.*, vol. 6, no. 1, 2018.
 - [31] N. Oconnell, P. Pinson, H. Madsen, and M. Omalley, “Benefits and challenges of electrical demand response: A critical review,” *Renewable and Sustainable Energy Reviews*, vol. 39, 2014.
 - [32] K. Christakou, D. C. Tomozei, J. Y. Le Boudec, and M. Paolone, “AC OPF in radial distribution networks – Part II: An augmented Lagrangian-based OPF algorithm,

- distributable via primal decomposition,” *Electr. Power Syst. Res.*, 2017.
- [33] A. R. Jordehi, “Optimisation of demand response in electric power systems, a review,” *Renewable and Sustainable Energy Reviews*. 2019.
 - [34] A. Ghasemi and M. Enayatzare, “Optimal energy management of a renewable-based isolated microgrid with pumped-storage unit and demand response,” *Renew. Energy*, vol. 123, 2018.
 - [35] A. Ajoulabadi, S. N. Ravadanegh, and Behnam Mohammadi-Ivatloo, “Flexible scheduling of reconfigurable microgrid-based distribution networks considering demand response program,” *Energy*, 2020.
 - [36] A. Samimi, M. Nikzad, and P. Siano, “Scenario-based stochastic framework for coupled active and reactive power market in smart distribution systems with demand response programs,” *Renew. Energy*, vol. 109, 2017.
 - [37] T. Cerovečki, M. Cvitanović, F. Damjanović, R. Ivković, J. Majcen, and I. Širić, “Optimal technical connection of PV plant on distribution grid.” 2019.
 - [38] RINA-C, “INSULAE - Energy Storage System - Conceptual design Unije,” 2019.
 - [39] “www.cropex.hr.” [Accessed: 05/03/2020]

PAPER 5

The role of the energy storage and the demand response in the robust reserve and network-constrained joint electricity and reserve market

^aMarko Mimica, ^cZoran Sinovčić, ^bAndrej Jokić, ^aGoran Krajačić

^aDepartment of Energy, Power Engineering and Environment, Faculty of Mechanical Engineering and Naval Architecture, 10 000 Zagreb

^bDepartment of Robotics and Production System Automation, Faculty of Mechanical Engineering and Naval Architecture, 10 000 Zagreb

^cCroatian Transmission System Operator, 10 000 Zagreb

e-mail: mmimica@fsb.hr

Abstract

Increase of the variable renewable energy sources in the power system is causing additional needs for the reserve in the system. On the other hand, the integration of energy storage and the demand response offers additional sources of flexibility in the system. Most of the current studies that model energy systems do not model the reserve market. Because of this, these studies eliminate the possibility to assess the full benefits of energy storage and demand response. The method proposed in this study enables the comparison between the two approaches and evaluates the benefits of energy storage and demand response for both approaches. The case study was conducted on the power system consisted of 13 interconnected nodes. The results showed that the operation cost of the system was 28.1% higher when the reserve constraints were imposed for the most pessimistic scenario. Moreover, the results showed that energy storage and flexible loads achieved significantly higher revenues when they were able to participate in the reserve market. The results indicated the need for the development of the reserve market as well as frameworks that will enable the energy storage and the demand response to participate in the reserve markets.

Keywords

Energy storage; Demand response; Power system analysis; Flexibility; Reserve markets

1. Introduction

The recent objectives set by the European Union (EU) in [1] described the necessity for the green energy transition. This is another document in a series of regulations regarding energy (e.g. [2] for energy balancing, [3] regarding the electricity market design) and other memorandums [4] and initiatives (e.g. Smart Islands initiative [5] and Clean Energy for all Europeans [6]) that emphasize the fact that the green energy transition is one of the top EU strategic objectives. Decarbonization of the electricity sector represents perhaps the most challenging issue. As the conventional generators that run on coal and gas are starting to phase out, the new variable renewable energy sources (VRES) such as wind and photovoltaic (PV) power plants are being integrated in the system. This results with additional uncertainty in the power system operation because VRES production depends on the current weather conditions in contrast to the coal and gas power plants that are controllable.

Many studies analysed the operation of future systems with high VRES share. The authors in [7] presented a case for complete decarbonization of the South-East Europe energy system. A subsampling method applied at the United Kingdom (UK) power systems over 36 year period in [8] resulted in significantly less variation in terms of system cost and hours of unmet demand in comparison to the models that observe individual years. The UK power system was also modelled in [9] but with consideration of different time resolutions, concluding that the systems with high wind and solar penetration should be modelled on a resolution finer than a one-hour resolution. Different tools for analysing the energy systems were developed over the years as well (e.g. EnergyPLAN used in [10], or H2RES applied in [11]). The value of interconnection was demonstrated in [12] where the authors analysed the islands of Korčula, Hvar, Lastovo and Vis. The results showed that Critical Excess Electricity Production decreased by 22% when the interconnection was considered for the most optimistic scenario. Another study [13] proposed a 30 MW solar and 22 MW wind energy mix for the island of Korčula. A 100% renewable energy system of island La Gomera was modelled in [14]. Similar results that indicate that it is possible to achieve 100% renewable production were achieved for the Åland Islands in [15]. The Markal model was coupled with the load flow model in [16] and showed that the integration of a 100 MW wind power plant resulted in a maximum of 21% line overload. Multi-energy microgrid operation was investigated in [17] where authors showed the flexibility benefits when

different sectors are jointly integrated. The possible pricing strategies for the battery storage in the residential microgrid with the photovoltaics were analysed in [18] and concluded that it would be optimal to apply the volumetric and the capacity tariffs. Different demand response models and energy storage systems were considered in the study [19] where authors concluded that optimal integration of renewable units with energy storage and the demand response results in a lower cost of the system. A multi-objective framework with AC OPF model was developed in [20] that analysed the operation of the demand response and the energy storage in the reconfigurable heat and power microgrid, however without including the reserve market. A similar study was conducted in [21] with a focus on including environmental aspects in the modelling and without the consideration of the reserve constraints. A soft-linking approach presented in [22] proved the necessity of more detailed modelling as there was grid code violation for the analysed energy planning scenario, however, the authors also did not include the reserve markets in the study. The studies [7-22] did not consider any kind of reserve constraints and used hourly time resolution (except [9] which compared different time resolution approaches). This paper presented a method that considered the reserve constraints incorporated in a DC OPF model on a 15-min time resolution. Moreover, the results of this study were obtained under demand uncertainty which is not considered in studies [7-22]. The proposed method filled in this research gap and the results demonstrated the necessity for more detailed modelling of the energy system.

Several studies proposed more detailed energy system models that included the reserve requirements. The authors in [23] analysed the Western Europe power system using the Dispa-SET tool. The study showed that the system can operate securely with a decrease in electricity price by 46.5% with an increase in renewable production of 11.7% by 2020 and 28.7% by 2030. The study did not, however, use a grid model where the power flow is a function of voltage angle difference between the two nodes. Another study [24] presented a joint energy and reserve model that did not include energy storage systems (ESS) and demand response (DR) as well as aggregated all technologies in one node. Joint energy and reserve model was presented in [25] where authors observed the influence of electric vehicle (EV) fleet on the system operation. Between the scenarios with 5, 50 and 500 EVs in the fleet, the lowest cost was achieved for the scenario with 50 EVs. However, the study did not consider the grid constraints which would enable better utilization of a fleet with a higher number of EVs. Another study [26] included EVs in the optimal management strategy of the energy and reserve markets, however without modelling of the grid constraints. A DC OPF model with reserve saturation was presented in

[27] where the authors provided a novel method for generator production and reserve provision control. The study does not consider the influence of ESS and DR on the system operation in the proposed model. The DR model was proposed in [28] in the AC OPF model, however, the reserve market was not modelled in this study.

The analysed studies indicated that the integration of VRES in power systems is increasing substantially. For these reasons, higher amounts of the reserve are required, while at the same there are fewer units that can provide the reserve as underlined in [29]. However, one of the solutions to this problem is the integration of flexible technologies such as ESS and DR [30]. The recent study [31] showed that ESS can successfully provide ancillary services to the system and maintain the voltage level below 1.05 p.u. However, the study focuses only on ancillary services regarding nominal voltage preservation. The study [32] considered an energy hub with included reserve constraints, however without enabling the possibility of reserve provision by the energy storage and without the comparison analysis to models without the reserve constraints. Another recent study [33] proposed a stochastic framework for integrating ESS as a reserve provider and compared four ESS reserve models. Both studies [31] and [33] used hourly time resolution and did not consider flexible load for providing reserve. Moreover, the studies did not provide insight into what benefits does reserve modelling offer in comparison to the existing energy system models. This paper analysed the differences between the two modelling approaches and quantified the impact on the overall system operation when the ESS and DR are included in the reserve market. The analysis of the previous studies shows that there is a research gap as there is no method that enables the comparison of different modelling approaches and that enables the comparison of the ESS and DR in such different models. This study fills this research gap by providing such robust method that enables the quantification of ESS and DR role under the uncertainty.

To the knowledge of the authors of this paper, no study compares the differences of the DC OPF model with and without the reserve constraints and includes ESS and DR reserve models under the demand uncertainty. A novel and original method for the comparison of energy system models is presented in this study. In addition, the presented method enables the comparison of ESS and DR roles in different models, thus provides an insight into the possible business models for providing flexibility on electric energy and reserve markets. This study hypothesises is that the inclusion of the reserve market in the power system modelling has a significant impact on the operation cost of the system as well as the operation and revenue of different stakeholders in the power system. The contributions of this study are listed below:

- A robust power system model under the demand uncertainty that includes the reserve market was modelled. The model includes the reserve models of ESS and DR.
- A comparative analysis between the joint model of electricity and reserve market and only electricity market was conducted
- A sensitivity analysis concerning different VRES share in the power system was conducted

This paper is organised in the following manner: an introduction and literature review are followed by the materials and methods section. The case study is described in the third section, the results are provided in the fourth section, the discussion in the fourth section and, in the final section, the conclusion is provided.

2. Materials and methods

This section provides a general overview of the proposed approach, a detailed mathematical representation of the models used in the paper, as well as a method for solving the proposed optimization problem.

2.1. General

The method developed in this study enables a comparison between the power system modelling with and without the reserve market. The method is designed for closed power systems, meaning that import and export were not allowed. This assumption was made because the method intends to demonstrate the operation of future power systems. These systems will include a high share of variable renewable energy sources (VRES) which means that it is assumed that the grid surrounding the observed system is also characterised by the high share of VRES. As similar VRES production can be expected for the observed system and the surrounding grid, energy exchange between the observed system and the surrounding grid is not considered.

It is assumed that the market price is equal to the marginal cost of production and reserve. The presented model is a network-constrained market clearing problem with energy dispatch as well as joint energy and reserve dispatch. The method offers the possibility to observe the impact of

the corrective actions that occur as a result of reserve market inclusion in the model. This enables the evaluation of the benefits when the reserve market is included in the energy system models that are being extensively discussed in the scientific community.

It should be noted that the study intends to focus on the role of ESS and DR in the power systems. The study aims to demonstrate the differences in the power system operation when ESS and DR are considered only in the environment of the electricity market in comparison to the case when joint electricity and reserve market. It is assumed that the transmission system operator (TSO) knows the parameters in equations (1) – (30) and that the joint electricity and reserve market is implemented. The overview of the proposed method is provided in Figure 1.

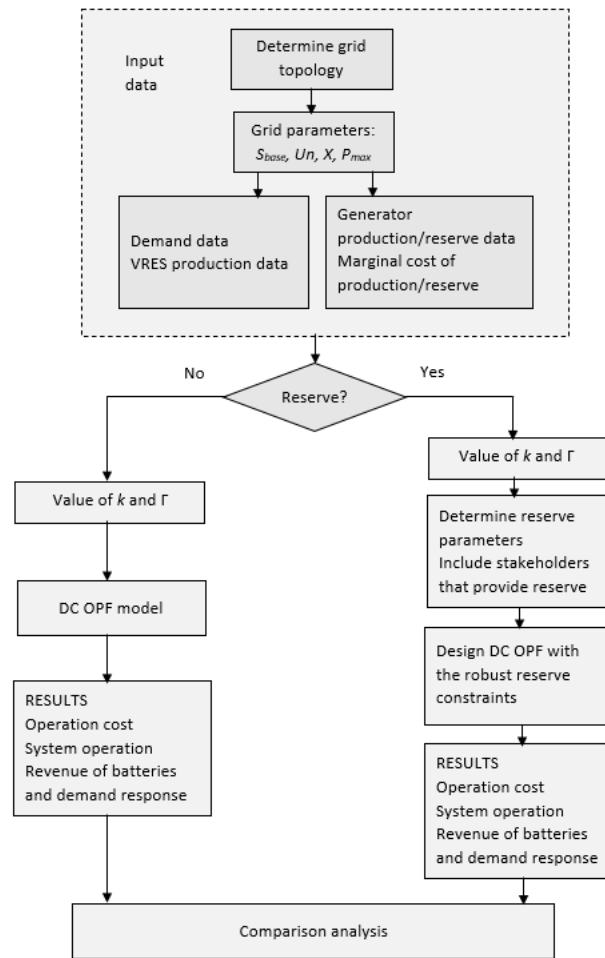


Figure 1. Flow diagram of the proposed method

2.2. Power system model without reserve market

The power system network is considered to be an undirected graph $G = (\mathcal{N}, \mathcal{E})$ where \mathcal{N} is a set of nodes and \mathcal{E} is a set of transmission lines or edges in the observed system. Other sets

include generators (\mathcal{R}), loads (\mathcal{L}), wind power plants (\mathcal{W}), photovoltaic power plants (\mathcal{S}), energy storages (\mathcal{B}) and flexible demand (\mathcal{V}). Set of all generation units is denoted as $\mathcal{G} := \mathcal{R} \cup \mathcal{W} \cup \mathcal{S}$. The power system operation is observed for the set of periods $\forall t \in \mathcal{T}$. The reactance of the transmission lines is represented with X_{ij} ($= X_{ji}$). The nomenclature can be found at the end of the paper.

Equation (1) presents the objective function of the problem. The objective function includes the cost of energy production from the regular generators and VRES, cost of load shedding (LS) and the cost of curtailed energy ($p_{i,t}^{curt}$) from the VRES. The objective of the proposed problem is to minimize the system operation cost as defined in equation (1). It should be noted that (1) will be changed when the reserve market is considered. The model includes grid constraints (2), (9) and (10), power balance at each node constraint (3), generator constraints (4)-(6), VRES constraints (7) and (8), ESS constraints (11)-(14) and DR constraints (15)-(17). The generation constraints define the ramping possibilities for the two consecutive time periods, equations (5) and (6), as well as minimum and maximum production from the units (4). The benefit of this model is that power flow balance needs to be satisfied in each node of the grid, as defined with equation (3), which is different from many other energy planning studies that do not consider the power grid as elaborated in the Introduction section. The ESS constraints (11)-(14) regulate the state of charge of the ESS at the given time period and limit the charging and discharging power of the ESS. Equation (17) ensures that the same amount of energy that is reduced as a consequence of the DR programme is retrieved. In other words, equation (17) ensures the preservation of energy. Binary variable $y_{i,t}$ was introduced to prevent simultaneous charging and discharging of the ESS, while binary variable $z_{i,t}$ was introduced to prevent simultaneous demand reduction and demand retrieval of the flexible loads. It should be noted that the constraints for the ESS and the DR will change as the reserve requirements will be included in the model. This can be seen in section 2.3. The k parameter associated with equations (7) and (8) was used to model the sensitivity analysis concerning the VRES share in the system. This will enable to observe the operation of the ESS and DR for the different share of renewables penetration in the system. For the sake of simplicity, the cost of generator production is assumed to be linear.

$$\min f \triangleq \min \sum_{t \in \mathcal{T}} \left(\sum_{i \in \mathcal{G}} p_{i,t}^G \cdot b_i + \sum_{i \in \mathcal{L}} LS_{i,t} \cdot VOLL + \sum_{i \in \mathcal{G} \setminus \{\mathcal{R}\}} CE \cdot p_{i,t}^{curt} \right) \cdot \Delta t \quad (1)$$

$$p_{ij,t} = \frac{\delta_{i,t} - \delta_{j,t}}{x_{ij}}, \quad i, j \in \mathcal{N}, \forall ij \in \mathcal{E}, \forall t \in \mathcal{T} \quad (2)$$

$$p_{i,t}^R + p_{i,t}^S + p_{i,t}^W + p_{i,t}^d - p_{i,t}^c + p_{i,t}^{drr} - p_{i,t}^{dr} - L_{i,t} = \sum_{j \in \mathcal{E}} p_{ij,t} : \lambda_{i,t}, \quad (3)$$

$$\forall i \in \mathcal{N}, \forall t \in \mathcal{T}$$

$$P_i^{min} \leq p_{i,t}^R \leq P_i^{max}, \quad \forall i \in \mathcal{R}, \forall t \in \mathcal{T} \quad (4)$$

$$p_{i,t+1}^R - p_{i,t}^R \leq RU_i, \quad \forall i \in \mathcal{R}, \forall t \in \mathcal{T} \quad (5)$$

$$p_{i,t-1}^R - p_{i,t}^R \leq RD_i, \quad \forall i \in \mathcal{R}, \forall t \in \mathcal{T} \quad (6)$$

$$p_{i,t}^W + p_{i,t}^{W,curt} \leq k \cdot \Lambda_{i,t}^W, \quad \forall i \in \mathcal{W}, \forall t \in \mathcal{T} \quad (7)$$

$$p_{i,t}^S + p_{i,t}^{S,curt} \leq k \cdot \Lambda_{i,t}^S, \quad \forall i \in \mathcal{S}, \forall t \in \mathcal{T} \quad (8)$$

$$-\frac{\pi}{2} \leq \delta_{ij,t} \leq \frac{\pi}{2}, \quad \forall ij \in \mathcal{E}, \forall t \in \mathcal{T} \quad (9)$$

$$-P_{ij}^{max} \leq p_{ij,t} \leq P_{ij}^{max}, \quad \forall ij \in \mathcal{E} \quad (10)$$

$$soc_{i,t} = soc_{i,t-1} + \left(p_{i,t}^c \cdot \eta_i^c - \frac{p_{i,t}^d}{\eta_i^d} \right) \cdot \Delta t, \quad \forall i \in \mathcal{B}, \forall t \in \mathcal{T} \quad (11)$$

$$SOC_i^{min} \leq soc_{i,t} \leq SOC_i^{max}, \quad \forall i \in \mathcal{B}, \forall t \in \mathcal{T} \quad (12)$$

$$p_{i,t}^d \leq P_i^{d-MAX} \cdot y_{i,t}, \quad \forall i \in \mathcal{B}, \forall t \in \mathcal{T} \quad (13)$$

$$p_{i,t}^c \leq P_i^{c-MAX} \cdot (1 - y_{i,t}), \quad \forall i \in \mathcal{B}, \forall t \in \mathcal{T} \quad (14)$$

$$p_{i,t}^{dr} \leq DR_{i,t}^{max} \cdot z_{i,t}, \quad \forall i \in \mathcal{V}, \forall t \in \mathcal{T} \quad (15)$$

$$p_{i,t}^{drr} \leq DRR_{i,t}^{max} \cdot (1 - z_{i,t}), \quad \forall i \in \mathcal{V}, \forall t \in \mathcal{T} \quad (16)$$

$$\sum_{t \in \mathcal{T}} p_{i,t}^{dr} = \sum_{t \in \mathcal{T}} p_{i,t}^{drr}, \quad \forall i \in \mathcal{V} \quad (17)$$

2.3. Power system model with reserve market

The complete DC OPF problem with reserve constraints included is given with the equations (2) – (30) and they form a joint electricity and reserve market clearing. It can be observed that the objective function (1) is now transformed into (18). The objective function (18) is expanded by including the cost of providing the up ($r_{i,t}^{UP}$) and down ($r_{i,t}^{DO}$) reserve from the generators, ESS and flexible loads. The objective of the problem remains to minimize the system operation costs but is defined as in equation (18). It is assumed that the marginal cost of the reserve for regular generators and ESS changes with respect to the change in the demand in the node where

generators and storage are connected. The intention is to model a simple bidding strategy that generators and storage would use to increase their revenues. Equations (19) and (20) describe the constraints for reserve requirements. Reserve requirements are defined with the current demand, wind and solar generation in the system. An increase of these values leads to higher requirements for the reserve. It should be noted that the system considers the demand to be uncertain. This means that the uncertain parameter is included in equations (19) and (20) which is why the robust model was developed as described in chapter 2.4. This allows the model to see the result parameters sensitivity with the respect to the different demand values in the system. Equations (21)-(24) are constraints for reserve provision from the regular generators, (25)-(28) are constraints for reserve provision from the ESS and (29)-(30) are constraints for reserve provision from the flexible load. It can also be seen that the generator, ESS and DR constraints were also modified in the model with included reserve constraints. Because these stakeholders (generators, ESS and DR) are participating in the reserve market, this has to be represented mathematically as well. Part of their capacity should be saved in case of reserve requirements defined by the model.

$$\begin{aligned}
\min f \triangleq \min \sum_{t \in \mathcal{T}} & \left[\sum_{i \in \mathcal{G}} p_{i,t}^G \cdot b_i^G + \sum_{i \in \mathcal{L}} LS_i \cdot VOLL \right. \\
& + \sum_{i \in \mathcal{G} \setminus \{\mathcal{R}\}} CE \cdot p_{i,t}^{curt} + \sum_{i \in \mathcal{V}} r_{i,t}^{DRR,UP} \cdot b_i^{DRR,UP} \\
& + \left(\sum_{i \in \mathcal{R}} r_{i,t}^{R,UP} \cdot b_i^{R,UP} + \sum_{i \in \mathcal{B}} r_{i,t}^{d,UP} \cdot b_i^{d,UP} \right) \left(1 + \frac{L_{i,t}}{L_i^{MAX}} \right) \\
& + \sum_{i \in \mathcal{V}} r_{i,t}^{DR,DO} \cdot b_i^{DR,DO} \\
& \left. + \left(\sum_{i \in \mathcal{R}} r_{i,t}^{R,DO} \cdot b_i^{R,DO} + \sum_{i \in \mathcal{B}} r_{i,t}^{c,DO} \cdot b_i^{c,DO} \right) \left(1 + \frac{L_{i,t}}{L_i^{MAX}} \right) \right] \cdot \Delta t
\end{aligned} \tag{18}$$

$$\begin{aligned}
\sum_{i \in \mathcal{R}} r_{i,t}^{R,UP} + \sum_{i \in \mathcal{B}} r_{i,t}^{d,UP} + \sum_{i \in \mathcal{V}} r_{i,t}^{dr,UP} & \geq J_L^{UP} \sum_{i \in \mathcal{L}} \widetilde{L}_{i,t} + J_W^{UP} \sum_{i \in \mathcal{W}} p_{i,t}^W + J_S^{UP} \sum_{i \in \mathcal{S}} p_{i,t}^S \\
& : \mu_t^{UP}, \forall t \in \mathcal{T}
\end{aligned} \tag{19}$$

$$\begin{aligned}
\sum_{i \in \mathcal{R}} r_{i,t}^{R,DO} + \sum_{i \in \mathcal{B}} r_{i,t}^{c,DO} + \sum_{i \in \mathcal{V}} r_{i,t}^{dr,DO} & \geq J_L^{DO} \sum_{i \in \mathcal{L}} \widetilde{L}_{i,t} + J_W^{DO} \sum_{i \in \mathcal{W}} p_{i,t}^W + J_S^{DO} \sum_{i \in \mathcal{S}} p_{i,t}^S \\
& : \mu_t^{DO}, \forall t \in \mathcal{T}
\end{aligned} \tag{20}$$

$$r_{i,t}^{UP} \leq p_i^{max} - p_{i,t}^R, \quad \forall i \in \mathcal{R}, \forall t \in \mathcal{T} \quad (21)$$

$$R_i^{UP-MIN} \leq r_{i,t}^{R,UP} \leq R_i^{UP-MAX}, \quad \forall i \in \mathcal{R}, \forall t \in \mathcal{T} \quad (22)$$

$$r_{i,t}^{DO} \leq p_{i,t}^R - p_i^{min}, \quad \forall i \in \mathcal{R}, \forall t \in \mathcal{T} \quad (23)$$

$$R_i^{DO-MIN} \leq r_{i,t}^{R,DO} \leq R_i^{DO-MAX}, \quad \forall i \in \mathcal{R}, \forall t \in \mathcal{T} \quad (24)$$

$$r_{i,t}^{d,UP} \leq \frac{SOC_i^{max} - soc_{i,t-1}}{\Delta t} - \frac{p_{i,t}^d}{\eta_i^d}, \quad \forall i \in \mathcal{B}, \forall t \in \mathcal{T} \quad (25)$$

$$r_{i,t}^{c,DO} \leq \frac{soc_{i,t-1} - SOC_i^{min}}{\Delta t} - \eta_i^c \cdot p_{i,t}^c, \quad \forall i \in \mathcal{B}, \forall t \in \mathcal{T} \quad (26)$$

$$r_{i,t}^{d,UP} \leq p_i^{d-MAX}, \quad \forall i \in \mathcal{B}, \forall t \in \mathcal{T} \quad (27)$$

$$r_{i,t}^{c,DO} \leq p_i^{c-MAX}, \quad \forall i \in \mathcal{B}, \forall t \in \mathcal{T} \quad (28)$$

$$r_{i,t}^{drr,UP} \leq DRR_{i,t}^{max} - p_{i,t}^{drr}, \quad \forall i \in \mathcal{V}, \forall t \in \mathcal{T} \quad (29)$$

$$r_{i,t}^{dr,DO} \leq DR_{i,t}^{max} - p_{i,t}^{dr}, \quad \forall i \in \mathcal{V}, \forall t \in \mathcal{T} \quad (30)$$

2.4. Uncertainty modelling

This paper used a robust approach for interpreting the uncertainty of the demand in the observed system. The robust approach presents an effective possibility for uncertainty modelling as it eliminates the need for modelling a large set of scenarios as is the case in the stochastic approach. It is considered that the demand value at node i and time t obtain the value in range between the minimum and maximum possible value of the demand as defined with the equation (31). This means that the minimum and maximum demand are the only input data that need to be known to model the uncertainty of the demand by using the robust approach. The input data is available from historic data as described in the Case study section.

$$\widetilde{L}_{i,t} \in U(\widetilde{L}_{i,t}) = \{\widetilde{L}_{i,t} : L_{i,t}^{min} \leq \widetilde{L}_{i,t} \leq L_{i,t}^{max}\}, \quad \forall i \in \mathcal{L}, \forall t \in \mathcal{T} \quad (31)$$

Modifying the equations (19) and (20) with the robust model results with the following equations (32) – (33). By introducing the auxiliary variables σ_i and $\varphi_{i,t}$ as well as conservativeness factor Γ_i the uncertain variable $\widetilde{L}_{i,t}$ can be replaced with the value $L_{i,t}^{min}$, $\forall i \in \mathcal{L}, \forall t \in \mathcal{T}$. This approach is described in [34]. The market-clearing process in a practical

context is based on expected demand values as well as bids from different generators. It is considered that the generators bid based on their marginal cost. In order to achieve a higher level of physical representation of the method, the market-clearing is conducted with deterministic demand values as is the case in real-time operation. The presented method allows observation of the system behaviour for various demand values when the ESS and DR are included in the joint electricity and reserve market.

Another assumption in this paper is that the perfect competition was considered. This assumption can be found in many publications, for example [35], and represents a market where all buyers and consumers have full and symmetric information. With this assumption, the Lagrange multiplier of the power balance constraint represents the electric energy price. In practical implementation, the energy prices are formed based on producers bids and expected demand. Thus, this model considers deterministic values in the power balance equation, while the uncertainty is implemented in the reserve constraints by the introduction of the auxiliary variables. This model aims to compare cases under the demand uncertainty controlled with the conservativeness factor Γ_i . Auxiliary variables σ_i and $\varphi_{i,t}$ change values as the conservativeness factor changes. For example, if the value of Γ_i is equal to zero, all the values will be contained in σ_i because of equation (34) and the most optimistic case will occur.

$$\begin{aligned} \sum_{i \in \mathcal{R}} r_{i,t}^{R,UP} + \sum_{i \in \mathcal{B}} r_{i,t}^{d,UP} + \sum_{i \in \mathcal{V}} r_{i,t}^{dr,UP} \\ \geq J_L^{UP} \sum_{i \in \mathcal{L}} (L_{i,t}^{min} + \sigma_i \cdot \Gamma_i + \varphi_{i,t}) + J_W^{UP} \sum_{i \in \mathcal{W}} p_{i,t}^W + J_S^{UP} \sum_{i \in \mathcal{S}} p_{i,t}^S : \mu_t^{UP}, \forall t \\ \in \mathcal{T} \end{aligned} \quad (32)$$

$$\begin{aligned} \sum_{i \in \mathcal{R}} r_{i,t}^{R,DO} + \sum_{i \in \mathcal{B}} r_{i,t}^{c,DO} + \sum_{i \in \mathcal{V}} r_{i,t}^{dr,DO} \\ \geq J_L^{DO} \sum_{i \in \mathcal{L}} (L_{i,t}^{min} + \sigma_i \cdot \Gamma_i + \varphi_{i,t}) + J_W^{DO} \sum_{i \in \mathcal{W}} p_{i,t}^W + J_S^{DO} \sum_{i \in \mathcal{S}} p_{i,t}^S : \mu_t^{DO}, \forall t \\ \in \mathcal{T} \end{aligned} \quad (33)$$

Equation (34) has to be considered so that the uncertainty range can be accounted for. With this equation (34), the auxiliary variables are assigned values greater or equal to the set range of the uncertain variable and the uncertainty range.

$$\sigma_i + \varphi_{i,t} \geq (P_{i,t}^{max} - P_{i,t}^{min}), \quad \forall i \in \mathcal{L}, \forall t \in \mathcal{T} \quad (34)$$

The variables of the described robust joint electricity and reserve market are provided with the (35).

$$Q = \left\{ \begin{array}{l} p_{i,t}^R, p_{i,t}^S, p_{i,t}^W, LS_{i,t}, p_{i,t}^{curt}, \delta_{i,t}, p_{ij,t}, \\ p_{i,t}^{drr}, p_{i,t}^{dr}, soc_{i,t}, y_{i,t}, z_{i,t}, p_{i,t}^d, p_{i,t}^c, r_{i,t}^{R,UP}, \\ r_{i,t}^{R,DO}, r_{i,t}^{d,UP}, r_{i,t}^{c,DO}, r_{i,t}^{drr,UP}, r_{i,t}^{dr,UP}, \sigma_i, \varphi_{i,t} \end{array} \right\} \quad (35)$$

The formulated model represents a mixed-integer problem and was solved with the CPLEX solver for continuous and discrete problems in the GAMS programming language on a 16 GB RAM machine. The model includes 6155 single variables and 144 binary variables.

2.5. Revenues for the ESS and DR under the marginal pricing

The proposed model suggests that three different commodities exist at each node. The three commodities are energy, up reserve and down reserve. Regular generators, wind and solar power plants sell the energy and the reserve can be offered by regular generators, ESS and flexible load (FL).

The defined robust optimization problem defines the market clearing process and results with the energy production and consumption of all units as well as with the up and down reserve values. The revenue of ESS and flexible load can be defined with the equations (36) and (37). The DR and ESS revenue is obtained as a sum of provided up and down reserve multiplied with the price of up and down reserve ($\mu_{i,t}^{UP}$ and $\mu_{i,t}^{DO}$) and the difference of sold and bought electricity on the market multiplied with the energy price ($\lambda_{i,t}$).

$$R_i^{ESS} = \sum_{t \in \mathcal{T}} \Delta t \cdot [\lambda_{i,t} (p_{i,t}^d - p_{i,t}^c) + \mu_{i,t}^{UP} \cdot r_{i,t}^{d,UP} + \mu_{i,t}^{DO} \cdot r_{i,t}^{c,DO}], \quad \forall i \in \mathcal{B} \quad (36)$$

$$R_i^{DR} = \sum_{t \in \mathcal{T}} \Delta t \cdot [\lambda_{i,t} (p_{i,t}^{dr} - p_{i,t}^{drr}) + \mu_{i,t}^{UP} \cdot r_{i,t}^{drr,UP} + \mu_{i,t}^{DO} \cdot r_{i,t}^{dr,DO}], \quad \forall i \in \mathcal{V} \quad (37)$$

3. Case study

The case study was conducted on the network consisted of 13 nodes and 15 transmission lines represented in Figure 2. Loads, generators (marked with the symbol for AC source), wind power plants (W), photovoltaic power plants (PV) and energy storages (ESS) can be connected to the node. The parameters for energy production units, ESS and flexible load are provided in Table 1 -Table 3. The production cost data in Table 1-Table 3 was obtained based on the report on energy production technologies [36] and [37] as well as the report on ESS [38]. The reserve costs were based on the report [39] that proposed margin cost values of the reserve for the peak and off-peak periods. It was assumed that the reserve cost from the flexible loads is significantly higher than the reserve from generators and the storage, especially for down reserve. This can be justified by the fact that the activation of the down reserve from the flexible loads would cause discomfort or loss for the industry or citizens providing it. The grid parameters for the observed system are provided in Table 4 calculated for the base power of 100 MVA. The grid parameters were obtained from [40] and represent the standard parameters of the transmission grid that include elements that operate on 110 kV voltage or higher. The reserve requirements for up and down reserve are equal and provided in Table 5. These values are specific for different parts of the grid and determined by the TSO. However, it can be assumed that these values depend on the demand, wind and PV production in the system as in [41].

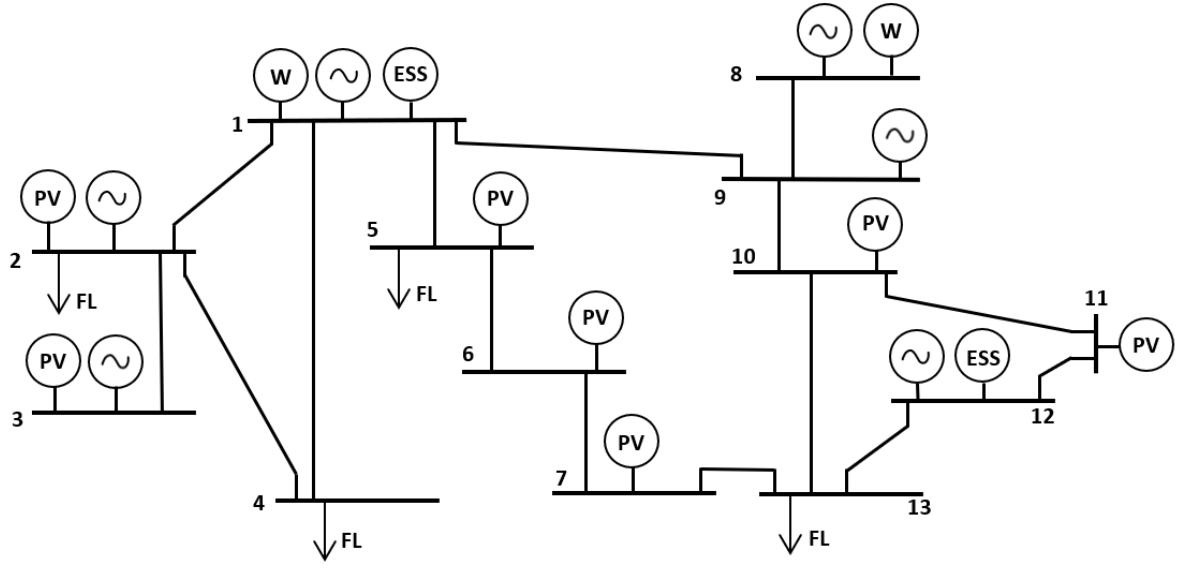


Figure 2. Grid topology of the analysed system with connection points of the production units, storage units and flexible load. The non-flexible load is present in every node but was not shown to preserve the clarity of the figure [40]

Table 1. Production unit data

Production unit	Node	P_{min} [MW]	P_{max} [MW]	RU [MW]	RD [MW]	b [€/MWh]	b^{UP} [€/MWh]	b^{DO} [€/MWh]
G1	1	10	35	17	17	65	12	8
G2	8	3	12	7	7	49	16	12
G3	9	2	10	6	6	51	18	14
G4	12	2	6	3	3	53	18	14
G5	3	2	10	6	6	55	17	11
G6	2	2	9	5	5	55	18	11
W1	1	0	12	-	-	6.8	-	-
W2	8	0	14	-	-	6.8	-	-
S1	2	0	4	-	-	5.3	-	-
S2	3	0	4	-	-	5.3	-	-
S3	5	0	6	-	-	5.3	-	-
S4	6	0	6	-	-	5.3	-	-
S5	7	0	4	-	-	5.3	-	-
S6	10	0	5	-	-	5.3	-	-
S7	11	0	3	-	-	5.3	-	-

Table 2. Energy storage system data

	Node	SOC_0 [MWh]	SOC_{min} [MWh]	SOC_{max} [MWh]	P^c_{max} [MW]	P^d_{max} [MW]	η_d	η_c	b^{UP} [€/MWh]	b^{DO} [€/MWh]
ESS1	1	4	0.8	7.2	4	4	0.97	0.98	11	11
ESS2	12	4	0.8	7.2	4	4	0.97	0.98	11	11

Table 3. Flexible load data

Flexible load	Node	DR_{max}	b^{UP} [€/MWh]	b^{DO} [€/MWh]
FL1	3	10%	30	55
FL2	9	12%	30	55
FL3	10	11%	30	55
FL4	20	10%	30	55

Table 4. Line parameters for the DC OPF model

N_i	N_j	X [p.u.]	P_{max} [MW]	N_i	N_j	X [p.u.]	P_{max} [MW]
1	2	0.0066	300	8	9	0.03388	110
2	3	0.01355	110	9	10	0.02711	110
2	4	0.03388	110	10	11	0.01694	110
1	4	0.03388	110	11	12	0.08471	110
1	5	0.08471	110	12	13	0.03388	110
5	6	0.13554	110	10	13	0.05083	110
6	7	0.23719	110	7	13	0.12149	80
1	9	0.02372	110				

Table 5. Reserve requirement parameters

Reserve requirement parameters	
J_L^{UP}, J_L^{DO}	0.05
J_W^{UP}, J_W^{DO}	0.1
J_S^{UP}, J_S^{DO}	0.05

The behaviour for the observed power system was obtained from the historical records [42], while the load data was obtained from [40]. The calculations are completed for one day on a 15-min level. The lower and upper boundaries of the load can be seen in Figure 3. The load

range boundaries were set to the 5th and 95th percentile of the analysed historical data. This ensures that 5% of the cases are under the lower boundary and that 95% of the cases are under the upper boundary. The production from renewable sources is presented in Figure 4 based on the historical values provided in [22].

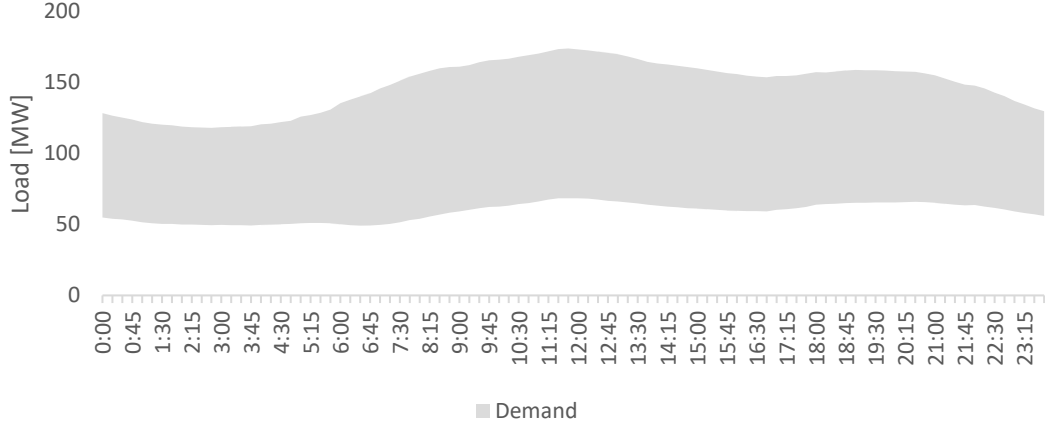


Figure 3. Load range for the observed power system

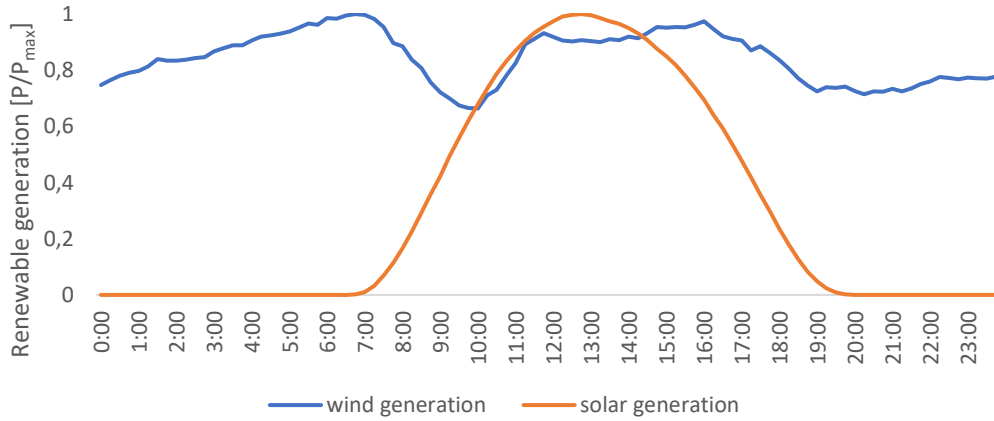


Figure 4. Generation from the renewable units

The penalty for the energy curtailment from the wind and photovoltaic power plants was assumed to be 45 €/MWh. The cost of the load shedding was set to a very high level of 10 000 €/MWh, thus ensuring the feasibility of the model.

Three different levels of VRES penetration were examined. This was modelled by adjusting the value of the k parameter. The three scenarios were the lowest VRES share ($k = 0.5$), the original scenario ($k = 1$) and the high VRES share ($k = 1.5$).

4. Results

The obtained results showed that there are significant differences in the power system operation for cases with and without the reserve market. The differences are visible for several parameters of the power system which are reported below. The results are presented in two sub-sections. The first sub-section presents the results of the comparison between models with and without the reserve market. The observed parameters include the operation cost of the system, marginal prices of energy as well as up and down a reserve, operation of the observed units in the system and detailed operation of the ESS. The second sub-section shows the revenue and the operation of ESS and DR when different levels of VRES are present in the system. The key results of the study show the necessity for reserve modelling for a more accurate representation of the energy systems as well as the need for the development of financial and regulatory frameworks for the inclusion of ESS and DR in the reserve markets.

4.1. Comparison between the model with and without RM

The operation cost of the system is illustrated in Table 6. When observing the difference between the modelling approaches, it can be seen that the inclusion of the reserve market caused the increase of the operation cost for all Γ values. This can be explained by the fact that the reserve requirements caused additional expenses because some of the capacities had to be reserved in case there would be the need for reserve activation. The reserved capacities may be used for electric energy production in the case when the reserve market is neglected. The difference in the operation cost between the modelling approaches became more expressed for more pessimistic scenarios. The maximum difference occurred for the most pessimistic scenario and increased by 28.1% in comparison to the scenario without consideration of the RM. The operation cost increased with the increase in demand conservativeness factor. This result was expected as the most optimistic case was presented for $\Gamma = 0$, while the most pessimistic case occurred for $\Gamma = 1$. The demand uncertainty had a lesser influence on the operation cost as the difference between the most optimistic case and most pessimistic was 6 095 €, while the difference for the most optimistic case when RM was considered in comparison with the case when RM was not considered was 16 836 €. This result further underlines the need for the inclusion of the RM in the energy system models. This will also become more important as the participation of different stakeholders in the provision of flexibility services will increase as a result of sector coupling.

Table 6. Operation cost for scenarios with and without RM

	Without RM	With RM ($\Gamma = 0$)	With RM ($\Gamma = 0.5$)	With RM ($\Gamma = 1$)
Operation cost [€]	59868	70609	73980	76704
Percentage change	-	17.9%	23.6%	28.1%

Figure 5 presents another interesting result of the study regarding the marginal price of power balance. Since the observed system is well interconnected, there was no congestion in the power system. As a result, the local marginal cost of the power balance was equal for each particular case. The differences in the dual variable of the power balance equation for different modelling approaches can be observed. The highest difference was equal to 0.5 €/MWh, with the highest energy cost of 13.75 €/MWh. The price difference is not significant as the market clearing was based on the deterministic demand values so that the optimization problem would have a better physical representation. However, if higher demand values would occur with less production from the renewables, one could expect higher prices of energy as marginal DR loads would have to be activated.

It should also be noted that this can influence the final electric energy price for the consumer. This price is usually dependent on many factors that include market price, taxes, distribution and transmission operator fee as well as any other fees set by the government. Increase in reserve requirements will make flexibility services more expensive which can lead to the increase of different fees as well as influence the market price of electric energy. In order to avoid dramatic increases, it is necessary to include the consumers in the energy transition process so that they are flexibility providers and that they can make revenue from providing the flexibility services. However, it is necessary to create proper regulatory and market mechanisms to enable such features. The technology for enabling such possibilities is already available as demonstrated on many research and innovation projects (e.g. [43]), however, it is necessary to invest efforts in the creation of the regulatory frameworks that will help to include consumers in the energy transition towards the decarbonised systems.

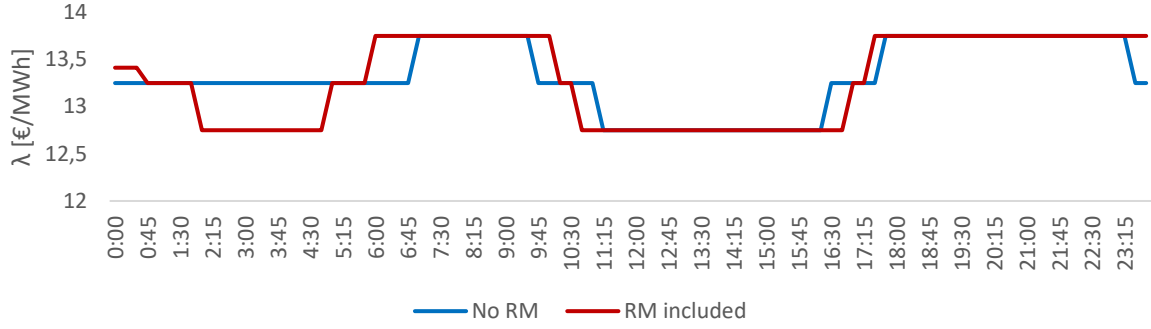


Figure 5. Marginal energy price of the observed system with and without the reserve market under the different robustness levels

Figure 6 and Figure 7 present the dual variables for the up and down reserve constraints. These dual variables represent the marginal cost of the reserve and can only be non-negative. The marginal cost of the reserve was significantly higher for the down reserve than for the up reserve. The more expensive controllable generators were mostly operating at their minimum due to the high penetration of the cheaper VRES units. Because of this, generators units were not able to provide the down reserve which means that the reserve requirements had to be met with the ESS and DR units. Although ESS units offer cheaper reserve, their capacity was not sufficient and the DR units have to be occupied for the provision of the reserve which resulted in a higher marginal cost of down reserve. This result is in line with other studies that showed that the down reserve will be more expensive than the up reserve and this is more detailly elaborated in the Discussion section.

Another finding of the paper revealed that the price of the reserve increased for more pessimistic scenarios (Figure 6 and Figure 7). For more pessimistic scenarios ($\Gamma \geq 0.5$), a sharp increase in up reserve price can be seen. The increase in marginal price occurred as the increased demand caused that units with more expensive up reserve had to provide it for that particular period.

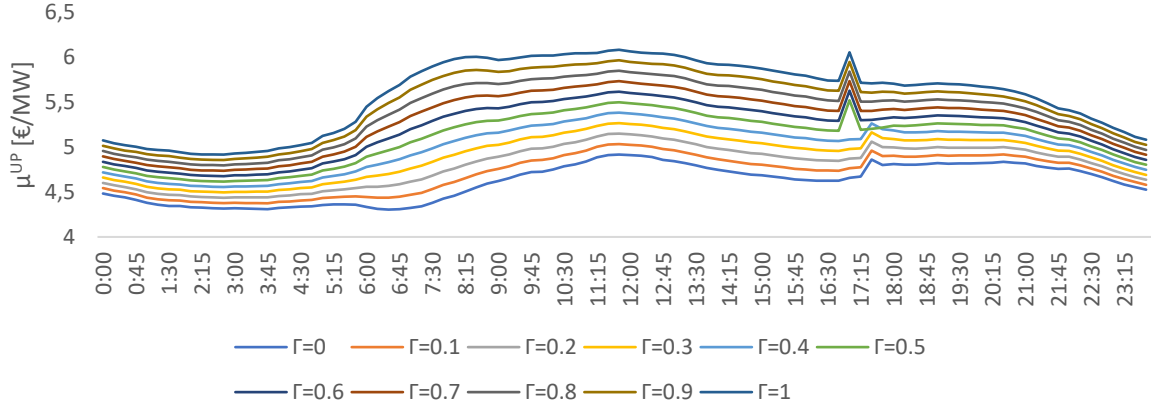


Figure 6. The marginal cost of upper reserve provision for different robustness levels

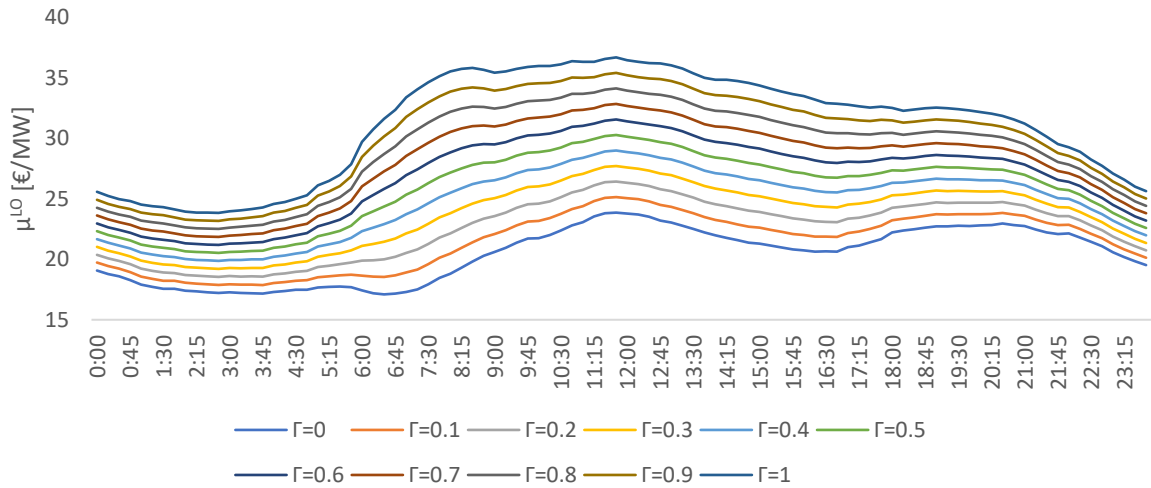


Figure 7. The marginal cost of lower reserve provision for different robustness levels

The ESS operation differs for models with and without the reserve market. Moreover, the presented spatially distributed model enables the observation of ESS units in different locations (Figure 8). This result showed that the inclusion of the reserve market in the modelling of the energy system would change the operating regime of the system as well. This means that many studies that deal with energy systems would produce different results if the reserve constraints were not neglected (e.g. [7-17]). The ESS operated differently when RM was considered as part of its capacity was preserved in order to be able to offer cheaper up reserve.

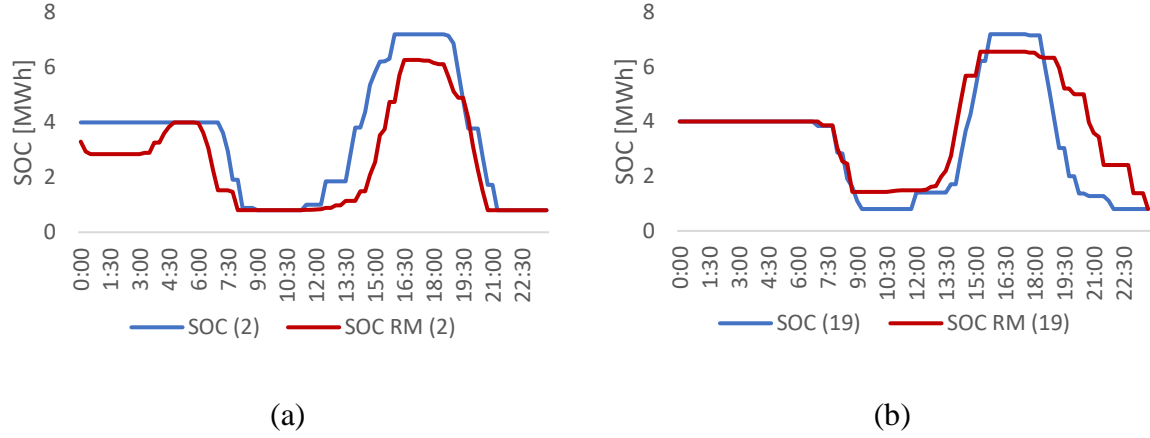


Figure 8. ESS operation at node 1 (a) and node 12 (b) for cases when the reserve market is considered (red line) and when the reserve market is not considered (blue line)

Figure 9 and Figure 10 show the overall system operation for cases with and without the RM for conservativeness factor 0.5. For the case without the RM, the DR was activated only for the marginal cases because of its' high marginal cost. The DR was not activated for the model with the reserve market because it is the marginal reserve provider. This result also showed that the model used the DR retrieval (increased demand) and charged battery during the periods of high wind and solar production. This indicates the need for flexible technologies in the systems with high VRES share.

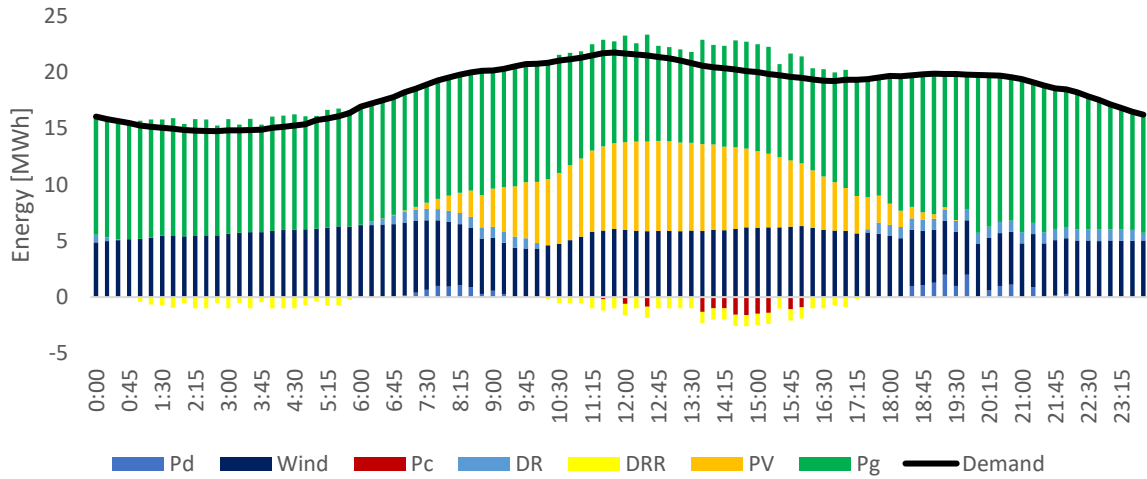


Figure 9. Energy system operation without the reserve market

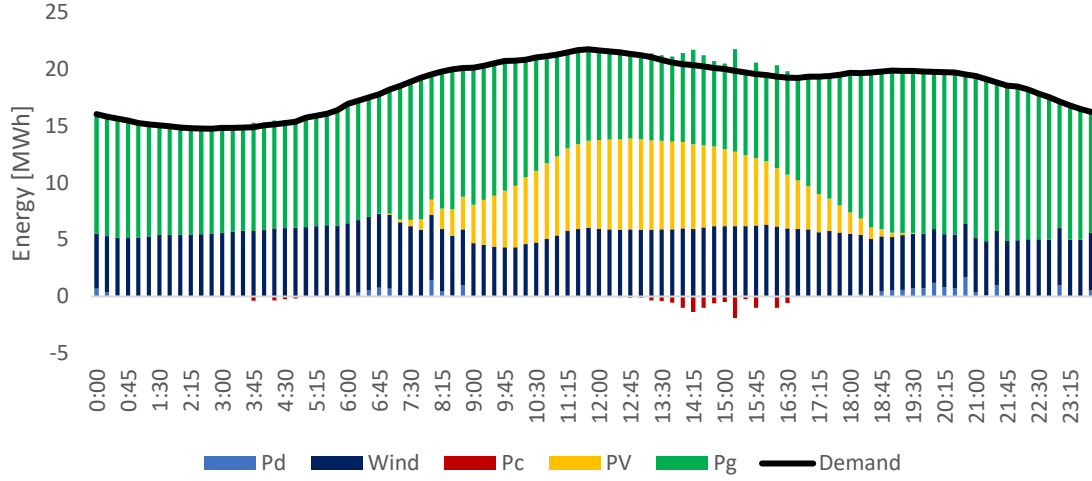


Figure 10. Energy system operation with the reserve market and conservativeness factor 0.5

4.2. Sensitivity analysis – different installed amounts of VOIE

The operation of the system was observed for three different levels of VRES installed power. The operation cost of the system was the highest for the case with the lowest share of VRES (Figure 11). This result was expected as the VRES are the cheapest units in the system although they create additional reserve requirements. Moreover, a higher share of VRES results in lower operation cost. The difference between the operation cost of the high VRES scenario ($k=1.5$) and the original scenario ($k=1$) was 15.2% for lowest demand ($\Gamma=0$) and it was 13.53% for the highest demand value ($\Gamma=1$). The results indicate that the share of VRES had a higher influence on the operation cost of the system than the demand uncertainty.

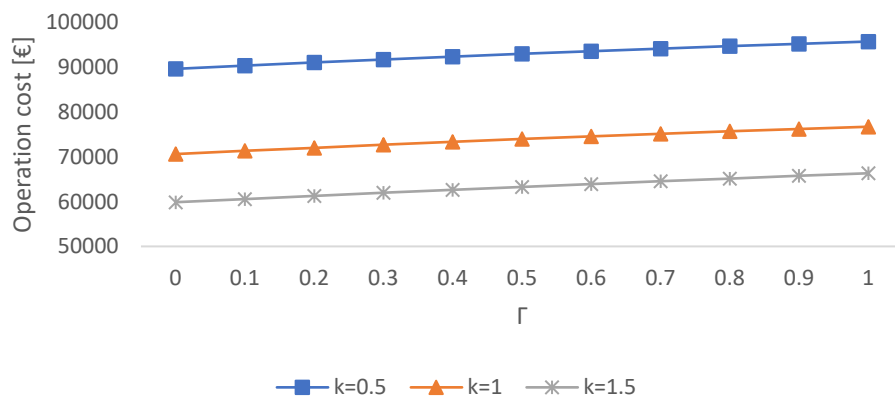


Figure 11. The operation cost of the power system for three different levels of VRES under the demand uncertainty

Another important finding of this study was that the ESS and the DR achieved significantly higher revenues when they were included in the RM. Figure 12 illustrates this result. It can be observed that the revenue increase from the reserve provision is more significant for the increase in the demand uncertainty than for the increase of VRES share. This is especially visible for the DR where the share of VRES did not significantly affect the revenue from the reserve provision. This result indicates that there is a need for sooner development of the reserve markets and the inclusion of the ESS and the DR as they can successfully contribute to the system operation even with the lower share of VRES. Additionally, frameworks that would enable the DR participation in the reserve markets would accelerate the inclusion of the citizens in the energy transition, which is one of the EU objectives.

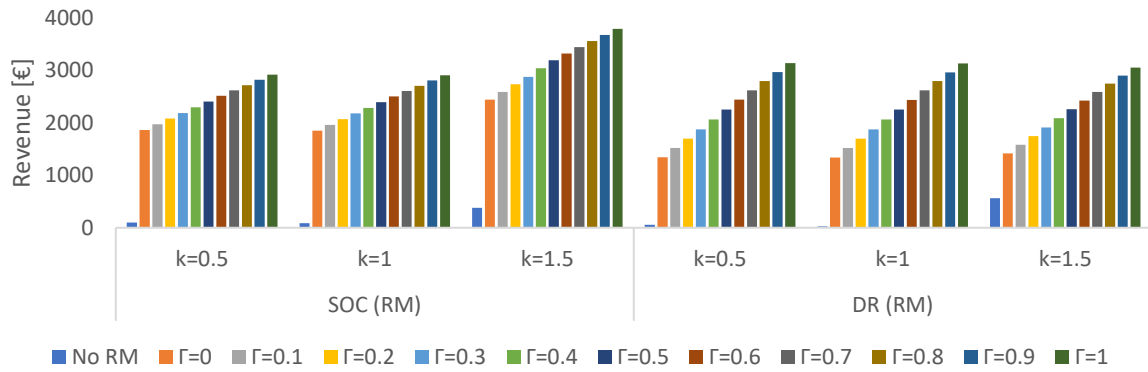


Figure 12. Energy storage and DR revenue from participation on the electric energy market and the reserve market under the demand uncertainty for different VRES levels

A complete schedule for reserve provision is provided in Figure 13 for the highest amount of VRES. It can be observed that the marginal reserve provider for the down reserve was the DR during most of the observed period. The up reserve is provided mostly from the ESS except for nine time periods (two hours and fifteen minutes) when the conventional generators participated in the reserve provision as well. The amount of required reserve does not change significantly for different periods which was expected because this was a direct consequence of the equations (19) and (20).

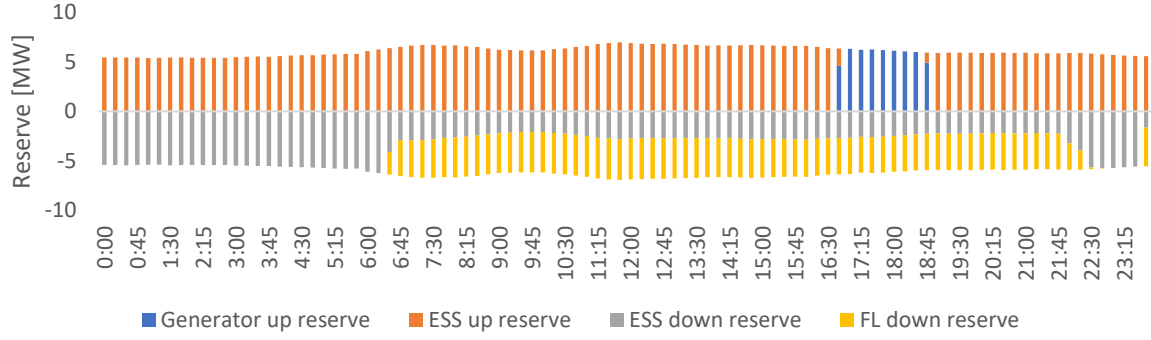


Figure 13. The reserve schedule for the observed period ($k=1.5$)

A detailed operation of the ESS in node 1 is provided in Figure 14. Interestingly, the ESS operation differs significantly for the different VRES shares. The SOC of the ESS was higher on average for the higher VRES share because there was a higher need for a down reserve. The upper reserve was provided mostly from the ESS because it can provide the cheapest reserve in comparison with the conventional generators and the DR.

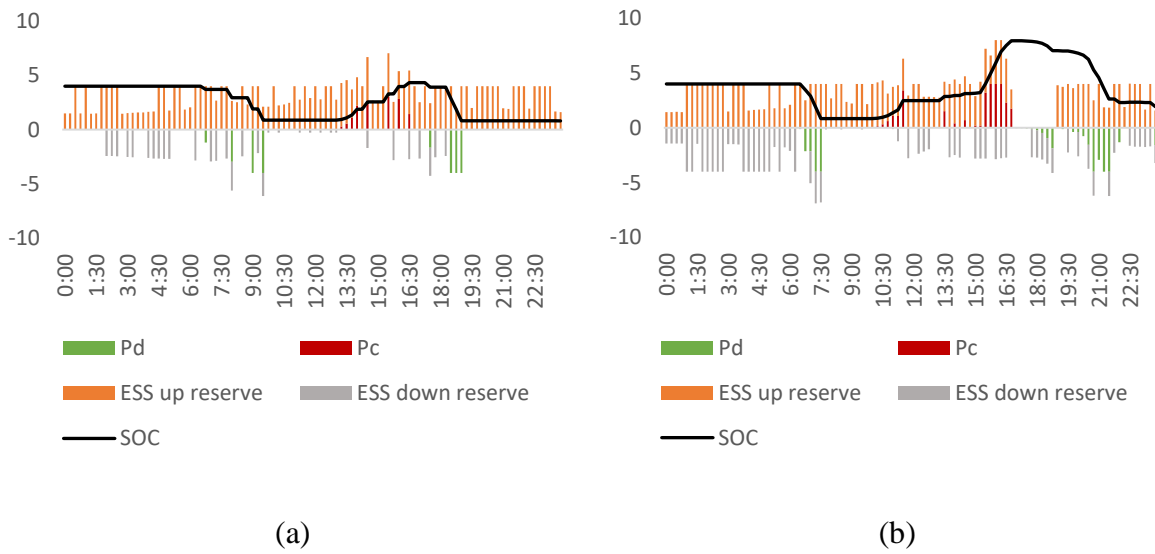


Figure 14. Battery storage operation in node 1 for different VRES shares $k=0.5$ (a) and $k=1.5$ (b) where SOC is measured in MWh and other parameters in MW

5. Discussion

One of the main objectives of this paper was to quantify the differences in power system modelling with and without the reserve market. There were three key findings of this study.

Firstly, the results showed that the inclusion of advanced technology such as the ESS and the DR in the reserve market resulted in significantly increased revenues for these stakeholders regardless of the VRES share in the system. Secondly, the proposed approach that incorporated the reserve market modelling resulted in significantly different operating parameters of the system. Finally, the results indicate the need for the development of legal and financial frameworks for the development of the reserve markets and the inclusion of different stakeholders in these markets.

To the best of the knowledge of the authors of this paper, the most extensive study on power system operation under reserve constraints was carried out in [44]. The authors found that 70% of the reserve was provided by the ESS while the marginal reserve provider for the observed period was flexible load and supplied 10% of the reserve. In this study, 69% of the overall reserve was provided by the ESS (for the $\Gamma=0.5$). However, the share of flexible demand in the overall reserve was 29% which is slightly different from the findings in [44].

The relation between the electric energy market and the reserve market in the high VRES share was investigated in [45]. The authors found that the total operation cost of the system changed between 2% and 2.5% when the PV share changed from 0-30%. The results of this study showed that the increase of VRES (PV and wind) for 50% (between $k = 1$ and $k = 1.5$ scenarios) would result in 15.2% - 13.53% lower operation cost depending on the level of conservativeness. This study also showed that the decrease of operation cost was more significant between the low share VRES scenario ($k = 0.5$) and original scenario ($k = 1$) than between high VRES ($k = 1.5$) and the original scenario. The operation cost was 21.2% lesser for the original scenario in comparison to the low VRES share scenario for the most optimistic case. This indicates that the integration of VRES in the systems with a low share of VRES would have a greater effect on the operation cost reduction than in the systems with a higher VRES share.

The changes that occurred in the operation of the observed system indicate the need for more detailed modelling of the energy systems. Current studies that offered different possibilities for the DR provision by the integration of different sectors (e.g. [46] for transport and electricity, [47] for water and electricity) illustrated the benefits of these technologies. However, the results from these studies could be expanded by applying the model from this paper. According to the results from this study, the DR technology can achieve significantly higher revenue from participation in the reserve market than in the electric energy market. This is partially related to the fact that the price of the down reserve, provided only from ESS and the DR, is significantly

higher than the upper reserve. This finding underlined the results of another study [48] that showed that the price of the down reserve can reach 93 €/MWh. The findings of this paper indicate the need for down reserve in future power systems with a high VRES share.

Moreover, this study showed that the ESS and DR achieve significantly higher revenues when they are allowed to provide the reserve. This is a valuable finding as it suggested that the inclusion of the ESS and DR on the reserve market is beneficial for all three stakeholders – ESS, DR as well as TSO. ESS and DR would be able to generate additional profit, while the TSO would have additional reserve providers.

One could argue that different reserve requirements that are dependable from one TSO to another would influence the final results of this study. Although this is a reasonable argument there are at least two reasons why this does not affect the key message of this study. First, the proposed method can be applied to any zone controlled by any TSO because the reserve requirements parameters can easily be changed. This allows any interested party can obtain its results. Second, the reserve requirements in the analysed case were set to a low value. Higher values of reserve would only increase the revenues from the reserve market, further emphasizing the findings of this study. Thus, it can be concluded that the system would operate similarly under different reserve requirements with ESS and flexible loads being significant reserve providers.

There are several limitations present in this study. Although this study introduced up and down reserve, additional types of the reserve were not considered. It can also be expected that the future energy system will be highly interconnected. This implicates that additional means of flexibility will emerge from the integration of an electric system with transport, heating, water system etc. Thus, there will be a possibility for reserve provision from a diverse spectrum of stakeholders. The representation of these stakeholders would require a more detailed model.

Finally, this study contributes to the understanding of the advanced technology role in future energy systems. The study underlines the necessity for the creation of the proper framework for the development of the reserve market, for the inclusion of the citizens in the electric energy and reserve markets and the more detailed energy and power system models.

6. Conclusion

This paper presented a novel method for the evaluation of the energy models that include the reserve market in comparison to the models without the reserve. The results of the study revealed significant differences in the two modelling approaches. Inclusion of the reserve constraints caused changes in the operating parameters of the system, marginal cost of electric energy production and revenues of the stakeholders in the system. The key findings of the study can be summarized as follows:

- The operation cost of the system increased by 16 836 € for the most pessimistic scenario with reserve market included in comparison to the scenario without the reserve market.
- The marginal cost of electric energy changed as a result of the inclusion of the reserve constraints
- The marginal cost of the down reserve was significantly higher than the marginal cost of the up reserve for all levels of VRES share in the system, which leads to the conclusion that there will be higher requirements for the down reserve units in the future due to the high excess production from the VRES
- The results showed that the revenue of ESS and flexible loads was significantly higher when they were allowed to participate in the reserve market. This indicates the need for the development of the reserve markets and the benefits of inclusion of the ESS and flexible load in the reserve market.

Future research will include more detailed modelling of different types of the reserve. It can also be expected that there will be requirements for a certain amount of inertia in future power systems with a high share of variable renewable energy sources. The inclusion of such requirements will also be a part of future research.

Acknowledgement

This work has been supported by the Young Researchers' Career Development Programme (DOK-01-2018) of Croatian Science Foundation which is financed by the European Union from European Social Fund and Horizon 2020 project INSULAE - Maximizing the impact of innovative energy approaches in the EU islands (Grant number ID: 824433). This support is gratefully acknowledged.

Nomenclature

Sets

\mathcal{N}	Set of nodes
\mathcal{E}	Set of edges
\mathcal{R}	Set of regular generators
\mathcal{W}	Set of wind power plants
\mathcal{S}	Set of PV power plants
\mathcal{G}	Set of all production units
\mathcal{L}	Set of loads
\mathcal{B}	Set of ESS
\mathcal{V}	Set of flexible loads
\mathcal{T}	Set of observed periods

Variables

$p_{i,t}^G$	Production from generators at node i at time t [MW]
$LS_{i,t}$	Load shedding value [MW]
$p_{i,t}^{curt}$	Curtailed power [MW]
$p_{ij,t}$	Power flow from node i to node j
$p_{i,t}^d, p_{i,t}^c$	Discharge and charge power from the ESS [MW]
$soc_{i,t}$	State of charge of the ESS [MWh]
$p_{i,t}^{drr}, p_{i,t}^{dr}$	Demand response retrieval and demand response power [MW]
$\delta_{i,t}$	Voltage angle at node i [rad]
$y_{i,t}, z_{i,t}$	Binary variables for ESS and flexible load
$r_{i,t}^{UP}, r_{i,t}^{DO}$	Up and down reserve at node i and time t [MW]
$\lambda_{i,t}$	The dual variable of the power balance equation
μ_t^{UP}, μ_t^{DO}	Dual variable of up and down reserve requirements equation

Parameters/notations

Δt	Difference between the two periods [h]
f	Objective function
b_i	The marginal cost of energy production [€/MWh]
$VOLL$	Value of lost load [€/MWh]
CE	Curtailed energy value [€/MWh]
X_{ij}	Reactance between node i and node j [p.u.]
S_{base}	Base power [MVA]
U_n	Nominal voltage [kV]
P_i^{min}, P_i^{max}	Minimum and maximum generator i power [MW]
RU_i, RD_i	Ramp-up and ramp-down values of the generator i [MW]
k	Sensitivity parameter related to the share of VRES
$\Lambda_{i,t}^W, \Lambda_{i,t}^S$	Forecasted wind and PV production [MW]
P_{ij}^{max}	Maximum power from node i to j [MW]
η_i^c, η_i^d	Charging and discharging efficiency of ESS
SOC_i^{min}, SOC_i^{max}	Minimum and maximum state of charge of ESS [MWh]
P_i^{c-MAX}, P_i^{d-MAX}	Maximum charging and discharging power of ESS [MW]
$DR_{i,t}^{max}, DRR_{i,t}^{max}$	Maximum demand response and demand response retrieval [MW]
b_i^{UP}, b_i^{DO}	The marginal cost of up and down reserve [€/MWh]
J_L^{UP}, J_L^{DO}	Reserve requirements parameters concerning current demand in the system
J_W^{UP}, J_W^{DO}	Reserve requirements parameters concerning wind production
J_S^{UP}, J_S^{DO}	Reserve requirements parameters concerning PV production
$R_i^{UP-MIN}, R_i^{UP-MAX}$	Minimum and maximum up reserve values of generators [MW]
$R_i^{DO-MIN}, R_i^{DO-MAX}$	Minimum and maximum down reserve values of generators [MW]

$\widetilde{L}_{i,t}$	Uncertain load variable	Γ_i	Conservativeness factor
φ_{ij}, σ_i	Auxiliary variables	R_i^{ESS}, R_i^{DR}	Revenues of ESS and flexible loads [€]

References

- [1] European Commission, “Communication from the Commission: The European Green Deal,” *COM(2019) 640 Final*, 2019.
- [2] The European Commission, “Commission Regulation (EU) 2017/2195 of 23 November 2017 establishing a guideline on electricity balancing,” *Off. J. Eur. Union*, vol. 2017, no. November, 2017.
- [3] European Parliament, “Directive (EU) 2019/944 of the European Parliament and of the Council of 5 June 2019 on common rules for the internal market for electricity,” *Official Journal of the European union*, vol. L158/125, no. 14.6.2019. 2019.
- [4] European Commission, *Clean energy for European Union islands: The memorandum of Split*. 2020.
- [5] DAFNI, “Smart Island Initiative,” *Network of Sustainable Greek Islands*, 2017. .
- [6] European Commission, “Clean energy for all Europeans Package,” *Clean energy all Eur. Packag.*, vol. 14, no. 2, 2017.
- [7] D. F. Dominković *et al.*, “Zero carbon energy system of South East Europe in 2050,” *Appl. Energy*, vol. 184, 2016.
- [8] A. P. Hilbers, D. J. Brayshaw, and A. Gandy, “Importance subsampling: improving power system planning under climate-based uncertainty,” *Appl. Energy*, vol. 251, 2019.
- [9] S. Pfenninger, “Dealing with multiple decades of hourly wind and PV time series in energy models: A comparison of methods to reduce time resolution and the planning implications of inter-annual variability,” *Appl. Energy*, 2017.
- [10] C. D. Yue, C. S. Chen, and Y. C. Lee, “Integration of optimal combinations of renewable energy sources into the energy supply of Wang-An Island,” *Renew. Energy*, vol. 86, 2016.
- [11] P. Prebeg, G. Gasparovic, G. Krajacic, and N. Duic, “Long-term energy planning of Croatian power system using multi-objective optimization with focus on renewable

- energy and integration of electric vehicles,” *Appl. Energy*, vol. 184, 2016.
- [12] A. Pfeifer, V. Dobravec, L. Pavlinek, G. Krajačić, and N. Duić, “Integration of renewable energy and demand response technologies in interconnected energy systems,” *Energy*, vol. 161, 2018.
 - [13] H. Dorotić, B. Doračić, V. Dobravec, T. Pukšec, G. Krajačić, and N. Duić, “Integration of transport and energy sectors in island communities with 100% intermittent renewable energy sources,” *Renewable and Sustainable Energy Reviews*. 2019.
 - [14] H. Meschede, M. Child, and C. Breyer, “Assessment of sustainable energy system configuration for a small Canary island in 2030,” *Energy Convers. Manag.*, 2018.
 - [15] M. Child, A. Nordling, and C. Breyer, “Scenarios for a sustainable energy system in the Åland Islands in 2030,” *Energy Convers. Manag.*, vol. 137, 2017.
 - [16] V. Taseska-Gjorgievska, M. Todorovski, N. Markovska, and A. Dedinec, “An integrated approach for analysis of higher penetration of variable renewable energy: Coupling of the long-term energy planning tools and power transmission network models,” *J. Sustain. Dev. Energy, Water Environ. Syst.*, vol. 7, no. 4, 2019.
 - [17] N. Holjevac, T. Capuder, N. Zhang, I. Kuzle, and C. Kang, “Corrective receding horizon scheduling of flexible distributed multi-energy microgrids,” *Appl. Energy*, 2017.
 - [18] I. Saviuc, K. Milis, H. Peremans, and S. Van Passel, “A cross-european analysis of the impact of electricity pricing on battery uptake in residential microgrids with photovoltaic units,” *J. Sustain. Dev. Energy, Water Environ. Syst.*, vol. 9, no. 3, 2021.
 - [19] L. Bagherzadeh, H. Shahinzadeh, H. Shayeghi, and G. B. Gharehpetian, “A short-term energy management of microgrids considering renewable energy resources, micro-compressed air energy storage and DRPs,” *Int. J. Renew. Energy Res.*, vol. 9, no. 4, 2019.
 - [20] M. Hemmati *et al.*, “Economic-environmental analysis of combined heat and power-based reconfigurable microgrid integrated with multiple energy storage and demand response program,” *Sustain. Cities Soc.*, vol. 69, 2021.
 - [21] L. Bagherzadeh, H. Shahinzadeh, and G. B. Gharehpetian, “Scheduling of Distributed Energy Resources in Active Distribution Networks Considering Combination of Techno-Economic and Environmental Objectives,” in *34th International Power System Conference, PSC 2019*, 2019.

- [22] M. Mimica, D. F. Dominković, V. Kirinčić, and G. Krajačić, “Soft-linking of improved spatiotemporal capacity expansion model with a power flow analysis for increased integration of renewable energy sources into interconnected archipelago,” *Appl. Energy*, vol. 305, p. 117855, Jan. 2022.
- [23] M. Pavičević, S. Quoilin, A. Zucker, G. Krajačić, T. Pukšec, and N. Duić, “Applying the dispa-SET model to the western balkans power system,” *J. Sustain. Dev. Energy, Water Environ. Syst.*, vol. 8, no. 1, 2020.
- [24] M. W. Hassan, M. B. Rasheed, N. Javaid, W. Nazar, and M. Akmal, “Co-optimization of energy and reserve capacity considering renewable energy unit with uncertainty,” *Energies*, vol. 11, no. 10, 2018.
- [25] N. Romero, K. van der Linden, G. Morales-España, and M. M. d. Weerdt, “Stochastic bidding of volume and price in constrained energy and reserve markets,” *Electr. Power Syst. Res.*, vol. 191, 2021.
- [26] V. C. Onishi, C. H. Antunes, and J. P. Fernandes Trovão, “Optimal energy and reserve market management in renewable microgrid-PEVs parking lot systems: V2G, demand response and sustainability costs,” *Energies*, vol. 13, no. 8, 2020.
- [27] R. Kannan, J. R. Luedtke, and L. A. Roald, “Stochastic DC optimal power flow with reserve saturation,” *Electr. Power Syst. Res.*, vol. 189, 2020.
- [28] M. Mimica, D. F. Dominković, T. Capuder, and G. Krajačić, “On the value and potential of demand response in the smart island archipelago,” *Renew. Energy*, vol. 176, 2021.
- [29] D. Al kez *et al.*, “A critical evaluation of grid stability and codes, energy storage and smart loads in power systems with wind generation,” *Energy*, vol. 205, 2020.
- [30] Ş. Kılıkış *et al.*, “Research frontiers in sustainable development of energy, water and environment systems in a time of climate crisis,” *Energy Conversion and Management*, vol. 199, 2019.
- [31] S. Massucco, P. Pongiglione, F. Silvestro, M. Paolone, and F. Sossan, “Siting and Sizing of Energy Storage Systems: Towards a Unified Approach for Transmission and Distribution System Operators for Reserve Provision and Grid Support,” *Electr. Power Syst. Res.*, vol. 190, 2021.
- [32] H. Shahinzadeh, J. Moradi, G. B. Gharehpetian, S. H. Fathi, and M. Abedi, “Optimal

- Energy Scheduling for a Microgrid Encompassing DRRs and Energy Hub Paradigm Subject to Alleviate Emission and Operational Costs,” in *Proceedings - 2018 Smart Grid Conference, SGC 2018*, 2018.
- [33] Z. Tang, J. Liu, Y. Liu, and L. Xu, “Stochastic reserve scheduling of energy storage system in energy and reserve markets,” *Int. J. Electr. Power Energy Syst.*, vol. 123, 2020.
 - [34] Y. Zhang, L. Fu, W. Zhu, X. Bao, and C. Liu, “Robust model predictive control for optimal energy management of island microgrids with uncertainties,” *Energy*, vol. 164, 2018.
 - [35] D. Kirschen and G. Strbac, *Fundamentals of Power System Economics*. 2005.
 - [36] Danish Energy Agency and Energinet, “Technology data - Energy plants for Electricity and District heating generation,” 2016.
 - [37] Danish Energy Agency and Energinet, “Technology data - Renewable fuels,” 2017.
 - [38] Danish Energy Agency and Energinet, “Technology data - Energy storage,” 2018.
 - [39] Economic Regulation Authority, “Spinning reserve ancillary service: margin values for the 2018–19 financial year,” Western Australia, 2018.
 - [40] Croatian Transmission System Operator, “Transmission grid in transmission area Rijeka (in Croatian),” 2012.
 - [41] U.S. Department of Energy - National Renewable Energy Laboratory, “Fundamental Drivers of the Cost and Price of Operating Reserves,” 2013.
 - [42] “<https://www.smard.de/home> [Accessed: 07-12-2020].” .
 - [43] “<http://insulae-h2020.eu/>.” .
 - [44] R. Mafakheri, P. Sheikhhahmadi, and S. Bahramara, “A two-level model for the participation of microgrids in energy and reserve markets using hybrid stochastic-IGDT approach,” *Int. J. Electr. Power Energy Syst.*, vol. 119, 2020.
 - [45] K. Van den Bergh and E. Delarue, “Energy and reserve markets: interdependency in electricity systems with a high share of renewables,” *Electr. Power Syst. Res.*, vol. 189, 2020.
 - [46] B. V. Mathiesen *et al.*, “Smart Energy Systems for coherent 100% renewable energy and

transport solutions,” *Applied Energy*. 2015.

- [47] H. Meschede, “Analysis on the demand response potential in hotels with varying probabilistic influencing time-series for the Canary Islands,” *Renew. Energy*, vol. 160, 2020.
- [48] K. Pandžić, I. Pavić, I. Andročec, and H. Pandžić, “Optimal Battery Storage Participation in European Energy and Reserves Markets,” *Energies*, vol. 13, no. 24, 2020.

PAPER 6

Cross-sectoral integration for increased penetration of renewable energy sources in the energy system – unlocking the flexibility potential of maritime transport electrification

Marko Mimica^{a*}, Maja Perčić^b, Nikola Vladimir^b, Goran Krajačić^a

^a*Department of Energy, Power and Environmental Engineering, Faculty of Mechanical Engineering and Naval Architecture, University of Zagreb, Ivana Lučića 5, 10002 Zagreb*

^b*Department of Naval Architecture and Offshore Engineering, Faculty of Mechanical Engineering and Naval Architecture, University of Zagreb, Ivana Lučića 5, 10002 Zagreb*

Abstract

The creation of smart energy systems is essential for the energy transition of the European Union. Electrification and smart integration of maritime transport with the power system is becoming highly important in order to successfully decarbonise maritime transportation and increase the possibility for the integration of renewable energy sources. This study presents a novel method for the analysis of maritime transportation integration with the power system. The method includes a novel model for electric ships that include all relevant engine, ship route and energy storage system aspects. By including the ship charging variable it is possible to connect the model to the distribution grid. The method provides the possibility to analyse the impact of maritime integration for different connection options and with the different shares of renewable energy sources present in the system. The study found that such smart integration can have a positive impact on the overall smart energy system. In particular, the smart integration of maritime transport with the power grid led to the reduction of curtailed energy by 3.9 MWh in the Kvarner archipelago for the maximum analysed penetration of renewable energy sources.

Nomenclature

Indices and sets

t	Time index	λ_t	Price on the electricity day-ahead market [€/MWh]
f	Ferry index	$CPV, VOLL$	Penalty for the curtailed energy and lost load [€/MWh]

i, j	Node indexes	Z_{ij}	Impedance between nodes i and j [Ω]
x	State of ship	θ_{ij}	Impedance angle between nodes i and j [rad]
k	Ferry route index	$l_{i,t}^P, l_{i,t}^Q$	Active and reactive power load [MW], [MVar]
T	Set of time periods	b	Line susceptance [μS]
N	Set of nodes	V_{min}, V_{max}	Minimum and maximum voltage values [kV]
F	Set of ferries	$\delta_{min}, \delta_{max}$	Minimum and maximum voltage angle [rad]
E	Set of edges	$\Lambda_{i,t}^{PV}$	Maximum available PV generation [MW]
S	Set of nodes with photovoltaic power plants	η_c, η_d	Battery charging and discharging efficiency
B	Set of nodes with energy storage systems	SOC_i^{min}, SOC_i^{max}	Minimum and maximum battery state of charge [MWh]
K	Set of ferry routes	Variables	
Parameters		$q_{i,t}^c$	Ship battery charging [MW]
$Q_f^{c,max}$	Maximum charging value of a ship f [MW]	$\psi_{f,t}$	Ship battery state of charge [MWh]
ψ_f^{max}	Maximum state of charge of ship battery [MWh]	$p_{i,t}^{imp}, p_{i,t}^{eks}$	Active power import and export to/from the grid [MW]
α, β	Battery parameters that define the minimum and maximum state of charge of ship battery	$q_{i,t}^{imp}, q_{i,t}^{eks}$	Reactive power import and export to/from the grid [Mvar]
μ_f^c	The efficiency of ship charging	$p_{i,t}^{PV}, p_{i,t}^d, p_{i,t}^c$	Active power production from PV, energy storage discharge and charge [MW]
τ_f	Loss of battery charge coefficient	$q_{i,t}^{PV}, q_{i,t}^d, q_{i,t}^c$	Reactive power production from PV, energy storage discharge and charge [Mvar]
$E_{f,k}^d$	Discharging from ship battery during the navigation [MWh]	$s_{ij,t}$	Apparent power [MVA]

$v_{f,d}$	Designed speed for ship f [kn]	$p_{i,t}^{PVC}$	Curtailed power from PV plants [MW]
$v_{f,ave}$	The average speed of ship f [kn]	$ls_{i,t}$	Load shed [MW]
$P_{f,ave}$	Average ship f operating capacity [MW]	$p_{ij,t}, q_{ij,t}$	Active and reactive power flow [MW], [MVar]
$P_{f,MEave}$	Average main engine capacity [MW]	$V_{i,t}$	Voltage at node i and time t [kV]
$P_{f,AEave}$	Average auxiliary engine load [MW]	$\delta_{i,t}$	Voltage angle at node i [rad]
l_k	The length of the route k [nm]	$i_{ij,t}$	Current through the line ij [A]
EC_f	Average energy consumption of ship f per distance [MWh/nm]	$soc_{i,t}$	State of the charge of the battery [MWh]
		OF	Objective function

Introduction

Environmental requirements regarding the Greenhouse Gases (GHGs) reduction forced the International Maritime Organization (IMO) towards setting an emission reduction target of 50% of annual GHG emissions from international shipping by 2050, compared to the 2008 levels [1]. According to the IMO decarbonization strategy, there are three levels of ambitions: short-term (2018-2023), mid-term (2023-2030) and long-term (2030-) ambitions. While the short-term ambitions refer to the beginning of GHGs reduction by tightening the Energy Efficiency Design Index (EEDI) or application of voluntary speed reduction, which results in lower fuel consumption and consequently significant GHGs reduction, the mid-term ambitions cover measures of the introduction of efficiency index for existing ships, i.e. Energy Efficiency Existing Ship Index (EEXI) [2], implementation of market-based measures and introduction of low-carbon fuels. The long-term ambitions focus on GHGs reduction up to 50% and higher, which is achievable with the development of innovative emission reduction technologies. Moreover, to achieve the ultimate GHGs reduction up to zero emissions from the international shipping sector by the end of this century, the development of zero-carbon fuels or carbon-neutral fuels is required [3]. These fuels, particularly hydrogen, ammonia, electricity, e-fuels, biofuels, etc., are investigated in a study by Korberg et al. [4] as advanced fuels for fossil-free ships, among which an electricity-powered ferry is highlighted as the most cost-effective option that offers zero-emission shipping, i.e. absence of tailpipe emissions during ship operation.

Although there are three different types of electrified ships, i.e. a hybrid ship, a plug-in hybrid ship and a full-electric ship, only the latter provide total elimination of the tailpipe emissions since it is powered by only energy storage [5]. Among different energy storage options, the implementation of a battery represents a better solution due to its high energy density and lower costs [6], where currently the most prominent battery for the maritime sector is Lithium-ion (Li-ion) battery [7]. Despite safe energy supply and mature technology, the main drawbacks of battery-powered ships are battery degradation, charging infrastructure and charging schedule [4]. Moreover, Gagatsi et al. [8] highlighted that the great disadvantage of the use of a battery for powering the ship is the limited range on which the ship can operate without recharging the battery. Battery-powered ships are currently only suitable for short-range routes in short-sea shipping, while the emission reduction for long-distance ships is achievable with other alternative low-carbon fuels [9]. However, with further development of metal-air batteries that have significantly higher energy density than a Li-ion battery [10], the full electrification of long-distance ships by using only a battery may be feasible.

The Life Cycle Assessment (LCA) has been widely used in many industries, as well as in the maritime industry [11]. Although battery-powered ships do not emit pernicious gases during navigation, when performing an environmental analysis of a ship, the main focus is put on the emissions generated by electricity production [12]. Perčić et al. [13] performed LCA and Life-Cycle Cost Assessment (LCCA) comparisons of nine different marine fuels implemented onboard three ferries operating in the Adriatic Sea and indicated that the battery-powered ship is the most environmentally friendly and cost-effective option among those investigated. Similar results are highlighted in a study by Wang et al. [14]. They performed LCA and LCCA comparisons of battery-powered catamaran ferry compared to the conventional ferry and indicated that fully electrification of the ship results in lower life-cycle GHG emissions and lifetime costs. The battery-powered ship is even more environmentally friendly when it is powered by electricity produced from RESs [13]. However, the available RESs in the coastal regions are often intermittent (solar, wind, waves) so special attention should be given to their integration into the new energy system. This is done by sector coupling and energy storage integrated into Smart energy systems. Sectors like electricity and transport were operated separately while increased electrification and development of digital technologies allowed their integration and optimisation in a new very complex and diverse environment. Smart energy systems must be supported by different platforms that will allow optimal energy and economy flows and business models for the flexibility provided by many new market players.

The analysis of energy systems has been widely conducted in the course of the previous two decades [15]. The importance of the energy planning models as decision support tools was emphasized in [16]. The EnergyPLAN tool was widely used for the smart energy system analysis as in [17] where the authors showed that there was no curtailed energy for the smart electrification scenario for the Madeira in comparison with the simple electrification scenario that had to curtail 7% of the production. The RenewIslands method was presented in [18] for analysing the effects of cross-sector integration on the islands. The approach presented in [19] analysed the microgrid operation with the availability of RES modelled as a chance constraint and found that the risk levels of not meeting (or exceeding) the energy demand higher than 30% did not correlate with additional microgrid benefits. The method for risk assessment of energy planning scenarios on islands was developed in [20], where the authors found that the zero import risk scenario for Unije island required a 3.5 MWh battery and a 0.5 MW PV plant. The tools for the meteorological forecasting that improve the energy planning process are also under development such as the FORCALM tool [21] demonstrated in the Sicily case.

The term flexibility is widely used by different authors in many recent studies in order to demonstrate the ability of smart energy systems to adapt their operation in order to reduce the cost of system operation [22]. Thus, the authors of the reported studies use the term flexibility to describe the energy management flexibilities of the system (e.g. inclusion of the battery system would increase the possibilities for energy management, thus would increase the flexibility of the energy system). However, the flexibility in the power systems is not related only to the energy, but also to the voltage flexibility, power or capacity flexibility and the flexibility in transmission capacity import and export. For the distributions systems, voltage flexibility and energy management flexibility are relevant as the installed capacities and capacity import and export are insignificant with the respect to the transmission system. Although this is the case, the authors of the reported studies considered only energy management flexibility. This study analyses also the voltage flexibility with a focus on maritime transportation, which is an important research contribution.

The recent energy planning methods focused more on flexibility and the demand response as in [23], where the authors concluded that the investments in microgrid reduce by 10.9% as a result of demand response implementation. The presented methods and tools include the effects of the flexibility sources on the energy planning scenarios, however, they did not provide a detailed technical assessment and implementation possibilities of different flexibility solutions. The significant operational changes that occur as a result of the flexibility provision, especially

from the large facilities (e.g. from industry facilities or maritime transportation as in this paper) can influence the conditions in the electric power grid. In this paper, the model that implemented relevant constraints imposed by the distribution system (e.g. voltage limits or power flow limits) was provided. This enabled the detailed evaluation of the electric and maritime sector integration, which was not previously done in the literature.

The study [24] showed that possible flexibility capacity as a result of a cross-sector integration is equal to 2.33 MW for the Krk island and 0.3 MW for the Vis island, however without specifying the contribution of maritime electrification to the systems' flexibility. Several studies proposed strategies for small islands decarbonisation, such as [25] on the example of the island of Ustica, however without the consideration of maritime electrification. A similar study was conducted for Cyprus [26] where the results showed that installation of 3 kW rooftop PV on 50% of households would require additional 191 MW for covering the entire electricity demand. Another study [27] concluded that the transition from diesel-based to photovoltaics-battery diesel hybrid system of the Philippines off-grid energy systems can decrease the levelized cost of electricity by 20%. The road transport integration with other sectors was considered in [28] for the Caribbean island, with the conclusion that 78% of demand can be covered by RES with 1% of curtailed energy. The studies [15 – 27], however, did not include the electrification of the maritime transport and its integration with other sectors in their analysis. In this paper, this knowledge gap was filled by placing a focus on the maritime transport in the analysis of cross-sector integration.

To the best of the authors' knowledge, there is no method that used the proposed mathematical model for electrified maritime transport and simultaneously integrated it into the detailed distribution system model in order to assess the impacts and consequences of smart cross-sector integration of maritime transport and electric power system. The proposed method enables the observation of electric system operation variables such as voltage, losses, operation cost, curtailed energy, battery system operation as well as the operation and charging schedule of electric ships under different energy storage and RES penetration values. A novel electric ship model includes parameters regarding the ships' engine characteristics, route and energy storage system (ESS) specifications with charging variables modelled so that the model can be integrated into the distribution system. The importance of the proposed approach is in its ability to provide insight into the flexibility of energy as well as voltage while considering relevant ship and maritime parameters. The main contributions of the study are:

- A novel mathematical model for the electric ship operation
- An integrated model of electrified maritime transport with the electric distribution grid
- Sensitivity analysis for different RES penetration shares

The rest of the paper is organized as follows- After the Introduction, the Materials and methods section is presented. The third section presents the results of the study. The Discussion is presented in the fourth section. The final section is the Conclusion.

Materials and methods

General overview

This paper presents a novel method for the evaluation of smart cross-sector integration of electrified maritime transport and the electric power system. The method can be used for the comparison of different scenarios that include maritime electrification with the traditional electric power systems. Moreover, the method enables the evaluation of such cross-sector integration in a different environment (e.g. connection of the ESS with the electric chargers or assessment with respect to different RES penetration). The method is divided into two key parts:

- Defining the mathematical model of the electric ship
- Defining the mathematical model of the observed energy system and including the electric ship model in the energy system

The proposed method is illustrated in Figure 1 and more detailly explained in the rest of the Materials and Methods chapter.

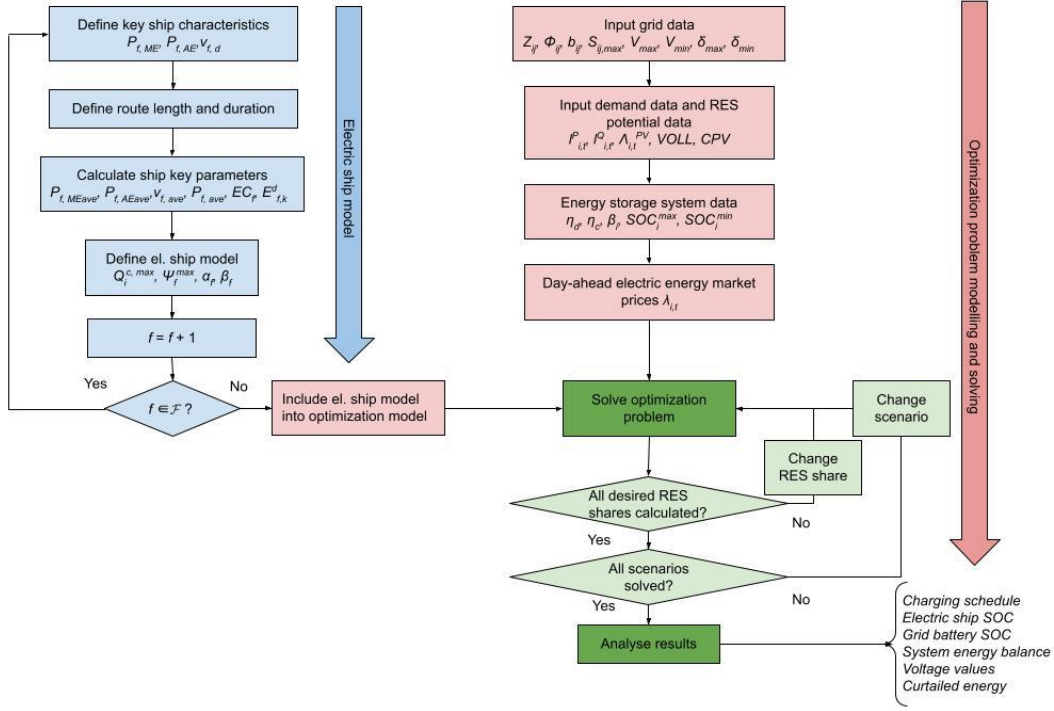


Figure 1. The proposed method for evaluation of maritime electrification

Electric ship mathematical model

Ships are designed to operate at certain speeds, i.e. design speeds ($v_{f,d}$), which corresponds to 70%–80% of the main engine load [29]. However, due to the rough weather conditions, strict operating schedule, voluntary speed reduction and others, the operating speed of a ship often differs from the design speed. The average operating speed of a ship ($v_{f,ave}$), can be calculated by dividing known route length by its duration. By considering the cubic relationship between ship speed and power, the average main engines capacity ($P_{f,MEave}$), is calculated with the equation (1) [13].

$$P_{f,MEave} = (P_{f,ME} \cdot 0.8) \cdot \left(\frac{v_{f,ave}}{v_{f,d}} \right)^3 \quad (1)$$

The average auxiliary engines power is calculated with the assumption that the average load of these engines is 50%. The total average ship power ($P_{f,ave}$), is calculated with the equation (2):

$$P_{f,ave} = P_{f,MEave} + P_{f,AEave} \quad (2)$$

The average energy consumption per distance, EC (kWh/nm), of an existing diesel-powered ship is calculated as follows:

$$EC_f = \frac{P_{f,ave}}{v_{f,ave}} \quad (3)$$

The energy consumption of a ship on a one-way route k is then described with the equation (4).

$$E_{f,k}^d = EC_f \cdot l_k \quad (4)$$

The l_k represents the length of a route k , $\forall k \in \mathcal{K}$. The capacity of ships' battery storage needs to be sufficient enough to ensure the ship's navigation on a particular route. Therefore, the battery parameter – maximum state of charge (ψ_f^{max}) has to be chosen so that the ship has enough energy to navigate to the next charging station, respect the timeline and account for the safety margins that reduce the negative effects of battery degradation (denoted with α and β).

For every ship, there are three different states $x_{f,t} \in \{0,1,2\}$, $\forall f \in \mathcal{F}$, $\forall t \in \mathcal{T}$, where $x_{f,t} = 0$ is assigned to the ship in port and not charging, $x_{f,t} = 1$ to the ship in the port and charging and $x_{f,t} = 2$ for the ship $f \in \mathcal{F}$ that is sailing at time $t \in \mathcal{T}$. The full mathematical model of the electric ship can then be described with equations (5) – (7).

$$\psi_{f,t} = \begin{cases} (1 - \tau_f) \psi_{f,t-1}, & x_{f,t} = 0 \\ \psi_{f,t-1} + q_{i,t}^c \mu_{i,f}^c \Delta t, & x_{f,t} = 1 \\ \psi_{f,t-1} - E_{f,k}^d, & x_{f,t} = 2 \end{cases} \quad (5)$$

$$q_{i,t}^c \begin{cases} \leq Q_i^{c,max}, & x_{f,t} = 1 \\ = 0, & else \end{cases} \quad (6)$$

$$\alpha_f \psi_f^{max} \leq \psi_{f,t} \leq \beta_f \psi_f^{max} \quad (7)$$

The state of charge of ships' battery ($\psi_{f,t}$) is given with the equation (5) and is dependent on the current state of the ship ($x_{f,t}$). The energy loss of battery when the ship is in port is modelled with a coefficient (τ_f). When in the port ($x_{f,t} = 1$), the ship is charged on a charger i with charging power $q_{i,t}^c$ and efficiency of the ship charger $\mu_{i,f}^c$. The ships' energy consumption of ferry f , on the route k is described with $E_{f,k}^d$. This amount of energy ($E_{f,k}^d$) is reduced from the ship's battery during the sailing time of the ship ($x_{f,t} = 2$) which results in the decrease of the ship's battery state of charge ($\psi_{f,t}$). Equation (6) describes the charging capacity ($q_{i,t}^c$) that has

to be less or equal to the maximum charging capacity ($Q_f^{c,max}$) for $x_{f,t} = 1$ and zero for other cases.

Mathematical model of the distribution system

The mathematical model used for the description of the energy system is a feasible non-linear optimisation problem. The model includes equations based on realistic constraints imposed by the distribution grid. The formed model is an NLP model solved in the GAMS tool with a CONOPT solver. The solver is suited for non-linear problems, especially effective for small-scale problems. Although the presented approach does not provide a solution with a global optimum, its results are sufficient for achieving the objectives of this paper, especially for the smaller distribution systems. The objective of the problem is to minimize the objective function OF defined in a manner described in equation (8).

$$\min OF \triangleq \min \left[\sum_{t \in T} \sum_{i \in N} \lambda_t (p_{i,t}^{imp} - p_{i,t}^{eks}) + CPV \sum_{t \in T} \sum_{i \in N} p_{i,t}^{PVC} + VOLL \sum_{t \in T} \sum_{i \in N} ls_{i,t} \right] \cdot \Delta t \quad (8)$$

Three types of costs are recognized in this method. The difference between the import and export ($p_{i,t}^{imp}, p_{i,t}^{eks}$) multiplied with the price on the day-ahead electricity market (λ_t) represents the first cost. Another cost is curtailed energy from RES ($p_{i,t}^{PVC}$) multiplied with a penalty for energy curtailment (CPV). Finally, the third cost is related to the lost load ($ls_{i,t}$) multiplied with the penalty or value of lost load ($VOLL$). The sum of these costs represents the overall cost of operation of the observed system.

The electric distribution grid constraints are introduced with equations (9) – (17). The constraints include a set of nodes and edges (lines or transformers). Afterwards, the renewable generation and the ESS are modelled (18) – (22). The input and output active and reactive power have to be equal at each node. This is modelled with equations (9) and (10), $\forall i \in \mathcal{N}, ij \in \mathcal{E}, \forall t \in \mathcal{T}$.

$$p_{i,t}^{imp} - p_{i,t}^{eks} + p_{i,t}^{PV} + p_{i,t}^d - p_{i,t}^c - l_{i,t}^P - q_{i,t}^c = \sum_j p_{ij,t} \quad (9)$$

$$q_{i,t}^{imp} - q_{i,t}^{eks} + q_{i,t}^{PV} + q_{i,t}^d - q_{i,t}^c - l_{i,t}^Q = \sum_j q_{ij,t} \quad (10)$$

The active power flow over between two nodes $ij \in \mathcal{E}$ is defined with the voltage at the beginning and the end of the line as well as the impedance of the line as in equation (11), $\forall ij \in \mathcal{E}, \forall t \in \mathcal{T}$. The active power flow is calculated as a squared voltage at the beginning node divided by the impedance minus the multiplication of beginning and end node voltage divided by the impedance. The expressions have to be multiplied by trigonometric function cosine because the active power ($p_{ij,t}$) represents a real part of the apparent power ($s_{ij,t}$). In addition to the parameters in (11), the reactive power flow is also defined with the susceptance as in equation (12), $\forall ij \in \mathcal{E}, \forall t \in \mathcal{T}$. Since the reactive power represent the imaginary part of the apparent power the expressions have to be multiplied by the sinus trigonometric function. The expression with susceptance (b) has to be also included in (12) because of the capacitive contributions of the lines.

$$p_{ij,t} = \frac{V_{i,t}^2}{Z_{ij}} \cos(\theta_{ij}) - \frac{V_{i,t}V_{j,t}}{Z_{ij}} \cos(\delta_{i,t} - \delta_{j,t} + \theta_{ij}) \quad (11)$$

$$q_{ij,t} = \frac{V_{i,t}^2}{Z_{ij}} \sin(\theta_{ij}) - \frac{V_{i,t}V_{j,t}}{Z_{ij}} \sin(\delta_{i,t} - \delta_{j,t} + \theta_{ij}) - \frac{bV_{i,t}^2}{2} \quad (12)$$

The apparent power flow between the two nodes is defined as a product of voltage and a complex conjugate of the current as in equation (13). Upper and lower values of the apparent power are defined with equation (14). Finally, the current ($i_{ij,t}$) between the nodes i and j is defined with the equation (15). The current is defined as the voltage difference between nodes i and j divided by the impedance between i and j with added capacitive currents defined by the susceptance (b). It should be noted that $s_{ij,t} \neq s_{ji,t}$, $\forall ij \in \mathcal{E}, \forall t \in \mathcal{T}$, and the difference between these two variables represent the losses of the system.

$$s_{ij,t} = (V_{i,t} \angle \delta_{i,t}) i_{ij,t}^* \quad (13)$$

$$-S_{ij,max} < s_{ij,t} < S_{ij,max} \quad (14)$$

$$i_{ij,t} = \frac{V_{i,t} \angle \delta_{i,t} - V_{j,t} \angle \delta_{j,t}}{Z_{ij} \angle \theta_{ij}} + \frac{bV_{i,t}}{2} \angle \left(\delta_{i,t} + \frac{\pi}{2} \right) \quad (15)$$

The minimum and maximum voltage values are given with equation (16), $\forall i \in \mathcal{N}, \forall t \in \mathcal{T}$, while the maximum voltage angle difference between the two nodes is given with (17), $\forall ij \in \mathcal{E}, \forall t \in \mathcal{T}$.

$$V_{min} \leq V_{i,t} \leq V_{max} \quad (16)$$

$$\delta_{min} \leq \delta_{ij,t} \leq \delta_{max} \quad (17)$$

The sum of produced energy and curtailed energy from the PV has to be equal to the overall production potential of the production from PV as in equation (18), $\forall i \in S, \forall t \in \mathcal{T}$.

$$p_{i,t}^{PV} + p_{i,t}^{CPV} = \Lambda_{i,t}^{PV} \quad (18)$$

The mathematical model of the ESS is given with equations (19) – (22), $\forall i \in \mathcal{B}, \forall t \in \mathcal{T}$. Equation (19) models the state of charge of the battery system. Maximum and minimum states of charge values are given with equation (20). Finally, maximum values of charging and discharging power of the ESS are given with equation (22).

$$soc_{i,t} = soc_{i,t-1} + (p_{i,t}^c \cdot \eta_c - \frac{p_{i,t}^d}{\eta_d}) \cdot \Delta t \quad (19)$$

$$SOC_i^{min} \leq soc_{i,t} \leq SOC_i^{max} \quad (20)$$

$$p_{i,t}^c \cdot \Delta t \leq \beta_i \cdot SOC_i^{max}, \beta_i \in [0,1] \quad (21)$$

$$p_{i,t}^d \cdot \Delta t \leq \beta_i \cdot SOC_i^{max}, \beta_i \in [0,1] \quad (22)$$

Case study

The case study in this research was conducted on the example of the Kvarner archipelago. The electrification of two Croatian ferries that operate on ferry line Valbiska-Merag, which connects the island of Krk with the island of Cres was investigated in this paper. The route length is 3.62 nm, while its duration is 25 min [30]. The ship specifications are obtained from the Croatian Register of Shipping [31] and presented in Table 1.

Table 1. Ship specifications

Ship's name	Kornati	Krk
Length between perpendiculars (m)	89.1	89.1
Breadth (m)	17.5	17.5
Draught (m)	2.40	2.40
Main engine(s) power, P_{ME} (kW)	1764	1764
Auxiliary engine(s) power, P_{AE} (kW)	840	1080
Design speed, v_{de} (knot)	12.3	12.3
Passenger capacity	616	616
Vehicle capacity	145	145

The observed electric power system is part of both the transmission and the distribution system (Figure 2). It is characterised by two main substations Krk 110/35 kV (between bus 1 and 2) connected to the mainland and Lošinj 110/35/10.5 kV (three winding between bus 12 and 13). A 110 kV line is connecting these two substations. On the lower voltage side of these transformers, a distribution system is connected. The 1 MW PV plant and 0.4MW/1.6MWh ESS are connected on the island of Unije (bus 23). Additionally, a 6.5 MW PV plant Orlec is installed at bus 7. This is considered to be a base case scenario (later noted as a 25% RES scenario).

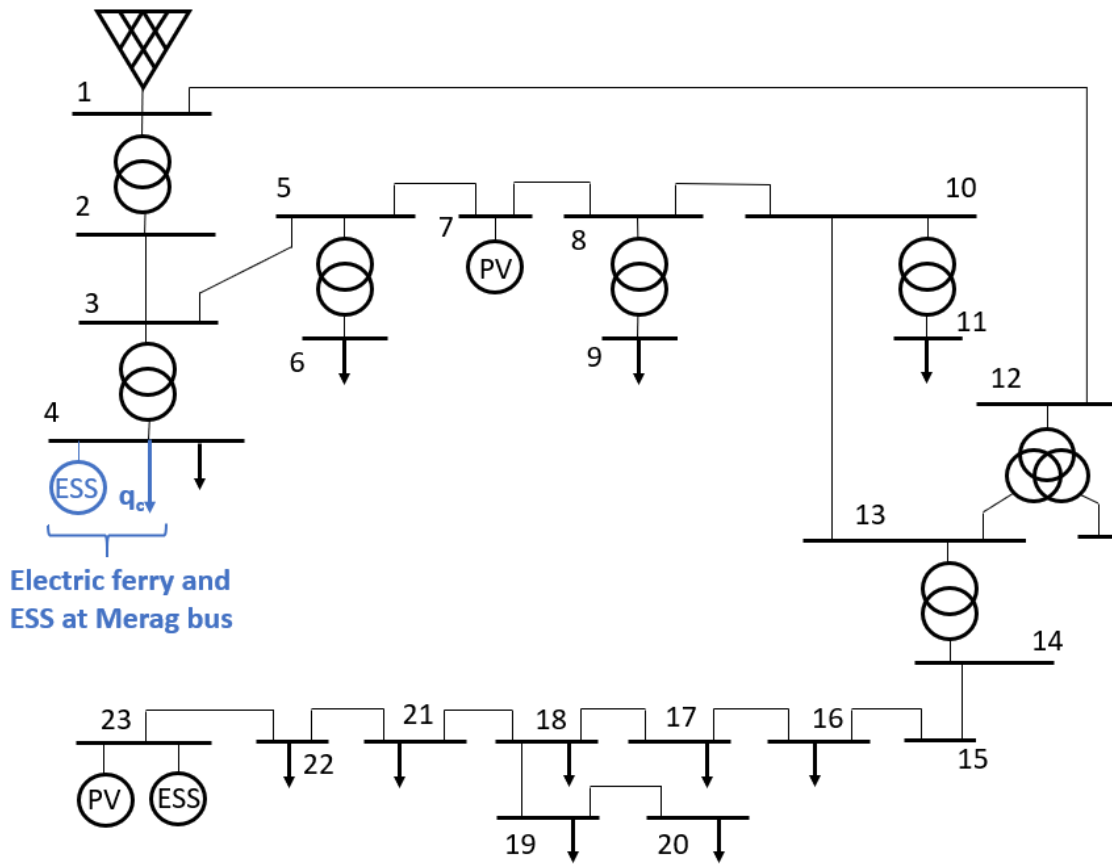


Figure 2. Scheme of the electric power system of the Kvarner archipelago

The demand and PV production as well as the data about grid elements were obtained from [33] (Table 2 and Table 3). The day-ahead market prices are available from the Croatian day-ahead market [34]. The elements of the system are modelled with detailed electrical parameters that include resistance, reactance, susceptance, voltage, types of windings and nominal capacities. The per-unit method [pu] was used for the expression of system characteristics in order to avoid

changes in system characteristics when referred from one side of the transformer to another (different voltage levels). The rest of the parameters used in the case study are provided in Table 4.

Table 2. Data about the lines in the system

<i>i</i>	<i>j</i>	Type	Length (km)	Voltage [kV]
2	3	Cu 3x150	10	35
3	5	Cu 3x50	15.64	35
1	12	AlČ 3x150	65	110
5	7	Cu 3x50	7	35
7	8	Cu 3x50	10	35
8	10	Cu 3x50	13.511	35
10	13	Cu 3x50	13.752	35
14	15	XHE 49-A 3x(1x185)	0.595	10
15	16	XHE 49-A 3x(1x150)	0.41	10
16	17	XHE 49-A 3x(1x150)	2.42	10
17	18	XHE 49-A 3x(1x185)*	5.567	10
18	19	RGS5H-10 JF 3x70	6.931	10
19	20	XHP 48-A 3x(1x95)	0.61	10
18	21	RGS5H-10 JF 3x70	3.024	10
21	22	RGS5H-10 JF 3x70*	7.353	10
22	23	XHE 49-A 3x(1x185)	1.2	10

**consisted of more line types, the longest one is taken*

Table 3. Transformer data in the observed grid

<i>i</i>	<i>j</i>	$u_k\%$	Type	Nominal capacity [MVA]
1	2	9	Yd5	8
3	4	4	Yd5	4
5	6	5.8	Yd5	8
8	9	5.8	Yd5	8
10	11	5.8	Yd5	8
12	13	11	YNyn0d5*	20
13	14	5.8	Dyn5	2.5

**three-winding transformer*

Table 4. Parameters used in the case study

Parameter	Value
η_d, η_c	0.95
μ^c	0.95
α	0.1
β	0.9
τ_f	0
CPV	150 €/MWh
VOLL	3000 €/MWh

The power system is characterised by two specific periods of operation – during minimum and maximum demand. The input data about the reference voltage at node 1 were taken from the measurements from the Krk substation [32]. The measurements indicate that system can operate normally during maximum demand, however, during minimum demand, the reference voltage at node 1 was higher, thus indicating the possible grid code violations during the period of minimum demand and high RES production. For this reason, all modelled scenarios were analysed for a day of operation for these two cases, which is detailly discussed in the Results as well as the Discussion section. The demand data for minimum and maximum case is provided in Figure 3. The system is analysed on for half – hourly periods.

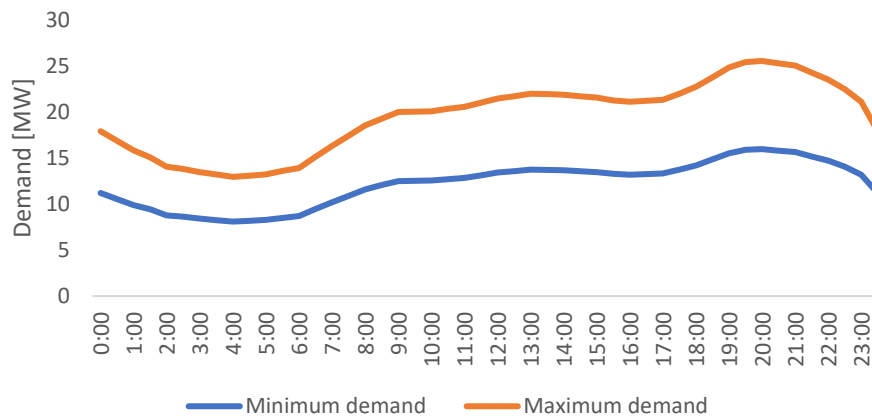


Figure 3. The demand for two analysed days

Finally, three different scenarios were analysed in this study and are presented in Table 5.

Table 5. Description of modelled scenarios

Scenario	S0	S1	S2
Description	No maritime electrification	Maritime transport electrification with 2.4 MW charger in node 4	S1 + connection of 1MW/2MWh ESS in node 4

For both scenarios, S1 and S2, it was considered that ships Krk and Kornati were electrified and that both ships are equipped each with a 2.4MW/1.2 MWh battery system. The batteries of such capacities are sufficient to follow the ships' timeline for winter and summer provided in Table 6. Merag port is located at node 4 and Valbiska in nearby node 2 in Figure 2. It was considered that the Krk ship (F1) started at Merag port and the Kornati ship (F2) started at Valbiska port.

Table 6. Timeline for Krk and Kornati ship for winter and summer periods

Winter			Summer	
Merag →	← Valbiska		Merag →	← Valbiska
05:30	05:00		05:00	05:30
07:00	06:30		06:30	07:00
09:00	08:30		08:30	09:00
10:30	10:00		10:00	10:30
13:00	12:30		11:30	12:00
15:30	15:00		13:00	13:30
18:00	17:30		14:30	15:00
20:00	19:30		16:00	16:30
22:00	21:30		17:30	18:00
23:30	23:00		19:00	19:30
			20:30	21:00
			22:00	22:30
			23:30	

The connection of charging infrastructure for electric ships requires a large intervention in the existing power system grid. This requires the installation of additional transformers, cables and additional electric equipment. Moreover, since the charging capacity is high, significant energy electronic equipment needs to be installed which can negatively affect the quality of electric energy. A significant number of ships operate on 60 Hz frequency, which can require additional electronic devices such as frequency converters. More types of connection is provided in the study [35]. In this study, it is considered that the Merag transformer was upgraded from 35/0.4 kV to 35/10 kV and that the connection of electrical chargers is on the 10 kV voltage.

Four scenarios with different RES shares were analysed in this study for each scenario (S0, S1 and S2), as well as minimum and maximum electricity demand (this corresponds to the winter and summer timeline of ships, respectively). The 25% RES scenario indicates the scenario with a total of 7.5 MW PV installed, while the 100% RES scenario is the scenario with 30 MW installed PV plants. Detailed connection points of added residential and utility PV plants are given in Table 7.

Table 7. Connection of PV generation for different RES share

Node	25% RES [MW]	50% RES [MW]	75% RES [MW]	100% RES [MW]
7	6.5	9	9	9
10	0	0	0	5
12	0	0	7.5	10
13	0	5	5	5
23	1	1	1	1
Total	7.5	15	22.5	30

Results

The results were observed for two base cases – maximum and minimum demand. The positive effects of smart sector integration are visible in both cases, however, the positive effects are more expressed for the minimum demand case due to the aggravated technical conditions in the electric grid. The results present the differences in the charging schedule of the electric ships, operation of the ESS, voltage values, curtailed energy values and the overall system operation for different scenarios and different RES shares.

The results regarding ship dimensioning are presented in Table 8. These results were obtained based on the data in Table 1 and equations (1) – (4) presented in the Methods section.

Table 8. Parameters for Krk and Kornati ship

Ship's name	Kornati	Krk
Average speed, v_{ave} (knot)	8.68	
Average main engine(s) power, $P_{ME,ave}$ (kW)	496.35	

Average auxiliary engine(s) power, $P_{AE,ave}$ (kW)	420	540
Total average ship power, P_{ave} (kW)	916.3	1036.3
Energy consumption per distance, EC (kWh/nm)	105.57	119.39

Maximum demand

The operation of both electric ships – Krk (F1) and Kornati (F2) for scenarios without (S1) and with (S2) ESS in node 4 is presented in Figure 4 and Figure 5. Figure 4 presents the charging of both electric ships at chargers installed at node 4. Both scenarios are presented in Figure 4 since the installation of the ESS in node 4 did not change the charging schedule of both electric ships. The charging schedule, however, did slightly change for different RES shares (e.g., charging of the Kornati ship increased by 0.3 MW at 9:00 for 100% RES in comparison to 25% RES). The blue arrows in Figure 4 point to the changes in the charging schedule for the first ship Krk (F1) and the red arrows point to the changes for the second ship Kornati (F2).

The charging schedule of the ships provides flexibility to the system so that it minimizes the operation cost. However, the system can exploit the flexibility only for a few periods because the charging schedule of the ships is primarily determined by the ship's navigation schedule. The installation of ESS in node 4 (S2 scenario) did not cause additional changes in the charging schedule of the ships because the battery provided additional flexibility during other periods when ship batteries were not able to provide it (see Figure 6). Similarly, the state of charge of the ships' batteries remains similar with slight changes caused by the penetration of different RES shares in the system (Figure 5).

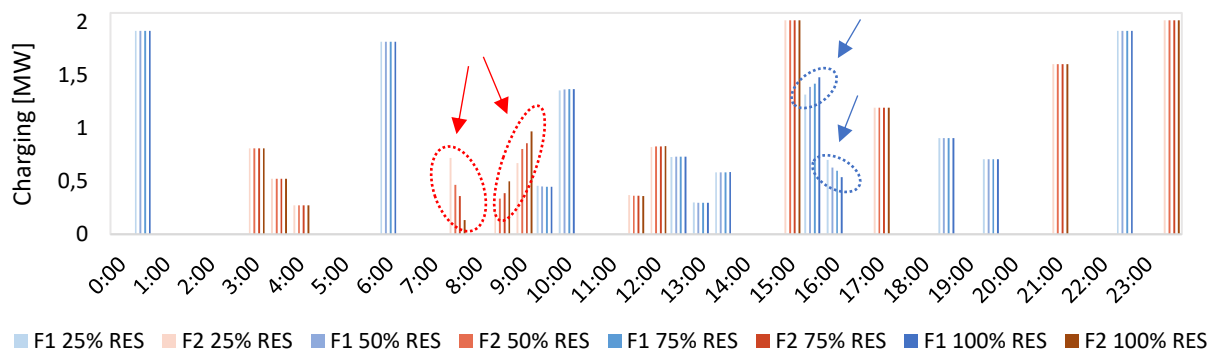


Figure 4. Ship charging values for scenarios S1 and S2 (without and with the ESS in node 4) – first ship Krk (F1) in blue columns and the second one Kornati (F2) in red columns

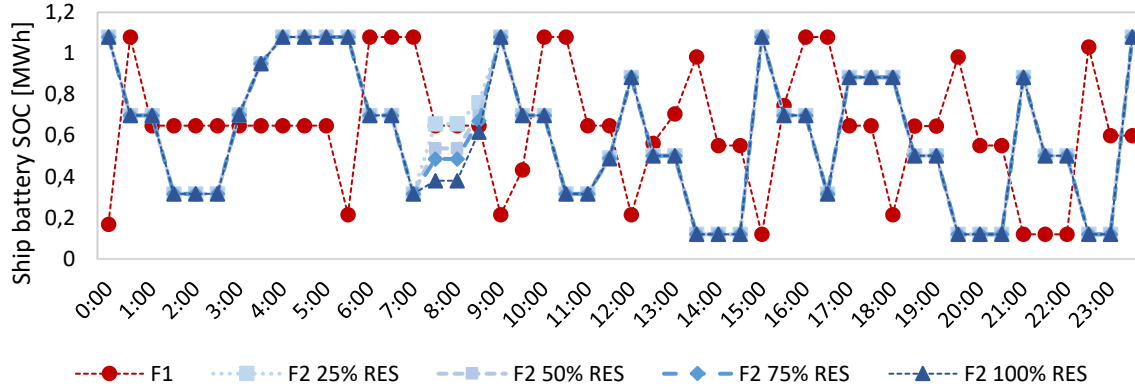


Figure 5. State of charge of the ferry batteries for scenarios S1 and S2 (without and with the ESS in node 4)

The operation of the ESS connected in node 4 (S2 scenario) is presented in Figure 6. The ESS did not change its operation as the RES share in the system increased. This result was expected because the system operates at a stable voltage for all scenarios. Because of that, the operation of the battery is only determined by the demand curve and the day-ahead electricity market prices. The battery charged during the night hours and low market prices and it increased during the evening and higher market prices.

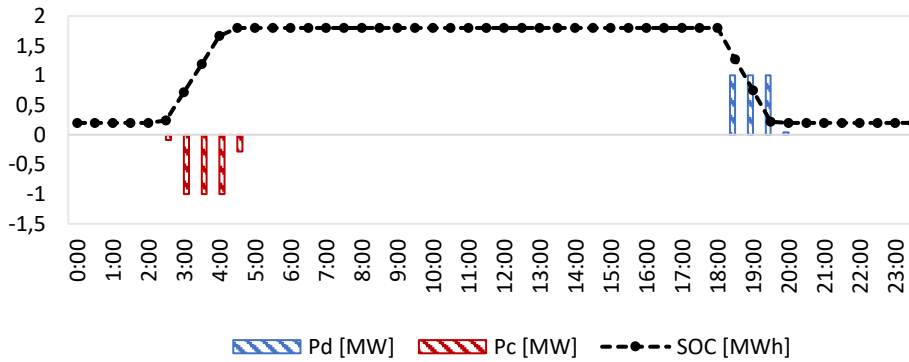


Figure 6. Battery operation at node 4 for scenario S3

Figure 7 presents the changes in the voltage at node 4 for different RES shares and all three scenarios. It can be seen that the increase in RES share caused the voltage level to increase as well. However, this did not impose significant constraints for the system operation because the voltage did not significantly approach the limits prescribed by the grid code. Another observation from Figure 7 regarding the maritime electrification effect and RES integration can be derived. It can be seen that the electrification of maritime transport (green and red lines in Figure 7) had a positive effect on the technical conditions in the grid. During the periods of

ship charging, the voltage at node 4 reduced and brought it closer to the nominal voltage (1 pu). The impact of the ESS connection at node 4 (green line) decreased the voltage during charging periods and increased during the discharging periods. However, the operation of the ESS and ship charging for the maximum demand case is primarily determined in a way that they decrease the overall system operation cost, but they also provide additional flexibility in technical terms so that there is a higher potential for the RES integration in the system. The lowest voltage value for the 100% RES S2 scenario was 0.98 pu, while the highest was 1.07 pu.

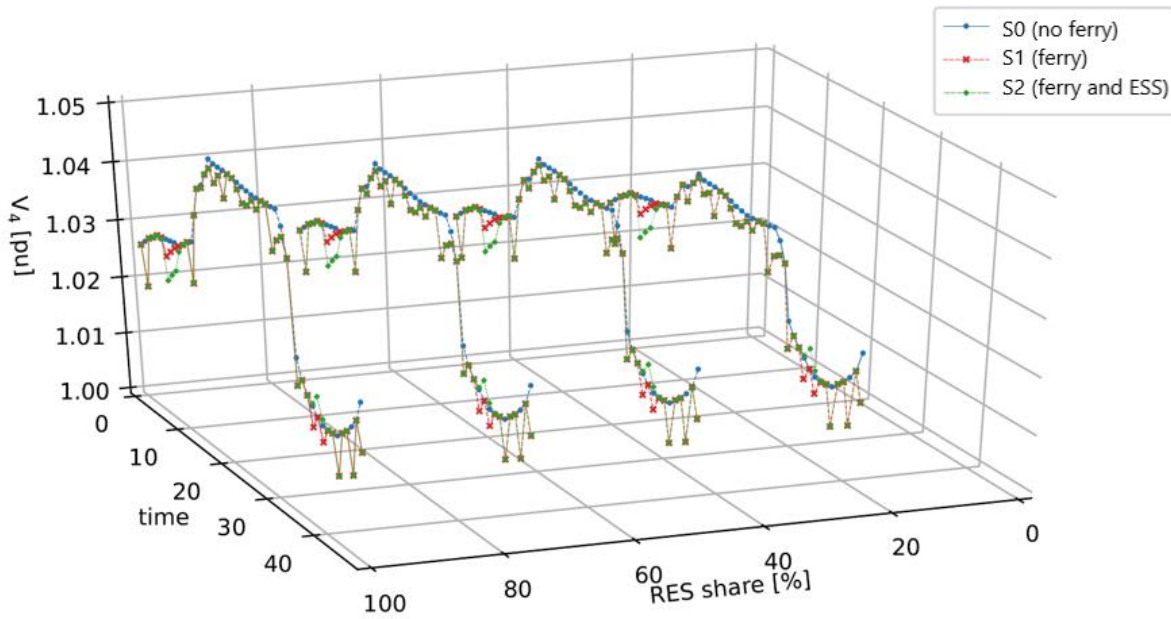


Figure 7. The voltage at node 4 for all three scenarios for maximum demand

The energy system operation for the S3 scenario and for the maximum demand case is presented in Figure 8. The figure shows the impact on the overall energy exchange as a result of ship charging and installed ESS. As shown in the figure, there were no curtailed energy values for the maximum demand case.

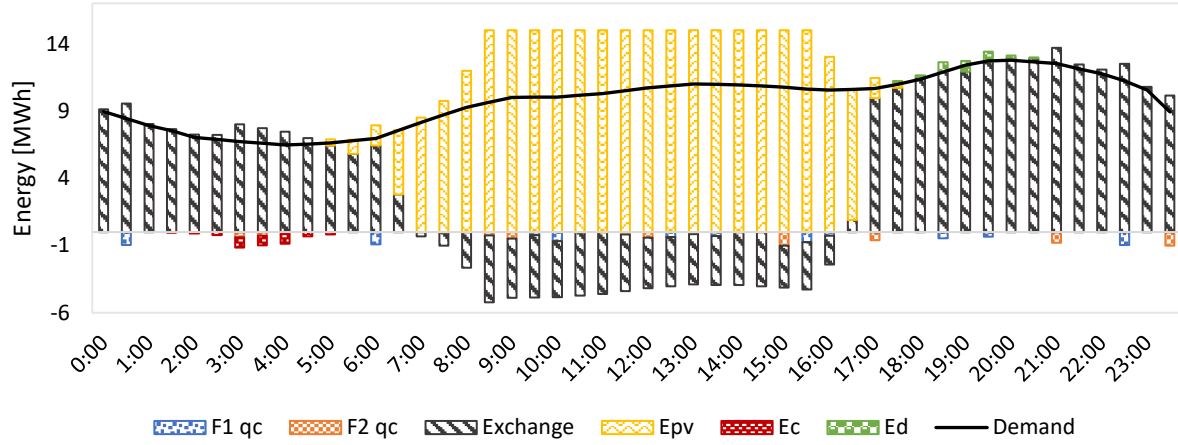


Figure 8. Energy system operation for scenario S2 for the maximum demand case

It is important to note that during the maximum demand there are no significant challenges to maintaining the system parameters within the limits prescribed by the grid code. This is why the flexibility provided by the ship charging stations and the installed ESS was not necessary for preventing violation of technical limits of the energy system but was used for decreasing the operation cost of the system, thus increasing overall social welfare. This will, however, change for the case with minimum demand as the voltage limits will rise closer to the upper limit (1.1 pu) because of increased reactive power flows.

Minimum demand

The case with minimum demand is characterised by high voltage, caused by the increased reactive power flow in the distribution and transmission grid. Increased RES share in such conditions can further aggravate the voltage conditions in the observed grid. However, the results indicate that enabling flexibility through smart cross-sectoral integration of maritime transport with the electric power system grid can improve the conditions, lower the curtailed energy from the RES and enable higher RES penetration.

Figure 9 and Figure 10 present the operation of the Krk and Kornati charging schedule for scenarios S1 and S2. In contrast to the case for the maximum demand, significantly more changes in the charging schedule for different RES shares occurred. In particular, the changes are most evident for the cases when RES share reaches 75% and 100%. This result was expected, because high RES penetration increased the system voltage, bringing it closer to prescribed limits (1.1 pu) on specific buses. This leads to the curtailment of renewable energy

and, in order to reduce the curtailed energy, the electric ships can provide flexibility to the extent possible so that the navigation schedule is respected. The results showed the necessity to invest in smart energy systems to integrate a large amount of RES.

Moreover, the results showed the difference in charging schedule between scenarios S1 and S2 as well. For example, the charging of the Krk ship (F1) was reduced by 10% at 13:00 for the 100% RES S3 scenario with the ESS in comparison to the S1 scenario (black arrow in Figure 9). Similarly, the charging for the Kornati ship was reduced by 7.4% at 15:30 for the same scenario comparison (Figure 10). More expressed changes for the Kornati ship can also be observed in Figure 10. For example, a 2.02 MW charging was scheduled at 10:30 only for the 100% RES S2 scenario and a 1.61 MW at 14:30 for the same scenario (noted with black arrows in Figure 10). It is interesting to observe that these changes are in line with the battery system operation for the S2 scenario shown in Figure 13 (e.g., ESS discharged at 10:30 and 14:30 when the ships charged and ESS charged at 15:30 when the charging of the Kornati ship was reduced).

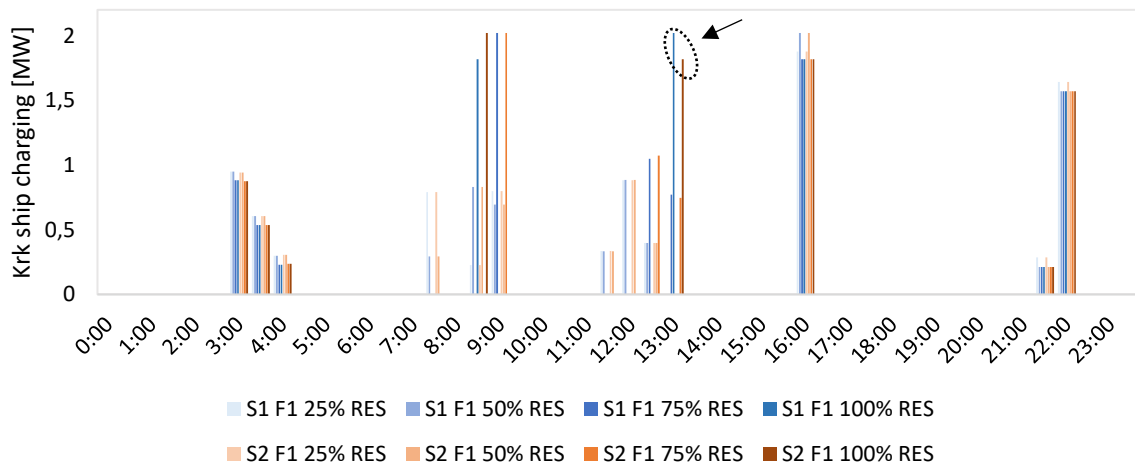


Figure 9. Krk ship (F1) charging values for scenarios without (S1) and with (S2) the ESS in node 4

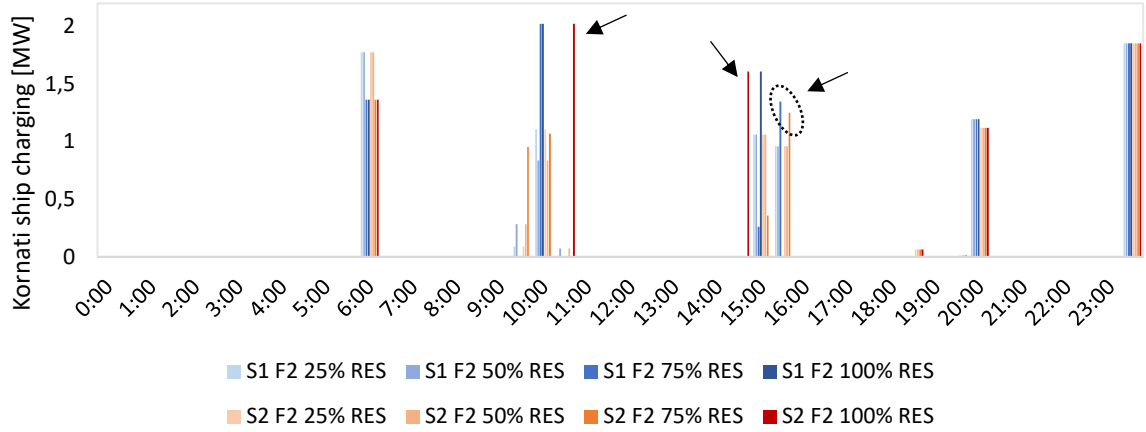


Figure 10. Kornati ship (F2) charging values for scenarios without (S1) and with (S2) the ESS in node 4

The changes in the charging schedule affect the state of charge of batteries on the ships. The changes between the state of charge of batteries on the ships for 25% and 100% RES are shown in Figure 11. The results shown in Figure 9, Figure 10 and Figure 12 demonstrate the ability of electrified maritime transport to provide flexibility to the observed system. The flexibility provided by maritime transport reduced the amount of curtailed renewable energy and increased the overall social welfare of the observed system.

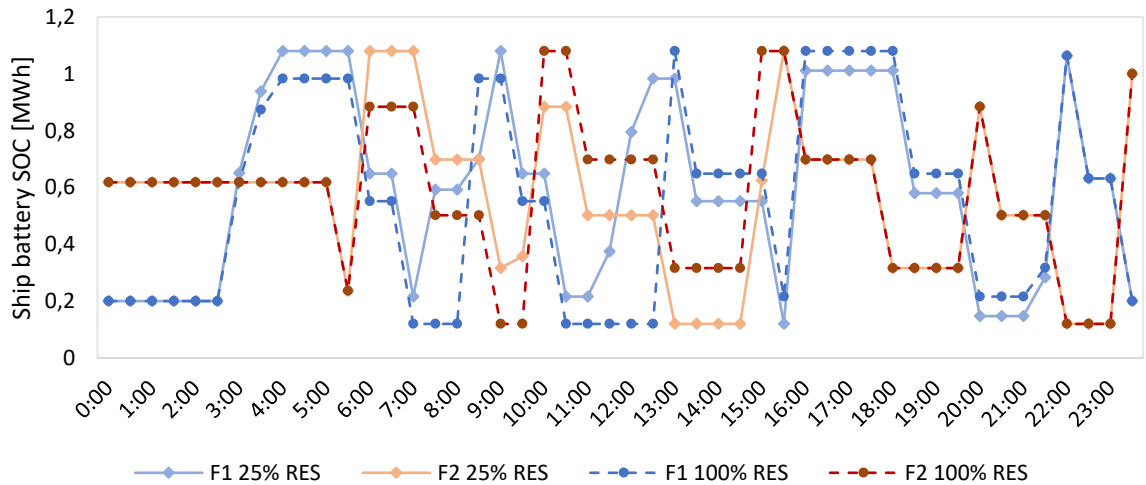


Figure 12. State of charge of Krk and Kornati batteries for 25% and 100% for the S1 scenario

The ESS operation for the S3 scenario is shown in Figure 13. The ESS connected at node 4 presents an additional source of flexibility for the system. It can be seen that the operation of the ESS for the 25% and 50% RES share did not change, however, significant differences can

be seen for 75% and 100% RES share. The ESS adjusts its operation to reduce the amount of curtailed energy from RES. This means that ESS operation was not determined only by prices of the day ahead electricity market, but also by the curtailed energy. The ESS aimed not only to reduce the amount of curtailed energy but also to reduce it when the market prices were high. Because of this ESS had to discharge at certain periods which caused voltage increase above values that occurred for the S0 scenario (but still below 1.1 pu), which was not the case for the maximum demand (see Figure 14).

Moreover, the operation of the ESS was aligned with the charging schedule of the ships. For example, the ESS discharges 1 MW at 9:30 and 10:30 for 75% and 100% RES share and, at the same periods, the Kornati ship was charging (0.95 MW at 9:30 for 75% RES and 2 MW for 100% RES at 10:30). This result implicates that for the large capacity chargers at high RES share, additional sources of flexibility such as ESS reduces the amount of curtailed energy and the operation cost of the system.

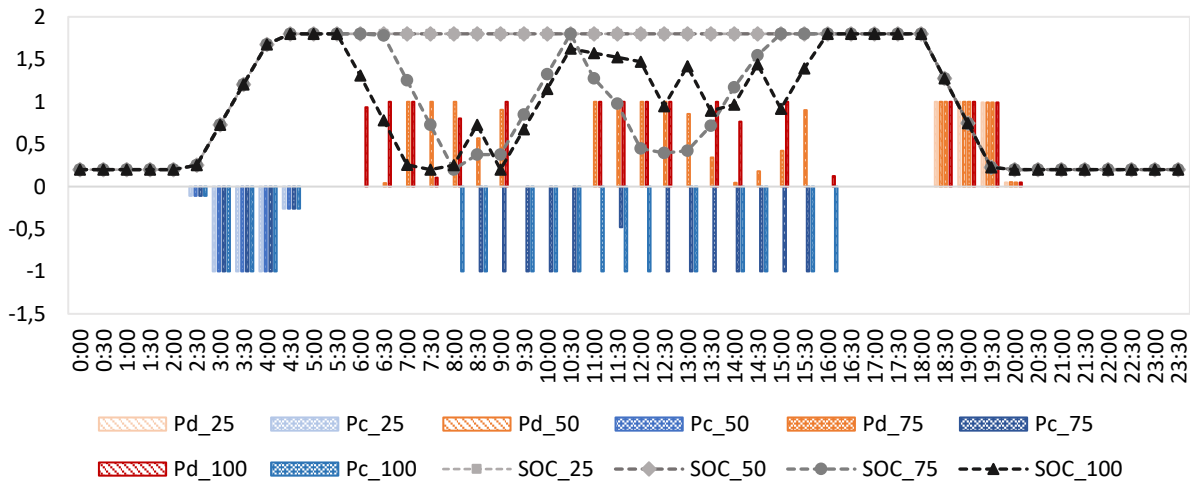


Figure 13. Battery system operation at node 4 for the S3 scenario for different RES share – charging and discharging (blue and red bars) are expressed in MW and the state of charge of batteries on the ships (lines) are expressed in MWh

The values of the curtailed energy for each scenario and RES share is given in Table 9. The results showed that there was no curtailed energy for the lowest RES share for any scenario. For the 50% RES share, there were low values of curtailed energy for the S0 scenario, while, for the S1 and S2 scenarios, the electric ships and the ESS provided enough flexibility to eliminate curtailed energy.

More significant values of curtailed energy appear for 75% and 100% RES shares. The effect of the flexibility provided by the smart electrification of the maritime transport and connection of the ESS at node 4 can be observed for these high RES cases. The electrification of the maritime transport and its integration with the electric system (the S1 scenario) reduced the amount of curtailed energy by 34.3% (1.92 MWh) in comparison to the base S0 scenario for 75% RES share and 9.8% (2.46 MWh) for 100% RES share. The additional connection of ESS at node 4 reduces the curtailed energy by 55.2% (3.1 MWh) for 75% RES share and 15.7% (3.9 MWh) for the 100% RES share.

Table 9. Curtailed energy [MWh] for each analysed scenario and different RES share

RES share / Scenario	S0	S1	S2
25%	0	0	0
50%	0.234	0	0
75%	5.6	3.68	2.51
100%	25.11	22.65	21.18

As elaborated in the Material and methods section, the proposed AC OPF model enables the calculation of losses in the energy system because $p_{ij} \neq p_{ji}$. The losses for all three scenarios and different RES shares are given in Table 10. It can be seen that the highest increase in losses is achieved for higher RES penetration which was expected because the increase of overall power flow in the grid will lead to higher losses. It is also possible to observe that the charging of the electrical ferry (S1) and the connection of the ESS (S2) did not cause a significant increase in losses. Because there is more curtailed energy for the S0 scenario (lower power flow in the grid) than for S1 and S2, the effect on the losses is even less expressed.

Table 10. Active losses [MWh] in the observed energy system

RES share / Scenario	S0	S1	S2
25%	3.72	3.74	3.75
50%	3.82	3.83	3.83
75%	3.81	3.87	3.93
100%	4.43	4.53	4.59

The voltage at node 4 for the minimum demand case is provided in Figure 14. The results indicate that, for the 25% and 50% RES share, the effect of the maritime transport electrification and additional ESS is similar to the case of maximum demand. The voltage for S1 and S2 was reduced closer to the nominal values, thus the technical grid conditions were improved.

However, differences occur for the 75% and 100% RES share, where the voltage for the S2 scenario raised above the voltage values that occurred for the scenario without maritime electrification (S0). Moreover, the significantly higher voltage reduction values (in comparison to S0 – blue line in Figure 14) occurred for 75% and 100% RES. These extremes are marked with a dotted black ellipse in Figure 14. This is connected to the previous results regarding battery storage operation and ship charging schedule. Besides lowering the overall curtailed values, the optimization algorithm adjusted the charging schedules as well as the ESS operation so that the curtailed values were the lowest for the lowest prices on the day-ahead electricity market. Because of this, increased ship charging values as well as the ESS charging and discharging values during the high PV production caused more frequent voltage deviation. The highest voltage at node 4 was 1.093 pu and, at the same period, the voltage at node 23 reached 1.1 pu. Further increase of voltage at node 4 would cause grid code violation for nodes 22 and 23.

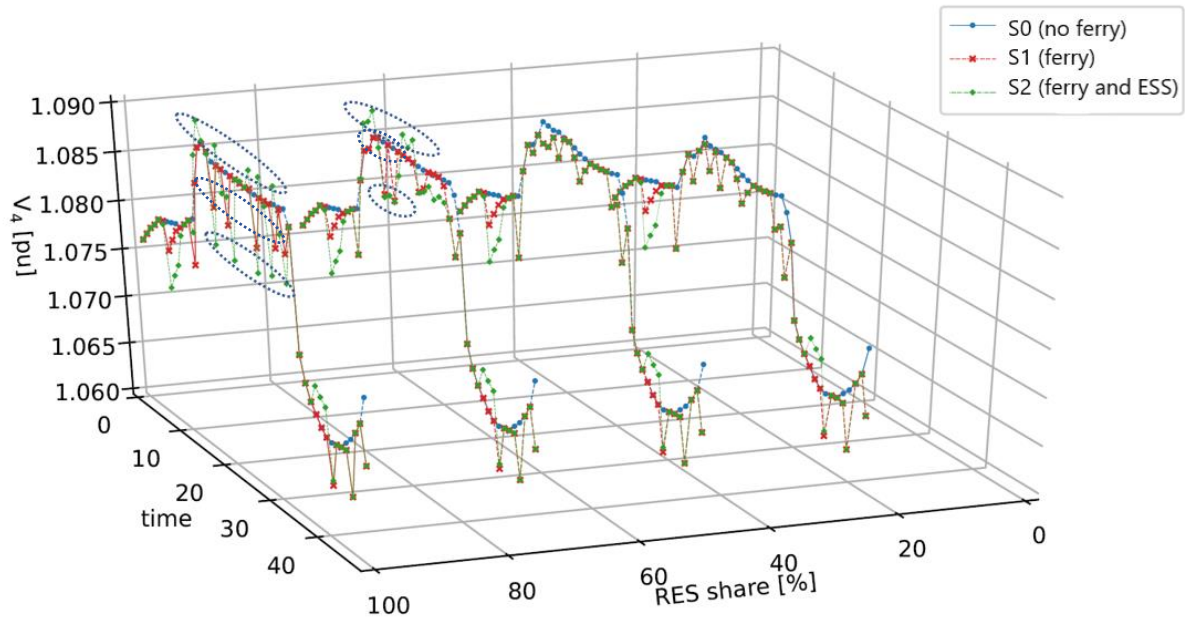


Figure 14. The voltage at node 4 for minimum demand and all scenarios at different RES share

Finally, the energy system operation for the minimum demand case is presented in Figure 15. The figure shows that the electrification of maritime transport and the installation of the ESS at node 4 had a higher impact on the overall system operation in comparison to the maximum

demand case (significant voltage increases and decreases are marked with blue dotted ellipses in Figure 14).

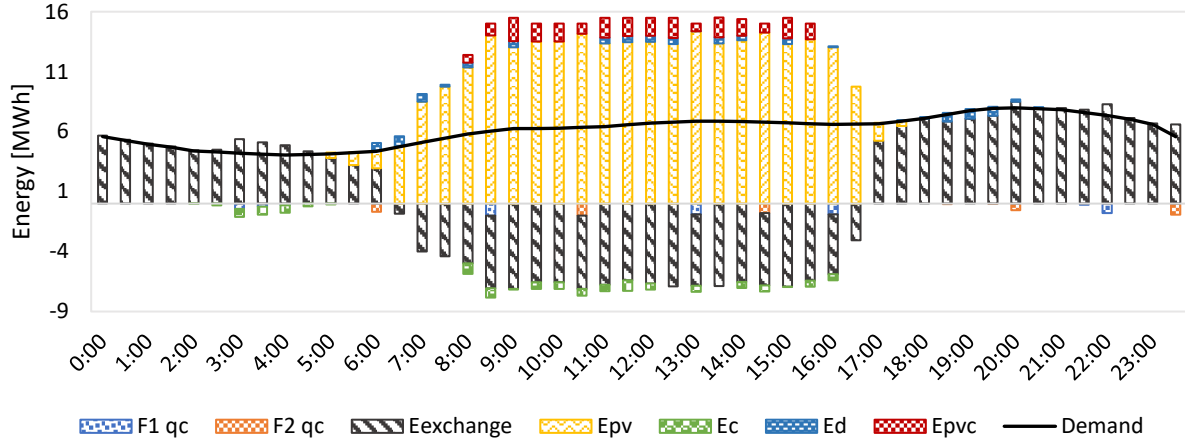


Figure 15. Energy system operation for scenario S2 for minimum demand case and 100% RES

The presented results showed the benefits of smart cross-sectoral integration, in particular the integration of maritime transport and the electric distribution system. Such integration can improve the technical conditions in the electric grid, enable the higher penetration of RES and increase overall social welfare. The solution where the ESS was connected at the same bus as the electric ship chargers only improved obtained results.

Discussion

The results of the study indicated that the proposed method and mathematical models can be used for the evaluation of the effects of the integration of the electric distribution grid and maritime transportation into smart energy systems.

The key findings of the study showed that such smart integration improved the technical conditions in the electric grid. The electrification of maritime transport lead to the reduction of the curtailed energy and influenced the electric system operation. The installation of ESS in the electric ferry connection point lead to further reduction of the curtailed energy. Moreover, the results showed that the charging schedule, as well as the ESS operation, changed with respect to the installed RES share. This effect was intensively visible for the high RES share for the

minimum demand case. Since the voltage was close to the limits for the minimum demand case, the charging schedule and the ESS operation were adjusted so that the system remained within stable conditions and that the lowest amount of energy was curtailed during periods of high price on the day-ahead electricity market.

To the best of our knowledge, the most relevant study that presented the electric vessel with PV, ESS and grid connection was carried out in [36]. The authors found that the ESS was mostly charged during the period of low prices in the electricity market. Although this is also true in our study for the maximum demand case, we also found out that the electric ships and the ESS were mostly charged during the peak PV production for the minimum demand scenario. This is the case because the method presented in this paper observed the entire distribution system of the archipelago, which enables to observe the full flexibility potential of maritime and the distribution system integration. This proved to be especially important for the periods when the system is close to the limits prescribed by the grid code limitations, which was not discussed in [36].

The detailed distribution system modelled in this study realistically captured the possible voltage violations and congestions. The application of such a detailed distribution system model, in combination with the presented electrical ferry model, enabled us to observe the impacts of smart integration of the maritime and electricity sector during both, the normal and disturbed operating parameters of the distributions system. A similar model was previously used in [37] for assessing the impact of the price-sensitive top-down demand response model. The model in [37] considered a smaller distribution system around Lošinj island and a maximum installed RES capacity of 20.5 MW. The maximum reduction of the curtailed energy was 3.5% lower for the scenario with demand response in comparison to the base scenario. This study considered a larger system around Krk island and considered a maximum of 30 MW RES installed. The maximum reduction of curtailed energy as a result of maritime electrification (S1) in this paper was 9.8% in comparison to base scenario S0. This means that the presented cross-sector integration had a larger impact than the price responsive demand response model. However, this was expected because the capacity of ship charging stations was approximately two times higher than the used price responsive demand response. Additionally, the charging stations were connected to one bus in the system which enabled a stronger local impact on the technical parameters of the observed system. The proposed model can also be used as a basis for further sector coupling and the creation of smart energy systems such as water and energy systems as in [38], or land transport integration as in [39].

The case study in this paper used the PV curve that represents the maximum daily PV production for both cases – maximum and minimum demand. Since the maximum demand is achieved during the summer period and the minimum demand is usually for the winter or autumn period, one could argue that a different PV curve that represents the average or minimum production should be used for the minimum demand case. Although it is reasonable to question this, there are at least two reasons why this should be avoided. First, the aim of the study is to demonstrate the effects of smart cross-sector integration for marginal system operation in high RES surrounding to observe the full effect of newly introduced flexibility in the system. Since the highest voltage will appear for the minimum demand and the highest generation, this scenario should be considered. Moreover, at least two technical studies ([40] and [33]) showed that maximum PV production can also occur during potential periods of minimum demand for the observed location, thus further underlining the necessity to analyse such a scenario. The second argument is that all of the results of the study were presented with respect to the different RES shares. Thus, the cases for lower PV production were analysed for 25% and 50% RES scenarios, which is considered enough to show the effects of lower PV production during minimum demand. The results were in accordance with the statements made in this chapter – that the most interesting case is for the highest RES production and the minimum demand. Thus, it can be concluded that the conducted sensitivity analysis well represents the system behaviour for different cases and that the minimum demand and 100% RES scenario fully demonstrate the possible exploitation of the flexibility potential of maritime electrification.

Although this study did propose a model that considered the ship battery energy loss when the ship is not sailing, the study did not include a battery degradation effect and this imposes a limit on this study. The degradation effect can have a long-term impact on the operation of the electric ships and should be investigated. However, in our study, it is acceptable to neglect this effect because this study aims at investigating the effects of cross-sector integration of maritime transport with the electrical grid, with a particular emphasis on the technical impacts on the power system grid. Moreover, since the variables and parameters used in the proposed approach are general and can be applied to any distribution system or electric ship, the proposed method can be applied to numerous case studies. It can be expected that similar results and conclusions would be achieved for other case studies, however, the precise impact will differ from one site to another and the proposed approach enables the quantification of these impacts for each site.

The presented study implicates the need to accelerate the creation of the financial and regulatory frameworks that will stimulate the smart electrification of maritime transport. In order to achieve the integration, it will be necessary to build the proper infrastructure and smart ports [41]. This will lead towards the increased penetration of RES in the energy systems and contribute to further sector coupling and energy transition.

Conclusion

This study presented a novel approach for the assessment of smart integration of the electrified maritime transport sector with the electric power system sector. The method proposed a mathematical model for the electric ships integrated into the detailed distribution system. The case study was conducted on the example of the Kvarner archipelago with the aim of observing the effects of cross-sector integration under the different penetration of renewable energy sources. The results of the study showed that:

- The cross-sector integration of maritime transport and electric power system with installed energy storage system resulted in the decrease of curtailed energy for 3.9 MWh when 30 MW of installed photovoltaics were installed in the grid in comparison to the case without the electrified maritime transport
- The integration of electrified maritime transport improved the voltage conditions during the maximum demand in the archipelago. The voltage at the ferry connection node reduced up to 0.845 kV when the ferries were connected in order to decrease the amount of the curtailed energy
- The charging schedule of the electric ships changed with the increased share of renewable energy sources while maintaining the passenger transport timeline. The changes went up to 2 MW of increased charging for the highest share of renewable energy sources present in the system
- The results of the study indicate the need for the creation of the supporting schemes and frameworks that will stimulate the electrification of maritime transport and its integration with the electric power system

The future research will be oriented towards the investigation of different possibilities of maritime transport electrification with an emphasis on their market integration. This will be done through the application of different incentives and support to electrified maritime transport.

Acknowledgement

This work has been supported by the Young Researchers' Career Development Programme (DOK-01-2018) of Croatian Science Foundation which is financed by the European Union from European Social Fund and Horizon 2020 project INSULAE - Maximizing the impact of innovative energy approaches in the EU islands (Grant number ID: 824433). This support is gratefully acknowledged.

References

- [1] International Maritime Organization, “Fourth IMO GHG Study-Executive Summary,” 2020.
- [2] DNV, “Energy Efficiency Existing Ship Index (EEXI).” .
- [3] DNV, “Achieving the IMO decarbonization goals.” .
- [4] A. D. Korberg, S. Brynolf, M. Grahn, and I. R. Skov, “Techno-economic assessment of advanced fuels and propulsion systems in future fossil-free ships,” *Renew. Sustain. Energy Rev.*, vol. 142, p. 110861, May 2021.
- [5] Sterling PlanB Energy Solutions (SPBES), “Electrification of ships.” .
- [6] C. Nuchturee, T. Li, and H. Xia, “Energy efficiency of integrated electric propulsion for ships – A review,” *Renew. Sustain. Energy Rev.*, vol. 134, p. 110145, Dec. 2020.
- [7] DNV GL AS Maritime, “Electrical Energy Storage for Ships,” 2020.
- [8] E. Gagatsi, T. Estrup, and A. Halatsis, “Exploring the Potentials of Electrical Waterborne Transport in Europe: The E-ferry Concept,” in *Transportation Research Procedia*, 2016, vol. 14, pp. 1571–1580.
- [9] I. Ø. Tvedten and S. Bauer, “Retrofitting towards a greener marine shipping future: Reassembling ship fuels and liquefied natural gas in Norway,” *Energy Res. Soc. Sci.*, vol. 86, p. 102423, Apr. 2022.
- [10] L. Wang, J. Hu, Y. Yu, K. Huang, and Y. Hu, “Lithium-air, lithium-sulfur, and sodium-ion, which secondary battery category is more environmentally friendly and promising

- based on footprint family indicators?,” *J. Clean. Prod.*, vol. 276, p. 124244, Dec. 2020.
- [11] E. Blanco-Davis and P. Zhou, “LCA as a tool to aid in the selection of retrofitting alternatives,” *Ocean Eng.*, vol. 77, pp. 33–41, Feb. 2014.
 - [12] M. Perčić, N. Vladimir, and A. Fan, “Techno-economic assessment of alternative marine fuels for inland shipping in Croatia,” *Renew. Sustain. Energy Rev.*, vol. 148, p. 111363, Sep. 2021.
 - [13] M. Perčić, N. Vladimir, and A. Fan, “Life-cycle cost assessment of alternative marine fuels to reduce the carbon footprint in short-sea shipping: A case study of Croatia,” *Appl. Energy*, vol. 279, p. 115848, Dec. 2020.
 - [14] H. Wang, E. Boulougouris, G. Theotokatos, P. Zhou, A. Priftis, and G. Shi, “Life cycle analysis and cost assessment of a battery powered ferry,” *Ocean Eng.*, vol. 241, p. 110029, Dec. 2021.
 - [15] D. F. Dominković, J. M. Weinand, F. Scheller, M. D’Andrea, and R. McKenna, “Reviewing two decades of energy system analysis with bibliometrics,” *Renew. Sustain. Energy Rev.*, vol. 153, p. 111749, Jan. 2022.
 - [16] F. Scheller, F. Wiese, J. M. Weinand, D. F. Dominković, and R. McKenna, “An expert survey to assess the current status and future challenges of energy system analysis,” *Smart Energy*, vol. 4, p. 100057, Nov. 2021.
 - [17] H. M. Marczinkowski and L. Barros, “Technical approaches and institutional alignment to 100% renewable energy system transition of madeira island-electrification, smart energy and the required flexible market conditions,” *Energies*, vol. 13, no. 17, 2020.
 - [18] N. Duić, G. Krajačić, and M. da Graça Carvalho, “RenewIslands methodology for sustainable energy and resource planning for islands,” *Renewable and Sustainable Energy Reviews*. 2008.
 - [19] Y. Matamala and F. Feijoo, “A two-stage stochastic Stackelberg model for microgrid operation with chance constraints for renewable energy generation uncertainty,” *Appl. Energy*, vol. 303, 2021.
 - [20] M. Mimica, L. Giménez de Urtasun, and G. Krajačić, “A robust risk assessment method for energy planning scenarios on smart islands under the demand uncertainty,” *Energy*, vol. 240, p. 122769, Feb. 2022.

- [21] F. Martorana, M. Giardina, P. Buffa, M. Beccali, and C. Zammuto, "A new tool to process forecast meteorological data for atmospheric pollution dispersion simulations of accident scenarios: A sicily-based case study," *J. Sustain. Dev. Energy, Water Environ. Syst.*, vol. 9, no. 3, 2021.
- [22] D. Groppi, A. Pfeifer, D. A. Garcia, G. Krajačić, and N. Duić, "A review on energy storage and demand side management solutions in smart energy islands," *Renew. Sustain. Energy Rev.*, vol. 135, 2021.
- [23] H. Hao, B. Huang, and P. Ji, "Optimal Configuration of An Island Microgrid Considering Demand Response Strategy," in *Proceedings - 2021 36th Youth Academic Annual Conference of Chinese Association of Automation, YAC 2021*, 2021.
- [24] M. Mimica and G. Krajačić, "The Smart Islands method for defining energy planning scenarios on islands," *Energy*, vol. 237, 2021.
- [25] D. Curto, V. FRANZITTA, M. Trapanese, and M. Cirrincione, "A Preliminary Energy Assessment to Improve the Energy Sustainability in the Small Islands of the Mediterranean Sea," *J. Sustain. Dev. Energy, Water Environ. Syst.*, vol. N/A, no. N/A, 2020.
- [26] R. A. Agathokleous and S. A. Kalogirou, "PV roofs as the first step towards 100% RES electricity production for Mediterranean islands: The case of Cyprus," *Smart Energy*, vol. 4, p. 100053, Nov. 2021.
- [27] J. D. Ocon and P. Bertheau, "Energy transition from diesel-based to solar photovoltaics-battery-diesel hybrid system-based island grids in the Philippines – Techno-economic potential and policy implication on missionary electrification," *J. Sustain. Dev. Energy, Water Environ. Syst.*, vol. 7, no. 1, 2019.
- [28] D. F. Dominkovic, G. Stark, B. M. Hodge, and A. S. Pedersen, "Integrated energy planning with a high share of variable renewable energy sources for a Caribbean Island," *Energies*, 2018.
- [29] R. Adland, P. Cariou, and F. C. Wolff, "Optimal ship speed and the cubic law revisited: Empirical evidence from an oil tanker fleet," *Transp. Res. Part E Logist. Transp. Rev.*, vol. 140, p. 101972, Aug. 2020.
- [30] Jadrolinija, "Ferry lines schedule." .

- [31] Croatian Register of Shipping, “Web report of a ship.” .
- [32] M. Mimica, D. F. Dominković, V. Kirinčić, and G. Krajačić, “Soft-linking of improved spatiotemporal capacity expansion model with a power flow analysis for increased integration of renewable energy sources into interconnected archipelago,” *Appl. Energy*, vol. 305, p. 117855, Jan. 2022.
- [33] T. Cerovečki, M. Cvitanović, F. Damjanović, R. Ivković, J. Majcen, and I. Širić, “Optimal technical connection of PV plant on distribution grid.” 2019.
- [34] “www.cropex.hr.” .
- [35] J. Kumar, A. A. Memon, L. Kumpulainen, K. Kauhaniemi, and O. Palizban, “Design and analysis of new harbour grid models to facilitate multiple scenarios of battery charging and onshore supply for modern vessels,” *Energies*, vol. 12, no. 12, 2019.
- [36] K. Hein, X. Yan, and G. Wilson, “Multi-objective optimal scheduling of a hybrid ferry with shore-to-ship power supply considering energy storage degradation,” *Electron.*, vol. 9, no. 5, 2020.
- [37] M. Mimica, D. F. Dominković, T. Capuder, and G. Krajačić, “On the value and potential of demand response in the smart island archipelago,” *Renew. Energy*, vol. 176, 2021.
- [38] E. Assareh, M. Delpisheh, S. M. Alirahmi, S. Tafi, and M. Carvalho, “Thermodynamic-economic optimization of a solar-powered combined energy system with desalination for electricity and freshwater production,” *Smart Energy*, p. 100062, Dec. 2021.
- [39] T. Boström, B. Babar, J. B. Hansen, and C. Good, “The pure PV-EV energy system – A conceptual study of a nationwide energy system based solely on photovoltaics and electric vehicles,” *Smart Energy*, vol. 1, p. 100001, Feb. 2021.
- [40] RINA-C, “INSULAE - Energy Storage System - Conceptual design Unije,” 2019.
- [41] J. Kumar, H. S. Khan, and K. Kauhaniemi, “Smart control of battery energy storage system in harbour area smart grid: A case study of vaasa harbour,” in *EUROCON 2021 - 19th IEEE International Conference on Smart Technologies, Proceedings*, 2021.